To the Graduate Council:

I am submitting herewith a dissertation written by Matthew D. Smith entitled "Chemical Approaches for the Investigation of Protein-Lipid Binding Interactions: Synthesis, Modification, and Evaluation of Novel Azido-Based Lipid Probes." I have examined the final electronic copy of this dissertation for form and content and recommend that it be accepted in partial fulfillment of the requirements for the degree of Doctor of Philosophy, with a major in Chemistry.

Michael Best
Major Professor

We have read this dissertation
and recommend its acceptance:

George Kabalka

Jimmy Mays

Engin Serpersu

Accepted for the Council:

Carolyn R. Hodges
Vice Provost and Dean of the Graduate School

(Original signatures are on file with official student records)

Chemical Approaches for the Investigation of Protein-Lipid Binding Interactions: Synthesis, Modification, and Evaluation of Novel Azido-Based Lipid Probes

A Dissertation
Presented for the
Doctor of Philosophy
Degree
University of Tennessee, Knoxville

Matthew Daniel Smith
May 2009

Dedication

This dissertation is dedicated to the memories of Burnis Hollingsworth and Dr. Rose West.

Paw-paw, while my memories of you are few, I do remember that you loved me like no one else. I hope that you are smiling down on me today the same way you used to smile to a blonde headed little boy.

Dr. West, you told me that no matter what I decided to become in life, just get the highest degree possible in my chosen career area. As I promised I would do, I have finally completed my doctorate degree. From taking your handwritten, one page exams to conversations in your office about our favorite reactions, your love for the science always showed. May I use all that I have learned and be able to pass the love for chemistry that you created and developed in me on to the students that cross my path with as I continue down this road called life.

Acknowledgements

So many people have helped me through this process. Before I begin thanking those individuals, if anyone feels their name should have been included but can't find it, you are probably correct. However, the absence of your name within this section does not mean that I intentionally left you out. If you happen to find yourself in the category, I ask that you attempt to write a dissertation while maintaining sanity and rational thought before giving me a hard time. At any rate, everyone involved in this undertaking from friends, family, students, labmates, and everyone else down to the guy at Folgers® who literally provided the fuel to carry on, thank you very much.

Mom and Dad: I am not sure that words can express what you two mean to me. You raised me well, taught me the value of hard work, to take pride in what I do, and to always love those that love me. You also taught me the faith in Christ that has gotten me through so many tough times, especially here lately. I know that my moving away was hard, but I hope you know that it was for me to gain what I thought best as I began my family. Your prayers have been much appreciated; please continue to do so. Please know that I love you both very much. My education has always been important to me, and I could not have asked for two parents to be any more supportive than you were.

While growing up and being the only boy in the family, one thing comes to mind: fighting with my sisters. Knowing that I did not always treat you right, as brothers often do, is something that I can not ever change. However, I think it suffices to say that you always got even. Trying to survive with three sisters is the only thing that I can think of

that would provide the determination and perseverance needed to complete what I am about to. Elisabeth and Grace: I will always be your big brother. I love you both and will always be there for you. May God bless all that you go through in life. Michaela: I see such potential in you. You are smarter than the three older children put together. Make life what you want it to be. You definitely are capable of becoming anything that you desire to be.

People often complain about their spouse's family. These people have obviously never met John, Ann, Jay, Granga, and Ken. Never have any people who are not blood relatives ever cared so much for me. It means so much to me to have people show so much interest about what I do. So many times at dinner discussion would turn towards how work was going. Having everyone make jokes about how simplistic that problem is, how you were just discussing that same topic the other day, or my personal favorite, how you know the answer but just are not going to tell me, caused me to step back from a hard day and smile. The next day was never as bad as the one before. I appreciate all that you have done for us. I will always consider you as dear family and am forever grateful for the love you show towards me.

Granny, Aunt Lois, Grandma and Grandpa: I have always felt nothing but love from you. From afterschool snacks to running through the kitchen as Batman with a towel around the neck, you have always been supportive of whatever I wanted to do. You looked at me with love and pride as a small boy, and I hope that is how you will always see me.

Two years into my graduate education, a student's worse nightmare happened. My advisor decided to change schools and go somewhere I had no intention of ever going. When this happened, someone was there to calm me down, and has been doing so ever since when things have taken a turn for the worse. Michael Best, you have taught me more chemistry than I ever knew existed. You are truly an advisor and not just a boss. I can tell that you have a desire to see me succeed and advance myself as a chemist and researcher. Your willingness to help me work through problems, even those that I am embarrassed to have to ask about, is endless. I truly enjoyed working for you, and I wish you all the success in the world as the research continues.

Without friends, life is short and dull. Graduate school provided me with friends like no others. My lab-mates have always been wonderful and supportive. May all of you continue to develop as strong scientists. If any of you guys or gals ever need anything, I am there for you. Jeremiah, I picked up two things from you. Without coffee and video games, these last years would have never passed. You are a true friend.

Lastly, there are two people who have changed my life more than any others. Beth Ann, when you said you would marry me, I bet you never anticipated this wild journey we would endure. As it is nearing completion, your constant support has always amazed me. You have provided me so much help during all of this; help that ranges from reading text that you did not understand and fixing commas all the way to never letting me give up. No one believes in me more than you do, myself included. Thanks for not letting me quit. Your love has kept me going when nothing else would….until you gave me our Norah-baby. Norah, I want you to know that all the late nights away from

home will soon be over. Holding you the day you were born made me realize that my most important job was now “Daddy”. Your laugh and chubby cheeks will put a smile on my face when nothing else will. Your love is wonderful. You and Mommy are my girls and “I’m gonna love you, like nobody’s loved you…..I’m with you always. I’m with you rain or shine.”

Abstract

Lipids such as diacylglycerol (DAG) and phosphatidic acid (PA) have been shown to play key roles in cell signaling events. The anchoring of proteins to the membrane via DAG or PA binding helps regulate protein function and localization and is also involved in normal and disease-related cellular processes. In order to fully understand these pathways, it is necessary to develop synthetic analogues that mimic the natural species, but that also have a means which allows investigation of the process at the molecular level. This dissertation will detail the design and synthesis of novel lipid-based probes possessing a reactive azide tag, which can then be functionalized via the 1,3-dipolar cycloaddition reaction (“click” chemistry) to produce a series of analogues with fluorescence and photo-cross-linking capabilities. Initial receptor-ligand binding results will be presented, along with the description of future studies that will provide insight into the mechanism of such interactions.

In addition, the immobilization of whole liposomes onto a surface will be discussed. Techniques such as measuring the fluorescence-after-immobilization and dye leakage assays were developed and optimized to prove that immobilization onto a surface had been achieved. This approach is then geared towards the development of a

high-throughput, micro-plate assay to detect the binding of a protein to a membrane. Here, liposomes which express a specific ligand at the surface will be immobilized and introduced to various receptors. Appropriate techniques will be employed to determine whether a given receptor binds to the expressed ligand.

Lastly, an initial attempt at the development of an artificial vesicle fusion system using “click” chemistry will be discussed.

Table of Contents

Chapter *Page*

Chapter 1: Introduction **1**

Chapter 2: Synthesis, Functionalization, and Biological Evaluations of Azide–Labeled Diacylglycerol (DAG) Analogues for the Modular Access to Lipid Probes **12**

Background and Significance **12**

Synthetic Procedures for DAG Analogues **15**

Biological Evaluation of DAG Analogues **28**

Experimental **31**

Chapter 3: Synthesis, Functionalization, and Biological Evaluations of Azide–Labeled Phosphatidic Acid (PA) Analogues for the Modular Access to Lipid Probes **76**

Background and Significance **76**

Synthesis of PA-based Lipid Probes **82**

Biological Evaluation of PA Analogues **95**

Experimental **98**

Chapter 4: Microplate-Based Analysis of Protein-Membrane Binding Interactions via Immobilization of Whole Liposomes via a Biotinylated Anchor **165**

Background and Significance **165**

Synthesis of Functionalized Lipids **169**

Immobilization of Whole Liposomes **172**

Detection of PKCα-DAG Interactions using Whole Liposome Immobilization **178**

Development of an Immobilization Assay for the Detection of Lectin-Carbohydrate Binding **180**

Experimental **189**

Chapter 5: Click Chemistry Using Azido and Alkyne Based Lipids Presented in Liposomes: Towards a Chemical Approach for Vesicle Fusion **212**

Background and Significance **212**

Synthesis of Lipids for Vesicle Fusion **213**

Surface Modification of Liposomes via “Click” Chemistry **215**

Attempts at Vesicle Fusion via “Click” Chemistry **222**

Experimental **226**

References **252**

Vita **264**

List of Figures

Figure		*Page*
Figure 1.1	Recruitment of peripheral proteins to the membrane surface	**2**
Figure 1.2	Three sections of the membrane bilayer	**5**
Figure 1.3	Various strategies for the modification of azides	**8**
Figure 2.1	Biosynthetic pathways for DAG	**13**
Figure 2.2	Chemical structure for azido-DAG analogue	**16**
Figure 2.3	Migration of the *sn*-2 acyl chain to the *sn*-3 position	**18**
Figure 2.4	PMB protecting group strategy for obtaining DAG analogues	**18**
Figure 2.5	^{1}H NMR containing migrated side product	**19**
Figure 2.6	TBDPS protecting group strategy for obtaining DAG analogues	**21**
Figure 2.7	DMTr protecting group strategy for obtaining DAG analogues	**23**
Figure 2.8	Deprotection and derivatization of DMTr-azido DAG	**25**
Figure 2.9	Comparison of analogues from PMB and DMTr routes by NMR	**27**
Figure 2.10	Affinity of PKCδ for DAG-containing membranes by SPR	**30**
Figure 2.11	HPLC trace for dansyl-DAG analogue	**52**
Figure 3.1	Biosynthesis of PA	**77**
Figure 3.2	Structures of currently developed PA probes	**81**
Figure 3.3	Conversion of azido-DAG scaffold into azido-PA scaffold	**84**
Figure 3.4	Initial attempts at early installation of phosphate headgroup	**84**
Figure 3.5	Synthesis of protected azido-PA scaffold	**85**

Figure 3.6 Attempts at optimizing the diol protecting group **87**

Figure 3.7 Derivatization and deprotection of PA scaffold to afford PA probes **89**

Figure 3.8 Synthesis of alkyne for development of bifunctional PA probe **91**

Figure 3.9 Failed attempts at the synthesis of bifunctional PA probe **93**

Figure 3.10 Efficient synthesis of a bifunctional PA probe **94**

Figure 3.11 Affinity of PKCα-C2 for PA-containing membranes by SPR **97**

Figure 4.1 Representation of membrane surface **166**

Figure 4.2 Structure of modifiable azido-lipid **170**

Figure 4.3 Synthesis of biotin-TEG-alkyne linker **171**

Figure 4.4 Synthesis of biotin and CBF-funtionalized lipids **173**

Figure 4.5 Immobilization and detection of whole liposomes via biotin anchor **174**

Figure 4.6 Fluorescence measurements after whole liposome immobilization **176**

Figure 4.7 Percent biotin required for efficient immobilization **177**

Figure 4.8 Results of dye leakage immobilization assay **179**

Figure 4.9 Assay for the detection of PKCα binding to whole liposomes **181**

Figure 4.10 Results of PKCα binding to immonilized whole liposomes **182**

Figure 4.11 Synthesis of mannose-lipid **184**

Figure 4.12 Initial results from ConA binding to immobilized liposomes **184**

Figure 4.13 Effects of Mn^{+2} on liposome immobilizations **185**

Figure 4.14 ConA binding following immobilization without Mn^{+2} and Ca^{+2} **187**

Figure 5.1 Structure of modifiable azido-lipid **214**

Figure 5.2 Synthesis of TEG-azido lipid **216**

Figure 5.3 Synthesis of TEG-alkyne lipid **217**

Figure 5.4 Synthesis of NBD and rhodamine lipids **218**

Figure 5.5 Using FRET to detect surface modification after “click” chemistry **220**

Figure 5.6 Fluorescence readings from surface modification experiments **221**

Figure 5.7 “Click” promoted vesicle fusion **223**

Figure 5.8 DLS results from vesicle fusion experiments **225**

List of Tables

Table *Page*

Table 2.1 Percent migration observed from PMB and TBDPS removal **19**

Table 2.2 Percent migration observed from DMTr removal **23**

Table 2.3 Binding properties of PKCδ with DAG analogues **29**

Table 3.1 Binding properties of PKCα-C2 with PA-analogues **96**

List of Abbreviations

p-ABA	*para*-Aminobenzoic acid
ABPP	Activity based protein profiling
AcOH	Acetic Acid
Ag_2O	Silver (I) oxide
Bn	Benzyl
Boc	*tert*-Butoxycarbonyl
Boc_2O	Di-*tert*-butyl dicarbonate
BSA	Bovine serum albumin
5(6)-CBF	5(6)-Carboxyfluorescein
Cbz	Benzyloxycarbonyl
ConA	Concanavalin A
m-CPBA	*meta*-Chloroperoxybenzoic acid
CuBr	Copper (I) bromide
CuI	Copper (I) iodide
CuOTf	Copper (I) triflate
$CuSO_4 \cdot 5H_2O$	Copper (II) sulfate pentahydrate
DAG	Diacylglycerol
DCC	Dicyclohexylcarbodiimide
DCM, CH_2Cl_2	Dichloromethane
DDQ	2,3-Dichloro-5,6-dicyano-1,4-benzoquinone
DGK	Diacylglycerol kinase
DIAD	Diisopropyl azodicarboxylate
DiC_{18}	*sn*-1,2-Dioleoylglycerol
DIEA	Diisopropylethylamine
DLS	Dynamic light scattering
DMAP	4-Dimethylaminopyridine
DMF	*N,N*-Dimethylformamide
DMTr	Dimethoxytrityl
DMTrCl	Dimethoxytrityl chloride
DMTrOH	Dimethoxytrityl alcohol
DPPA	Diphenylphosphoryl azide
DTT	Dithiothreitol
Et_2O	Ethyl ether
Et_3N	Triethylamine
EtOAc	Ethyl acetate

FRET	Förster resonance energy transfer
G3P	Glycerol 3-phosphate
GNL	Galanthus Nivalis Lectin
HA	Hemagglutinin
HCl	Hydrochloric acid
HEPES	(4-(2-Hydroxyethyl)-1-piperazineethanesulfonic acid)
HRP	Horse radish peroxidase
ITC	Isothermal calorimetry
KI	Potassium Iodide
$LiALH_4$	Lithium aluminum hydride
LPA	Lysophosphatidic acid
MeOH	Methanol
MMTr	Monomethoxytrityl
MsCl	Methanesulfonyl chloride
NaCl	Sodium chloride
NaH	Sodium hydride
NaN_3	Sodium azide
NaOH	Sodium hydroxide
NBDCl	4-Chloro-7-nitrobenzofurazan
NMM	*N*-Methylmorpholine
NPE	2-Nitrophenylethyl
OPG	Alcohol protecting group
PA	Phosphatidic acid
PAPs	Phosphatidic acid phosphohydrolases
PC	Phosphatidylcholine
PE	Phosphatidylethanolamine
PG	Phosphatidylglycerol
PIP_ns	Phosphoinositides (n refers to location of phosphates)
PKC	Protein kinase C
PLC	Phospholipase C
PLD	Phospholipase D
PMB	*para*-Methoxybenzyl
PMBCl	*para*-Methoxybenzyl chloride
PMP	*para*-Methoxybenzylidene
POPA	1-Palmitoyl-2-oleoyl-*sn*-glycero-3-phosphatidic acid
POPC	1-Palmitoyl-2-oleoyl-*sn*-glycero-3-phosphocholine
POPE	1-Palmitoyl-2-oleoyl-*sn*-glycero-3-phosphoethanolamine
POPS	1-Palmitoyl-2-oleoyl-*sn*-glycero-3-phosphoserine
PPh_3	Triphenylphosphine

SATE	*S*-Acetylthioethyl
SEC	Size exclusion chromatography
SPR	Surface plasmon resonance
TBAF	Tetrabutylammonium fluoride
TBDPS	*tert*-Butyldiphenylsilyl
TBDPSCl	*tert*-Butyldiphenylsilyl chloride
TEG	Tetraethylene glycol
TFA	Trifluoroacetic acid
THF	Tetrahydrofuran
TMSBr	Bromotrimethylsilane
TsCl	Tosyl chloride
p-TsOH	*p*-Toluenesulfonic acid

Chapter 1: Introduction

Lipids are biological molecules that consist of a polar headgroup, typically a phosphoester, and hydrophobic acyl tails. The lipids align themselves to form a bilayer structure which constitutes the bulk of cellular membranes. Although membrane surfaces may be decorated with a litany of biological molecules, and integral membrane proteins may be embedded within the bilayer, the main components of the membrane are lipids. These lipids are divided into two main classes. Bulk lipids including phosphatidylcholine (PC), phosphatidylethanolamine (PE), and phosphatidylglycerol (PG) account for the majority of the lipid composition, and signaling lipids such as diacylglycerol (DAG), phosphatidic acid (PA), and the phosphoinositides (PIP_ns) account for minor percentages of the lipid composition. It is now known that DAG,[1-5] PA,[5-7] and PIP_ns[8-14] are linked to a litany of crucial cellular events. One particular function involves the docking of peripheral proteins onto membrane surfaces through targeted interactions with a specific signaling lipid(s). These interactions generally regulate the location of proteins within the cell and also regulate their function (figure **1.1**).[2, 3, 15, 16] Biological function of the receptor can be directly regulated through such binding interactions or indirectly regulated, as often times binding of the receptor to another membrane bound protein occurs.[2, 3, 15, 17] These binding interactions also control protein localization within the cell. Since the concentrations and locations of

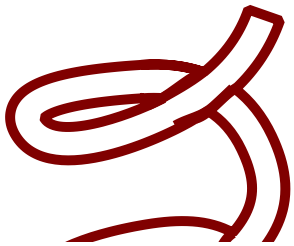

Figure 1.1. Representation of the recruitment of peripheral proteins to the membrane surface through interactions with signaling lipids.

signaling lipids within the cell are closely regulated, lipid-specific receptors can be recruited to specific cellular locations based upon where the lipid is presented.[18] Upon binding to the lipid a signal is sent to the protein. In certain cases, detachment of the protein followed by relocation to a different cellular location allows transfer of that signal to various pathways. Because many of these interactions have been linked to various diseases, it is important to elucidate the exact details of the protein-lipid binding events.

While specific examples will be discussed in detail in relevant chapters, it suffices to say that the actual processes are much more nuanced than depicted in figure **1.1**. Many complex factors are involved and must be characterized in order to decipher the binding mechanism. Such is the case with the protein kinase C (PKC) family. The inability to completely characterize the binding specificity and cellular localization of each isozyme, of which at least eleven are known, has hindered the elucidation of the specific function of each.[19]

One aspect that can complicate determining the binding specifics is the possibility for the receptor to bind to the membrane in a multivalent fashion.[20, 21] In such a case, one must consider that each of the domains may possess identical or varying affinities for the ligand. It is known that within the PKC family, which bind DAG with two tandem domains, the affinity for DAG and molecules that compete for the DAG binding sites vary from isozyme to isozyme as well as between the two domains.[2] Another related factor involves the actual specificity for the lipid by a domain. An example of this presents itself in the study of the PIP_ns. It is well documented that the PIP_ns are targeted not by a specific domain, but instead by a multitude of them including the PH,

FYVE, PX, PROPPIN,[22] ENTH, ANTH, FERM, and Tubby domains.[9, 10, 14] Characterization of binding events between PIP_ns and receptors containing these domains is complicated by varying affinities for each domain, low sequence homologies among some of the domains, and the number of PIP_n isomers, each of which will have different specificities for binding to each type of domain.

Another aspect that deserves consideration when probing binding events is the manner in which the protein interacts with the membrane. The cellular membrane is divided into three sections (figure **1.2**).[2, 23] Initially, the recruitment of the protein to the polar membrane surface is driven primarily by electrostatic interactions, as all membranes contain some amount of anionic phospholipids and most peripheral proteins contain some positive amino acid residues.[2] Other interactions that occur at the polar surface, such as ion-ion and ion-dipole attractions, between signaling lipid and receptor may also be responsible for membrane recruitment,[23] but studies have shown that these initial nonspecific electrostatic interactions are required.[2, 24] Proteins that specifically interact at the polar surface are termed headgroup-driven (S-type)[2] and will generally recognize probes primarily via the headgroup.[10] Following this initial anchoring, other types of interactions may occur, which greatly enhance binding energy leading to full anchoring onto the membrane that in turn regulates activity.[2] For example, proteins that possess hydrophobic and aromatic residues around the binding domain may penetrate into the other regions of the bilayer. Depending upon the depth of the penetration, these proteins are termed I-type (interfacial region) or H-type (hydrophobic core).[2] Interactions at the interfacial region are predominantly ion- dipole

Figure 1.2. The membrane bilayer is divided into three different sections, each with different polarities, and thus, different types of interactions between molecules.

and ionic-hydrogen bonds, while those occurring in the hydrophobic core consist of van der Waals interactions and non-ionic hydrogen bonding.[23] The study of proteins that bind to the membrane via these interactions would require the membrane environment and full lipid analogues when probing the binding event.

Lipid probes have proven to be very useful in scrutinizing these binding events.[14, 25-33] A probe is an analogue of a natural lipid that is tagged with a reporter moiety capable of providing details related to a specific event.[34] When designing the probe, there are several factors that should be considered. First, the lipid probe must be designed in a manner such that it mimics the natural lipid, and the receptor still recognizes it as a ligand. Second, the synthesis should produce the target probes from simple, economically feasible, commercially available, and enantiopure starting materials. While specific examples for manipulation of the headgroup and acyl tails via enzymatic means have been used in the synthesis of lipids and probes,[30, 35-37] they are often expensive, require small scale reaction conditions, limit the variations in the types of probes that can be obtained, and often give rise to a mixture of products instead of a single species. Also, one must determine the most beneficial location for the placement of the reporter molecule, which will allow investigation of the interaction at the molecular level by providing a means for the direct detection of binding. Attaching it directly to the headgroup could greatly interfere with binding. If it is incorporated into the tail, it must be non-polar such that it remains embedded within the hydrophobic membrane core. The other potential location for a modification to be made is in place of a hydrogen at the *sn*-1 position. This has rarely been pursued due to the synthesis and manipulation of

functional groups required to readily place a synthetic handle at this location.[32] However, this site could be a very appealing location for modifying the lipid structure as it places the reporter molecule in proximity of the headgroup to allow for a more sensitive detection of binding, yet as far away as possible from the phosphodiester binding motif.

One of the main goals in lipid probe design is to produce analogues via a process that is as efficient as possible. Many synthetic procedures for lipid probes require the full synthesis to be carried out for each probe.[14, 25, 26, 28-33] Therefore, a modular approach is beneficial as it allows for the synthetic generation of a common lipid precursor followed by the ability to efficiently modify this scaffold in order to obtain an arsenal of probes of use for different studies. The key to developing a modular approach is the incorporation of a synthetic handle that is stable under most conditions, yet reacts efficiently via a specific reaction. The azide functionality has become a popular choice as a synthetic handle due its ability to meet these requirements.

Azides are relatively small, so they pose no steric limitations for remaining synthetic steps. They are fairly stable under acidic and basic conditions, and at moderate temperatures, yet they efficiently react through the copper-catalyzed 1,3-dipolar cycloaddition ("click" chemistry),[38-40] as shown in figure **1.3**. "Click" chemistry has become increasingly popular since its discovery for several reasons. First, it is carried out under very mild conditions. Second, the reaction is specific for the azide and alkyne, thereby increasing the efficiency of the reaction and decreasing the amount of side reactions. Lastly, the reaction is bio-orthogonal. Azides and alkyne generally do

Figure 1.3. Various chemical reactions for the modification of azides that can be used to functionalize lipids to generate probes.

not react with species found within the cell, which maintains the high selectivity of the reaction when carried out *in vivo*.

Azides can also be efficiently modified via the Staudinger ligation,[41-43] which is also a bio-orthogonal reaction (figure **1.3**). The conditions are not as mild as those for the "click" reaction, so certain functionalities may not be as tolerant of this modification strategy. Azides can also be used as a masking group for amines, generating the amine upon reduction (figure **1.3**).[44] Using these approaches, a variety of reporter molecules can be incorporated onto the lipid structure at various locations through single step manipulation of the azide synthetic handle.

The use of a fluorescent tag as the reporter molecule is a popular strategy among previously reported lipid probes.[34] For example, Schultz and coworkers have developed a probe containing alkyne functionalities in the lipid tails.[45] The lipid was incorporated into living cells and, following the attachment of a fluorophore via "click" chemistry, distribution of the probe within cellular membranes was monitored.

The use of fluorescence to monitor binding events can be taken one step further. Förster resonance energy transfer (FRET) is a radiationless energy transfer from an excited donor molecule to an acceptor molecule through long-range (10–100 Å) dipole-dipole couplings.[46-48] Thus, FRET is a useful technique for detecting changes in proximity between the donor and acceptor, as it is highly dependent upon the distance between them. The closer the donor is to the acceptor, the more FRET is observed and vice versa. The effectiveness of this approach is evidenced through the work of Swanson and co-workers.[49, 50] Here, a FRET based approach was used to detect and

monitor the multivalent binding of cholera toxin to gangliosode GM1.

Another approach to investigating protein-lipid binding is photoaffinity labeling.[51] In this application, tags are incorporated that generate highly reactive species, such as radicals or carbenes, upon exposure to light. These reactive intermediates then form a covalent bond to the lipid-bound receptor. Prestwich and co-workers have developed a series of photoaffinity probes, designed around the phosphoinositides, capable of interacting with various PIP receptors.[14, 26, 31, 33] Photoaffinity labeling can also be extended to protein profiling, a method in which a series of proteins that target a specific lipid are fished out of a complex mixture of proteins.[27] Here, cross-linking is coupled with a secondary tag that allows purification or detection of the receptor-ligand complex. Ultimately, both processes can be used for the identification of new receptors and in mapping the sequence of the binding domain.

One final tag that is of great importance in lipid probes is biotin. Due to its tight binding to the protein streptavidin ($K_d \approx 10^{-15}$ M),[52] biotin can be used to purify conjugates away from species not tagged with the biotin, as in protein profiling. The incorporation of biotin onto lipids has also proven useful for the immobilization of liposomes onto an avidin coated surface.[52-56]

The work presented within this dissertation is focused around two common themes. First, the design, synthesis, and evaluation of signaling lipid probes will be explored. Each family of probe will be accessed from a common scaffold bearing an azide. “Click” chemistry will then be used to functionalize the probes with a litany of reporter molecules. Receptors that target the natural lipid will be used to determine how

effective our probes serve as a mimic of the natural lipid. Analogues that exhibit comparable binding constants as the natural ligand will be used in further investigation of the binding event. Second, unnatural lipids accessed from a modular azido-scaffold will be synthesized and used in the development of techniques such as microplate binding assays via liposome immobilization and a specific, chemically promoted vesicle fusion system.

Chapter 2: Synthesis, Functionalization, and Biological Evaluations of Azide–Labeled Diacylglycerol (DAG) Analogues for the Modular Access to Lipid Probes

Background and Significance

Diacylglycerol (DAG) is a glycerolipid that contains two fatty acid tails at the *sn*-1 and *sn*-2 positions and a primary hydroxyl group at the *sn*-3 as shown in figure **2.1**. Most of the DAG present in the cell arises from lysophosphatidic acid (LPA) (figure **2.1**).[1] Following acylation of LPA to furnish phosphatidic acid (PA), PA phosphohydrolases (PAPs) transform PA into DAG. The enzymes phospholipase C (PLC) and phospholipase D (PLD) are both involved in DAG production via hydrolysis of phospholipids, although these are not mainstream routes for the generation of DAG (figure **2.1**). Despite its simplistic structure, DAG has been linked to various diseases such as diabetes[57] and cancer.[19, 58] In order to learn exactly how DAG is involved in the generation or promotion of such diseases, the details that govern the binding of receptors to DAG need to be understood.

A well studied class of DAG receptors is the protein kinase C (PKC) family of proteins. PKC enzymes bind to DAG producing a direct relationship between binding and action.[59] There are at least eleven different isozymes of PKC and three classes of PKC enzyme, each of which bind DAG in a unique fashion. Conventional PKC enzymes are dependent upon calcium, DAG, and anionic phospholipid. Novel PKC enzymes are

Figure 2.1. Biosynthesis of DAG adapted from ref **1**. Major pathways are indicated with red reaction arrows. Minor pathways that produce DAG that is not consumed for metabolic purposes are indicated with blue reaction arrows.

dependent upon the presence of DAG and anionic phospholipid, but require no calcium for binding. Atypical PKC enzymes are DAG, calcium and phospholipid independent.[1-4, 59] In order to bind DAG, PKC enzymes require two cysteine-rich, highly conserved (C1) domains. Conventional and novel PKC enzymes bind DAG using two C1 domains, denoted C1A and C1B. In addition to the tandem C1 domains, conventional and novel PKC enzymes contain a conserved 2 (C2) domain. C2 domains recognize anionic phospholipids on the membrane surface, to which they are attracted to through electrostatic interactions.[2] In order for C2 domains of conventional PKC enzymes to bind the anionic phospholipid, calcium must be present. The C2 domains of novel PKC enzymes bind to the anionic phospholipid without calcium. Atypical isozymes only contain a single C1 domain and therefore do not bind DAG or its analogues.[59]

PKCs have long been known to play a role in tumorigenesis.[19, 58, 60] Deciphering this role is a daunting task due to the number of isozymes, each of which play various, and often opposing, roles in cellular pathways. A current hypothesis is that subtle differences in binding patterns between isozymes promote their different and distinct cellular locations.[3, 16] In turn, these variations in cellular location govern their involvement in specific pathways. The binding mechanism is further complicated by the multivalent interactions discussed above, which allow variations in affinity and specificity to occur between isozymes. For example, PKCε and PKCγ both contain C1 domains that bind DAG with high affinity at each domain.[2] PKCα and PKCδ, on the other hand, tightly bind DAG with only their C1A domain.[61] Anionic lipid specificities also arise as some isozymes prefer phosphatidylserine (PS) while others prefer PA.[62, 63] The complex

nature of these events requires DAG-based probes that will provide the ability to investigate association at the molecular level so as to actually detect and monitor the binding event.

Synthetic Procedures for DAG Analogues

Although synthetic lipid probes have been utilized to scrutinize protein–lipid binding events,[14, 25-33] these investigations are often limited by the lack of an efficient synthesis of each probe. Due to the absence of a modular approach in many of the syntheses, obtaining a library of probes requires that each probe be synthesized in an individual manner, rather than through the derivatization of a common scaffold. Therefore, we sought to design a lipid scaffold containing a versatile, reactive tag that could be functionalized at a late stage in the synthesis in order to obtain a family of DAG-based probes. The choice of an appropriate reactive tag is crucial, as the tag modification must be tolerant of the other functional groups present in the lipid structure. For this purpose we chose to incorporate an azide functionality at the *sn*-1 position. The azide is a bio-orthogonal species that is easily modified via the 1,3-dipolar cycloaddition ("click" chemistry),[38-40] a strategy that will not interfere with the core structure of the lipid.

The initial azido-DAG target is represented by lipid **2.2.1** (figure **2.2**). This compound not only serves as a scaffold for obtaining other, more complex probes through manipulation of the azide but can itself serve as a probe for the investigation of binding events.

Figure 2.2. Structure of initial azido-DAG target compound.

Before embarking on the actual synthesis of **2.2.1**, there was one aspect that warranted consideration in the synthetic design. The migration of the *sn*-2 acyl chain to the *sn*-3 position is a common occurrence in lipid synthesis (figure **2.3**). The migration is known to be catalyzed via both acid and base mechanisms, as well as facilitated by prolonged exposure to silica gel.[64] Therefore, deprotection of the *sn*-3 hydroxyl group must be done in a manner so as to avoid migration. Side reactions of the deprotection should also be minimized, as silica chromatography, which would be needed to purify the final product, must be performed rapidly. Ultimately three different approaches were designed and each carried out in order to obtain **2.2.1** and analogues thereof.

The initial approach utilized the commercially available C_2 symmetric tartrate **2.4.2** as shown in figure **2.4**. Following modified a literature procedure[65] the diol of **2.4.2** was protected with an acetonide to furnish **2.4.3** and subsequently reduced to generate bis-hydroxymethyl compound **2.4.4**. Mono *p*-methoxybenzyl (PMB) protection of **2.4.4** furnished known alcohol **2.4.5**,[66] which was converted to azide **2.4.6** via a Mitsunobu reaction. The acetonide protecting group was removed under acidic conditions to yield diol **2.4.7**. Stearic acid was coupled to the hydroxyl groups to furnish the PMB-protected azido DAG **2.4.8a**. Oxidative removal of the PMB protecting group to afford **2.2.1**, however, also yielded migration byproduct **2.2.1a,** as observed in the proton NMR (figure **2.5**, table **2.1**). Although this reaction has been used to produce a primary alcohol on a similar lipid structure with no reports of migration,[32] when used in our synthesis, **2.2.1a** was always produced as a byproduct. Previous accounts using this reaction to produce DAG-based structures were carried out in systems that contained

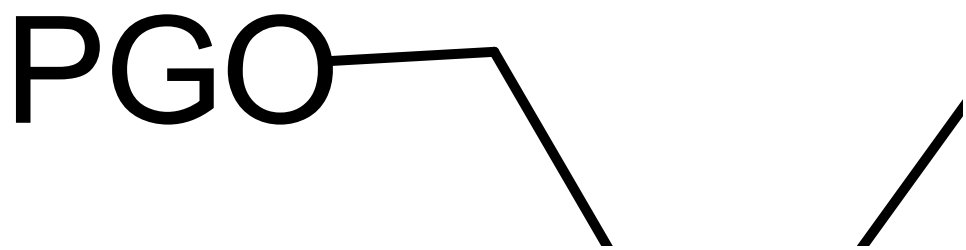

Figure 2.3. Migration of the *sn*-2 acyl chain upon removal of the *sn*-3 protecting group.

Figure 2.4. Synthesis of **2.2.1** via PMB protecting group route.

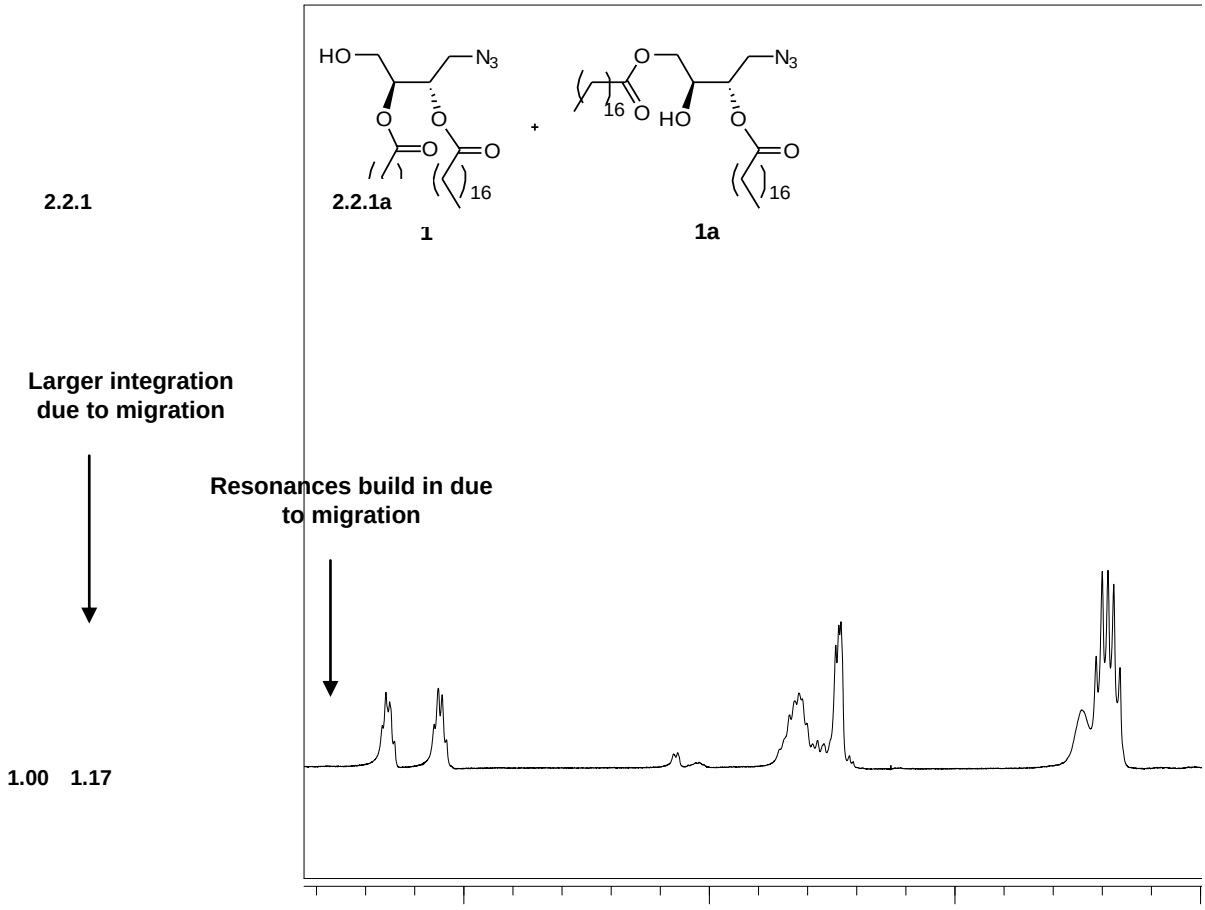

Figure 2.5. ^{1}H NMR of mixture of **2.2.1** and **2.2.1a** obtained after PMB deprotection.

Table 2.1. Percentages of **2.2.1** and **2.2.1a** based upon analysis of ^{1}H NMR spectra following PG removal.

Protecting Group (PG)	Method of Deprotection	% 2.2.1	% 2.2.1a
PMB (**2.4.8a**)	Wet DDQ	85%	15%
TBDPS (**2.6.8b**)	TBAF	0%	100%
TBDPS (**2.6.8b**)	TBAF/AcOH	83%	17%

no modification at the *sn*-1position. We reasoned that replacing a hydrogen atom with the azido methyl may lead to the observed migration due to an increase in sterics.

In an attempt to circumvent the migration of the *sn*-2 acyl chain to the *sn*-3 position, a synthesis utilizing a silyl protecting group for the *sn*-3 hydroxyl group was designed as shown in figure **2.6**. It is documented that removal of a silyl protecting group leads to reduced acyl migration in lipid synthesis.[67] Mono *tert*-butyldiphenylsilyl (TBDPS) protection of **2.4.4** furnished **2.6.9**[68, 69] which was then converted to azide **2.6.10** via Mitsunobu conditions. The acetonide was removed under acidic conditions to provide diol **2.6.11,** and coupling with stearic acid under standard ester forming conditions afforded TBDPS-protected azido DAG **2.6.8b**. Removal of the silyl group was attempted via two forms of tetrabutylammonium fluoride (TBAF) deprotection as shown in table **2.1**. Deprotection using only TBAF facilitated complete conversion to the migrated product **2.2.1a**. While this could be reduced by addition of acetic acid (AcOH),[67, 70] the percentage of migrated product present was comparable to that observed in the PMB-protection approach.

These results indicate that the addition of the azidomethyl group at the *sn*-1 position is responsible, at least in part, for the increased observance of migrated product, as we had originally theorized. Increasing the steric bulk at this position would promote the tendency for migration to occur for several reasones. First, migration would greatly alleviate steric strain in the molecule caused by having the azidomethyl group and the two large acyl chains in proximity. Second, the effective molarity of the migration reaction would be rather large, as the reaction is intramolecular. Also, the

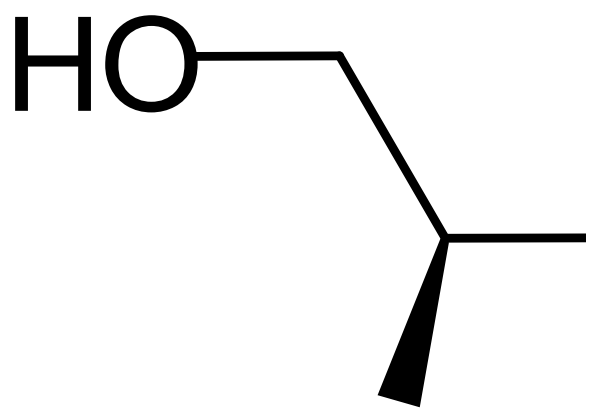

Figure 2.6. Synthesis of **2.2.1** via TBDPS protecting group route.

removal of PMB and TBDPS groups occurs via basic mechanisms, which are also known to promote migration. The observation that both DDQ and TBAF neutralized with AcOH deprotections provided similar amounts of migrated product further indicates that some factor other than reaction conditions causes increased susceptibility of our system to furnish the migrated byproduct.

At this stage we sought to design a synthesis utilizing a protecting group that could be removed very rapidly and under very mild conditions. Finally, the dimethoxytrityl (DMTr) protecting group was decided upon. This protecting group has been used in the protection of *sn*-3 hydroxyl groups,[71] and is known to be removed under mildly acidic conditions.[72] The synthesis for the DMTr protected scaffold is outlined in figure **2.7**. Monotosylation of compound **2.4.4** furnished **2.7.12**, which was directly converted to the azide **2.7.13**.[65, 73] Normally *sn*-3 the hydroxyl protecting group would be introduced at this point, but the DMTr would not survive the acidic conditions necessary to remove the acetonide. However, DMTr is selective for primary alcohols.[72] Therefore, acidic deprotection of the acetonide was used to access known azido-triol **2.7.14**,[74] which was then converted to the DMTr compound **2.7.15**. Introduction of stearate acyl tails using traditional ester forming conditions afforded DMTr-protected azido DAG **2.7.8c**. A monomethoxytrityl (MMTr) analogue **2.7.8d** was also synthesized, but ultimately, the DMTr synthesis was more efficient.

After obtaining compounds **2.7.8c** and **2.7.8d**, a series of deprotection conditions were carried out as shown in table **2.2**. Initially, MMTr deprotection with *p*-toluenesulfonic acid (*p*-TsOH) furnished only migrated product **2.2.1a**. DMTr removal

Figure 2.7. Synthesis of DMTr-protected azido DAG analogues.

Table 2.2. Deprotection conditions for the trityl-protected azido DAG analogues.

Protecting Group (PG)	**Method of Deprotection**	**% 2.2.1**	**% 2.2.1a**
MMTr (**2.7.8d**)	*p*-TsOH	0%	100%
DMTr (**2.7.8c**)	AcOH/*p*-ABA or pyrrole	98%	2%
DMTr (**2.7.8c**)	$Cl_2HCCOOH$	0%	100%
DMTr (**2.7.8c**)	AcOH/*p*-ABA or pyrrole; direct "click"	>99.5%	<0.5%

using dichloroacetic acid was attempted but also resulted in only **2.2.1a** being obtained. Since a scavenger for the DMTr carbocation is always needed,[75] and since the DMTr can be removed under milder conditions, a system of AcOH and pyrrole as the scavenger was utilized. Proton NMR analysis of the crude reaction mixture indicated no migration had occurred during the course of the reaction. After rapid chromatography, a mixture of **2.2.1** and **2.2.1a** was obtained. Based upon NMR analysis, approximately 2% of **2.2.1a** was present in the mixture. However, due to the rapid elution, reaction byproducts such as dimethoxytritylmethanol (DMTrOH) and the DMTr-pyrrole adduct were also recovered. More careful purification led to increased migration due to prolonged exposure to the silica gel. *p*-Aminobenzoic acid (*p*-ABA) was in turn used as the cation scavenger. It was reasoned that the carboxylate would prevent co-elution of the DMTr-*p*-ABA adduct, however, the DMTrOH still co-eluted with **2.2.1**, and the NMR analysis for migration was similar to that observed with AcOH/pyrrole. While these results were drastically improved as compared to those observed with PMB and TBDPS synthetic routes, we still sought to develop a system that furnished no detectable migration.

It was discovered that while the byproducts of the DMTr deprotection hinder purification of **2.2.1**, they can be readily removed after “click” modification of **2.2.1**. In order to achieve this, **2.7.8c** was deprotected using AcOH/pyrrole and subsequent “click” reactions were carried out using a variety of functionalized alkynes, as shown in figure **2.8**. The mild reaction conditions of the azide-alkyne cycloaddition did not promote any migration, as determined by proton NMR analysis of the reaction prior to

Figure 2.8: Derivatization of **2.7.8c** via deprotection and direct “click” reaction.

silica chromatography. The incorporation of the triazole ring also facilitated the purification of the final compounds. The aforementioned byproducts are considerably less polar than the functionalized product. Therefore, they are efficiently separated from the final compounds allowing rapid purification and minimal exposure to the silica. All final compounds were obtained in >99.5% **2.2.1** as analyzed by ^{1}H NMR. The ^{1}H NMR spectra of benzophenone analogue **2.8.16e** obtained from the PMB route and from the DMTr route are shown in figure **2.9** as a comparison for the amount of migration produced by the two procedures.

"Click" chemistry functionalization utilized a series of fluorescent (**2.8.17a–d**) and photoaffinity (**2.8.17e**) alkynes, which were accessed in one step from propargyl amine, to furnish the DAG analogues **2.8.16a–e**. The fluorescent analogues (**2.8.16a–d**) were designed so as to include various FRET donors and acceptors. These probes will be utilized to study the multivalent interactions of DAG receptors. As FRET is highly dependent upon distance, any change in the proximity of the donor and acceptor upon binding should be visualized by monitoring the fluorescence signals. This will provide valuable insight as to how the receptor interacts not only with the ligand, but also the membrane. DAG probe **2.8.16e** was functionalized with a benzophenone to serve as a photoaffinity label. This probe will be used towards the process of mapping the binding domains of new DAG receptors.

PMB Route

DMTr Route

Figure 2.9: ^{1}H NMR comparison of analogue **2.8.16e** obtained through the PMB and DMTr synthetic routes. Only the region containing resonances corresponding to migration are shown.

Biological Evaluation of DAG Analogues

Having developed a series of DAG analogues, we next sought to determine how effective each probe would be in the monitoring of DAG-binding events. In order to analyze this, we monitored the binding of each analogue with PKCδ, a well known DAG receptor. In collaborative efforts with Dr. Robert Stahelin, surface plasmon resonance (SPR) equilibrium binding analysis was performed. Vesicles composed of 1-palmitoyl-2-oleoyl-*sn*-glycero-3-phosphocholine (POPC), 1-palmitoyl-2-oleoyl-*sn*-glycero-3-phosphoserine (POPS), and DAG (78:20:2, respectively) were used as an active binding surface alongside vesicles containing only POPC as a control. *sn*-1,2-Dioleoylglycerol (DiC_{18}) served as a reference standard, as binding of PKCδ to vesicles containing this lipid are well documented.[61] Liposomes containing DiC_{18} bound PKCδ with a K_d of 24nM as indicated in table **2.3** and figure **2.10**. In identical fashion, DAG analogues **2.8.16a–e** were incorporated into vesicles with POPC and POPS, and their ability to bind PKCδ was analyzed. Naphthyl analogue **2.8.16a** displayed the lowest K_d (16 nM) and the 5(6)-carboxyfluorescein analogue **2.8.16d** displayed the highest (28 nM). However, the K_d values, as well as the binding isotherms, indicate that each DAG probe can effectively bind this DAG receptor. This data also confirms that the *sn*-1 position is an acceptable location for the placement of a reporter molecule. The tag is placed as close to the binding motif as possible to facilitate optimal detection, yet still far enough away so as not to deter the binding event.

Table 2.3. Binding properties of PKCδ with different DAG analogues.

Lipid	K_d (nM) using POPC/POPS/DAG (78:20:2)
DiC_{18}	24 ± 4
Synthetic DiC_{18}	19 ± 2
Naphthyl-DAG (**2.8.16a**)	16 ± 3
Dansyl-DAG (**2.8.16b**)	20 ± 3
Coumarin-DAG (**2.8.16c**)	18 ± 2
5(6)-CBF DAG (**2.8.16d**)	28 ± 5
Benzophenone-DAG (**2.8.16e**)	21 ± 3

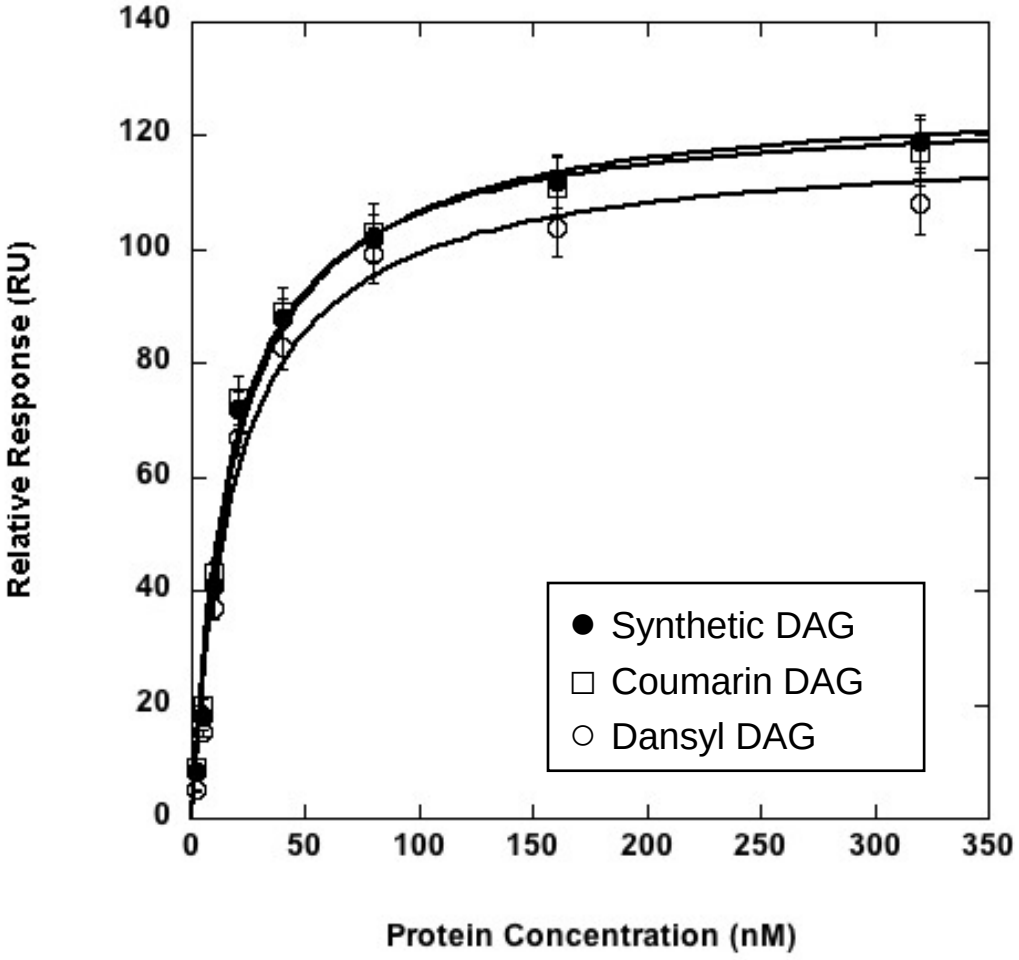

Figure 2.10. Affinity of PKCδ for DAG-containing membranes determined by SPR analysis. SPR measurements were used to determine K_ds of PKCδ for POPC/POPS/DAG (78:20:2) vesicles where DAG represents synthetic DAGs reported above. PKCδ was injected at varying concentrations at a flow rate of 5 μL/min and the subsequent association and dissociation were monitored. From these plots, the saturation response (R_{eq}, equilibrium value) was determined. In order to calculate the K_d of PKCδ for the DAG containing vesicles, the equilibrium value (saturating response (R_{eq}) of protein bound) determined from each sensorgram was then plotted versus respective protein concentration (2, 5, 10, 20, 40, 80, 160, and 320 nM). The solid lines represent theoretical curves constructed from R_{max} and K_d values determined by nonlinear least squares analysis of the isotherms using $R_{eq} = R_{max}/(1 + K_d/C)$.

Experimental

General Considerations

All reagents were purchased from Aldrich or Acros and used as received. Dry solvents were obtained from a Pure Solv solvent delivery system purchased from Innovative Technology, Inc. Column chromatography was performed using 230 - 400 mesh silica gel purchased from Sorbent Technologies. NMR spectra were obtained using a Bruker AC250 spectrometer updated with a TecMag data collection system, a Varian Mercury 300 spectrometer, and a Bruker Avance 400 spectrometer. Mass spectra were obtained with JEOL DART-AccuTOF spectrometer with high resolution capabilities. Optical rotation values were obtained using a Perkin-Elmer 241 polarimeter. HPLC data was obtained using an HP series 1100 HPLC with an Alltech Lichrosphere SI 60 5U column with HPLC grade solvents purchased from Fisher. 1-Palmitoyl-2-oleoyl-*sn*-glycero-3-phosphocholine (POPC), 1-palmitoyl-2-oleoyl-*sn*-glycero-3-phosphoserine (POPS), and *sn*-1,2-dioleoylglycerol (DiC_{18}) were purchased from Avanti Polar Lipids, Inc. (Alabaster, AL).

Experimental Procedure for the PMB Protection Synthesis

((4S,5S)-2,2-Dimethyl-1,3-dioxolane-4,5-diyl)dimethanol (2.4.4). A solution of diethyl-L-tartrate **2.4.2** (6.76 mL, 39.5 mmol) and *p*-toluenesulfonic acid (128 mg, 0.672 mmol) in benzene (80 mL) was prepared in a flame-dried round-bottom flask. To the solution was added with stirring 2,2-dimethoxypropane (6.03 mL, 48.6 mmol). The solution was heated to 80 °C for 3 h and the azeotrope was collected in a Dean-Stark trap. The

solution was allowed to cool to room temperature, at which point sodium carbonate (200 mg, 1.89 mmol) was added and stirring was continued for 2 h. The solution was filtered and concentrated on a rotary evaporator to yield crude **2.4.3**.

A solution of lithium aluminum hydride (3.0 g, 79 mmol) in anhydrous THF (70 mL) was prepared in a flame-dried, 3-neck round-bottom flask. The suspension was cooled to 0 °C and kept under nitrogen. The crude mixture containing **2.4.3** was dissolved in anhydrous THF (20 mL) and added dropwise to the reaction over 30 minutes. The reaction mixture was stirred at 0 °C for 1 h, then at room temperature for 1 h and was then cooled back to 0 °C. The reaction was quenched by the dropwise addition of 3 mL water, 3 mL of 10% NaOH, and 9 mL more of water. Vigorous stirring was continued for 20 minutes while the mixture returned to room temperature. Anhydrous magnesium sulfate was added with stirring for 1 h to dry the reaction. The reaction was filtered and the solvent was removed by rotary evaporation. Column chromatography with silica gel and a gradient solvent system of 3 to 5% methanol/dichloromethane afforded **2.4.4** as a clear oil (4.5 g, 70% over 2 steps).

Characterizations matched previous reports.[65]

^{1}H NMR (250 MHz, $CDCl_3$) δ 4.02–4.00 (m, 2H), 3.83–3.71 (m, 4H), 2.49–2.45 (m, 2H), 1.44 (s, 6H)**.**

((4S,5S)-5-((4-Methoxybenzyloxy)methyl-2,2-dimethyl-1,3-dioxolan-4-yl)methanol (2.4.5). A modified literature procedure was used to prepare **2.4.5**.[66] A solution of sodium hydride (162 mg, 4.06 mmol, 60% purity) in anhydrous DMF (20 mL) was

prepared in a flame-dried round-bottom flask under nitrogen and cooled to 0 °C with stirring. Diol **2.4.4** (658 mg, 4.06 mmol) was dissolved in anhydrous DMF (20 mL) and added dropwise. Stirring was continued at 0 °C for 10 min and then at room temperature for 20 min. At this point the reaction mixture was cooled to 0 °C and 4-methoxybenzyl chloride (606 µL, 4.47 mmol) was added dropwise. The mixture was then stirred at room temperature overnight. The reaction was quenched with ~50 mL water, and the mixture was extracted with dichloromethane (2 x 50 mL). The organic layer was then dried with magnesium sulfate and filtered, and the solvent was removed by rotary evaporation. Column chromatography with silica gel and a gradient solvent system of 20 to 60% ethyl acetate/hexanes afforded **2.4.5** as a clear oil (908 mg, 79%). ^{1}H NMR (300MHz, $CDCl_3$) δ 7.24 (d, *J* = 8.7 Hz, 2H), 6.87 (d, *J* = 8.7 Hz, 2H), 4.56–4.47 (m, 2H), 4.05–3.99 (m, 1H), 3.94–3.88 (m, 1H), 3.79 (s, 3H), 3.78–3.63 (m, 3H), 3.54–3.49 (m, 1H), 2.56–2.52 (m, 1H), 1.41 (s, 6H); ^{13}C NMR (62.9 MHz, $CDCl_3$) δ 159.4, 129.6, 129.5, 113.9, 109.3, 79.8, 76.5, 73.4, 70.1, 62.5, 55.2, 27.0; HRMS $[M-H]^+$ calcd: 281.13890, found: 281.13718.

(4S,5S)-4-(Azidomethyl)-5-((4-methoxybenzyloxy)methyl)-2,2-dimethyl-1,3-dioxolane (2.4.6). Alcohol **2.4.5** (589 mg, 2.09 mmol) was dissolved in dry THF (15 mL) along with triphenylphosphine (1.096 g, 4.18 mmol). The solution was placed under nitrogen and diisopropyl azodicarboxylate (810 µL, 4.18 mmol) was added with stirring. Diphenylphosphoryl azide (901 µL, 4.18 mmol) was dissolved in dry THF (5 mL) and added to the reaction, which was then stirred overnight at room temperature. The

solvent was removed with a rotary evaporator, and column chromatography with silica gel and a gradient solvent system of 10 to 20% ethyl acetate/hexanes afforded **2.4.6** as a clear oil (507 mg, 79%).

^{1}H NMR (300 MHz, $CDCl_3$) δ 7.23 (d, *J* = 8.6 Hz, 2H), 6.87 (d, *J* = 8.6 Hz, 2H), 4.53–4.45 (m, 2H), 4.06–3.96 (m, 2H), 3.79 (s, 3H), 3.63–3.47 (m, 3H), 3.30–3.24 (m, 1H), 1.45 (s, 3H), 1.41 (s, 3H); ^{13}C NMR (75 MHz, $CDCl_3$) δ 159.4, 129.8, 129.3, 113.8, 109.9, 78.1, 76.5, 73.2, 69.9, 55.2, 52.0, 27.0, 26.8; HRMS $[M\text{-}N_2+H]^+$ calcd: 280.15488, found: 280.15483.

(2S,3S)-1-Azido-4-(4-methoxybenzyloxy)butane-2,3-diol (2.4.7). Compound **2.4.6** (820 mg, 2.67 mmol) was dissolved in THF (14 mL) and 1 N HCl (14 mL) was added. The reaction was stirred at room temperature for 48 h and was then quenched with saturated sodium bicarbonate. The mixture was then diluted with water (50 mL) and extracted with dichloromethane (2 x 50 mL). The organic layer was then dried with magnesium sulfate and filtered, and the solvent was removed by rotary evaporation. Column chromatography with silica gel and a gradient solvent system of 50 to 90% ethyl acetate/hexanes afforded **2.4.7** as a clear oil (627 mg, 88%).

^{1}H NMR (250 MHz, $CDCl_3$) δ 7.23 (d, *J* = 8.5 Hz, 2H), 6.88 (d, *J* = 8.5 Hz, 2H), 4.50–4.40 (m, 2H), 3.79 (s, 3H) 3.79–3.72 (m, 2H), 3.55–3.53 (m, 2H), 3.37–3.33 (m, 2H), 3.19 (*b* s, 1H), 3.06 (*b* s, 1H); ^{13}C NMR (62.9 MHz, $CDCl_3$) δ 159.5, 129.6, 129.5, 114.0, 73.3, 71.7, 71.3, 70.2, 55.3, 53.6; HRMS $[M\text{-}N_2+H]^+$ calcd: 240.12358, found: 240.12340.

(2S,3S)-1-Azido-4-(4-methoxybenzyloxy)butane-2,3-diyl distearate (2.4.8a). Diol **2.4.7** (375.2 mg, 1.40 mmol) was dissolved in anhydrous dichloromethane (15 mL). With stirring was added stearic acid (1.194 g, 4.2 mmol), 4-dimethylaminopyridine (188 mg, 1.54 mmol), and *N,N*-dicyclohexylcarbodiimide (866 mg, 4.2 mmol). The reaction was stirred at room temperature for 3 h at which point it was filtered. Column chromatography with silica gel and a gradient solvent system of 0 to 10% ethyl acetate/hexanes afforded **2.4.8a** as a white solid (1 g, 89%).

^{1}H NMR (300 MHz, $CDCl_3$) δ 7.22 (d, *J* = 8.7 Hz, 2H), 6.87 (d, *J* = 8.7 Hz, 2H), 5.34–5.29 (m, 1H), 5.25–5.20 (m, 1H), 4.49–4.37 (m, 2H), 3.80 (s, 3H), 3.52–3.44 (m, 3H), 3.37–3.31 (m, 1H), 2.34–2.29 (m, 4H), 1.63–1.58 (m, 4H), 1.25 (*b* s, 56H), 0.88 (t, *J* = 6.8 Hz, 6H); ^{13}C NMR (75 MHz, $CDCl_3$) δ 172.9, 172.8, 159.4, 129.5, 129.46, 113.9, 73.0, 70.59, 70.55, 67.5, 55.2, 51.0, 34.3, 34.2, 32.0, 29.73, 29.69, 29.5, 29.4, 29.3, 29.2, 25.0, 24.9, 22.7, 14.1; HRMS $[M\text{-}N_2+H]^+$ calcd: 772.64551, found: 772.64821.

(2S,3S)-1-Azido-4-hydroxybutane-2,3-diyl distearate (2.2.1). Compound **2.4.8a** (592 mg, 0.740 mmol) was dissolved in dichloromethane (7 mL) and 2,3-dichloro-5,6-dicyano-1,4-benzoquinone (DDQ) (410 mg, 1.81 mmol) and water (700 µL, 10%) were added with stirring. Stirring was continued at room temperature for 6 h at which point the reaction was quenched with saturated sodium bicarbonate. The reaction mixture was extracted with dichloromethane (2 x 50 mL), and the organic layer was dried with magnesium sulfate and filtered. The solvent was then removed by rotary evaporation. The crude product was placed on a high vacuum line overnight to assist in the removal

of volatile side products. Column chromatography with silica gel and a gradient solvent system of 0 to 20% ethyl acetate/hexanes afforded **2.2.1** and **2.2.1a** as white solids (426 mg, 85% combined).

Experimental Procedures for the TBDPS Protection Synthesis

((4S,5S)-5-((*tert*-butyldiphenylsilyloxy)methyl-2,2-dimethyl-1,3-dioxolan-4-yl)methanol (2.6.9). Compound **2.4.4** (700 mg, 4.32 mmol) was dissolved in anhydrous THF (7.5 mL) and added dropwise to a solution of NaH (173 mg, 4.32 mmol, 60% purity) in anhydrous THF (7.5 mL) at 0 °C under a nitrogen atmosphere. Sitrring was continued at that temperature for 30 minutes at which time *tert*-butyldiphenylsilyl chloride (1.12 mL,4.32 mmol) was added. Stirring was continued for 30 minutes and the reaction was quenched with water (30 mL). The product was extracted with ethyl acetate, dried with magnesium sulfate, and concentrated under reduced pressure. Column chromatography with silica gel and a gradient solvent system of 20 to 40% ethyl acetate/hexanes afforded **2.6.9** as a colorless oil (1.380 g, 80%).

Characterization matches previous reports.[68, 69]

^{1}H NMR (300 MHz, $CDCl_3$) δ 7.74–7.68 (m, 4H), 7.45–7.39 (m, 6H), 4.17–4.10 (m, 1H), 4.04–3.98 (m, 1H), 3.89–3.77 (m, 2H), 3.70–3.66 (m, 1H), 2.61 (*b* s, 1H), 1.45 (s, 3H), 1.43 (s, 3H), 1.10 (s, 9H).

(4S,5S)-4-(Azidomethyl)-5-((*tert*-butyldiphenylsilyloxy)methyl)-2,2-dimethyl-1,3-dioxolane (2.6.10). To a solution of alcohol **2.6.9** (440 mg, 1.1 mmol) in anhydrous THF

(12 mL) at room temperature was added diisopropyl azodicarboxylate (426 µL, 2.2 mmol) and triphenylphosphine (577 mg, 2.2 mmol). Diphenylphosphoryl azide (474 µL, 2.2 mmol) was dissolved in dry THF (3 mL) and added to the reaction which was stirred overnight at room temperature. After the reaction was complete the mixture was concentrated under reduced pressure and column chromatography with silica gel and a gradient solvent system of 0 to 10% ethyl acetate/hexanes afforded **2.6.10** as a pale yellow oil (380 mg, 81%).

$[\alpha]_D^{296K}$ -25.97 (c = 1.155, $CHCl_3$); ^{1}H NMR (300 MHz, $CDCl_3$) δ 7.71–7.66 (m, 4H), 7.49–7.39 (m, 6H), 4.20–4.15 (m, 1H), 4.02–3.96 (m, 1H), 3.87–3.73 (m, 2H), 3.63–3.57 (m, 1H), 3.33–3.27 (m, 1H), 1.48 (s, 3H), 1.42 (s, 3H), 1.09 (s, 9H); ^{13}C NMR (75 MHz, $CDCl_3$) δ 135.5, 132.9, 132.8, 129.9, 129.8, 127.8, 109.7, 78.0, 77.6, 64.0, 52.2, 27.0, 26.9, 26.8, 19.2; HRMS $[M\text{-}N_2+H]^+$ calcd: 398.21514, found: 398.21530.

(2S,3S)-1-Azido-4-(*tert*-butyldiphenylsilyloxy)butane-2,3-diol (2.6.11). Azide **2.6.10** (350 mg, 0.822 mmol) was dissolved in 8 mL 90% acetic acid and heated at reflux for 10 minutes. The reaction was then slowly cooled to room temperature and concentrated under reduced pressure and purified via column chromatography with silica gel and a gradient solvent system of 10 to 50% ethyl acetate/hexanes to afford **2.6.11** as a pale yellow oil (235 mg, 74%).

$[\alpha]_D^{296K}$ +5.21 (c = 0.845, $CHCl_3$); ^{1}H NMR (300 MHz, $CDCl_3$) δ 7.69–7.65 (m, 4H), 7.47–7.39 (m, 6H), 3.88–3.66 (m, 4H), 3.44–3.32 (m, 2H), 2.89–2.87 (m, 1H), 2.72–2.70 (m, 1H), 1.09 (s, 9H); ^{13}C NMR (75 MHz, $CDCl_3$) δ 135.49, 135.45, 132.5, 132.4, 130.0,

127.9, 71.1, 70.9, 65.6, 53.6, 26.8, 19.1; HRMS $[M+NH_4]^+$ calcd: 403.21654, found: 403.21717.

(2S,3S)-1-Azido-4-(*tert*-butyldiphenylsilyloxy)butane-2,3-diyl distearate (2.6.8b). Diol **2.6.11** (220 mg, 0.571 mmol), stearic acid (487 mg, 1.71 mmol), 4-dimethylaminopyridine (209 mg, 1.71 mmol), and dicyclohexylcarbodiimide (353 mg, 1.71 mmol) were combined in dichloromethane (8 mL). The reaction was stirred at room temperature overnight at which point it was filtered. Column chromatography with silica gel and a gradient solvent system of 0 to 10% ethyl acetate/hexanes afforded **2.6.8b** as a white solid (524 mg, 100%).

$[\alpha]_D^{296K}$ -2.78 (c = 0.360, $CHCl_3$); ^{1}H NMR (300 MHz, $CDCl_3$) δ 7.66–7.63 (m, 4H), 7.47–7.36 (m, 6H), 5.43–5.38 (m, 1H), 5.23–5.18 (m, 1H), 3.78–3.67 (m, 2H), 3.55–3.39 (m, 2H), 2.34–2.26 (m, 4H), 1.62–1.61 (m, 4H), 1.27 (*b* s, 56H), 1.06 (s, 9H), 0.89 (t, *J* = 6.0 Hz); ^{13}C NMR (75 MHz, $CDCl_3$) δ 172.8, 172.7, 135.6, 135.5, 132.8, 132.7, 129.9, 127.8, 127.7, 72.0, 70.3, 62.0, 51.0, 34.2, 34.1, 31.9, 29.7, 29.65, 29.62, 29.5, 29.35, 29.28, 29.26, 29.2, 29.1, 26.7, 24.84, 24.70, 22.7, 19.1, 14.1.

(2S,3S)-1-Azido-4-hydroxybutane-2,3-diyl distearate (2.2.1). Compound **2.6.8b** (57 mg, 0.062 mmol) was dissolved in THF (2 mL). Acetic acid (3.5 µL, 0.062 mmol) and TBAF·$3H_2O$ (19.6 mg, 0.062 mmol) were each dissolved in THF (2 mL) and added successively to the reaction. The reaction was stirred at room temperature for 80 minutes, and the solvent was removed with reduced pressure. The product was

extracted using a solution of 30 mL $CHCl_3$, 20 mL MeOH, and 10 mL H_2O. The bottom layer was kept and concentrated. Quick chromatography with a short column of silica gel and a gradient solvent system of 10 to 100% ethyl acetate/hexanes afforded **2.2.1** and **2.2.1a** as white solids (31.3 mg, 74%, 11% TBDPS byproduct that was not separable).

Experimental Procedure for the DMTr Protection Synthesis

((4S,5S)-5-(azidomethyl)-2,2-dimethyl-1,3-dioxolan-4-yl)methanol (2.7.13). Diol **2.4.4** (990 mg, 6.10 mmol) was suspended in anhydrous dichloromethane (36 mL). With stirring was added silver (I) oxide (2.12 g, 9.15 mmol), tosyl chloride (1.28 g, 6.71 mmol), and crushed potassium iodide (203 mg, 1.22 mmol). The reaction was stirred at room temperature for 2 hours at which point it was filtered through a short plug of silica using ethyl acetate as an eluant and concentrated under reduced pressure to afford crude **2.7.12**.

The crude solution of **2.7.12** was dissolved in anhydrous DMF (60 mL) and sodium azide (1.19 g, 18.3 mmol) was added. The reaction was heated to 85 °C and stirred overnight. The crude reaction was extracted with ethyl acetate, dried with magnesium sulfate, and concentrated under reduced pressure. Column chromatography with silica gel and a gradient solvent system of 20-60% ethyl acetate/hexanes afforded **2.7.13** as a colorless oil (934 mg, 82% over 2 steps).

Characterization matches previous reports.[73]

^{1}H NMR (300 MHz, $CDCl_3$) δ 4.12-3.97 (m, 2H), 3.84–3.78 (m, 1H), 3.69–3.55 (m, 2H),

3.37–3.31 (m, 1H), 2.39 (t, *J* = 6 MHz, 1H), 1.47 (s, 1H), 1.44 (s, 1H).

(2S,3S)-4-azidobutane-1,2,3-triol (2.7.14). Alcohol **2.7.13** was dissolved in 10 mL of 90% acetic acid. The solution was heated to reflux for 10 minutes and then slowly cooled to room temperature. Solvent was removed under reduced pressure and column chromatography with silica gel and 10% methanol/dichloromethane afforded compound **2.7.14** as a yellow syrup (232 mg, 92%).

^{1}H NMR (300 MHz, CD_3OD) showed removal of the acetonide protecting group.The R_f value by TLC analysis matched previous reports,[74] and compound **2.7.14** was used without any further characterization.

(2S,3S)-1-azido-4-((4,4'-dimethoxytrityl)methoxy)butane-2,3-diol (2.7.15). Triol **2.7.14** (75.3 mg, 0.512 mmol) was dissolved in pyridine (5 mL), and a small amount of 4Å MS was added to the reaction flask. With stirring, 4,4'-dimethoxytrityl chloride (260 mg, 0.768 mmol) was added. The reaction was placed under nitrogen and stirred at room temperature overnight. The reaction was then filtered with dichloromethane, and the solvent was removed under reduced pressure at low temperature (45 °C). Column chromatography with silica gel and a gradient solvent system of 30-80% ethyl acetate/hexanes afforded **2.7.15** as a yellow oil (143 mg, 62 %).

$[\alpha]_D^{296K}$ -5.53 (c = 1.428, $CHCl_3$); ^{1}H NMR (300 MHz, $CDCl_3$) δ 7.42–7.18 (m, 9H), 6.82 (d, *J* = 8.7 Hz, 4H), 3.82–3.64 (m, 8H ($OC\underline{H}_3$ + 2 $C\underline{H}OH$)), 3.38–3.18 (m, 4H), 2.98 (d, *J* = 4.8 Hz, 1H), 2.82 (d, *J* = 6 Hz, 1H); ^{13}C NMR (100.6 MHz, $CDCl_3$) δ 158.6, 144.5,

135.7, 135.5, 130.0, 128.02, 127.97, 127.0, 113.3, 86.7, 71.3, 70.7, 65.2, 55.2, 53.6; HRMS $[M + Cl^-]^-$ calcd: 484.16392, found: 484.16204.

(2S,3S)-1-azido-4-((4,4'-dimethoxytrityl)methoxy)butane-2,3-diyl distearate (2.7.8c). Diol **2.7.15** (289 mg, 0.643 mmol), stearic acid (549 mg, 1.93 mmol), 4-dimethylaminopyridine (79 mg, 0.643 mmol), and dicyclohexylcarbodiimide (398 mg, 1.93 mmol) were combined in dichloromethane (7 mL). The reaction was stirred at room temperature for 7 hours, at which point it was filtered with ethyl acetate. Column chromatography with silica gel and 10% ethyl acetate/hexanes afforded **2.7.8c** as a white solid (546 mg, 86%).

$[\alpha]_D^{296K}$ +3.10 (c = 0.967, $CHCl_3$); ^{1}H NMR (300 MHz, $CDCl_3$) δ 7.42–7.18 (m, 9H), 6.82 (d, *J* = 8.7 Hz, 4H), 5.45–5.40 (m, 1H), 5.27–5.23 (m, 1H), 3.78 (s, 6H), 3.45–3.39 (m, 1H), 3.31–3.19 (m, 2H), 3.11–3.06 (m, 1H), 2.39–2.22 (m, 4H), 1.67–1.54 (m, 4H), 1.26 (*b* s, 56H), 0.88 (t, *J* = 6.6 Hz, 6H); ^{13}C NMR (100.6 MHz, $CDCl_3$) δ 172.8, 172.7, 158.6, 144.3, 135.6, 135.4, 129.96, 129.90, 128.0, 127.9, 126.9, 113.2, 86.3, 71.2, 70.7, 61.7, 55.2, 50.9, 34.4, 34.1, 32.0, 29.73, 29.69, 29.68, 29.67, 29.5, 29.4, 29.3, 29.28, 29.2, 25.0, 24.8, 22.7, 14.1; $[M + O_2]^-$ calcd: 1013.70683, found: 1013.71083.

(2S,3S)-1-Azido-4-hydroxybutane-2,3-diyl distearate (2.2.1). Compound **2.7.8c** (35 mg, 0.036 mmol) and p-aminobenzoic acid (49 mg, 0.360 mmol) were combined in 2 mL of solvent in a ratio of dichloromethane : acetic acid : water (1 : 8.5 : 0.5). The solution was stirred at room temperature for 12.5 hours. The reaction was extracted with

dichloromethane (50 mL) and dried with magnesium sulfate. The solvent was removed under reduced pressure. Column chromatography was carried out on a short plug of silica gel using 30% ethyl acetate/hexanes. Because compound **2.2.1** is known to undergo acyl chain migration on silica, purification was performed rapidly. As a result of not being able to carefully purify the reaction, **2.2.1** was not obtained in pure form, but the trityl adduct impurities did not effect the next reaction and were easily removed during purification of the subsequent DAG analogues.

^{1}H NMR (300 MHz, $CDCl_3$) δ 5.33–5.30 (m, 1H), 5.12–5.07 (m, 1H), 3.68–3.61 (m, 2H), 3.49–3.46 (m, 2H), 2.44–2.33 (m, 5H, O<u>H</u> buried), 1.66–1.60 (m, 4H), 1.26 (*b* s, 56H), 0.88 (t, *J* = 6.3 Hz, 6H); ^{13}C NMR (62.9 MHz, $CDCl_3$) δ 173.7, 173.2, 72.5, 70.5, 60.8, 51.1, 34.2, 32.0, 29.7, 29.5, 29.4, 29.3, 29.2, 25.0, 24.9, 22.7, 14.1; HRMS $[M\text{-}H_2O + H]^+$ calcd: 662.58358, found: 662.58257.

<u>Experimental Procedures for Alkyne-Functionalized reagents</u>

Standard amide bond-forming coupling conditions were employed to obtain alkyne-functionalized fluorescent and cross-linking groups. Generally, the coupling reagent *N,N*-dicyclohexylcarbodiimide (DCC) was used to produce the highly non-polar alkyne conjugates. For the more polar alkyne conjugates, such as fluorescein, other coupling reagents, exemplified by 1-Ethyl-3-(3-dimethylaminopropyl)carbodiimide hydrochloride (EDC), were used to avoid problems with separating the products from the urea byproduct of DCC.

Naphthyl alkyne (2.8.17a). 2-Naphthylacetic acid (100 mg, 0.537 mmol), *N,N*-dicyclohexylcarbodiimide (166.2 mg, 0.806 mmol), 4-dimethylaminopyridine, (32.8 mg, 0.269 mmol) and propargylamine (44 µL, 0.644 mmol) were dissolved in methylene chloride (6 mL). The reaction was stirred at room temperature in the dark overnight. The reaction was extracted with dichloromethane (2 x 50 mL) from water (50 mL), and the organic layer was dried with magnesium sulfate and filtered, and the solvent was removed by rotary evaporation. Column chromatography with silica gel and a gradient solvent system of 25 to 50% ethyl acetate/hexanes afforded **2.8.17a** as a white solid (95 mg, 79%).

^{1}H NMR (300 MHz, $CDCl_3$) δ 7.87-7.81 (m, 3H), 7.73 (s, 1H), 7.54–7.47 (m, 2H), 7.39–7.36 (m, 1H), 5.58, (*b* s, 1H), 4.02 (dd, *J* = 5.3, 2.6 Hz, 2H), 3.77 (s, 2H), 2.16 (t, *J* = 2.6 Hz, 1H); ^{13}C NMR (62.9 MHz, $CDCl_3$) δ 170.5, 133.5, 132.6, 131.9, 128.8, 128.3, 127.7, 127.7, 127.3, 126.4, 126.1, 79.4, 71.5, 43.6, 29.3; HRMS $[M+H]^+$ calcd: 224.10754, found: 224.10790.

Dansyl alkyne (2.8.17b). Compound **2.8.17b** was synthesized according to a literature procedure[76] using dansyl chloride (100 mg, 0.371 mmol), propargylamine (31 µL, 0.445 mmol), and triethylamine (62 µL, 0.445 mmol). The reaction mixture was extracted with dichloromethane (2 x 50 mL) from water (50 mL), and the organic phase was then dried with magnesium sulfate and filtered. Next, the solvent was removed by rotary evaporation. Column chromatography with silica gel and a gradient solvent system of 25 to 50% ethyl acetate/hexanes afforded **2.8.17b** as a yellow solid (97 mg, 90%).

Characterization agreed with previous literature reports. HRMS $[M+H]^+$ calcd: 289.10107, found: 289.10202.

Coumarin Alkyne (2.8.17c). Coumarin-3-carboxylic acid (191 mg, 1 mmol) was dissolved in dry DMF (10 mL) and HBTU (455 mg, 1.2 mmol) and hydroxybenzotriazole (162 mg, 1.2 mmol) were added. The sides of the reaction flask were rinsed with dry DMF (1 mL), and diisopropylethylamine (198 µL, 1.2 mmol) was added and stirred for 5 min. Propargylamine (82 µL, 1.2 mmol) was dissolved in DMF (1 mL) and added to the reaction mixture, which was then allowed to stir in the dark at room temperature overnight. After the reaction was complete, DMF was removed on a rotary evaporator, and the residue was extracted with ethyl acetate (2 x 50 mL) from 10% sodium bicarbonate (50 mL). The organic phase was then dried with magnesium sulfate and filtered, and the solvent was removed by rotary evaporation. Column chromatography with silica gel and a gradient solvent system of 20 to 70% ethyl acetate/hexanes afforded **2.8.17c** as a pale yellow solid (161 mg, 71%).

^{1}H NMR (300 MHz, $CDCl_3$) δ 9.01 (*b* s, 1H), 8.29 (s, 1H), 7.72–7.66 (m, 2H), 7.43–7.39 (m, 2H), 4.26 (dd, *J* = 5.1, 2.4 Hz, 2H), 2.28 (t, *J* = 2.4 Hz, 1H); ^{13}C NMR (69.2 MHz, $CDCl_3$) δ 161.4, 154.6, 148.8, 134.3, 129.9, 125.4, 118.6, 118.0, 116.7, 79.1, 71.6, 29.5; HRMS $[M+H]^+$ calcd: 228.06607, found: 228.06633.

5(6)-CBF alkyne (2.8.17d). Propargylamine (34.3 µL, 0.5 mmol), 4-dimethylaminopyridine (61.1 mg, 0.5 mmol), *N*-methylmorpholine (82.5 µL, 0.75 mmol),

and 5(6)-carboxyfluorescein (226 mg, 0.6 mmol) were dissolved in a 1:1 mixture of dry DMF and dichloromethane (4 mL) at room temperature. 1-Ethyl-3-(3-dimethylaminopropyl)carbodiimide hydrochloride (EDC, 115 mg, 0.6 mmol) was added. The reaction mixture was stirred at room temperature overnight in the dark. After the reaction was complete, the mixture was extracted with ethyl acetate (2 x 50 mL) from 2 N HCl (50 mL), and the organic layer was dried with magnesium sulfate and filtered. The solvent was then removed by rotary evaporation. Column chromatography with silica gel and a gradient solvent system of 5 to 15% methanol/chloroform with 0.1% acetic acid afforded **2.8.17d** as an orange solid (140 mg, 68%). Note: Since both isomers were present in the ^{1}H NMR spectra for compounds **2.8.17d** and **2.8.16d** and the ratio of each isomer is unknown in the commercially available acid, integration values are not reported. ^{13}C NMR data for compounds **2.8.17d** and **2.8.16d** are not reported due to poor solubility of the compounds and the complex nature of the spectra due to the isomeric mixture.

^{1}H NMR (300 MHz, CD_3OD), δ 8.75 (*b* s), 8.52–8.43 (m), 8.22–8.07 (m), 7.93 (*b* s), 7.62 (s), 7.32–7.30 (m), 6.69–6.52 (m), 4.21 (d, *J* = 2.4 Hz), 4.08 (d, *J* = 4.08 Hz), 2.66 (t, *J* = 2.3 Hz), 2.56 (t, *J* = 2.3 Hz); HRMS $[M+H]^+$ calcd: 414.09776, found: 414.09632.

Benzophenone alkyne (2.8.17e). A solution of 4-benzoylbenzoic acid (200 mg, 0.884 mmol), *N,N'*-dicyclohexylcarbodiimide (273.5 mg, 1.33 mmol), and 4-dimethylaminopyridine (54 mg, 0.442 mmol) was prepared in dry dichloromethane and allowed to react for 30 min. Propargylamine (72.8 µL, 1.06 mmol) was added, and the

reaction mixture was stirred at room temperature overnight in the dark. After the reaction was complete, the mixture was extracted with dichloromethane (2 x 50 mL) from water (50 mL), and the organic layer was dried with magnesium sulfate and filtered, followed by solvent removal. Column chromatography with silica gel and a gradient solvent system of 20 to 70% ethyl acetate/hexanes afforded **2.8.17e** as a white solid (145 mg, 62%).

^{1}H NMR (300 MHz, $CDCl_3$) δ 7.92–7.84 (m, 4H), 7.82–7.78 (m, 2H), 7.65–7.60 (m, 1H), 7.53–7.48 (m, 2H), 6.37 (*b* s, 1H), 4.30 (dd, *J* = 2.6, 5.25 Hz, 2H), 2.32 (t, *J* = 2.6 Hz, 1H); ^{13}C NMR (62.9 MHz, $CDCl_3$) δ 196.0, 166.4, 140.3, 137.0, 136.9, 132.9, 130.1, 128.5, 127.1, 79.3, 72.0, 29.9; HRMS $[M+H]^+$ calcd: 264.10245, found: 264.10361.

Experimental Procedures for Obtaining DAG Analogues Modified by "Click" Chemistry

Compound **2.7.8c** (1 eq) and pyrrole (2.05 eq) or p-ABA (10 eq) were dissolved in 2 mL of solvent consisting of dichloromethane : AcOH : H_2O (1 : 8.5 : 0.5). The solution was stirred at room temperature for 6 hours if using pyrrole or 12.5 hours if using p-ABA. The reaction was extracted with dichloromethane (2 x 25 mL) and dried with magnesium sulfate. The solvent was removed under reduced pressure. The crude residue containing unmigrated **2.2.1** was then dried under high vacuum for 1-3 hours and used directly in the click reactions as described below.

Naphthyl-DAG (2.8.16a). Alkyne **2.8.17a** (14.3 mg, 0.064 mmol) and **2.2.1** (0.064

mmol) were dissolved in dry THF (0.5 mL). Copper sulfate pentahydrate (16 mg, 0.064 mmol) and sodium ascorbate (12.7 mg, 0.064 mmol) were added along with water (0.5 mL). The reaction was stirred in the dark at room temperature overnight. The reaction was extracted with dichloromethane (2 x 50 mL) from water, and the organic phase was dried with magnesium sulfate, filtered and the solvent was removed by rotary evaporation. Column chromatography on a short plug of silica gel and a gradient solvent system of 50 to 100% ethyl acetate/hexanes afforded **2.8.16a** as a white solid (29 mg, 50% (2 steps)).

$[\alpha]_D^{296K}$ -11.0 (c = 0.963, $CHCl_3$); ^{1}H NMR (300 MHz, $CDCl_3$) δ 7.82–7.77 (m, 3H), 7.69 (s, 1H), 7.57 (s, 1H), 7.51–7.45 (m, 2H),7.36–7.33 (m, 1H), 6.30 (t, *J* = 5.7 Hz, 1H), 5.55–5.50 (m, 1H), 5.02–4.97 (m, 1H), 4.54 (d, *J* = 6 Hz, 2H), 4.42 (d, *J* = 5.7 Hz, 2H), 3.79–3.56 (m & s overlapped, 4H), 2.71 (*b* s, 1H), 2.38–2.24 (m, 4H), 1.64–1.51 (m, 4H), 1.25 (*b* s, 56H), 0.88 (t, *J* = 6.2 Hz, 6H); ^{13}C NMR (75 MHz, $CDCl_3$) δ 173.4, 173.1, 171.1, 144.9, 133.5, 132.5, 131.9, 128.9, 128.3, 127.71, 127.65, 127.2, 126.4, 126.1, 123.3, 72.0, 70.0, 60.5, 50.3, 43.8, 35.0, 34.1, 33.9, 29.72, 29.68, 29.5, 29.4, 29.3, 29.2, 29.1, 24.9, 24.8, 22.7, 14.1; HRMS $[M+H]^+$ calcd: 903.69386, found: 903.68995.

Dansyl-DAG (2.8.16b). Alkyne **2.8.17b** (16.4 mg, 0.057 mmol) and **2.2.1** (0.057 mmol) were dissolved in dry THF (0.5 mL). Copper sulfate pentahydrate (14.2 mg, 0.057 mmol) and sodium ascorbate (11.3 mg, 0.057 mmol) were added along with water (0.5 mL). The reaction mixture was stirred in the dark at room temperature overnight. The reaction was extracted with dichloromethane (2 x 50 mL) from water and the organic

phase was dried with magnesium sulfate, filtered and the solvent was removed by rotary evaporation. Column chromatography on a short plug of silica gel and a gradient solvent system of 50 to 100% ethyl acetate/hexanes afforded **2.8.16b** as a greenish solid (30 mg, 55% (2 steps)).

$[\alpha]_D^{296K}$ -12.2 (c = 1.01, $CHCl_3$); ^1H NMR (300MHz, $CDCl_3$) δ 8.55 (d, *J* = 8.7 Hz, 1H), 8.27–8.24 (m, 2H), 7.58–7.50 (m, 2H), 7.43 (s, 1H), 7.19 (d, *J* = 7.5 Hz, 1H), 5.51–5.44 (m, 2H, NH buried), 4.98–4.93 (m, 1H), 4.48 (d, *J* = 6 Hz, 2H), 4.18 (d, *J* = 6 Hz, 2H), 3.79–3.58 (m, 2H), 2.89 (s, 6H), 2.64 (*b* s, 1H), 2.39–2.27 (m, 4H), 1.66–1.53 (m, 4H), 1.25 (*b* s, 56H), 0.88 (t, *J* = 6.5 Hz, 6H); ^{13}C NMR (75 MHz, $CDCl_3$) δ 173.4, 173.2, 151.9, 144.4, 134.4, 130.6, 129.8, 129.6, 129.5, 128.6, 123.3, 123.2, 118.7, 115.3, 72.0, 69.8, 60.5, 50.2, 45.4, 38.7, 34.1, 33.9, 31.9, 29.72, 29.68, 29.5, 29.4, 29.3, 29.26, 29.2, 29.1, 24.9, 24.8, 22.7, 14.1; HRMS $[M+H]^+$ calcd: 968.68739, found: 968.68743.

Coumarin-DAG (2.8.16c). Alkyne **2.8.17c** (12.7 mg, 0.056 mmol) and **2.2.1** (0.056 mmol) were dissolved in dry THF (0.5 mL). Copper sulfate pentahydrate (14 mg, 0.056 mmol) and sodium ascorbate (11.1 mg, 0.056 mmol) were added along with water (0.5 mL). The reaction mixture was stirred in the dark at room temperature overnight. Solvent was removed, and column chromatography on a short plug of silica gel and a gradient solvent system of 20 to 100% acetone/chloroform afforded **2.8.16c** as a tan solid (31 mg, 60% (2 steps)).

$[\alpha]_D^{296K}$ -14.6 (c = 1.224, $CHCl_3$); ^1H NMR (300 MHz, $CDCl_3$) δ 9.29 (bs, 1H), 8.91 (s, 1H), 7.71–7.65 (m, 3H), 7.42–7.36 (m, 2H), 5.60–5.55 (m, 1H), 5.07–5.02 (m, 1H), 4.73

(*b*s, 2H), 4.61–4.60 (m, 2H), 3.80–3.59 (m, 2H), 2.64–2.62 (m, 1H), 2.39–2.28 (m, 4H), 1.65–1.53 (m, 4H), 1.25 (*b* s, 56H), 0.88 (t, *J* = 6.6 Hz, 6H); ^{13}C NMR (75 MHz, $CDCl_3$) δ 173.4, 173.1, 161.8, 161.2, 154.5, 148.5, 144.8, 134.3, 129.8, 125.3, 123.3, 118.5, 118.1, 116.7, 72.1, 70.0, 60.5, 50.3, 35.4, 34.1, 33.9, 31.9. 29.72, 29.67, 29.5, 29.4, 29.3, 29.2, 29.1, 24.9, 24.8, 22.7, 14.2; HRMS $[M+H]^+$ calcd: 907.65239, found: 907.65176.

5(6)-CBF DAG (2.8.16d). Alkyne **2.8.17d** (19.8 mg, 0.048 mmol) and **2.2.1** (0.048 mmol) were dissolved in dry THF (0.5 mL). Copper sulfate pentahydrate (12 mg, 0.048 mmol) and sodium ascorbate (9.5 mg, 0.048 mmol) were added along with water (0.5 mL). The reaction was stirred in the dark at room temperature overnight. Solvent was removed and column chromatography on a short plug of silica gel and a gradient solvent system of 30 to 100% acetone/chloroform afforded **2.8.16d** as an orange solid (25 mg, 47% (2 steps)). Note: since both fluorescein isomers (5 and 6-carboxy) were present in the ^{1}H NMR spectra for compounds **2.8.16d** and **2.8.17d**, and the ratio of each isomer is unknown in the commercially available acid, integration values are not reported. ^{13}C NMR data for compounds **2.8.16d** and **2.8.17d** are not reported due to poor solubility of the compounds and the complex nature of the spectra due to the isomeric mixture.

$[\alpha]_D^{296K}$ -8.5 (c = 0.823, 1 Acetone : 1 $CHCl_3$); ^{1}H NMR (300 MHz, $CDCl_3$: $(CD_3)_2CO$ (1 : 1)) δ 9.05 (*b* s), 8.60 (*b* s), 8.50 (*b* s), 8.33–8.30 (m), 8.24–8.21 (m), 8.04–8.01 (m) 7.91 (*b* s), 7.81–7.78 (m), 7.74 (s), 7.31–7.28 (m), 6.77–6.56 (m), 5.61–5.51 (m), 5.04–4.99

(m), 4.72–4.59 (m) 4.30–4.17 (m), 3.83–3.65 (m), 2. 39–2.18 (m), 1.62–1.43 (m), 1.27 (*b* s), 0.88 (t, *J* = 6.3 Hz); HRMS $[M+H]^+$ calcd: 1093.68408, found: 1093.68461.

Benzophenone-DAG (2.8.16e). Alkyne **2.8.17e** (13.6 mg, 0.052 mmol) and **2.2.1** (0.052 mmol) were dissolved in dry THF (0.5 mL). Copper sulfate pentahydrate (13 mg, 0.052 mmol) and sodium ascorbate (10 mg, 0.052 mmol) were added along with water (0.5 mL). The reaction was stirred in the dark at room temperature overnight. The reaction was extracted with dichloromethane (2 x 50 mL) from wate,r and the organic phase was dried with magnesium sulfate, filtered, and the solvent was removed by rotary evaporation. Column chromatography on a short plug of silica gel and a gradient solvent system of 50 to 100% ethyl acetate/hexanes afforded **2.8.16e** as a white solid (34 mg, 69% (2 steps)).

$[\alpha]_D^{296K}$ -11.4 (c = 1.127, $CHCl_3$); ^{1}H NMR (300 MHz, $CDCl_3$) δ 7.92 (d, *J* = 8.1Hz, 2H), 7.84–7.73 (m, 5H), 7.61 (t, *J* = 7.4 Hz, 1H), 7.49 (m, 2H), 7.33 (*b* s, 1H), 5.61–5.57 (m, 1H), 5.06–5.01 (m, 1H), 4.77–4.71 (m, 2H), 4.62–4.59 (m, 2H), 3.81–3.75 (m, 1H), 3.67–3.60 (m, 1H), 2.39–2.27 (m, 4H), 1.64–1.49 (m, 4H), 1.25 (*b* s, 56H), 0.88 (t, *J* = 6.6 Hz, 6H); ^{13}C NMR (100.6 MHz, $CDCl_3$) δ 195.9, 173.3, 173.2, 166.6, 144.7, 140.2, 137.2, 137.0, 132.9, 130.1, 128.4, 127.1, 123.6, 72.1, 70.0, 60.6, 50.4, 35.4, 34.2, 34.0, 31.9, 29.7, 29.5, 29.4, 29.3, 29.2, 29.1, 24.9, 24.8, 22.1, 14.1; HRMS $[M+H]^+$ calcd: 943.68877, found: 943.68741.

HPLC trace for functionalized DAG Probe 16b

As discussed in the text above, the acyl chains of diacylglycerols are known to migrate in the presence of silica. NMR analysis of analogs obtained via removal of the PMB protecting group indicated that migration was occurring. Removal of the DMT group and direct modification via "click" chemistry followed by purification produced compounds with NMRs that showed virtually no migration. However, upon HPLC analysis, two peaks appeared (chromatogram for **2.8.16b** shown below in figure **2.11**), one for the migrated product and one for the unmigrated product. The same sample was reanalyzed by NMR after HPLC analysis and no migration was detected, leading to the conclusion that the migration was observed on the column.

Protein Binding Analysis (This analysis was performed by our collaborator Dr. R. V. Stahelin at Indiania University School of Medicine-South Bend.)

The DAG binding protein PKCδ was purified from Sf9 cells as previously described.[61] Lipid vesicles were prepared as previously described[61] and consisted of POPC/POPS/DAG (78:20:2 where DAG is any synthetic DAG tested). POPC vesicles were prepared for the control surface. All surface plasmon resonance (SPR) experiments were performed at 25 °C using a Biacore X as described previously.[77] Equilibrium SPR measurements were carried out at the flow rate of 5 μl/min with coating of the L1 sensor chip (GE Healthcare) done as previously reported.[77] After injecting 85 μl of PKCδ, the protein-lipid association and dissociation were measured for 1020 s and

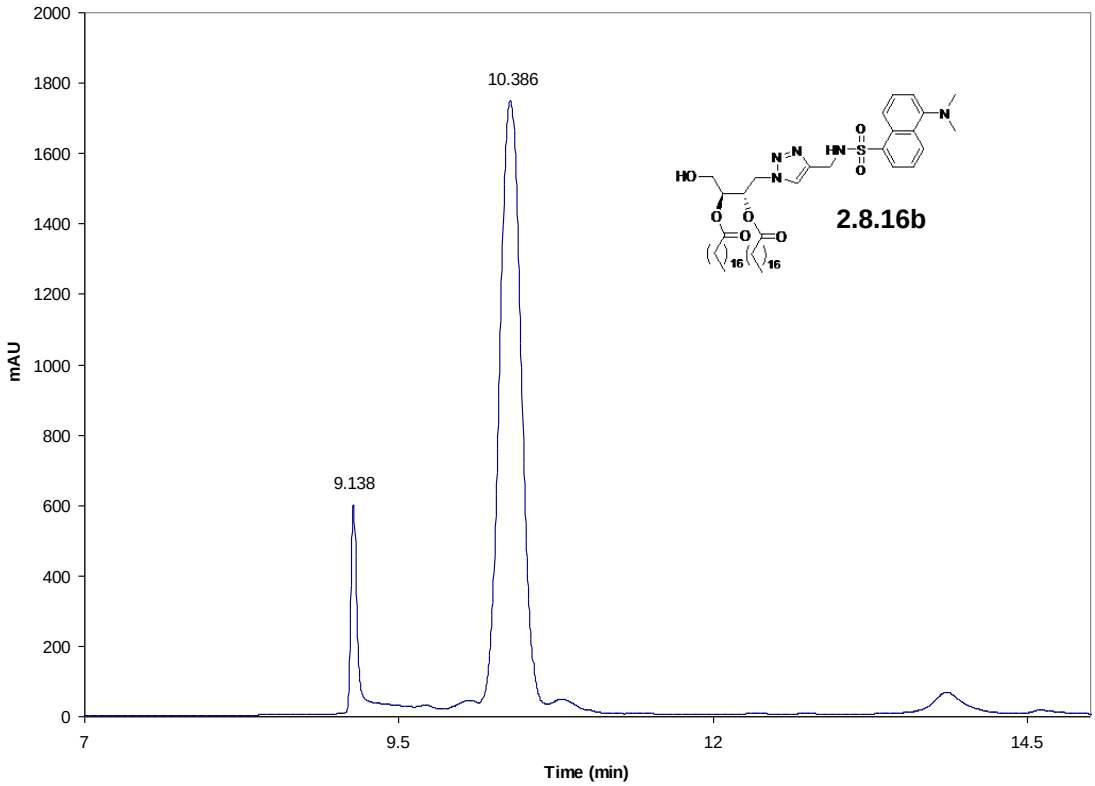

Figure 2.11. HPLC trace for Dansyl DAG analogue.

500 s, respectively. The sensorgrams were obtained using five or more different concentrations of the protein (within a 10-fold range of K_d) for each condition tested. The sensorgrams were corrected for refractive index change by subtracting the control surface response. The maximal response (R_{eq}, saturation value) was determined from the plots and then plotted *versus* protein concentrations (C). The K_d value was determined by a nonlinear least squares analysis of the binding isotherm using an equation, $R_{eq} = R_{max}/(1 + K_d/C)$.[78]

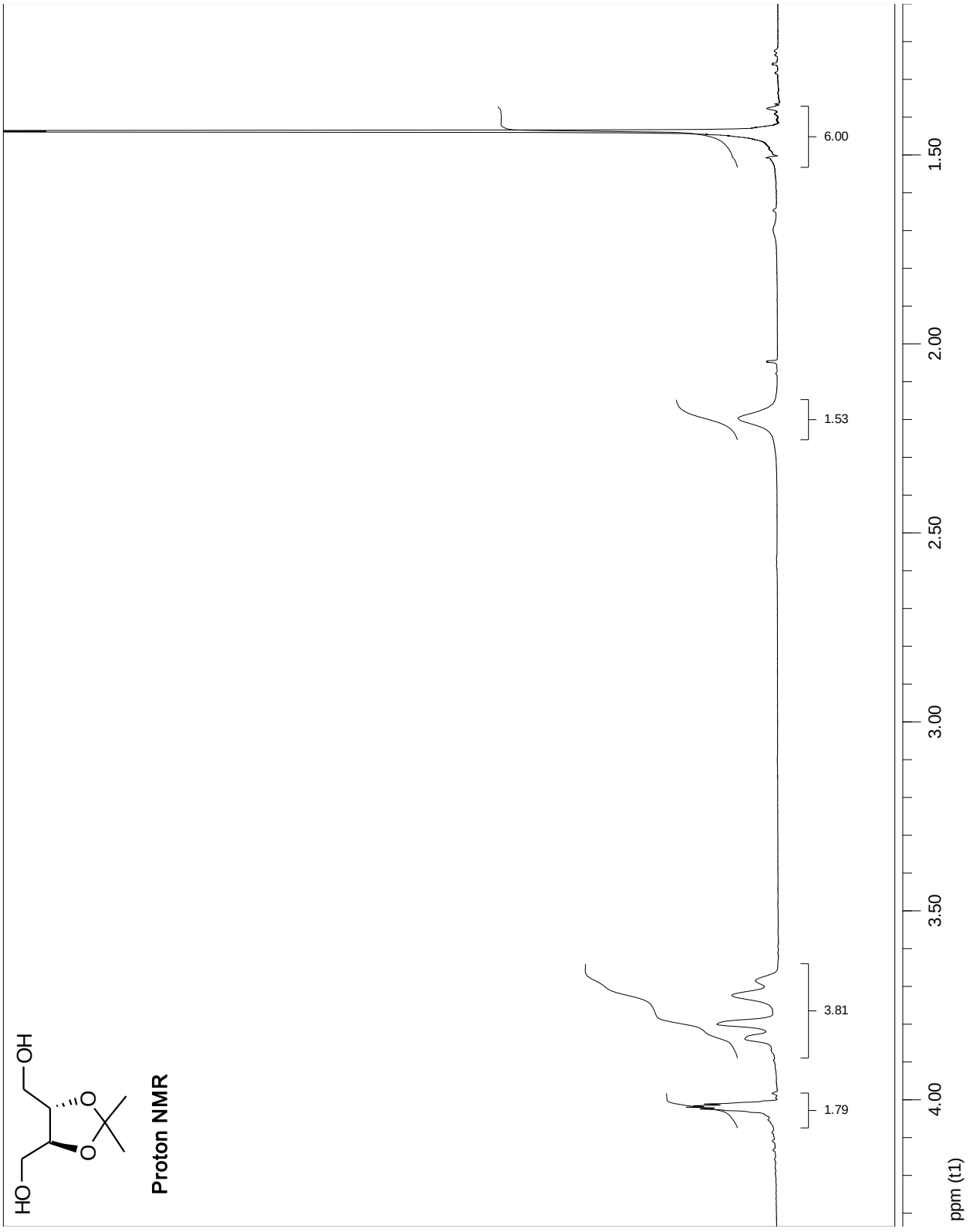
HO
OH
O
O
Proton NMR
6.00
1.53
3.81
1.79
1.50
2.00
2.50
3.00
3.50
4.00
ppm (t1)

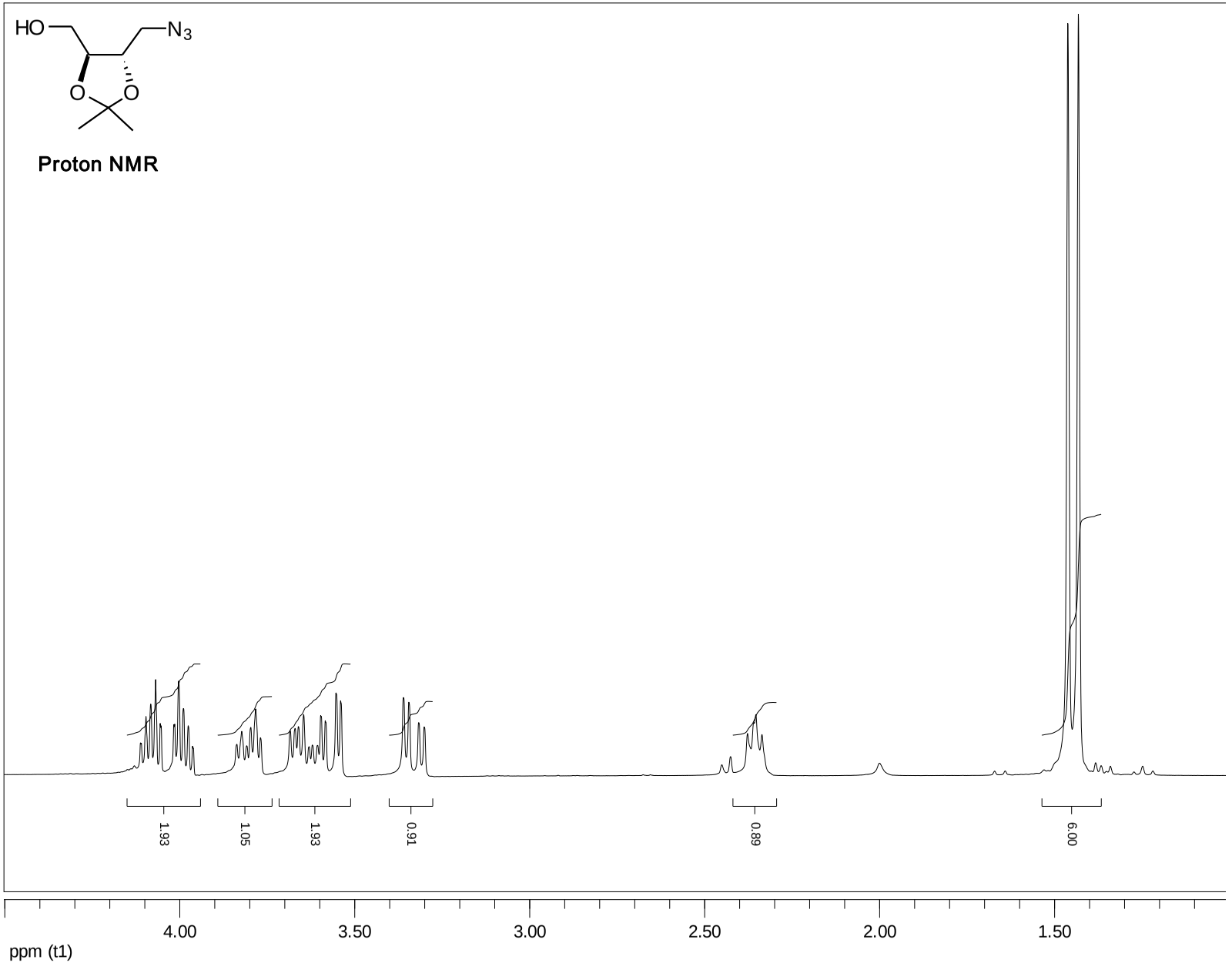
HO
N3
O
O
Proton NMR
1.93
1.05
1.93
0.91
0.89
6.00
4.00
3.50
3.00
2.50
2.00
1.50
ppm (t1)

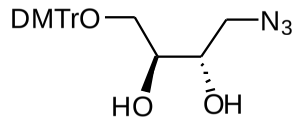

Proton NMR

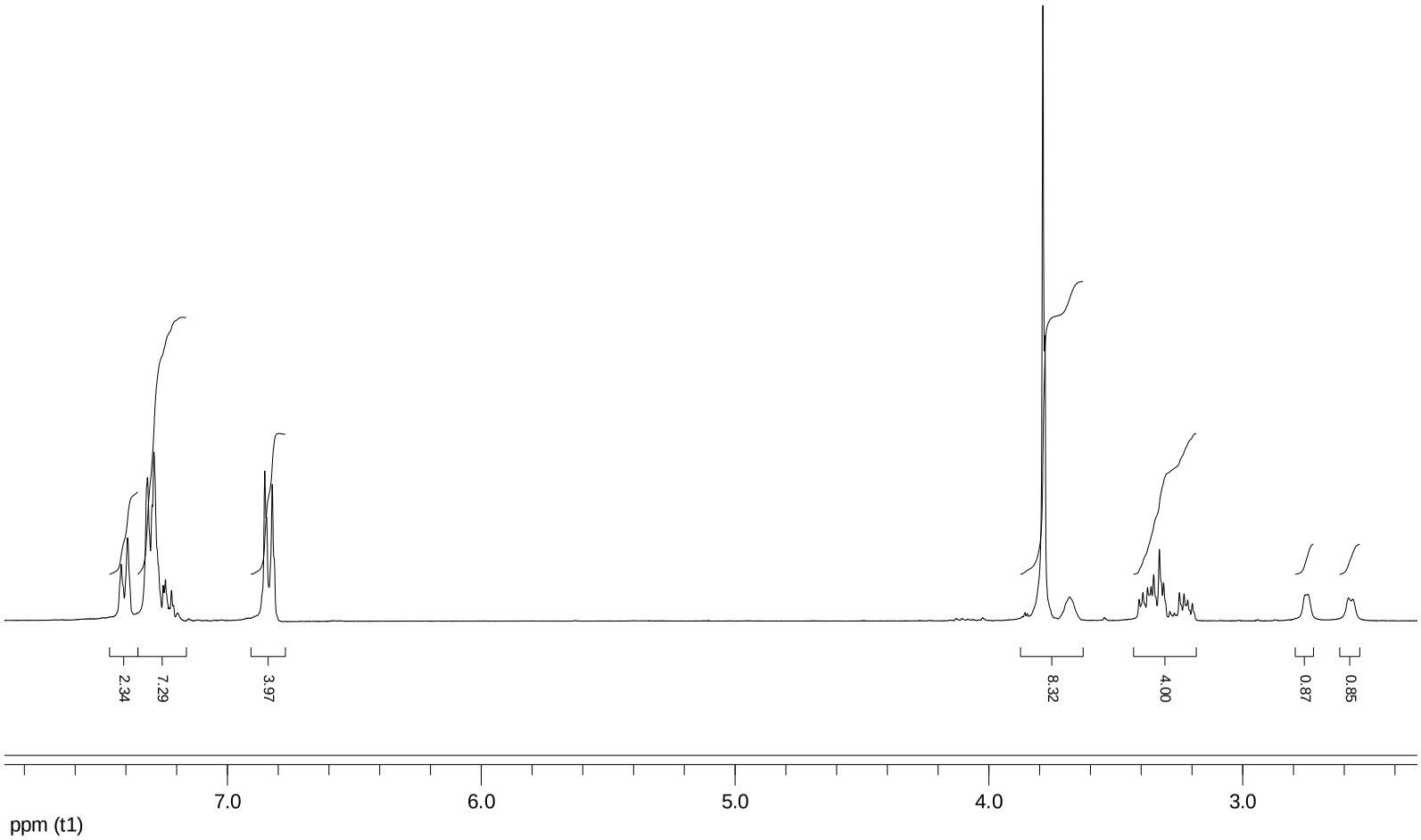

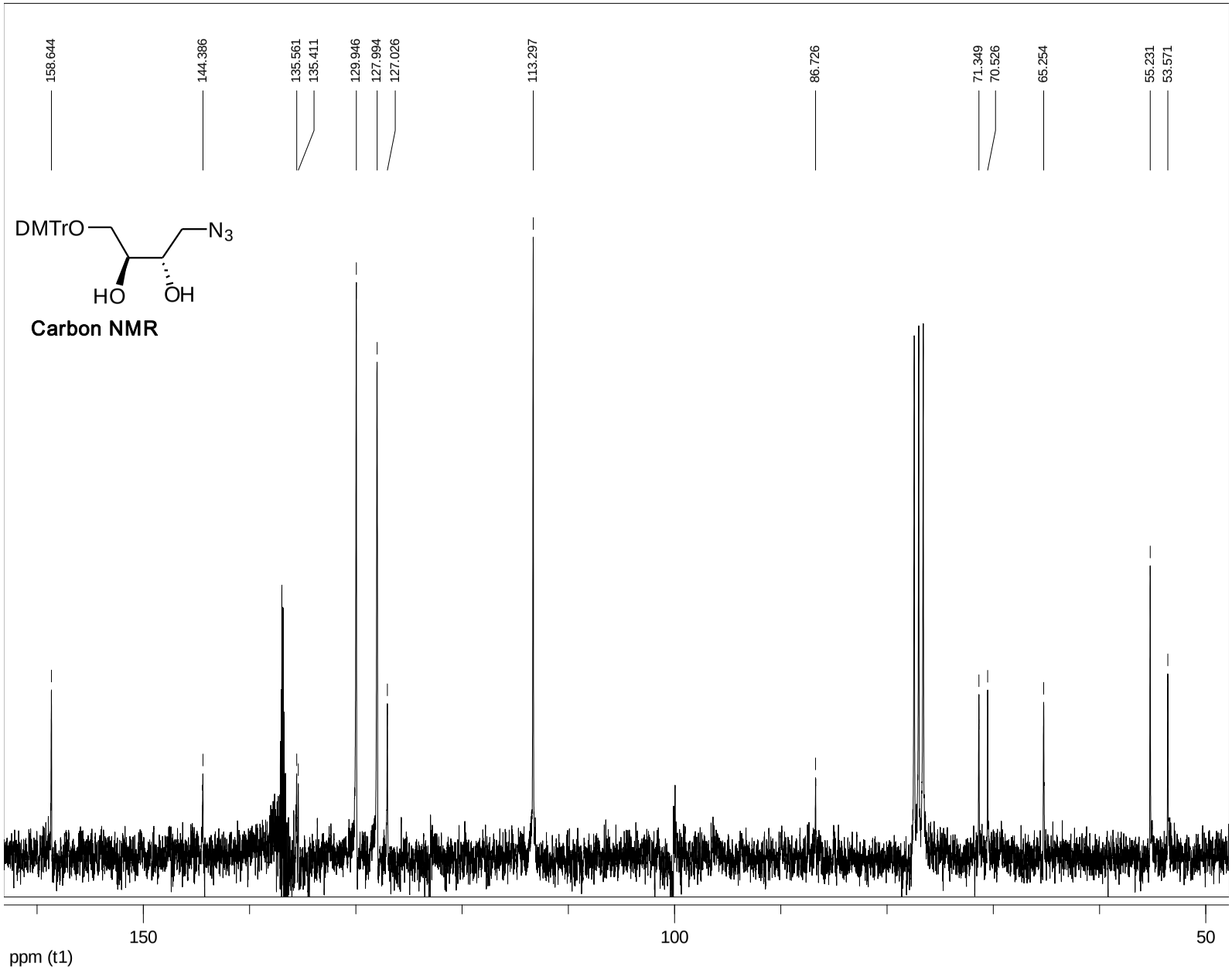
158.644
144.386
135.561
135.411
129.946
127.994
127.026
113.297
86.726
71.349
70.526
65.254
55.231
53.571
DMTrO
N3
HO
OH
Carbon NMR
150
100
50
ppm (t1)

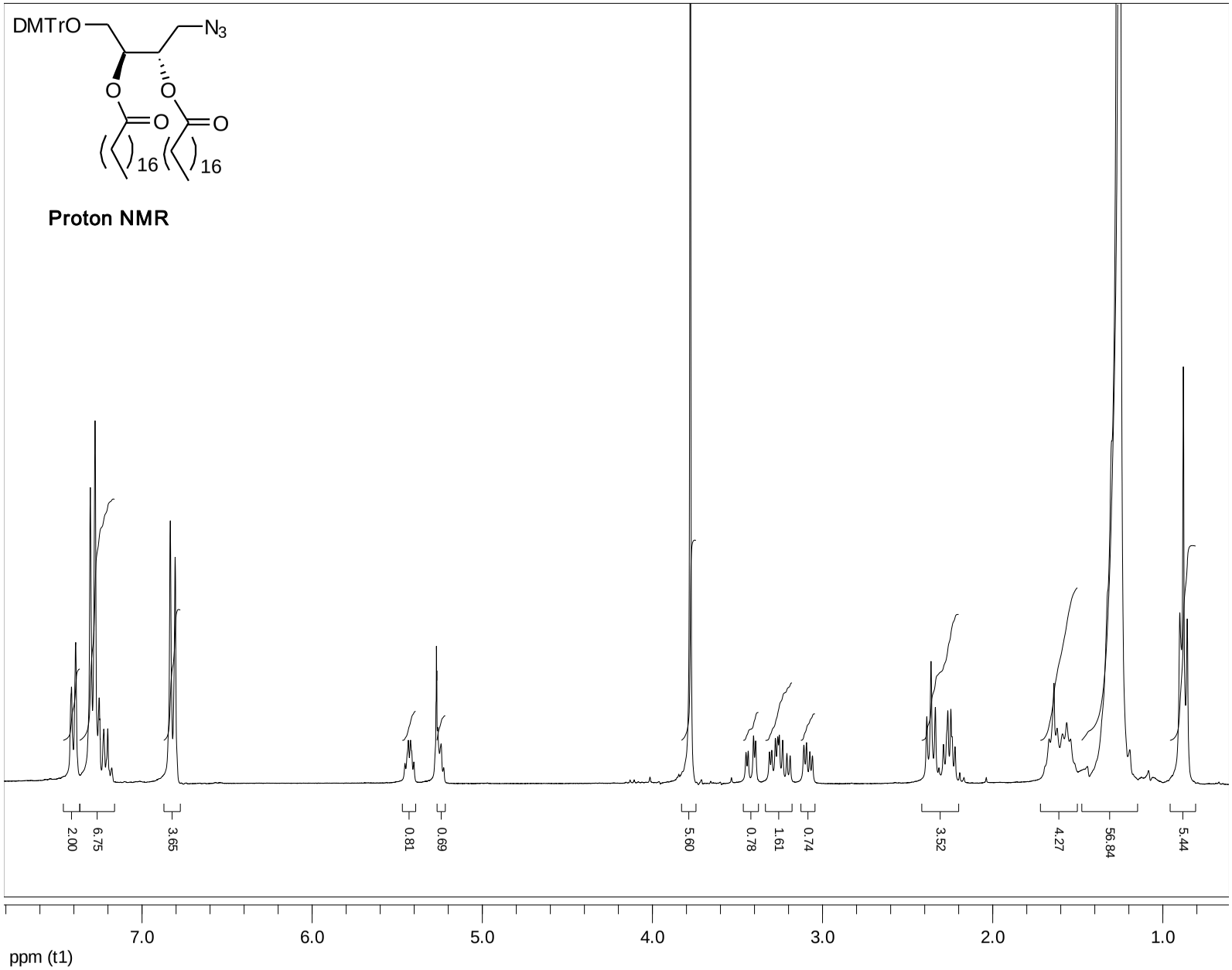
DMTrO
N3
O
O
O
O
O
16
16
Proton NMR
2.00
6.75
3.65
0.81
0.69
5.60
0.78
1.61
0.74
3.52
4.27
56.84
5.44
7.0
6.0
5.0
4.0
3.0
2.0
1.0
ppm (t1)

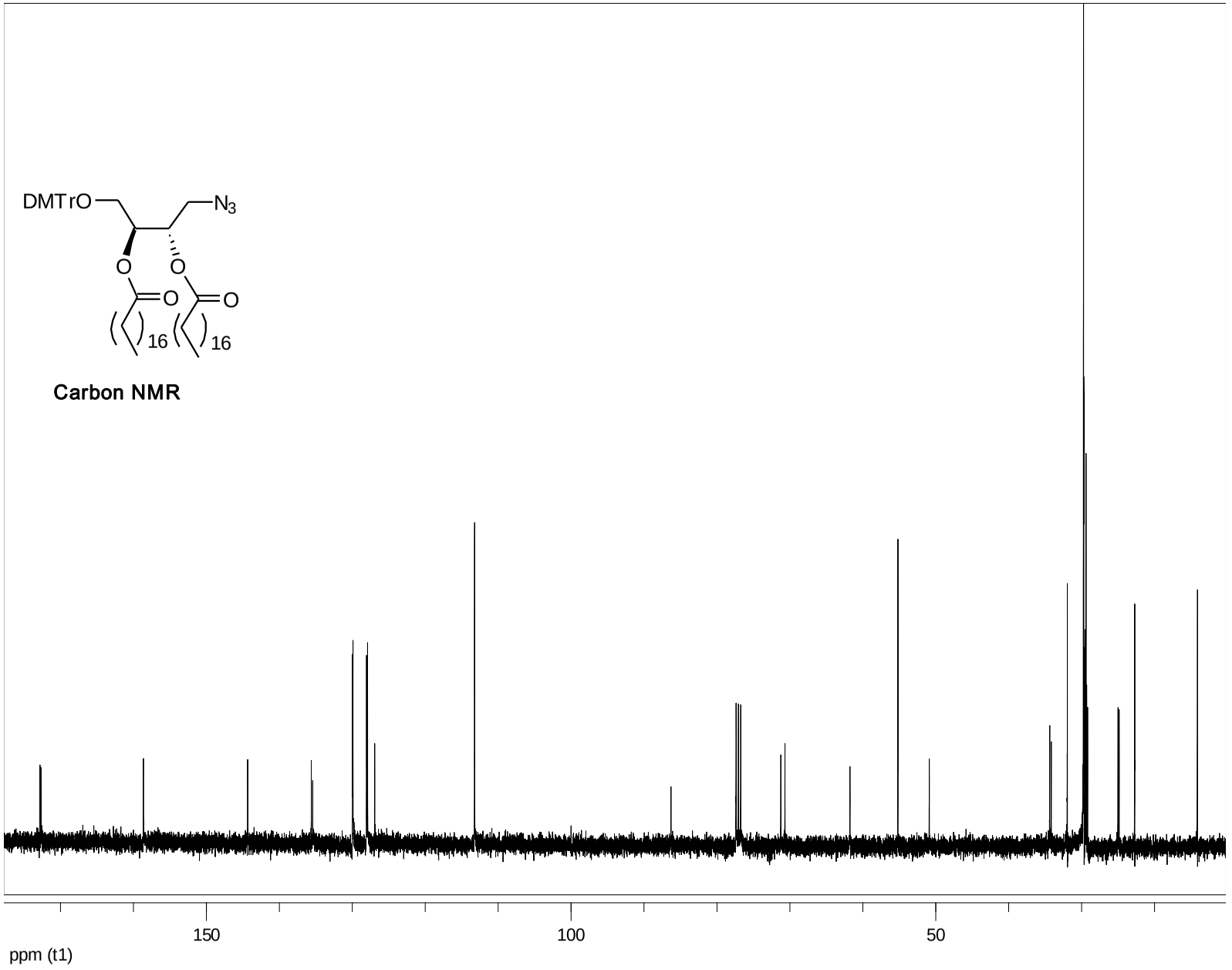
DMTrO
N3
O
O
O
O
16
16
Carbon NMR
150
100
50
ppm (t1)

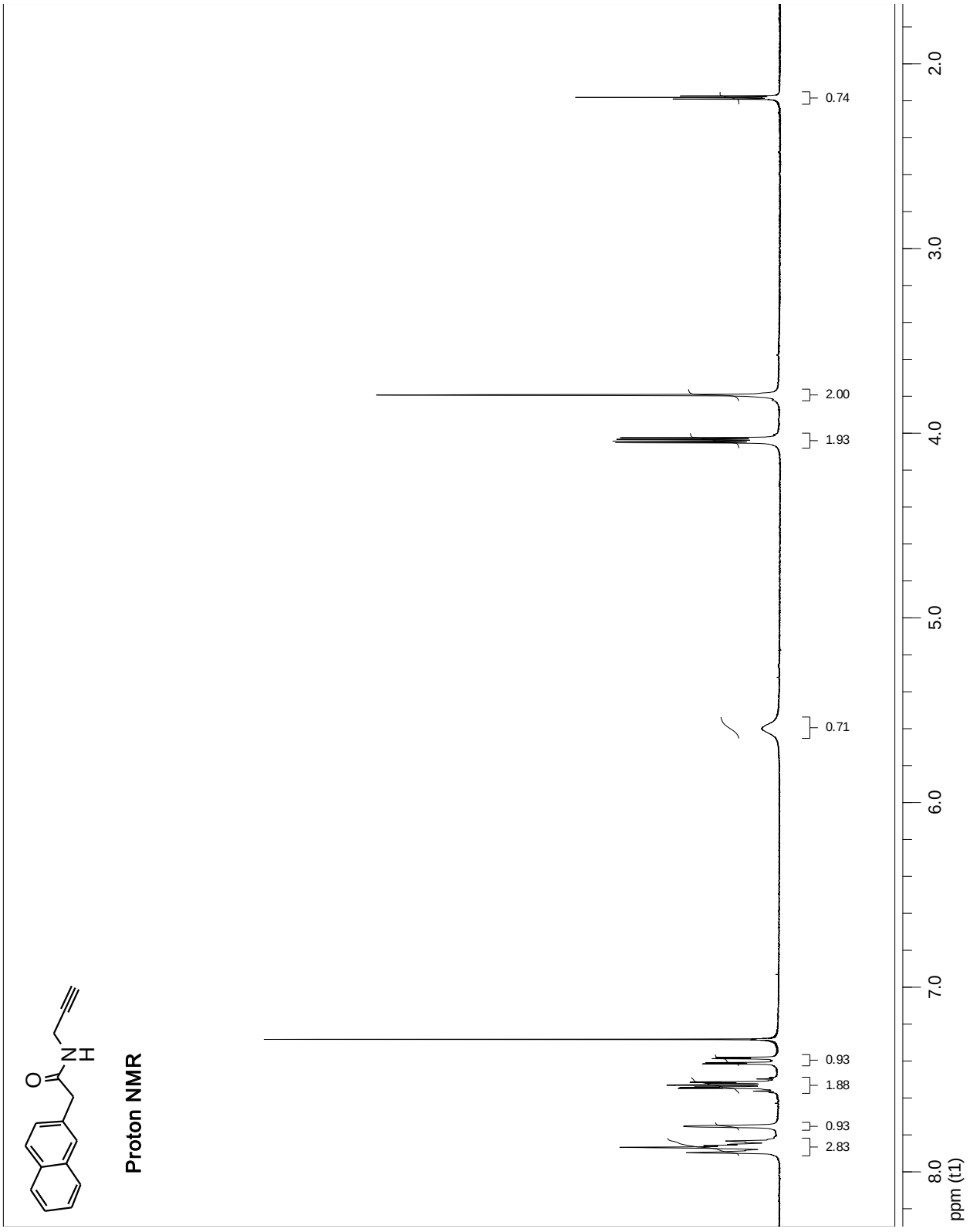
Proton NMR
0.74
2.00
1.93
0.71
0.93
1.88
0.93
2.83
2.0
3.0
4.0
5.0
6.0
7.0
8.0
ppm (t1)

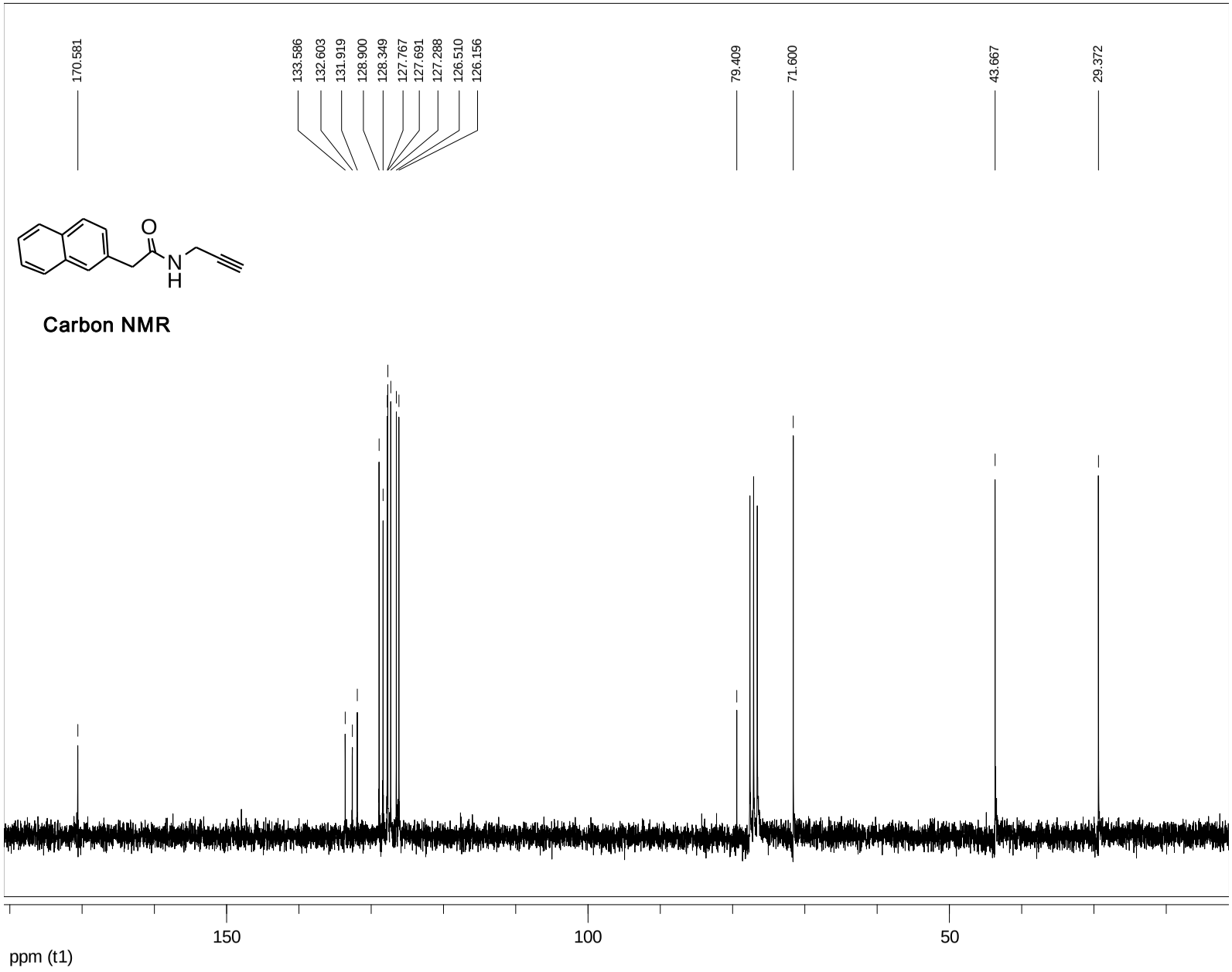
170.581
133.586
132.603
131.919
128.900
128.349
127.767
127.691
127.288
126.510
126.156
79.409
71.600
43.667
29.372
O
N
H
Carbon NMR
150
100
50
ppm (t1)

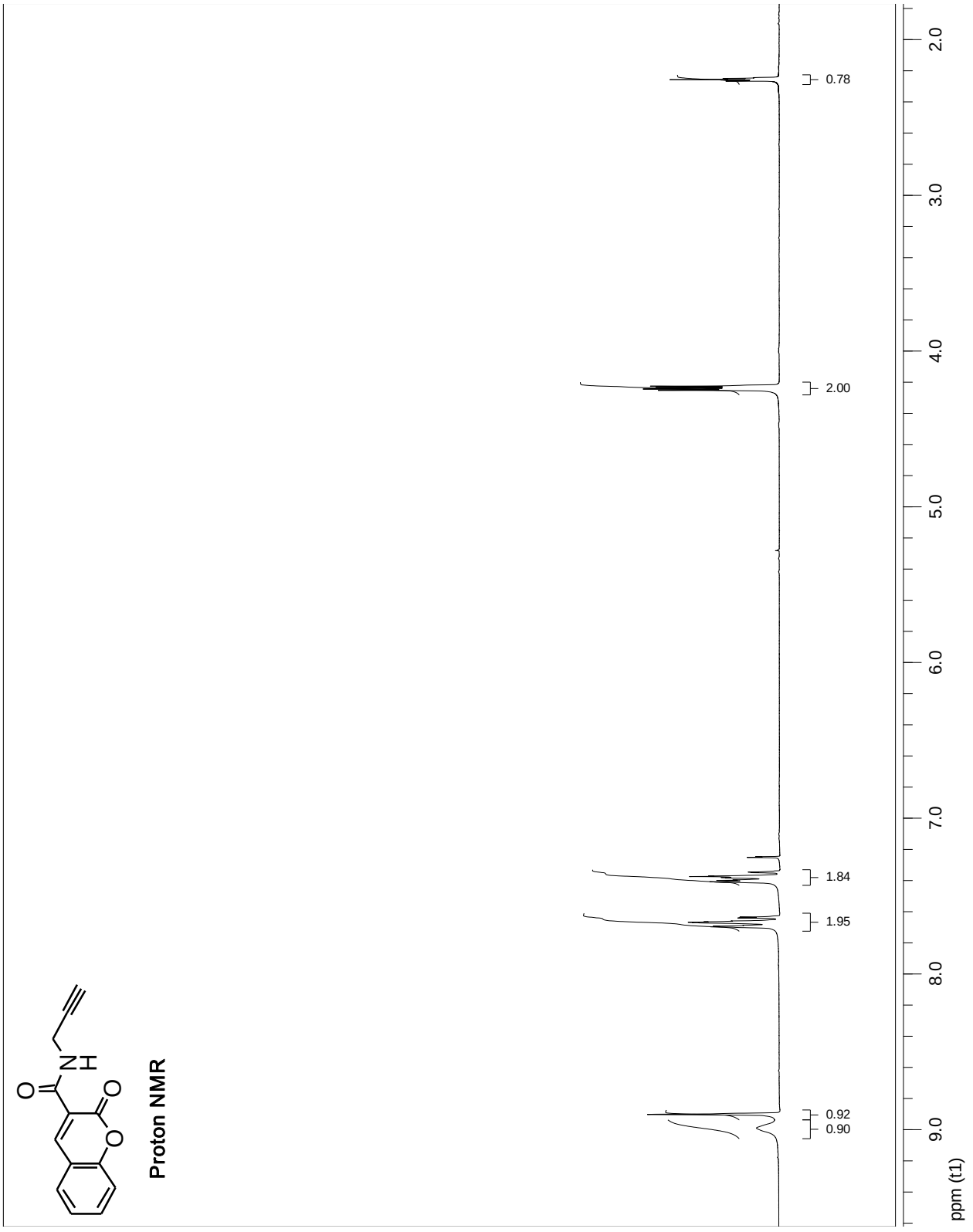
Proton NMR
0.78
2.00
1.84
1.95
0.92
0.90
2.0
3.0
4.0
5.0
6.0
7.0
8.0
9.0
ppm (t1)

161.333
154.526
148.794
134.278
129.890
125.365
118.543
118.021
116.714
79.110
71.627
29.469
Carbon NMR
ppm (t1)
150
100
50

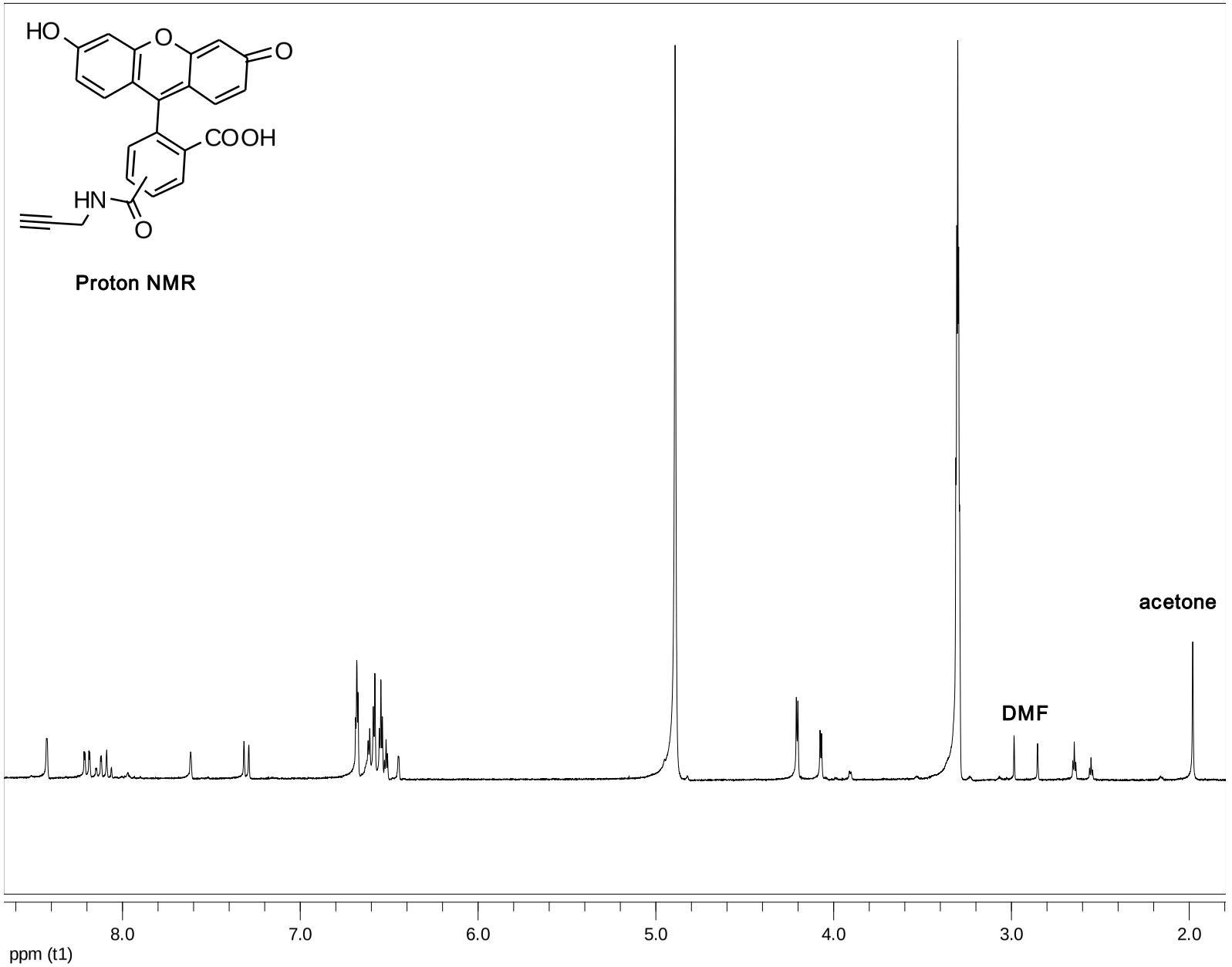
HO
O
O
COOH
HN
O
Proton NMR
acetone
DMF
8.0
7.0
6.0
5.0
4.0
3.0
2.0
ppm (t1)

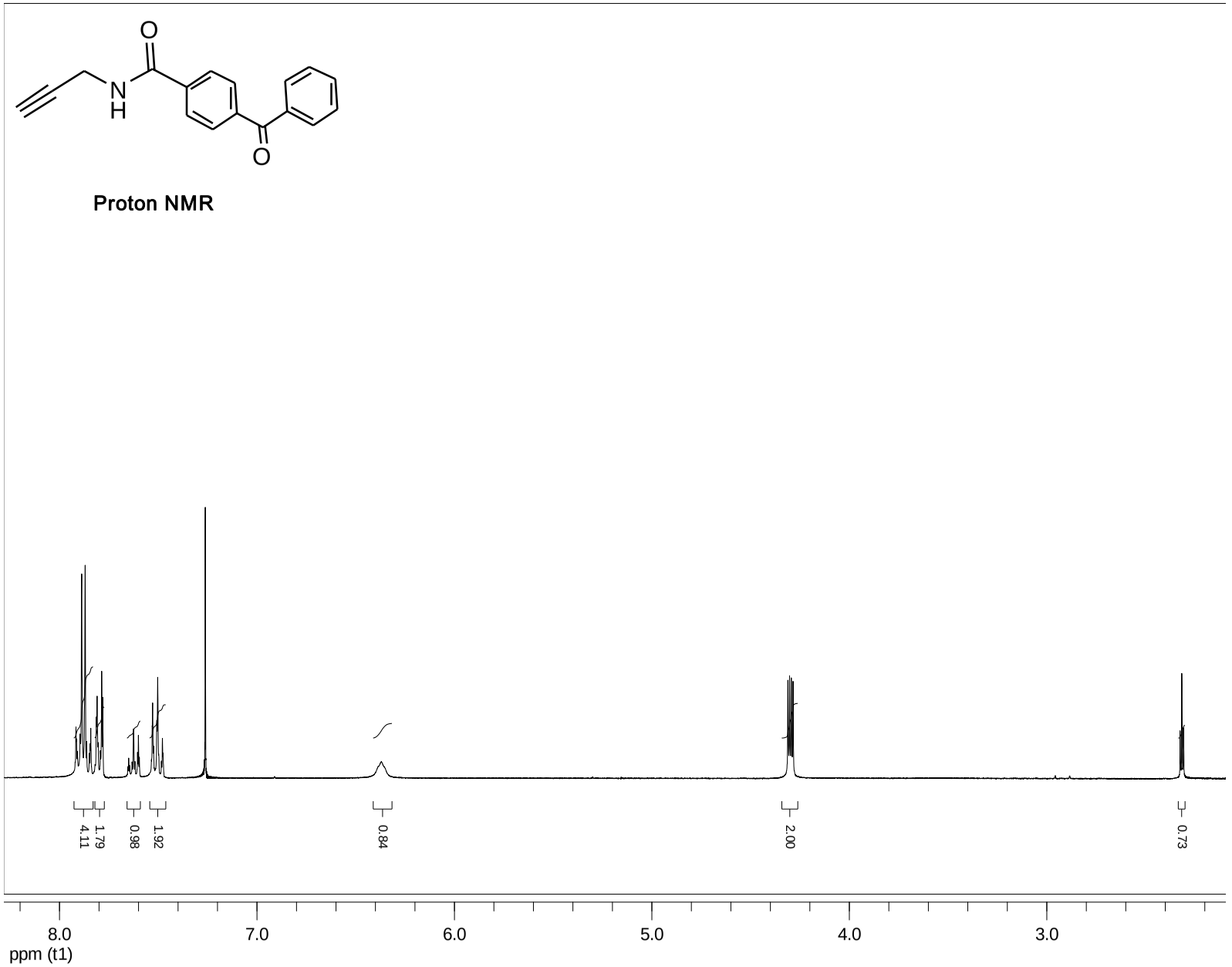
O
N
H
O
Proton NMR
4.11
1.79
0.98
1.92
0.84
2.00
0.73
8.0
7.0
6.0
5.0
4.0
3.0
ppm (t1)

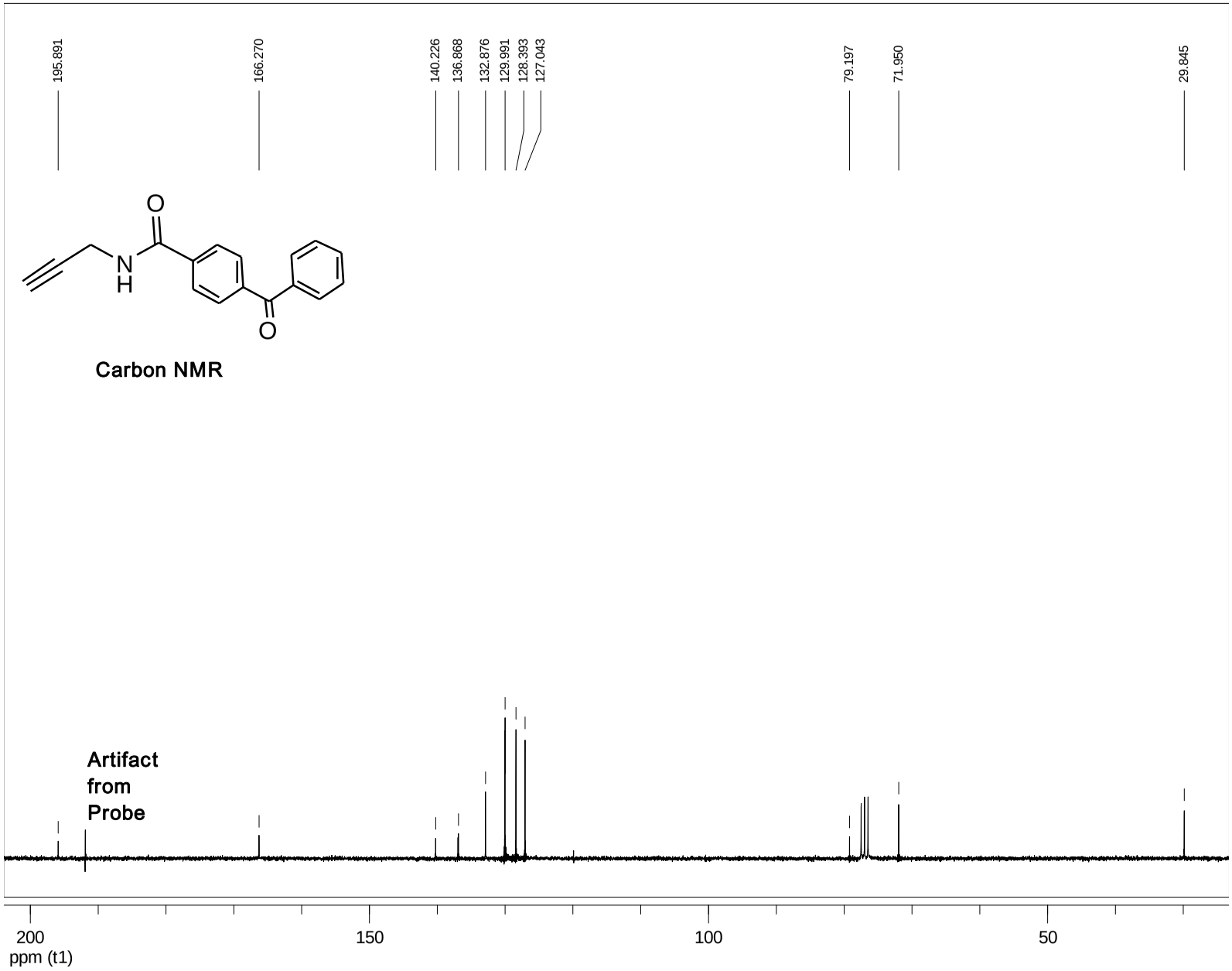
195.891
166.270
140.226
136.868
132.876
129.991
128.393
127.043
79.197
71.950
29.845
O
N
H
O
Carbon NMR
Artifact
from
Probe
200
150
100
50
ppm (t1)

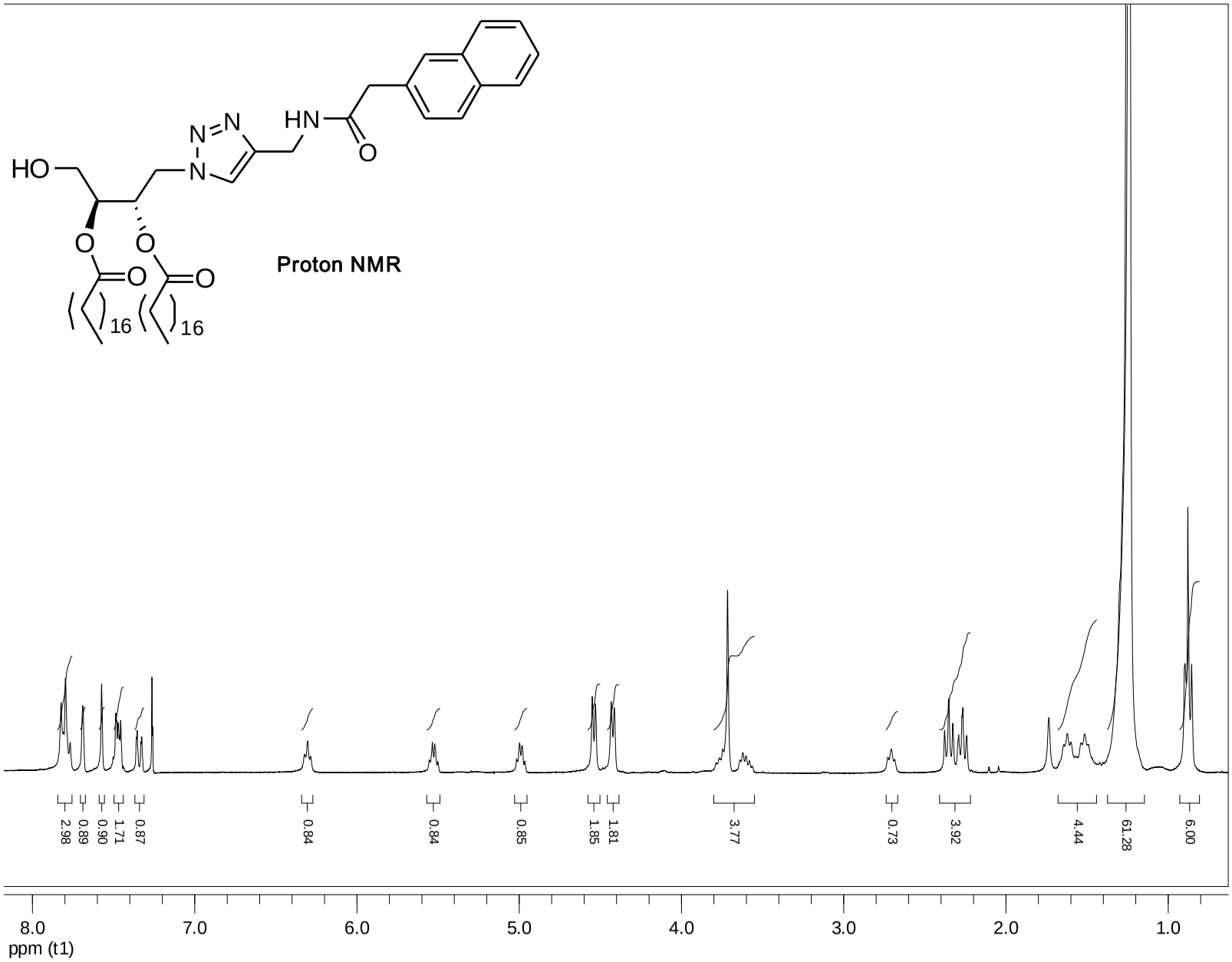
HO
N
N
N
HN
O
O
O
O
O
16
16
Proton NMR
2.98
0.89
0.90
1.71
0.87
0.84
0.84
0.85
1.85
1.81
3.77
0.73
3.92
4.44
61.28
6.00
8.0
7.0
6.0
5.0
4.0
3.0
2.0
1.0
ppm (t1)

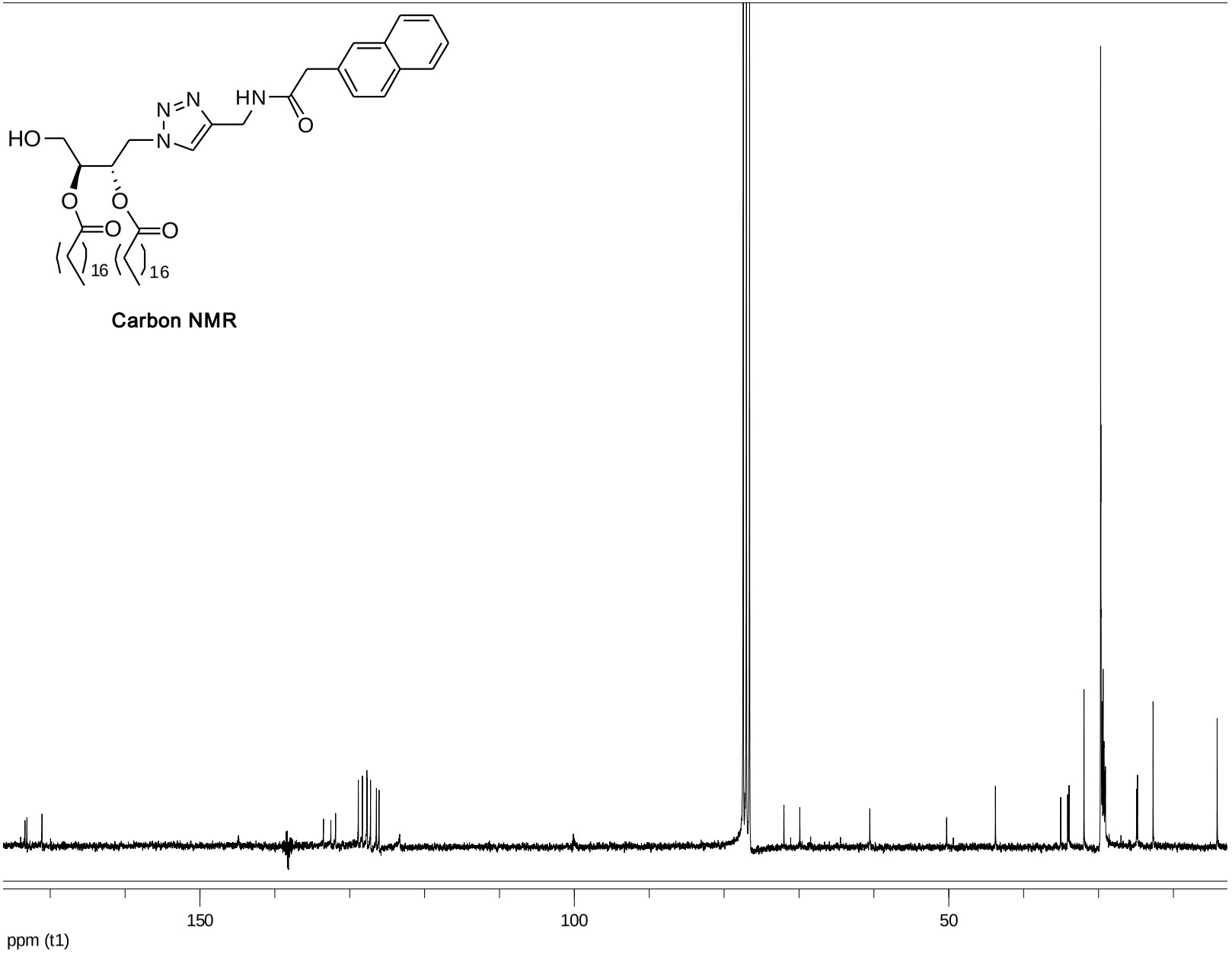

Carbon NMR

69

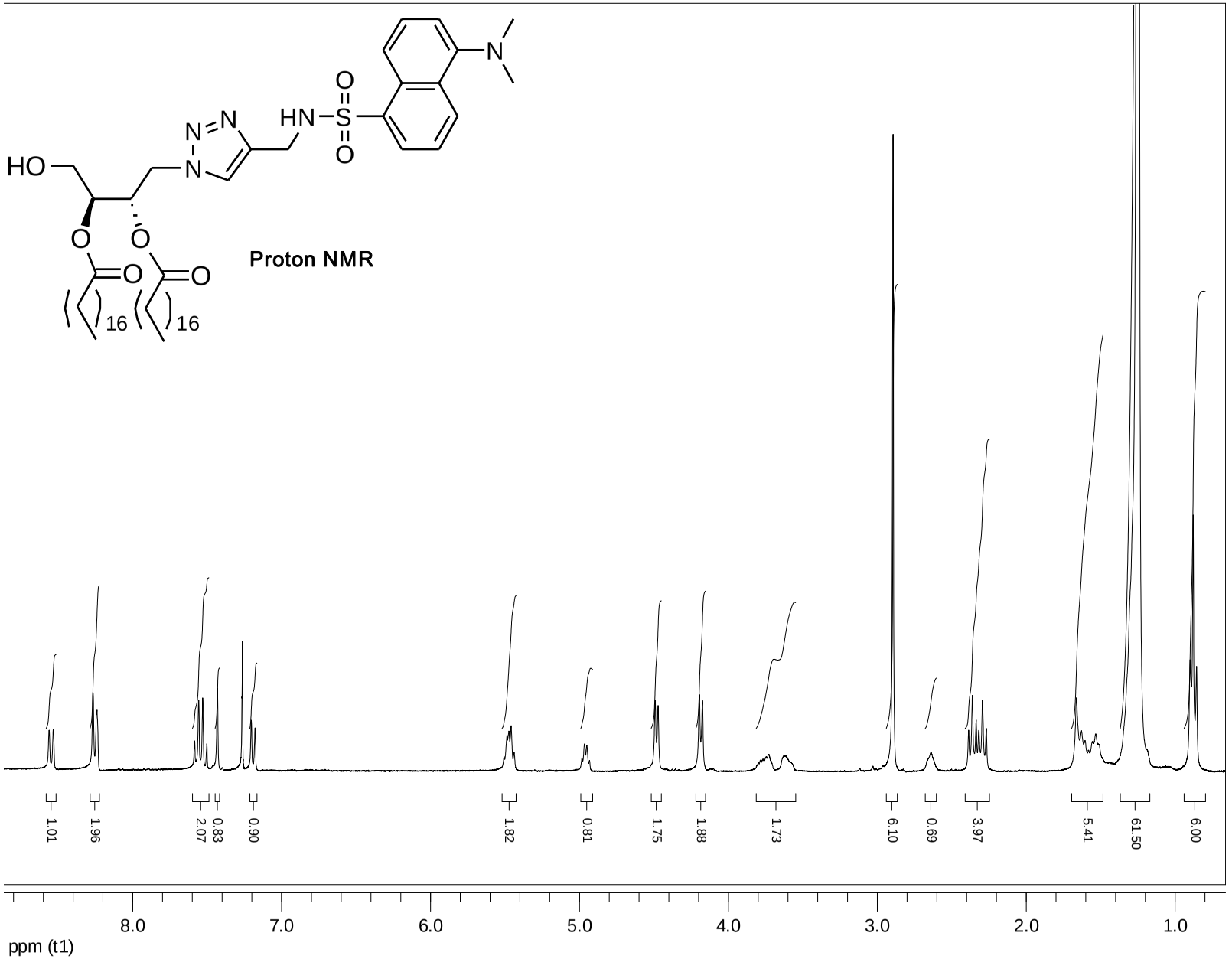
Proton NMR
HO
N
N
N
HN
S
O
O
O
O
O
O
16
16
1.01
1.96
2.07
0.83
0.90
1.82
0.81
1.75
1.88
1.73
6.10
0.69
3.97
5.41
61.50
6.00
8.0
7.0
6.0
5.0
4.0
3.0
2.0
1.0
ppm (t1)

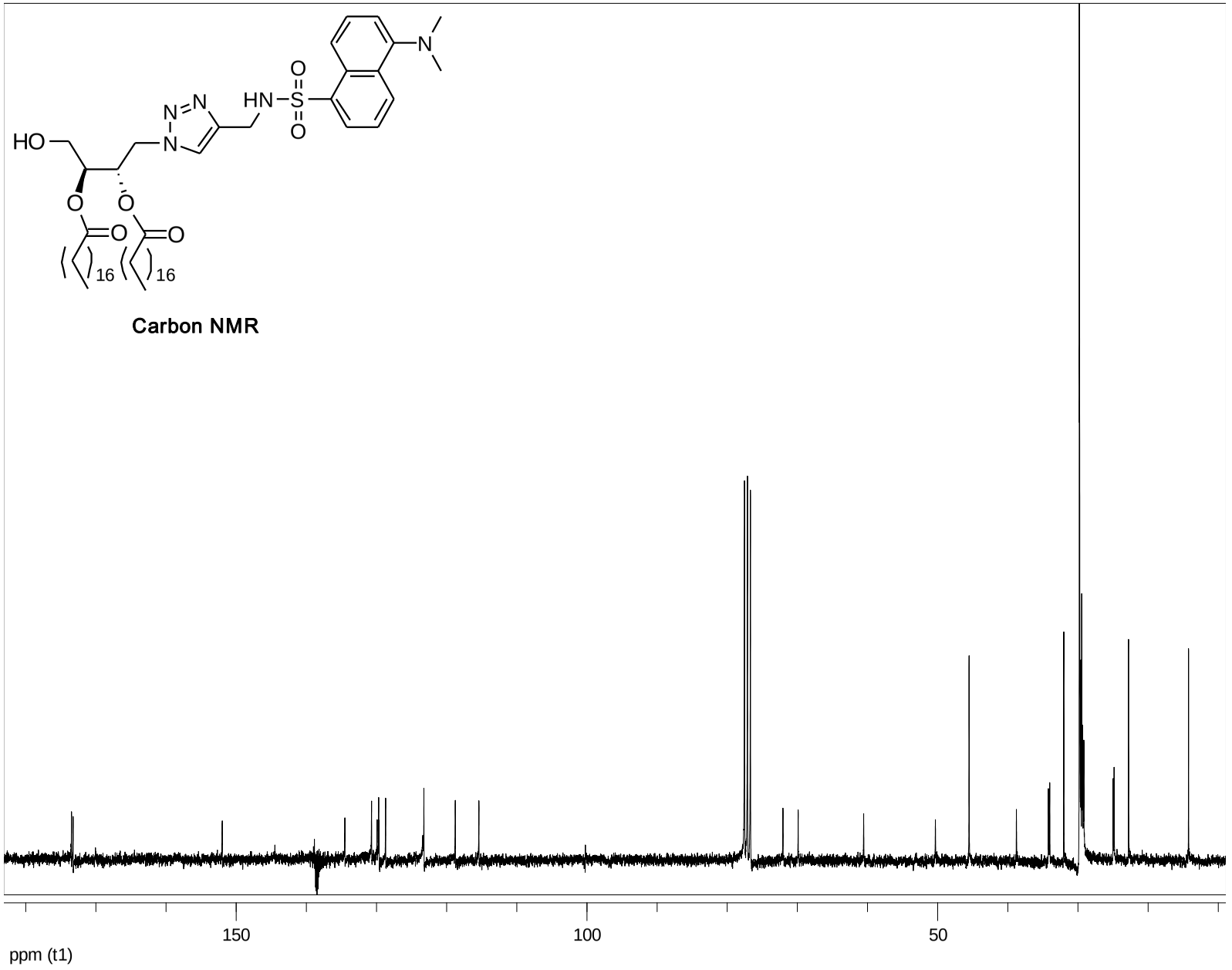
HO
N
N
N
HN
S
O
O
O
O
O
O
16
16
Carbon NMR
150
100
50
ppm (t1)

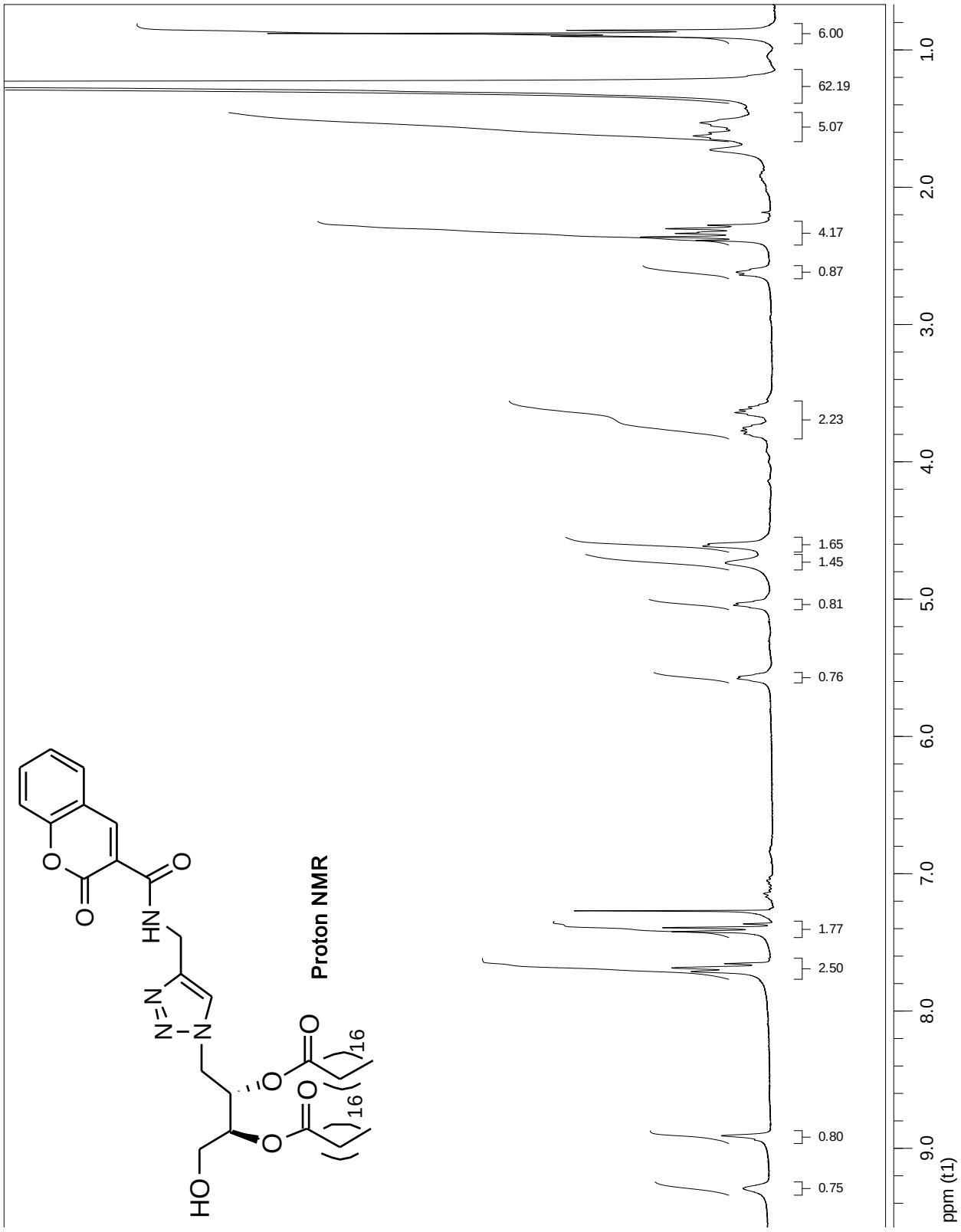
Proton NMR
6.00
62.19
5.07
4.17
0.87
2.23
1.65
1.45
0.81
0.76
1.77
2.50
0.80
0.75
1.0
2.0
3.0
4.0
5.0
6.0
7.0
8.0
9.0
ppm (t1)

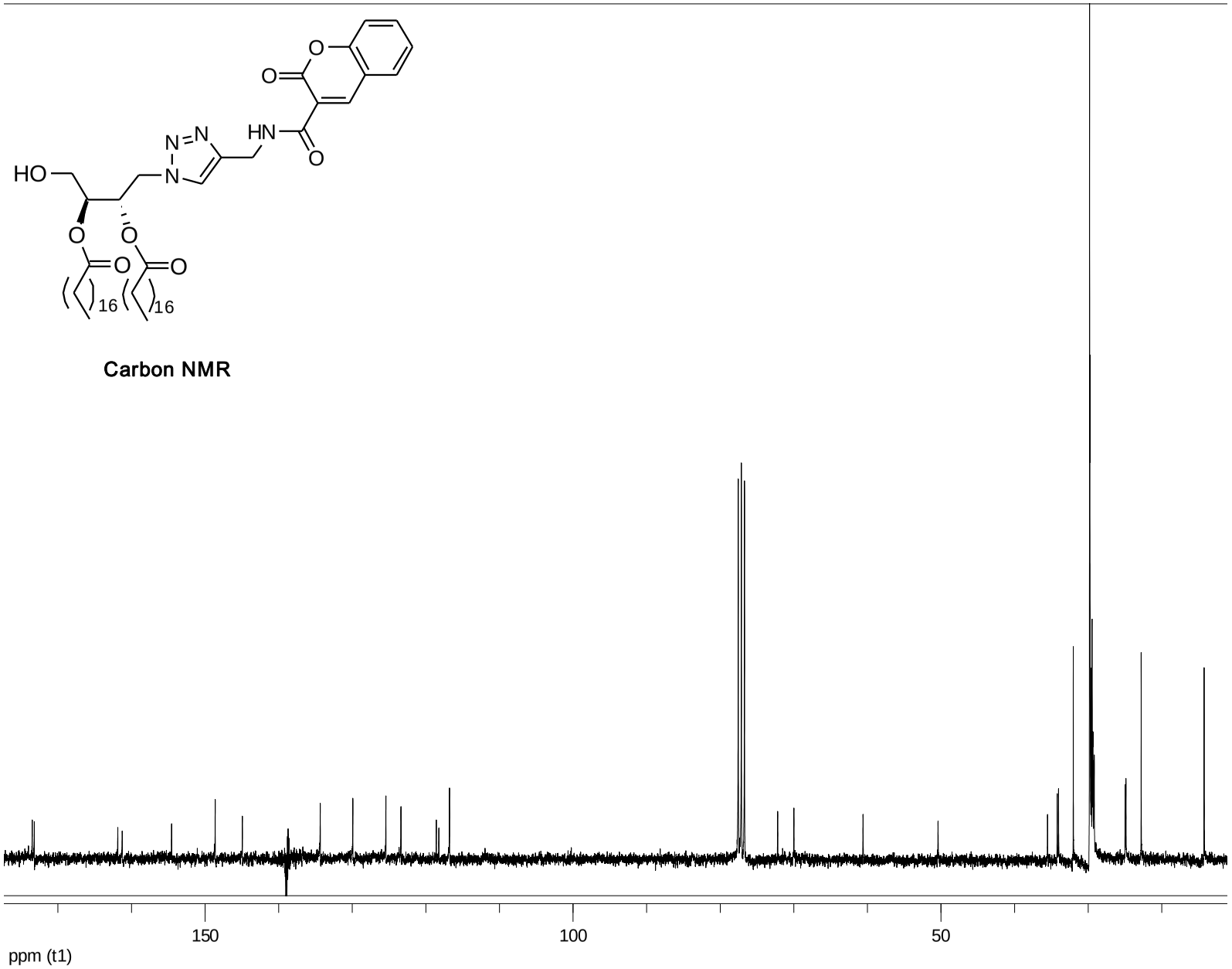

Carbon NMR

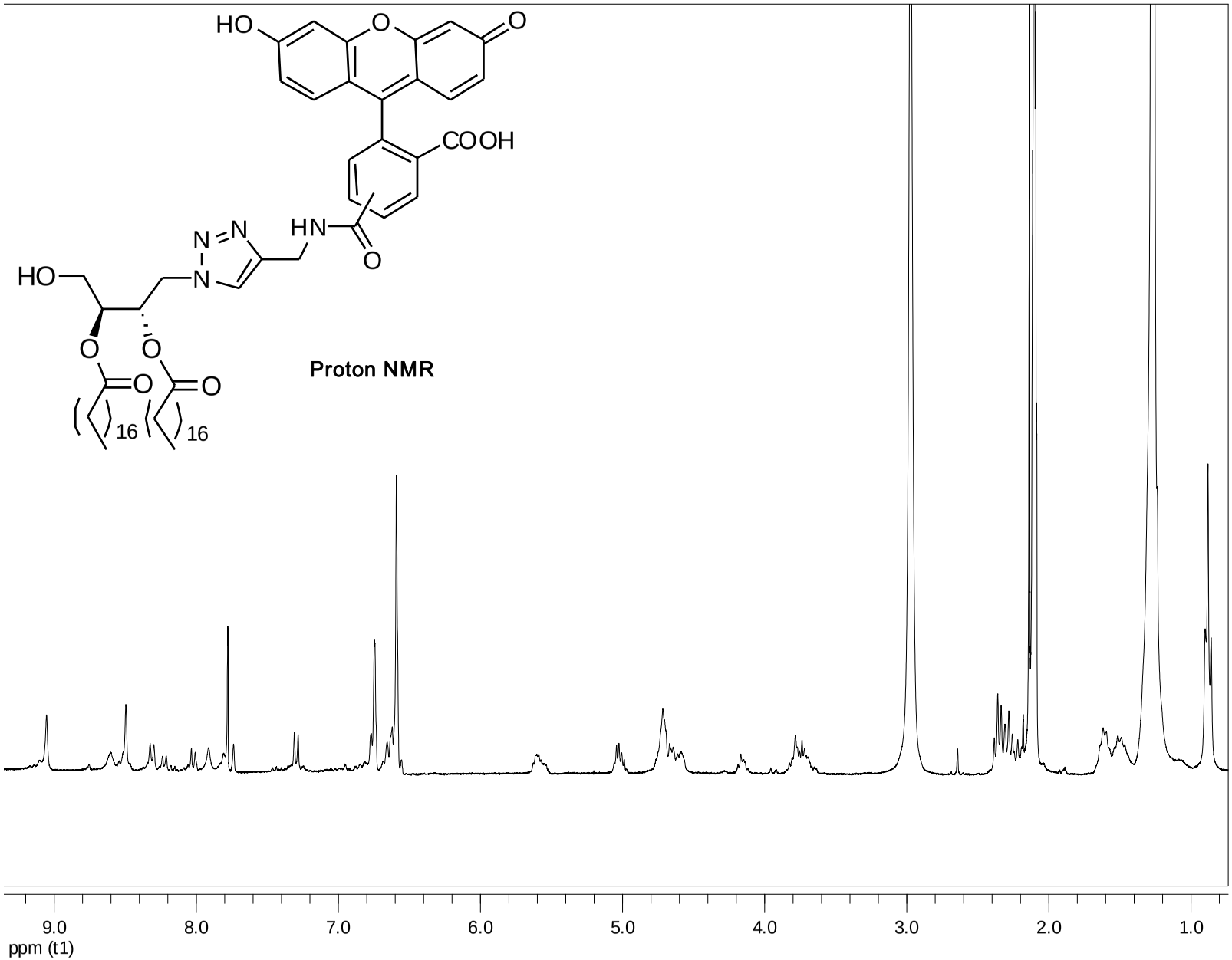
HO
O
O
COOH
HN
O
N
N
N
HO
O
O
O
O
16
16
Proton NMR
9.0
8.0
7.0
6.0
5.0
4.0
3.0
2.0
1.0
ppm (t1)

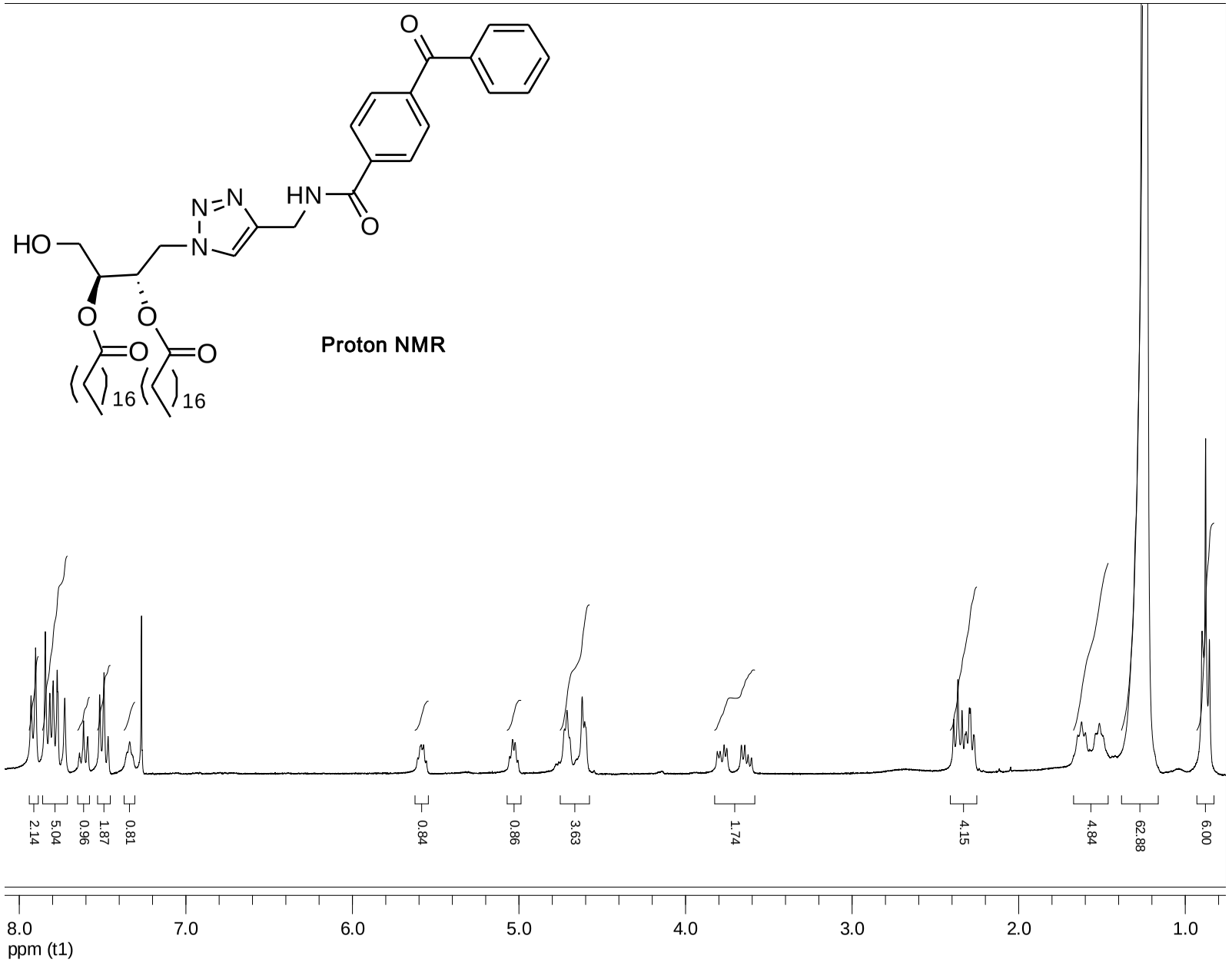
HO
O
O
O
O
O
16
16
N=N
N
HN
O
O
Proton NMR
2.14
5.04
0.96
1.87
0.81
0.84
0.86
3.63
1.74
4.15
4.84
62.88
6.00
8.0
7.0
6.0
5.0
4.0
3.0
2.0
1.0
ppm (t1)

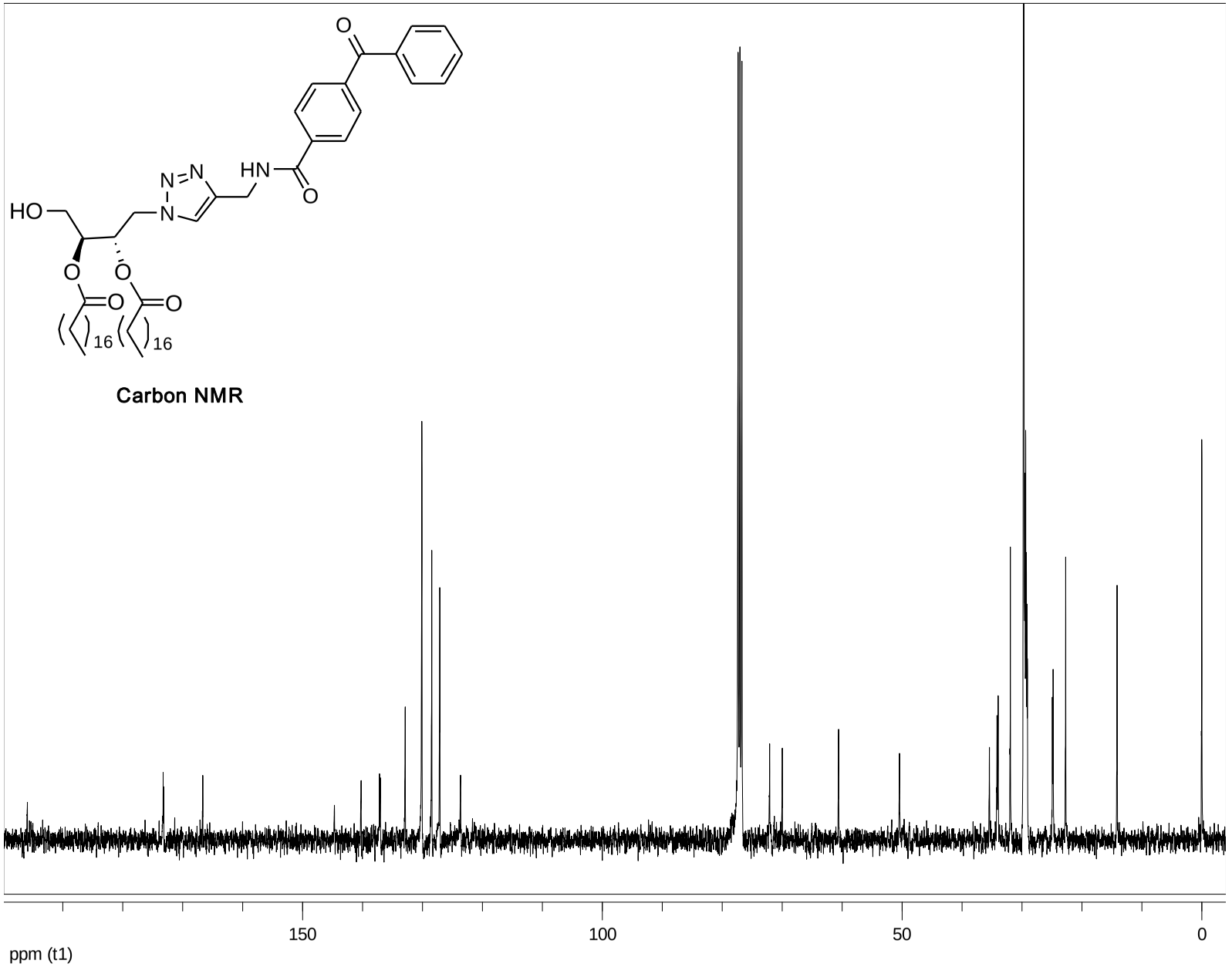
HO
O
O
O
O
16
16
N=N
N
HN
O
O
Carbon NMR
150
100
50
0
ppm (t1)

Chapter 3: Synthesis, Functionalization, and Biological Evaluations of Azide–Labeled Phosphatidic Acid (PA) Analogues for the Modular Access to Lipid Probes

Background and Significance

Phosphatidic acid (PA) is a phospholipid that consists of two acyl chains at the *sn*-1 and *sn*-2 positions and a phosphomonoester (phosphate group) at the *sn*-3 position. PA is generated and consumed by different methods within the cell, depending upon the specific application for which it is to be used (Figure **3.1**).[6] One method for the generation of PA involves the reaction between glycerol 3-phosphate (G3P) and fatty acyl CoA. PA generated via this route constitutes biological stores of the lipid that are used in the synthesis of other lipids such as phosphatidylcholine (PC), phoshatidylserine (PS) and the phosphoinositides (PIP_ns).[5-7] PA can also be produced from other lipids, such as through the cleavage of the choline group from PC by phospholipase D (PLD) or the hydrolysis of various phospholipids to produce diacylglycerol (DAG), which is then phosphorylated by diacylglycerol kinases (DGK). PA that is produced via these processes is generally involved in signaling pathways and the recruitment of proteins to the membrane surface. Despite the simplicity of its structure, PA has emerged as an important signaling lipid involved in several physiological and pathophysiological processes.[5-7, 79, 80] Interactions between these signaling lipids and their receptors are often connected to disease onset, and in fact, PA has been linked to

Figure 3.1. Various synthetic routes of PA. This figure has been adapted from reference **6**. Blue arrows indicate generation and consumption of PA for biosynthetic purposes. Red arrows indicate processes that utilize PA as a signaling lipid.

carcinogenesis through its indirect involvement with Ras enzymes.[79, 80]

There are currently a number of known PA receptors[6, 7] including protein kinases[81-83], protein phosphatases[84-86], and cAMP-specific phosphodiesterases.[87, 88] By far, the best studied and characterized PA receptor is Raf-1 kinase. Binding of Raf-1 kinase to PA facilitates association of the protein with the membrane, which brings it into proximity with Ras GTPase. This protein-protein interaction activates Raf-1 kinase and leads to the initiation of the Ras/Raf/MEK/ERK cell proliferation pathway[89-96]. It is also known that the C2 domain of certain protein kinase C isozymes, such as PKCα[97] and PKCε,[98] have affinity for PA. Study of these interactions is important as the PKC family is known to be heavily involved in cancer.[19, 58, 60]

Despite this recent increase in the number of known PA receptors, there is still much to be learned as to how a simple lipid such as PA can play such a profound role in cellular pathways, and bind receptors with such high specificity. de Kruijff and coworkers have proposed an electrostatic/hydrogen bond switch mechanism in attempts to explain these principles.[99, 100] Monodeprotonated PA is stabilized by an intramolecular hydrogen bond that preserves the -1 charge. Basic residues in proteins/peptides are attracted to the negatively charged membrane surface through electrostatic interactions with the PA. Once bound to the surface, the basic side chains can form hydrogen bonds to the PA headgroup, which immediately leads to full deprotonation (-2 charge on PA). This increase in negative charge enhances the attractive forces between the amino acid and PA and results in the specificity related to PA receptors. Another factor believed to contribute to the specificity and binding of PA

receptors is the shape of PA.[100] At physiological pH, PA exists as a cone-shaped lipid. As a result of its shape, PA lies below the membrane surface in the interfacial region which is mildly polar.[23] This aspect is thought to enhance the penetration of hydrophobic residues into the membrane around the PA binding domain. Indeed, both aspects seem viable in terms of explaining the specificity observed for PA by its receptors as the PA binding domains in Raf-1 kinase,[90, 91, 100] PKCα,[97] and PKCε[98] all contain basic amino acids that have been deemed crucial for PA recognition as well as hydrophobic residues that penetrate the membrane upon binding.

Despite these advancements in understanding the actions of PA as a ligand, the full scope of PA-targeting proteins is not yet clear. The number of identified receptors is still relatively small compared to the biological processes that show PA-dependence. A primary complication in the discovery of PA-binding proteins is that these receptors generally do not possess conserved domains that can be employed for sequence homology searching.[6, 7, 10] The PA binding domains established to date are diverse and consist of sequences that were not previously known the bind lipids.[6, 7] In fact, the only common link that many of the PA binding domains share are small clusters of basic (Arg, Lys, Trp) amino acids.[6, 7, 10, 100] However, this feature alone can not sufficiently explain the high specificity of these domains for PA over other lipids bearing negative charge.[6, 7, 100] Such lipids are often significantly more abundant than PA and attempts at determining proteins that bind PA based solely on sequence holomogy searching often leads to the misidentification of PA receptors.[6, 100] Due to this inability to discover PA-binding receptors via structure searches, experimental approaches are crucial for

elucidating binding interactions. As such, chemical probes are vital for studying and characterizing protein–PA binding interactions at the molecular level. Generation of probes from scratch has several benefits including the ability to purify to homogeneity at the end of the synthesis, the ability to incorporate reporter tags that will allow the investigation of the event in any way one chooses, and that it is often much more cost efficient than modifying natural lipids. Despite these advantages, the synthesis of lipid probes has been rarely pursued due to the required synthesis.[32]

Synthetic PA probes have previously proven effective for probing receptors that target this lipid (figure **3.2**). For example, Gadella and coworkers developed a caged PA analogue that was used to induced flagellar excision in algae.[101] Here, the introduction of a 2-nitrophenylethyl (NPE) caging moiety allowed the probe to cross the membrane, and photolysis produced an increase of PA within the cell that caused a decrease in the swimming of the algae. In this case, commercially available lipids were used as precursors to the caged probes. Picq and coworkers developed a photoaffinity-tagged PA probe that was used in the covalent labeling of type 4 cAMP-phosphodiesterases (PDE4).[30] The photoaffinity label was incorporated into the acyl tails, which is effective for proteins that interact significantly with lipid chains buried within the hydrophobic membrane core. Probe synthesis again utilized commercial lipids as precursors and enzymatic installation of the PA headgroup. Ktistakis and coworkers have designed a fully synthetic PA probe that was attached to beads via an amine incorporated into the *sn*-1 acyl tail.[28, 29] The resulting PA-functionalized resin was employed for affinity chromatography to selectively purify receptors that target this lipid. While efficient in the

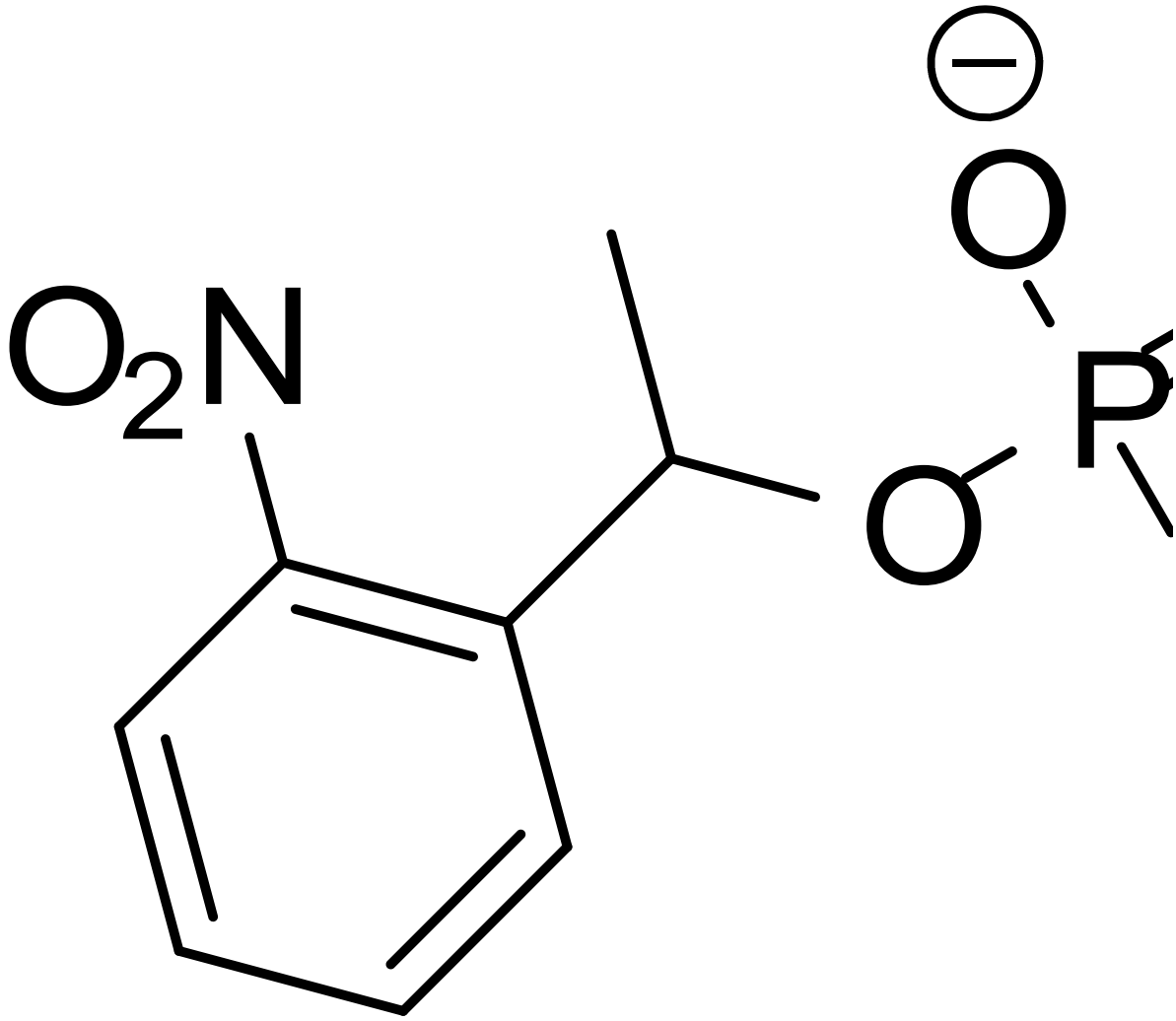

Figure 3.2. General structures of currently developed PA-based probes.

analysis of certain PA receptors, this particular probe can not be incorporated into a membrane-type environment, and therefore not all PA receptors will bind to it.[6] Stabilized derivatives of PA, such as fluoromethylene phosphonate analogues developed by Prestwich and coworkers, have been shown to be capable of activating the mTOR pathway.[102] Schultz and coworkers have developed PA probes with terminal alkynes and cyclooctynes attached to the acyl tail, which have proven effective for the fluorescence labeling of lipids in cells.[45]

While each example has proven capable of investigating PA activity through interactions with various receptors or monitoring its movement within the cell, a modular scaffold that will allow easy access to a wide range of PA probes still remains undeveloped. Also, based upon the results obtained with our DAG analogues, we feel that the *sn*-1 position is a prime location of the installation of a reporter molecule. Installation of such a tag at any location of the headgroup is a characteristic absent in each example presented above.

Synthesis of PA-based Lipid Probes

The development of lipid probes is crucial to further the understanding of protein-lipid binding events, as such probes allow investigation of the binding on the molecular level via the incorporation of appropriate reporter molecules. Generation of these probes from scratch is particularly advantageous as it reduces the cost of the probe, allows the incorporation of an array of reporter molecules, and purification allows a single compound to be obtained and utilized in biological studies. However, the

synthesis of such probes is difficult, and therefore few accounts synthetic probes exist.[32]

Following the development of an efficient and modular approach for diacylglycerol (DAG)-based probes,[103] we sought to extend this same methodology towards the synthesis of a litany of PA-based probes from a common scaffold **(3.3.1)**, as shown in figure **3.3**. However, initial attempts at direct installation of a protected phosphate headgroup onto the DAG scaffold proved to be problematic. The phosphoramidite chemistry used to install the phosphate headgroup is not as mild as the "click" chemistry used for DAG modification. Thus, a significant amount of *sn*-2 to *sn*-3 acyl migration was observed, forcing us to redesign the synthesis so as to incorporate the headgroup prior to introducing the acyl tails.

In order to install the headgroup early in the synthesis, we initially attempted to utilize intermediate **2.7.13** from the DAG synthesis as shown in figure **3.4**. However, phosphotriester **3.4.3** was difficult to purify due to co-elution with byproducts. Furthermore, acidic removal of the acetonide protecting group afforded only approximately 10% of diol **3.4.4**. Presumably, the electron withdrawing properties of the phosphotriester deter protonation of the oxygen during the first step of the deprotection. Attempts at forcing the deprotection, such as heating in 90% acetic acid, led to decreased yields and decomposition of the phosphotriester. In order to circumvent the low yield, we turned our focus towards other 1,2-diol protecting groups that are more efficiently cleaved.

The new approach, shown in figure **3.5**, began with commercially available diethyl-L-tartrate **2.4.2**. Following installation of the cyclopentylidene acetal to furnish

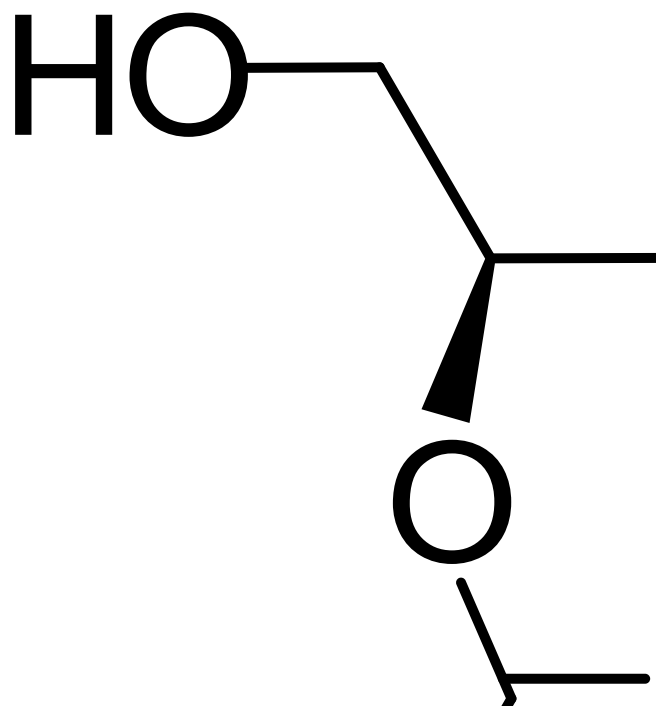

Figure 3.3. Scaffolds for DAG and PA lipids possessing an azide as a synthetic handle for the modular access to a library of probes.

Figure 3.4. Initial attempts at early installation of the PA headgroup.

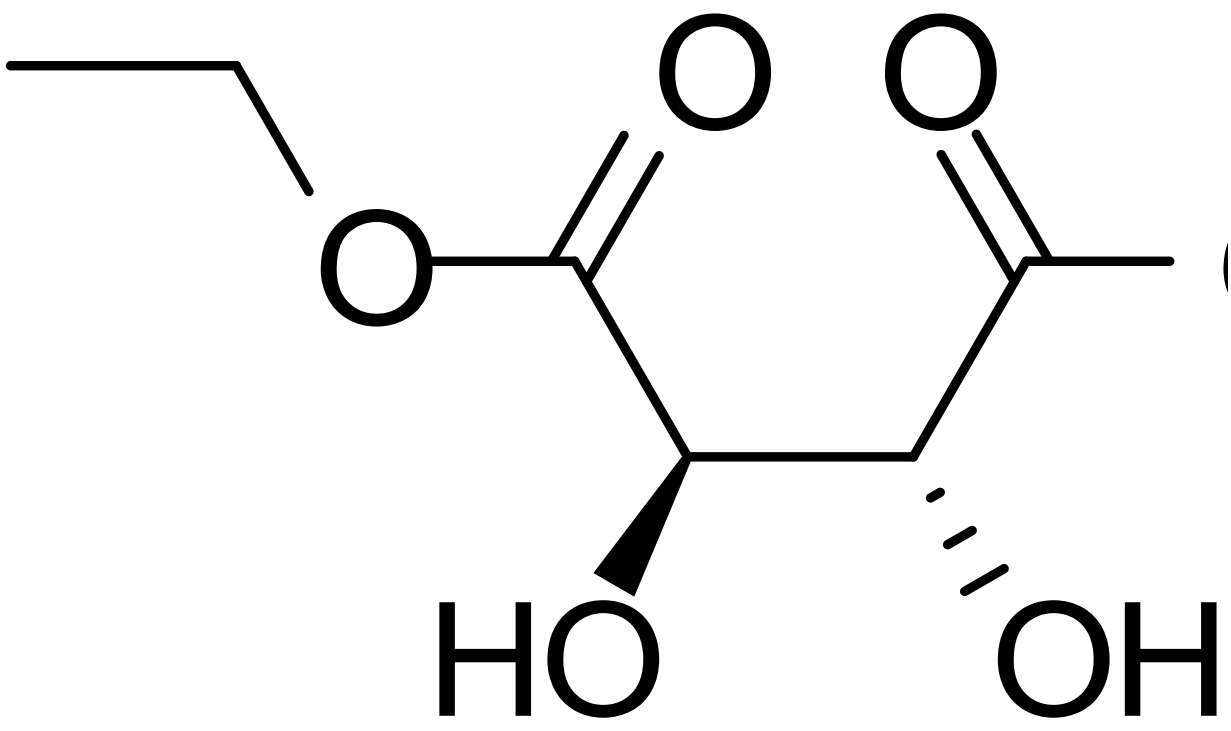

Figure 3.5. Synthesis of protected azido PA probes incorporating early installation of the headgroup.

3.5.5, the esters were reduced to provide the bis-hydroxymethyl intermediate **3.5.6**.[32, 103] Mono-tosylation followed by direct conversion to the azide[73, 103] furnished **3.5.7**. The headgroup, which was protected as a phosphotriester, was installed using dibenzyl diisopropylphosphoramidite **3.4.2** to afford **3.5.8**. Removal of the cyclopentylidene acetal under acidic conditions was then employed to generate diol **3.4.4** in 52% yield. The ester tails were then coupled on to the diol using standard coupling reagents to produce protected PA scaffold **3.5.9**.

While the cyclopentylidene acetal was a better choice of protecting group for the diol than was the acetonide, we sought to determine if it was the optimal choice. Therefore, a variety of protecting group strategies shown in figure **3.6** were attempted in hopes of improving the deprotection yield. Initially, the *p*-methoxybenzylidene (PMP) analogue **3.6.10** was synthesized. However, the *m*-CPBA oxidative conditions required to install the phosphotriester and afford compound **3.6.11** led to partial deprotection of the PMP group. The use of milder oxidants also facilitated partial deprotection. Focus was then turned towards the individual protection of each alcohol. Attempts at installing two *p*-methoxybenzyl (PMB) groups onto the diol of **2.4.2** to furnish **3.6.12** were unsuccessful due to steric hindrance and side product formation. While two silyl groups could be installed on the diol of **2.4.2** to yield **3.6.13** following literature procedures,[104, 105] they were subsequently removed during the reduction of the ester groups in attempt to access **3.6.14**. While compounds **3.6.15**[106] and **3.6.17** could be synthesized, attempts at the bis-silylation of each to furnish **3.6.16** and **3.6.18,** respectively, were again unsuccessful due to steric hindrance. Thus, after exhausting all potential possibilities for

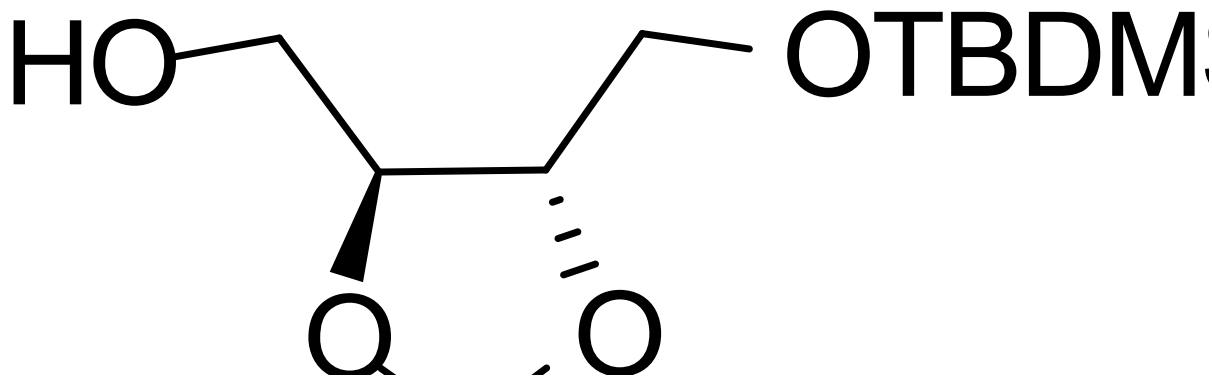

Figure 3.6. Diol protecting group strategies attempted in the optimization of PA scaffold **3.5.9**.

diol protections tolerant of other functionalities present in the core structure, the decision to return to the cyclopentylidene acetal was made, as it was the most efficient approach attempted.

Having developed an efficient synthesis for protected PA scaffold **3.5.9**, we now sought to derivatize the core scaffold utilizing the reactive azide tag in order to obtain a litany of PA probes. Following the reasoning and methods set forth in the synthesis of DAG-based probes,[103] we again chose to modify the azide via “click” chemistry. The route for obtaining PA probes via modification of **3.5.9** is outlined in figure **3.7**. Initial introduction of a variety of reporter molecules was accomplished through cycloaddition of **3.5.9** with multiple alkynes (**2.8.17a-c, e; 3.7.19d**).[103] The functionalized protected PA scaffolds **3.7.20a-e** were then deprotected with bromotrimethylsilane (TMSBr) and ion exchange was performed to produce the ammonium salts of PA probes **3.7.21a-e**. Functionalization prior to benzyl deprotection was determined to be optimal as benzyl deprotection followed by cycloaddition conditions produced no observed product (**3.7.21a-e**). Likewise, TMSBr deprotection of the benzyl groups was superior to hydrogenolysis for several reasons. First, the hydrogenolysis reactions never went to completion, even after prolonged reaction times. Second, it was observed that the benzophenone moiety was reduced to the corresponding alcohol under such conditions. Thus, TMSBr removal provided quick and efficient deprotection of the benzyl groups in one hour and maintained a uniform synthetic procedure for all PA probes **3.7.21a-e**. This strategy was efficient in obtaining a variety of PA probes modified with fluorescent tags (naphthyl (**3.7.21a**), dansyl (**3.7.213b**), coumarin (**3.7.21c**), and rhodamine

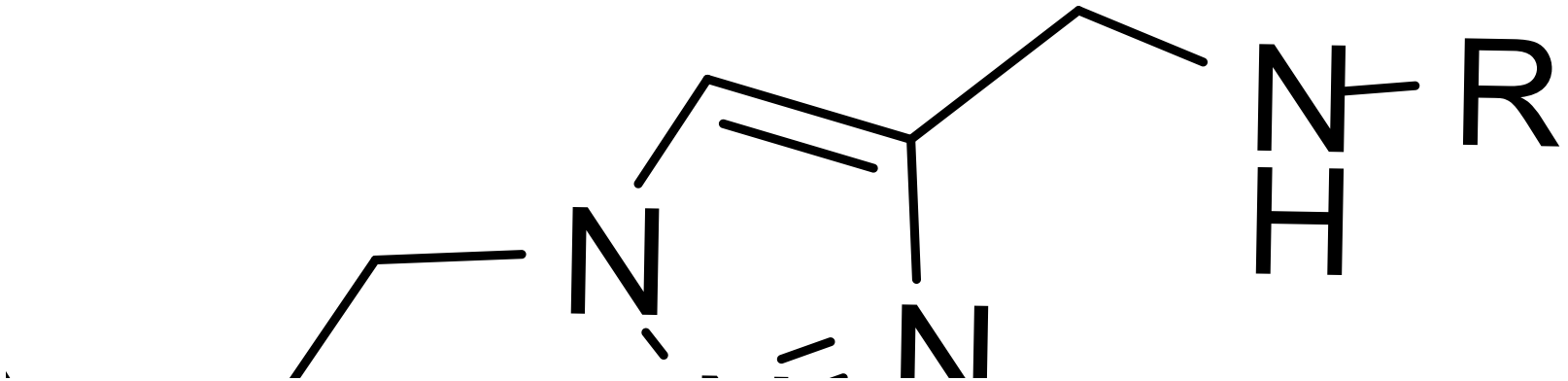

Figure 3.7. Derivatization of protected PA scaffold **3.5.9** via “click” chemistry to furnish a variety of PA probes.

(**3.7.21d**)) as well as a photoaffinity tag (benzophenone (**3.7.21e**)). The fluorescent analogues were designed such that various Förster resonance energy transfer (FRET) pairs were included. Since FRET is highly dependent upon the distance between donor and acceptor,[46-50, 107-109] these probes will be highly useful in detecting changes in proximity of the molecules upon protein binding. Installation of the benzophenone tag will be utilized in photo-cross-linking studies[51] in order to characterize and map binding sites of PA receptors.

As discussed earlier, the primary hindrance to the discovery of new PA receptors is the lack of a consensus sequence of the PA binding domain. A common approach for the identification of new enzymes is activity based protein profiling (ABPP).[110-118] In ABPP, probes are designed that target enzymes based upon their activity. As such, a multitude of new proteins can be targeted and identified from a complex mixture. Most ABPP probes contain a crosslinking group for attachment to the protein, along with a secondary reactive tag that allows detection or isolation of the covalently linked receptor–probe. New lipid receptors can be rapidly identified from the same complex mixture of proteins using a similar approach in which bifunctional lipid probes are designed. For example, de Kroon and coworkers have developed such probes derived from the structure of PC.[27] Each probe contains a crosslinking group along with a secondary azide tag for chemical modification and purification/detection.

Therefore, we sought to design a bifunctional probe utilizing the azido PA scaffold **3.3.1**. Figure **3.8** outlines the synthesis of an alkyne (**3.8.19f**) that was utilized in development of the activity based probe. Commercially available lysine precursor

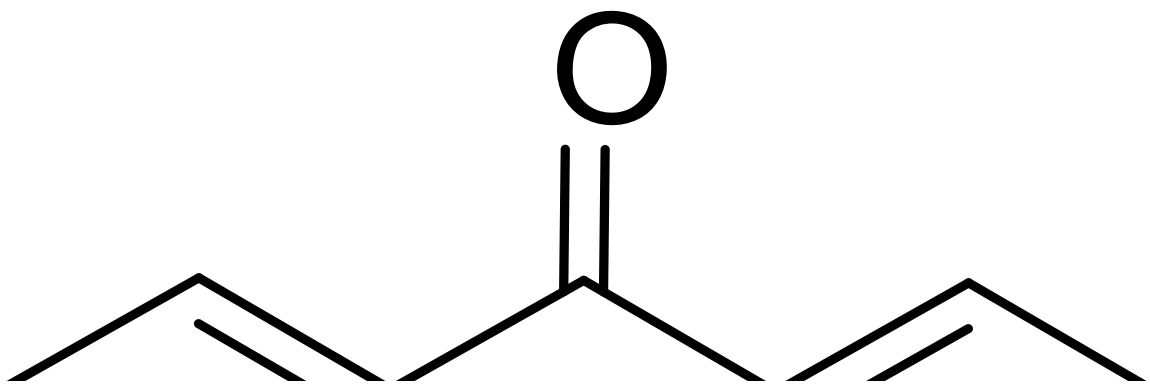

Figure 3.8. Synthesis of alkyne **3.8.19f** for incorporation into a bifunctional PA probe.

3.8.22 is subjected to hydrogenolysis to remove the carbobenzyloxy (Cbz) N-terminal protecting group, followed by coupling to 4-benzoylbenzoic acid to furnish intermediate **3.8.23**. Hydrolysis of the methyl ester followed by coupling with propargyl amine yielded alkyne **3.8.19f**.

Having installed the photoaffinity label for cross-linking capability and the alkyne for attachment to the azido PA scaffold, the next task was how to convert the *tert*-butoxycarbonyl (Boc) protected lysine side-chain amine into an azide, which will be used as the secondary reactive tag. Several approaches are outlined in figure **3.9**. Initially, the Boc group of **3.8.19f** was deprotected and the amine was coupled to glycolic acid, which was subsequently reacted with **3.5.9** to afford **3.9.24**. However, conversion of the alcohol to an azide via Mitsunobu conditions was deemed inefficient as inconsistent and low yields were observed. Next, following removal of the Boc group of **3.8.19f**, the alkyne was directly reacted with **3.5.9** to provide **3.9.25**. Amine **3.9.25** was subjected to diazo transfer reaction conditions to convert the amine to an azide.[119] However, these conditions also led to decomposition of the phosphotriester. Knowing that we could access compound **3.9.25**, it was reasoned that coupling of **3.8.19f** following Boc-deprotection to an azido-carboxylic acid derived from compounds such as **3.9.26** or **3.9.27** would provide a protected activity based PA probe. However, diazo transfer conditions afforded little to no azide from the corresponding amino acids.

At this point, a viable synthesis was designed that is outlined in figure **3.10**. Here, following Boc deprotection of **3.8.19f**, the resulting amine was attached to **3.5.9** via “click” chemistry. 6-Azidohexanoic **3.10.28** prepared from the corresponding bromide[120]

Figure 3.9. Failed attempts at accessing a bifunctional PA probe.

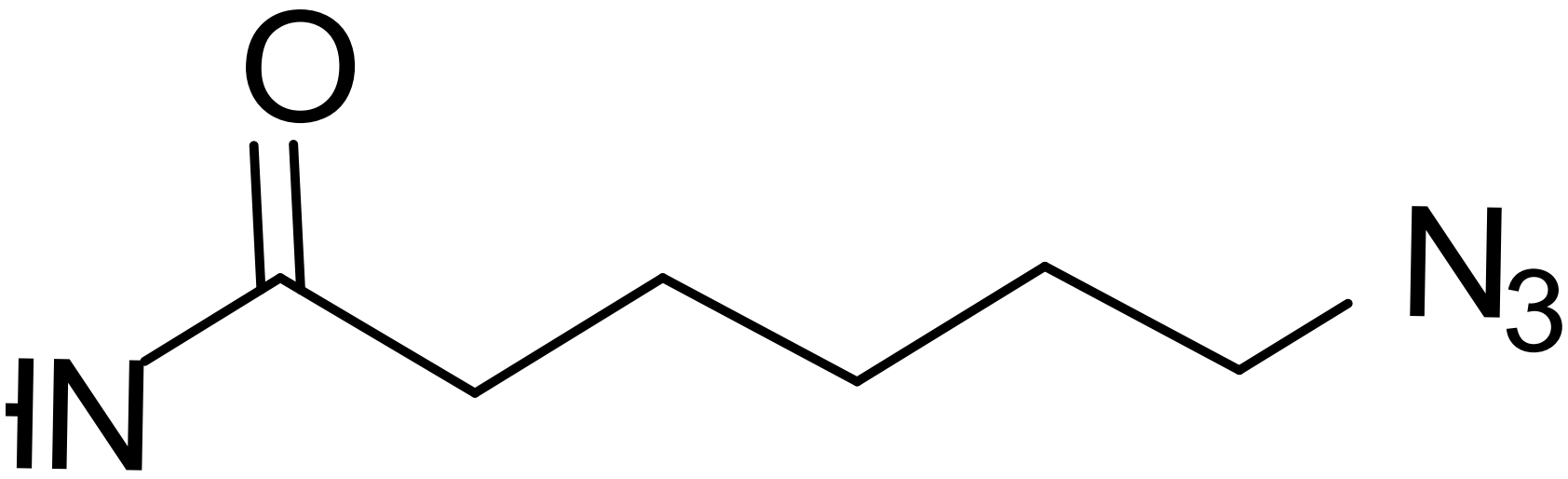

Figure 3.10. Synthesis of bifunctional PA probe **3.10.21f**.

was coupled onto the amine to furnish protected PA probe **3.10.20f**. TMSBr deprotection of the benzyl groups provided the activity based PA probe **3.10.21f**.

Biological Evaluation of PA Analogues

Having developed seven new PA-based probes, we next sought to evaluate their efficacy as ligands for known PA receptors. In order to do so, we monitored the binding the C2 domain of PKCα to vesicles containing each of the probes **3.7.21a-e, 3.10.21f**. In collaborative efforts with Dr. Robert Stahelin, surface plasmon resonance (SPR) equilibrium binding analysis was performed using liposomes containing 1-palmitoyl-2-oleoyl-*sn*-glycero-3-phosphocholine (POPC), 1-palmitoyl-2-oleoyl-*sn*-glycero-3-phosphoethanolamine (POPE), and PA (40 : 40 : 20) as an active surface for recruitment of the protein. Synthetic 1-palmitoyl-2-oleoyl-*sn*-glycero-3-phosphatidic acid (POPA) was used as a control standard as binding of PKCα-C2 to these vesicles is well documented.[121] The observed K_d for PKCα-C2 to these vesicles was 440 ± 50 nM as shown in table **3.1**. Systematic analysis of each of the probes **3.7.21a-e, 3.10.21f** revealed K_ds similar to that for POPA as shown in table **3.1** and figure **3.11**.

These results indicate that all of the synthesized probes are effective for recruiting this PA receptor as each displayed a K_d value no larger than two times that for synthetic version of natural PA. Along these lines, this data also confirms that the *sn*-1 position is an acceptable location for the placement of a reporter molecule, as was also seen with the DAG analogs.[103] The tag is placed as close to the binding motif as possible so as to facilitate optimal detection, yet seemingly still far enough away so as

Table 3.1. K_d values obtained from binding of PKCα-C2 with vesicles containing different PA compounds.

Liposome (POPC : POPE : PA (40:40:20)	**K_d (nM)[a]**
POPA	440 ± 50
Azido PA **3.3.1**	640 ± 140
Naphthyl PA **3.7.21a**	780 ± 50
Dansyl PA **3.7.21b**	800 ± 70
Coumarin PA **3.7.21c**	850 ± 120
Rhodamine PA **3.7.21d**	510 ± 90
Benzophenone PA **3.7.21e**	570 ± 150
Bifunctional PA **3.10.21f**	520 ± 80

[a] Binding experiments conducted in 25 mM Tris HCl pH 7.4, 150 mM NaCl, 1 mM $CaCl_2$, and 1 mM DTT.

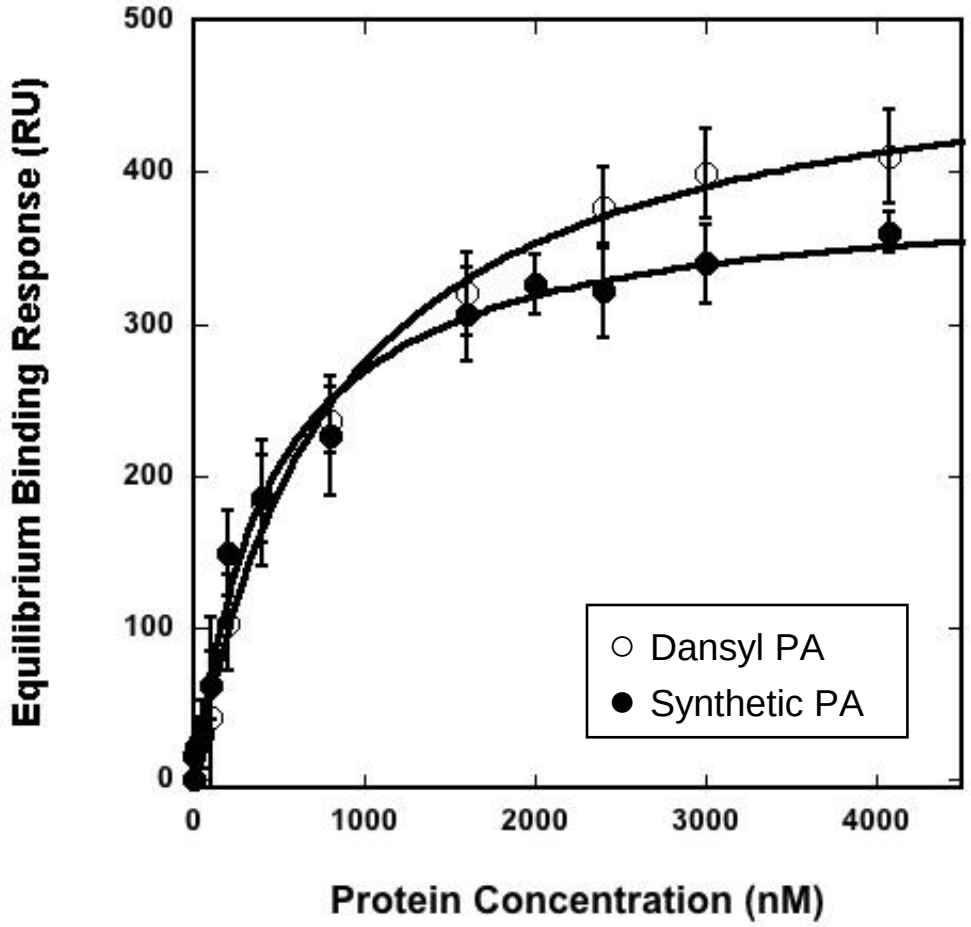

Figure 3.11. Afinity of the PKCαC2 domain for PA-containing membranes determined by SPR analysis. SPR measurements were used to determine K_ds of PKC-α C2 for POPC/POPE/PA (40:40:20) vesicles where PA represents synthetic PA analogues reported above. PKCαC2 was injected at varying concentrations to generate a binding isotherm of resonance units bound (saturating response units) versus protein concentrations. The solid lines represent a theoretical curve obtained based on R_{max} and K_d values determined by nonlinear least squares analysis. Error bars are indicative of the standard deviation calculated from three separate measurements.

not to significantly deter the binding event. While some of the probes displayed tight binding affinities (rhodamine (**3.7.21d**) and bifunctional PA probe (**3.10.21f**)) as compared to POPA, there seems to be no correlation at this point between structure and physiochemical properties of the probes and their ability to bind PKCα-C2.

Experimental

General Considerations

All reagents were purchased from Aldrich or Acros and used as received. Dry solvents were obtained from a Pure Solv solvent delivery system purchased from Innovative Technology, Inc. Column chromatography was performed using 230 – 400 mesh silica gel purchased from Sorbent Technologies. NMR spectra were obtained using a Bruker AC250 spectrometer updated with a TecMag data collection system, a Varian Mercury 300 spectrometer, and a Bruker Avance 400 spectrometer. High Resolution Mass spectra were obtained with JEOL DART-AccuTOF and ABI Voyager DE Pro MALDI spectrometers. Optical rotation values were obtained using a Perkin-Elmer 241 polarimeter. HPLC data was obtained using an HP series 1100 HPLC with an Alltech Lichrosphere SI 60 5U column with HPLC grade solvents purchased from Fisher. Cbz-Lys(Boc)-OMe was purchased from Chem-Impex International (wood Dale, IL). 1-Palmitoyl-2-oleoyl-*sn*-glycero-3-phosphocholine (POPC), 1-palmitoyl-2-oleoyl-*sn*-glycero-3-phosphoethanolamine (POPE), and 1-palmitoyl-2-oleoyl-*sn*-glycero-3-phosphatidic acid (POPA) were purchased from Avanti Polar Lipids, Inc. (Alabaster, AL). Experimental procedures and characterizations for azide **2.7.13** and alkynes

2.8.17a-c, e were given in chapter 2.

Synthetic Procedures

(2*R*,3*R*)-diethyl 1,4-dioxaspiro[4.4]nonane-2,3-dicarboxylate (3.5.5). Fully protected tartrate **3.5.5** was obtained following a slightly modified literature procedure in which the synthesis of the enantiomer was described.[32] Diethyl-L-tartrate **2.4.2** (4.05 g, 19.6 mmol) was dissolved in toluene (130 mL). To this stirring solution was added cyclopentanone (8.7 mL, 98 mmol) and *p*-toluenesulfonic acid (373 mg, 1.96 mmol). A Dean–Stark trap was attached and the reaction was heated at 130 °C overnight. Solid sodium bicarbonate (329 mg, 20%) was added and stirring was continued for 10 min. The reaction mixture was filtered and the filtrate was condensed under reduced pressure. Column chromatography with silica gel and a gradient solvent system of 0–20% ethyl acetate to hexanes afforded **3.5.5** as a yellow oil (4.19 g, 79%).

Characterizations matched the enantiomer of **3.5.5** but for the change in sign of the optical rotation.[32]

$[\alpha]_D^{296K}$ – 31.5(*c* = 2.92, $CHCl_3$); ^{1}H NMR (300 MHz, $CDCl_3$) δ 4.71 (s, 2H), 4.26 (q, *J* = 7.2 MHz, 4H), 2.03–1.67 (m, 8H), 1.30 (t, *J* = 7.2 MHz, 6H); ^{13}C NMR (75.5 MHz, $CDCl_3$) δ 169.7, 123.3, 77.0, 61.9, 36.6, 23.5, 14.1; HRMS $[M + H]^+$ calcd: 273.13381, found: 273.13516.

(2*S*,3*S*)-1,4-dioxaspiro[4.4]nonane-2,3-diyldimethanol (3.5.6). Compound **3.5.6** was obtained using a procedure modified from reports of the enantiomer[32] and a similar compound.[103] Diester **3.5.5** (2.5 g, 9.18 mmol), dissolved in anhydrous THF (8 mL), was

added dropwise to a solution of lithium aluminum hydride (700 mg, 18.36 mmol) in anhydrous THF at 0 °C under nitrogen. After the addition was complete, stirring was continued for 1 h at 0 °C and then at room temperature for an addition 1 h. The solution was cooled to 0 °C and the nitrogen was removed. Carefully, water (1 mL), 10% NaOH (1 mL), and water (2 mL) were added to quench the reaction. Stirring was continued for 30 min at room temperature. Anhydrous magnesium sulfate was added and stirring was continued for 30 min. The solution was filtered and concentrated under reduced pressure. Column chromatography with silica gel and a gradient solvent system of 0–10% methanol to ethyl acetate afforded **3.5.6** as a clear oil which solidified upon refrigeration (1.70 g, 99%).

Characterizations matched the enantiomer of **3.5.6** but for the change in sign of the optical rotation.[32]

$[\alpha]_D^{296K}$ – 6.50 (*c* = 1.692, $CHCl_3$); ^{1}H NMR (300 MHz, $CDCl_3$) δ 3.97–3.94 (m, 2H), 3.81–3.69 (m, 4H), 2.30–2.05 (m, 2H), 1.89–1.60 (m, 8H); ^{13}C NMR (75.5 MHz, $CDCl_3$) δ 119.4, 78.0, 62.3, 37.4, 23.4; HRMS $[M + H]^+$ calcd: 189.11268, found: 189.11238.

((2*S*,3*S*)-3-azidomethyl)-1,4-dioxaspiro[4.4]nonan-2-yl)methanol (3.5.7). Azide **3.5.7** was obtained following procedures reported for similar compounds.[73, 103] Diol **3.5.6** (720 mg, 3.83 mmol) was suspended in dichloromethane (20 mL). With stirring, silver (I) oxide (1.33 g, 5.75 mmol), tosyl chloride (803 mg, 4.21 mmol) and finely crushed potassium iodide (64 mg, 0.383 mmol) were added. The resulting solution was stirred at room temperature for 2 h and then filtered through a plug of silica gel with 100% ethyl

acetate as the eluant. The filtrate was concentrated under reduced pressure, and then DMF (40 mL) and sodium azide (622 mg, 9.58 mmol) were added. The solution was stirred at 85 °C overnight, concentrated, extracted with chloroform (2 x 100 mL), dried with magnesium sulfate, and concentrated under reduced pressure. Column chromatography with silica gel and 50% ethyl acetate to hexane as eluant afforded **3.5.7** as a clear oil (636 mg, 78%).

$[\alpha]_D^{296K}$ – 57.8 (*c* = 1.492, $CHCl_3$); ^{1}H NMR (300 MHz, $CDCl_3$) δ 4.05–3.90 (m, 2H), 3.81–3.62 (m, 2H), 3.55–3.51 (m, 1H), 3.30–3.33 (m, 1H), 2.65 (*b* s, 1H), 1.89–1.67 (m, 8H); ^{13}C NMR (75.5 MHz, $CDCl_3$) δ 119.8, 78.5, 76.1, 62.0, 52.0, 37.3, 37.2, 23.5, 23.3; HRMS $[M - N_2 + H]^+$ calcd: 186.11302, found: 186.11384.

((2*S*,3*S*)-3-(azidomethyl)-1,4-dioxaspiro[4.4]nonan-2-yl)methyldibenzyl phosphate (3.5.8). Azido alcohol **3.5.7** (425 mg, 1.99 mmol) was dissolved in anhydrous dichloromethane. 1*H*-tetrazole (13.3 mL, 5.98 mmol, 0.45 M stock) was added and the solution was cooled to 0 °C under nitrogen. Dibenzyl diisopropylphosphoramidite (**3.4.2**, 721 µL, 2.19 mmol) was then added dropwise. Stirring was continued for 10 min at 0 °C and then at room temperature for 1 h. At this point the reaction solution was cooled to 0 °C and *m*-chloroperoxybenzoic acid (1.81 g, 5.98 mmol, 57% purity) was added and stirring was continued for 1.5 h. The reaction was quenched with the addition of saturated sodium bicarbonate, extracted with dichloromethane (2 x 100 mL), dired with magnesium sulfate, and concentrated under reduced pressure. Column chromatography with silica gel and 50% ethyl acetate to hexane as eluant afforded

3.5.8 as a pale yellow oil (803 mg, 85%).

$[\alpha]_D^{296K}$ – 24.3 (*c* = 1.68, $CHCl_3$); ^1H NMR (300 MHz, $CDCl_3$) δ 7.42–7.32 (m, 10H), 5.11–4.99 (m, 4H), 4.09–3.87 (m, 4H), 3.43–3.37 (m, 1H), 3.24–3.18 (m, 1H), 1.89–1.60 (m, 8H); ^{13}C NMR (75.5 MHz, $CDCl_3$) δ 135.7, 135.6, 128.7, 128.6, 128.0, 120.2, 76.8, 76.0, 75.9, 69.6, 69.5, 66.7, 66.6, 51.8, 37.3, 37.1, 23.5, 23.4; ^{31}P NMR (121.5 MHz, $CDCl_3$) δ 0.143; HRMS $[M - N_2 + H]^+$ calcd: 446.17325, found: 446.17276.

(2*S*,3*S*)-4-azido-2,3-dihydroxybutyl dibenzyl phosphate (3.4.4). Phosphotriester **3.5.8** (1.07 g, 2.26 mmol) was dissolved in methanol (15 mL). With stirring was added *p*-toluenesulfonic acid (43 mg, 0.226 mmol). The solution was stirred at room temp overnight and quenched with saturated sodium bicarbonate and extracted with chloroform (2 x 100 mL), dried with magnesium sulfate, and concentrated under reduced pressure. Column chromatography with silica gel and a gradient solvent system of 80-100% ethyl acetate to hexanes afforded **3.4.4** as a clear oil (482 mg, 52%).

$[\alpha]_D^{296K}$ + 8.04 (*c* = 1.48, $CHCl_3$); ^1H NMR (300 MHz, $CDCl_3$) δ 7.37–7.31 (m, 10H), 5.05–5.02 (m, 4H), 4.04–4.00 (m, 2H), 3.72–3.69 (m, 2H), 3.43–3.26 (m, 4H); ^{13}C NMR (75.5 MHz, $CDCl_3$) δ 135.4, 135.3, 128.8, 128.7, 128.1, 70.2, 70.1, 69.9, 69.8, 69.7, 68.54, 68.46, 53.3; ^{31}P NMR (121.5 MHz, $CDCl_3$) δ 0.928; HRMS $[M - N_2 + H]^+$ calcd: 380.12630, found: 380.12495.

(2*S*,3*S*)-1-azido-4-(bis(benzyloxy)phosphoryloxy)butane-2,3-diyl distearate (3.5.9). Diol **3.4.4** (482 mg, 1.18 mmol), stearic acid (1.01 g, 3.55 mmol), dicyclohexylcarbodiimide (732 mg, 3.55 mmol) and 4-dimethylaminopyridine (144 mg, 1.18 mmol) were dissolved in dichloromethane (12 mL) and stirred at room temperature overnight. The reaction was filtered using ethyl acetate and concentrated under reduced pressure. Column chromatography with silica gel and a gradient solvent system of 10–30% ethyl acetate to hexanes afforded **3.5.9** as a white solid (820 mg, 74%). $[\alpha]_D^{296K}$ – 4.26 (*c* = 1.315, $CHCl_3$); ^{1}H NMR (300 MHz, $CDCl_3$) δ 7.35–7.26 (m, 10H), 5.20 (*b* s, 2H), 5.04–5.01 (m, 4H), 4.13–3.90 (m, 2H), 3.45–3.28 (m, 2H), 2.35–2.24 (m, 4H), 1.65–1.58 (m, 4H), 1.26 (*b* s, 56H), 0.88 (t, *J* = 6.5 Hz, 6H); ^{13}C NMR (75.5 MHz, $CDCl_3$) δ 172.7, 172.6, 135.6, 135.5, 128.7, 128.6, 128.03, 127.99, 70.0, 69.9, 69.7, 69.6, 69.5, 65.1, 65.0, 50.6, 34.0, 31.9, 29.72, 29.68, 29.5, 29.4, 29.3, 29.1, 24.81, 24.78, 22.7, 14.1; ^{31}P NMR (121.5 MHz, $CDCl_3$) δ 0.038; MALDI–HRMS $[M + Na]^+$ calcd: 962.6358, found: 962.6332.

Rhodamine-Alkyne (3.7.19d). Lissamine Rhodamine B sulfonyl chloride (141 mg, 0.244 mmol) was dissolved in DMF (10 mL). Propargyl amine (17 µL, 0.244 mmol) and triethyl amine (170 µL, 1.22 mmol) were added with stirring. Stirring was continued in the dark at room temperature overnight at which time the solvent was removed under reduced pressure. Column chromatography with silica gel and a gradient solvent system of 2–7% methanol to dichloromethane afforded **3.7.19d** as a purple solid (55 mg, 38%).

^{1}H NMR (300 MHz, $CDCl_3$) δ 8.74 (m, 1H), 8.13–8.10 (m, 1H), 7.37 (d, *J* = 8.1 Hz, 1H), 7.15 (d, *J* = 9.3 Hz, 2H), 6.93–6.89 (m, 2H), 6.82–6.81 (m, 2H), 3.93 (d, *J* = 2.4 Hz, 2H), 3.64 (q, *J* = 7.2 Hz, 8H), 2.44 (t, *J* = 2.5 Hz, 1H), 1.33 (t, *J* = 7.2 Hz, 12H); ^{13}C NMR (62.9 MHz, $CDCl_3$) δ 158.3, 157.4, 156.0, 146.6, 142.7, 134.4, 133.0, 130.7, 128.6, 127.6, 114.5, 114.1, 96.2, 78.6, 73.5, 46.2, 32.8, 12.7; MALDI–HRMS $[M + Na]^+$ calcd: 618.1703, found: 618.1699.

Benzophenone-Lys(Boc)-OMe (3.8.23). Cbz-Lys(Boc)-OMe (**3.8.22**, 535 mg, 1.36 mmol) was dissolved in methanol (15 mL). Palladium (II) hydroxide (10% wt) was added with stirring. A hydrogen atmosphere was established and stirring was continued overnight. The reaction mixture was filtered through celite and washed with methanol and the solvent was removed under reduced pressure. The residue was dissolved in DMF (10 mL). With stirring 4-benzoylbenzoic acid (308 mg, 1.36 mmol), 4-dimethylaminopyridine (199 mg, 1.63 mmol), and N-methylmorpholine (523 µL, 4.76 mmol) were added. After 5 min EDCI·HCl (313 mg, 1.63 mmol) was added and stirring was continued 7 h. The solvent was removed under reduced pressure and column chromatography with silica gel and a solvent system of 50% ethyl acetate to hexanes afforded **3.8.23** as a white foam (561 mg, 88%).

$[\alpha]_D^{296K}$ + 8.89 (c = 5.544, $CHCl_3$); ^{1}H NMR (300 MHz, $CDCl_3$) δ 7.96 (d, *J* = 8.4 Hz, 2H), 7.84–7.77 (m, 4H), 7.62 (t, *J* = 7.5 Hz, 1H), 7.52–7.47 (m, 2H), 7.26 (d, *J* = 7.5 Hz, 1H), 4.81–4.77 (m, 2H), 3.78 (s, 3H), 3.13–3.11 (m, 2H), 2.00–1.40 (m, 15H); ^{13}C NMR (100.6 MHz, $CDCl_3$) δ 195.9, 172.9, 166.5, 156.2, 140.3, 137.1, 137.0, 132.9, 130.23,

130.20, 128.4, 127.2, 79.1, 52.7, 52.5, 40.0, 31.9, 29.7, 28.4, 22.6; HRMS [M - Boc + 2H]$^{+}$ calcd: 369.18143, found: 369.18007.

Benzophenone-Lys(Boc)-Alkyne (3.8.19f). Compound **3.8.23** (561 mg, 1.20 mmol) was dissolved in methanol (5 mL). With stirring was added 2 N NaOH (5 mL). Stirring was continued 20 min and TLC analysis showed no starting material. The solution was neutralized with Dowex®50WX8–200 H^{+} resin to pH ~4. The solution was filtered and the filtrate concentrated under reduced pressure. The residue was washed with toluene, concentrated, and dried under high vacuum 5 h. The residue was then dissolved in dichloromethane (15 mL) and with stirring propargyl amine (99 µL, 1.44 mmol), 4-dimethylaminopyridine (146 mg, 1.20 mmol), EDCI·HCl (276 mg, 1.44 mmol) and N-methylmorpholine (395 µL, 3.59 mmol) were added. Stirring was continued overnight at room temperature at which time the solvent was removed under reduced pressure. Column chromatography with silica gel and a gradient solvent system of 50–80% ethyl acetate to hexanes afforded **3.8.19f** as a white solid (550 mg, 93%, 2 steps).
$[\alpha]_D^{296K}$ + 1.07(c = 0.935, $CHCl_3$); ^{1}H NMR (300 MHz, $CDCl_3$) δ 7.96–7.92 (m, 2H), 7.81–7.74 (m, 4H), 7.61–7.44 (m, 5H), 4.82–4.75 (m, 2H), 4.12–3.96 (m, 2H), 3.08–3.07 (m, 2H), 2.19 (t, *J* = 2 Hz, 1H), 2.00–1.77 (m, 2H), 1.59–1.38 (m, 12H); ^{13}C NMR (75.5 MHz, $CDCl_3$) δ 195.9, 171.8, 166.8, 156.2, 140.3, 136.9, 136.8, 132.9, 130.1, 130.0, 128.5, 127.3, 79.3, 79.1, 71.7, 53.5, 40.1, 32.3, 29.6, 29.2, 28.4, 22.7; HRMS [M – Boc + 2H]$^{+}$ calcd: 392.19742, found: 392.19514.

General Procedure for Click Chemistry Derivatization to Produce Phosphotriesters 3.7.20a-e.

Compound **3.5.9** and derivatized alkynes (**2.8.17a-c, e; 3.7.19d**) were dissolved in THF (1.5–2 mL). Copper sulfate pentahydrate and sodium ascorbate were added along with H_2O (0.5 mL). The solution was stirred at room temperature overnight at which point the solvent was removed under reduced pressure. Column chromatography with silica gel afforded compounds **3.7.20a-e**. Due to the amphipathic nature of the phosphotriesters, the integration values in the proton NMR did not always correspond to the exact correct value. However, they were always close. The values listed below correspond to the value that should be observed. Actual NMR copies are included that show the observed values.

Naphthyl Phosphotriester (3.7.20a). Alkyne **2.8.17a** (33.7 mg, 0.151 mmol), **3.5.9** (141.6 mg, 0.151 mmol), copper sulfate pentahydrate (113 mg, 0.453 mmol), and sodium ascorbate (179 mg, 0.906 mmol) were utilized. Column chromatography with a gradient solvent system of 70–100% ethyl acetate to hexanes afforded **3.7.20a** as a white solid (151 mg, 86%).

$[\alpha]_D^{296K}$ – 4.41 (*c* = 3.79, $CHCl_3$); ^{1}H NMR (300 MHz, $CDCl_3$) δ 7.80–7.75 (m, 3H), 7.69 (s, 1H), 7.48–7.43 (m, 3H), 7.36–7.33 (m, 11H), 6.52 (t, *J* = 5.4 Hz, 1H), 5.44–5.39 (m, 1H), 5.03–4.97 (m, 5H(1 + 4 H)), 4.43–4.41 (m, 4H), 4.18–4.06 (m, 2H), 3.71 (s, 2H), 2.29–2.18 (m, 4H), 1.56–1.48 (m, 4H), 1.25 (*b* s, 56H), 0.88 (t, *J* = 6 Hz, 6H); ^{13}C NMR (75.5 MHz, $CDCl_3$) δ 172.6, 172.2, 171.1, 144.9, 135.5, 135.4, 133.5, 132.4, 132.2,

128.7, 128.6, 128.1, 128.0, 127.96, 127.3, 126.2, 125.9, 123.5, 69.65, 69.57, 69.1, 64.82, 64.81, 49.9, 49.8, 43.6, 34.9, 33.9, 33.8, 31.9, 29.71, 29.67, 29.5, 29.4, 29.3, 29.12, 29.07, 24.8, 24.7, 22.7, 14.1; ^{31}P NMR (121.5 MHz, $CDCl_3$) δ 0.005; MALDI–HRMS $[M + Na]^+$ calcd: 1185.7355, found: 1185.7310.

Dansyl Phosphotriester (3.7.20b). Alkyne **2.8.17b** (33.4 mg, 0.116 mmol), **3.5.9** (109 mg, 0.116 mmol), copper sulfate pentahydrate (87 mg, 0.348 mmol), and sodium ascorbate (138 mg, 0.696 mmol) were utilized. Column chromatography with a gradient solvent system of 50–80% ethyl acetate to hexanes afforded **3.7.20b** as a green glass (121 mg, 85%).

$[\alpha]_D^{296K}$ – 4.40 (*c* = 1.796, $CHCl_3$); ^{1}H NMR (300 MHz, $CDCl_3$) δ 8.55 (d, *J* = 8.7 Hz, 1H), 8.29–8.25 (m, 2H), 7.53 (q, *J* = 7.9 Hz, 2H), 7.34 (*b* s, 11H), 7.18 (d, *J* = 7.2 Hz, 1H), 5.52 (*b* s, 1H), 5.40–5.35 (m, 1H), 5.08–4.97 (m, 5H(1 + 4H)), 4.39-4.37 (m, 2H), 4.17–4.05 (m, 4H), 2.89 (s, 6H), 2.30–2.21 (m, 4H), 1.56–1.50 (m, 4H), 1.25 (*b* s, 56H), 0.88 (t, *J* = 6.6 Hz, 6H); ^{13}C NMR (75.5 MHz, $CDCl_3$) δ 172.6, 172.3, 151.9, 144.4, 135.45, 135.46, 134.6, 130.5, 129.9, 129.6, 129.5, 128.7, 128.6, 128.5, 128.03, 127.99, 123.4, 123.1, 118.8, 115.3, 69.7, 69.6, 69.1, 64.92, 64.86, 49.8, 45.4, 38.7, 33.9, 33.8, 31.9, 29.72, 29.67, 29.5, 29.4, 29.29, 29.27, 29.13, 29.07, 24.8, 24.7, 22.7, 14.1; ^{31}P NMR (121.5 MHz, $CDCl_3$) δ -0.058; MALDI–HRMS $[M + Na]^+$ calcd: 1250.7290, found: 1250.7317.

Coumarin Phosphotriester (3.7.20c). Alkyne **2.8.17c** (36.1 mg, 0.159 mmol), **3.5.9** (149.3 mg, 0.159 mmol) copper sulfate pentahydrate (119 mg, 0.477 mmol), and sodium ascorbate (189 mg, 0.954 mmol) were employed. Column chromatography with a gradient solvent system of 70–100% ethyl acetate to hexanes afforded **3.7.20c** as a white solid (153 mg, 83%).

$[\alpha]_D^{296K}$ – 6.96 (*c* = 6.132, $CHCl_3$); ^{1}H NMR (300 MHz, $CDCl_3$) δ 9.28–9.25 (m, 1H) 8.90 (s, 1H), 7.69–7.64 (m, 2H), 7.58 (s, 1H), 7.41–7.34 (m, 12H), 5.49–5.44 (m, 1H), 5.09–4.98 (m, 5H(1+4H)), 4.73–4.71 (m, 2H), 4.49–4.47 (m, 2H), 4.19–4.09 (m, 2H), 2.30–2.22 (m, 4H), 1.57–1.42 (m, 4H), 1.25 (*b* s, 56H), 0.88 (t, *J* = 6.5 Hz, 6H); ^{13}C NMR (100.6 MHz, $CDCl_3$) δ 172.5, 172.2, 161.7, 161.1, 154.5, 148.4, 144.9, 135.6, 135.5, 134.2, 129.8, 128.7, 129.0, 125.3, 123.3, 115.5, 118.3, 116.7, 69.7, 69.2, 64.9, 49.9, 35.5, 34.0, 33.8, 32.9, 29.7, 29.5, 29.4, 29.3, 29.2, 24.8, 24.7, 22.7, 14.1; ^{31}P NMR (121.5 MHz, $CDCl_3$) δ 0.027; MALDI–HRMS $[M + Na]^+$ calcd: 1189.6940, found: 1189.6920.

Rhodamine Phosphotriester (3.7.20d). Alkyne **3.7.19d** (21.4 mg, 0.036 mmol), **3.5.9** (34 mg, 0.036 mmol) copper sulfate pentahydrate (27 mg, 0.108 mmol), and sodium ascorbate (43 mg, 0.215 mmol) were used. Column chromatography with 10% methanol / chloroform as eluant afforded **3.7.20d** as a pink solid (44 mg, 80%).

No optical rotation was obtained due to the high propensity of the compound to stain; ^{1}H NMR (300 MHz, $CDCl_3$) δ 8.52 (s, 1H), 7.93–7.91 (m, 2H), 7.30 (*b* s, 12H), 7.10 (d, *J* = 7.5 Hz, 1H), 6.90 (d, *J* = 8.7 Hz, 2H), 6.63–6.62 (m, 3H), 5.47 (*b* s, 1H), 5.01–4.97 (m,

5H(1 + 4H)), 4.73–4.69 (m, 1H), 4.58–4.45 (m. 3H), 4.16 (s, 2H), 3.65–3.52 (m, 8H), 2.21–2.18 (m, 4H), 1.47–1.45 (m, 4H), 1.31–1.20 (m, 68H), 0.88 (t, *J* = 6.6 Hz, 6H); ^{13}C NMR (100.6 MHz, $CDCl_3$) δ 172.6, 172.3, 159.0, 157.8, 155.7, 155.5, 147.4, 142.3, 135.83, 135.76, 133.73, 133.67, 133.3, 129.6, 128.6, 128.5, 128.4, 128.0, 127.4, 127.2, 125.1, 114.3, 113.7, 113.6, 95.6, 70.0, 69.9, 69.63, 69.57, 69.5, 69.4, 68.9, 65.2, 50.1, 45.8, 38.8, 34.1, 33.9, 31.9, 29.7, 29.5, 29.4, 29.1, 24.8, 24.7, 22.7, 14.1, 12.6; ^{31}P NMR (121.5 MHz, $CDCl_3$) δ -0.247; MALDI–HRMS $[M + Na]^+$ calcd: 1557.8169, found: 1557.8251.

Benzophenone Phosphotriester (3.7.20e). Alkyne **2.8.17e** (38 mg, 0.144 mmol), **3.5.9** (123 mg, 0.131 mmol), copper sulfate pentahydrate (98 mg, 0.392 mmol), and sodium ascorbate (155 mg, 0.785 mmol) were used. Column chromatography with a gradient solvent system of 70–100% ethyl acetate to hexanes afforded **3.7.20e** as a white solid (135 mg, 86%).

$[\alpha]_D^{296K}$ – 5.27 (*c* = 2.544, $CHCl_3$); ^{1}H NMR (300 MHz, $CDCl_3$) δ 7.94 (d, *J* = 7.8 Hz, 2H), 7.83–7.76 (m, 4H), 7.64–7.58 (m, 2H), 7.48 (t, *J* = 7.7 Hz, 3H), 7.33 (*b* s, 10H), 5.49–5.43 (m, 1H), 5.11–4.96 (m, 5H(1 + 4H)), 4.78–4.71 (m, 2H), 4.55–4.49 (m, 2H), 4.19–4.09 (m, 2H), 2.30–2.22 (m. 4H), 1.56–1.49 (m, 4H), 1.25 (*b* s, 56H), 0.88 (t, *J* = 6.5 Hz, 6H); ^{13}C NMR (100.6 MHz, $CDCl_3$) δ 195.8, 172.6, 172.2, 166.5, 140.1, 137.2, 137.1, 135.54, 135.47, 132.8, 130.0, 128.6, 128.4, 128.0, 127.97, 127.1, 123.6, 69.7, 69.6, 69.2, 64.9, 64.8, 50.0, 35.5, 34.0, 33.8, 31.9, 29.7, 29.5, 29.4, 29.3, 29.14, 29.10, 24.8, 24.7, 22.7, 14.1; ^{31}P NMR (121.5 MHz, $CDCl_3$) δ -0.058; MALDI–HRMS $[M + H]^+$ calcd:

1203.7485, found: 1203.7488.

Bifunctional Phosphotriester (3.10.20f). Alkyne **3.8.19f** (84 mg, 0.171 mmol) was dissolved in dichloromethane (2 mL) and with stirring was added trifluoroacetic acid (2 mL). Stirring was continued for 2 h and the solvent was removed under reduced pressure and placed under high vacuum for 2 h. The residue was dissolved in THF (1.5 mL) and **3.5.9** (161 mg, 0.171 mmol) was added along with copper sulfate pentahydrate (43 mg, 0.171 mmol), sodium ascorbate (68 mg, 0.342 mmol), and H_2O (0.5 mL). Stirring was continued overnight at room temperature at which point the solvent was removed under reduced pressure and placed under high vacuum 2 h. This residue was dissolved in anhydrous DMF (3 mL) and 6-azidohexanoic acid **3.10.28**[120] (32 mg, 0.205 mmol) was added. 4-Dimethylaminopyridine (21 mg, 0.171 mmol), EDCI·HCl (72 mg, 0.376 mmol), and N-methylmorpholine (94 µL, 0.855 mmol) were added and stirring was continued overnight at room temperature at which point the solvent was removed under reduced pressure. Column chromatography with silica gel and a gradient solvent system of 30–50% acetone to chloroform afforded **3.10.20f** as a white solid (110 mg, 44%, 3 steps).

$[\alpha]_D^{296K}$ – 4.91 (*c* = 4.36, $CHCl_3$); ^{1}H NMR (300 MHz, $CDCl_3$) δ 7.98 (d, *J* = 8.4 Hz, 2H), 7.80 (t *J* = 8.4 Hz, 4H), 7.64–7.47 (m, 6H), 7.34 (*b* s, 10H), 6.16–6.12 (m, 1H), 5.47–5.42 (m, 1H), 5.07–4.96 (m, 5H(1 + 4H)), 4.68–4.66 (m, 1H), 4.52–4.52 (m, 4H), 4.13–4.07 (m, 2H), 3.26–3.19 (m, 4H), 2.30–2.23 (m, 4H), 2.12 (t, *J* = 7.5 Hz, 2H), 1.96–1.84 (m, 2H), 1.63–1.24 (m, 70H), 0.88 (t *J* = 6.5 Hz, 6H); ^{13}C NMR (100.6 MHz, $CDCl_3$) δ

195.8, 173.2, 172.6, 173.3, 171.8, 166.7, 144.8, 140.3, 137.0, 135.5, 135.4, 132.9, 130.1, 130.0, 128.72, 128.67, 128.4, 128.0, 127.96, 127.3, 123.3, 69.72, 69.67, 69.2, 64.9, 53.6, 51.2, 49.9, 38.6, 36.4, 35.1, 34.0, 33.9, 31.9, 29.7, 29.6, 29.4, 29.3, 29.14, 29.06, 28.6, 26.4, 25.2, 24.80, 24.76, 22.7, 22.5, 14.1; ^{31}P NMR (121.5 MHz, $CDCl_3$) δ -0.254; MALDI–HRMS $[M + Na]^+$ calcd: 1492.8999, found: 1492.9028.

General Procedure for Deprotection of Phosphotriesters to Access PA Analogues 3.3.1 / 3.7.21a-e / 3.10.21f.

Phosphotriesters **3.5.9** / **3.7.20a-e** / **3.10.20f** were dissolved in dichloromethane at 0 °C under argon. Bromotrimethylsilane was added and stirring was continued at room temperature for 1 h. Solvent was removed under reduced pressure and the residue was placed on a high vacuum line to remove any residual solvents. Methanol (2 mL) was added and the solution was stirred at room temperature for 1 h. The solid that formed was collected via filtration. The solid was dissolved in methanol–chloroform (1:4) and extracted with 8 mM ammonium acetate. The organic layer was concentrated under reduced pressure to afford **3.3.1 / 3.7.21a-e / 3.10.21f**.

Azido PA (3.3.1). Azido phosphotriester **3.5.9** (65 mg, 0.069 mmol), dichloromethane (2.45 mL), and bromotrimethylsilane (0.55 mL) afforded **3.3.1** as a white solid (30 mg, 56%).

^{1}H NMR (300 MHz, $CDCl_3$: CD_3OD (1:1)) δ 5.29 (*b* s, 2H), 4.09 (*b* s, 2H), 3.61–3.52 (m, 2H), 2.38–2.37 (m, 4H), 1.64 (*b* s, 4H), 1.27 (*b* s, 56H), 0.89 (t, *J* = 6.3 Hz, 6H); ^{31}P

NMR showed no resonance in any solvent tried; MALDI–HRMS $[M - NH_4 + 2Na]^+$ calcd: 804.5238, found: 804.5143.

Naphthyl PA (3.7.21a). Naphthyl phosphotriester **3.7.20a** (67 mg, 0.058 mmol), dichloromethane (1.64 mL), and bromotrimethylsilane (0.36 mL) afforded **3.7.21a** as a brownish solid (40 mg, 70%).

^{31}P NMR (121.5 MHz, $CDCl_3$) δ 1.44; MALDI–HRMS $[M - NH_4 + 2Na]^+$ calcd: 1027.6235, found: 1027.6273.

Dansyl PA (3.7.21b). Dansyl phosphotriester **3.7.20b** (80 mg, 0.065 mmol), dichloromethane (1.64 mL) , and bromotrimethylsilane (0.36 mL) afforded **3.7.21b** as a green solid (74 mg, quantative yield).

^{31}P NMR (121.5 MHz, $CDCl_3$) δ 1.09; MALDI–HRMS $[M - NH_4 + 2Na]^+$ calcd: 1092.6171, found: 1092.6128.

Coumarin PA (3.7.21c). Coumarin phosphotriester **3.7.20c** (60 mg, 0.051 mmol), dichloromethane (1.64 mL), and bromotrimethylsilane (0.36 mL) afforded **3.7.21c** as a white solid (40 mg, 78%).

^{31}P NMR (121.5 MHz, $CDCl_3$) δ 1.39; MALDI–HRMS $[M - NH_4 + 2Na]^+$ calcd: 1031.5821, found: 1031.5857.

Rhodamine PA (3.7.21d). Rhodamine phosphotriester **3.7.20d** (44mg, 0.029 mmol), dichloromethane (1.64 mL), and bromotrimethylsilane (0.36 mL) Column chromatography with silica gel and a solvent system of 7 chloroform : 2.5 methanol : 0.5 water was necessary to purify the phosphate. The resulting solid was dissolved in methanol–chloroform (1:4) and extracted with 8 mM ammonium acetate. The organic layer was concentrated under reduced pressure to afford **3.7.21d** as a purple solid (34 mg, 85%).

^{31}P NMR no resonance could be detected in any solvent tried; MALDI–HRMS [M - NH_4 + 2Na]$^+$ calcd: 1399.7049, found: 1399.6963.

Benzophenone PA (3.7.21e). Benzophenone phosphotriester **3.7.20e** (41.5 mg, 0.035 mmol), dichloromethane (1.64 mL), and bromotrimethylsilane (0.36 mL) afforded **3.7.21e** as a pinkish white solid (26 mg, 73%).

^{31}P NMR (121.5 MHz, $CDCl_3$) δ 1.25; MALDI–HRMS [M - NH_4 + 2Na]$^+$ calcd: 1067.6185, found: 1067.6116.

Bifunctional Benzophenone/Azido PA (3.10.21f). Bifunctional benzophenone/azido phosphotriester **3.10.20f** (52 mg, 0.035 mmol), dichloromethane (1.64 mL), and bromotrimethylsilane (0.36 mL) afforded **3.10.21f** as a white solid (38 mg, 83%).

^{31}P NMR (121.5 MHz, $CDCl_3$) δ 1.12; MALDI–HRMS [M - NH_4 + 2Na]$^+$ calcd: 1334.7880, found: 1334.7890.

PA Binding Analysis with Surface Plasmon Resonance. (This analysis was performed by our collaborator Dr. R. V. Stahelin at Indiania University School of Medicine-South Bend.)

All surface plasmon resonance (SPR) binding measurements were performed at room temprature (25°C). PA lipid stocks were dissolved in a chloroform:methanol (80:20) mixture from which liposomes were prepared as POPC:POPE:PA (40:40:20) for different PA compounds. Aliquots of lipid mixtures to prepare a final concentration of 0.5 mg/ml of vesicles were dried under nitrogen and rehydrated with 500 µl binding buffer (25 mM Tris HCl pH 7.4, 150 mM NaCl, 1 mM $CaCl_2$ and 1 mM DTT). Lipid solutions were vortexed for 15 min and sonicated for 15 min. Lipid vesicles were then passed 19 times through a 100 nm polycarbonate membrane in an Avanti Mini-Extruder at room temperature. The liposome coating of the Pioneer L1 sensor chip (GE Healthcare) has been described in detail previously.[78, 122] Briefly, the sensor chip surface was washed and then coated by injecting 85 µl of vesicles containing various analogs of PA at a 5 µl/min flow rate to yield a response of 5,000 resonance units (RU). Each lipid layer was stabilized by injecting 10 µl of 50 mM NaOH three times at 100 µl/min flow rate. Typically, no decrease in lipid signal was seen after the first injection. Various concentrations of PKCα-C2 (within a 10-fold range of K_d) were injected to study the equilibrium binding and viability of synthetic analogs of PA. PKCα-C2 was expressed and purified as previously described.[123] For Equilibrium SPR measurements, the flow rate was set at 10 µl/min to allow sufficient time for the association phase, which in turn allows RU values to reach saturating response values (R_{eq}). Following collection of

three data sets for each PA analogue, R_{eq} values were plotted *versus* respective protein concentrations (C), and the K_d value was calculated by a non-linear least squares analysis of the binding isotherm using an equation, $R_{eq} = R_{max}/(1 + K_d/C)$,[78] where R_{max} is a theoretical maximum R_{eq} value.

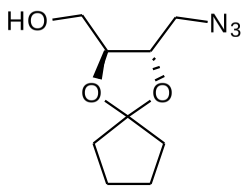

Proton NMR

116

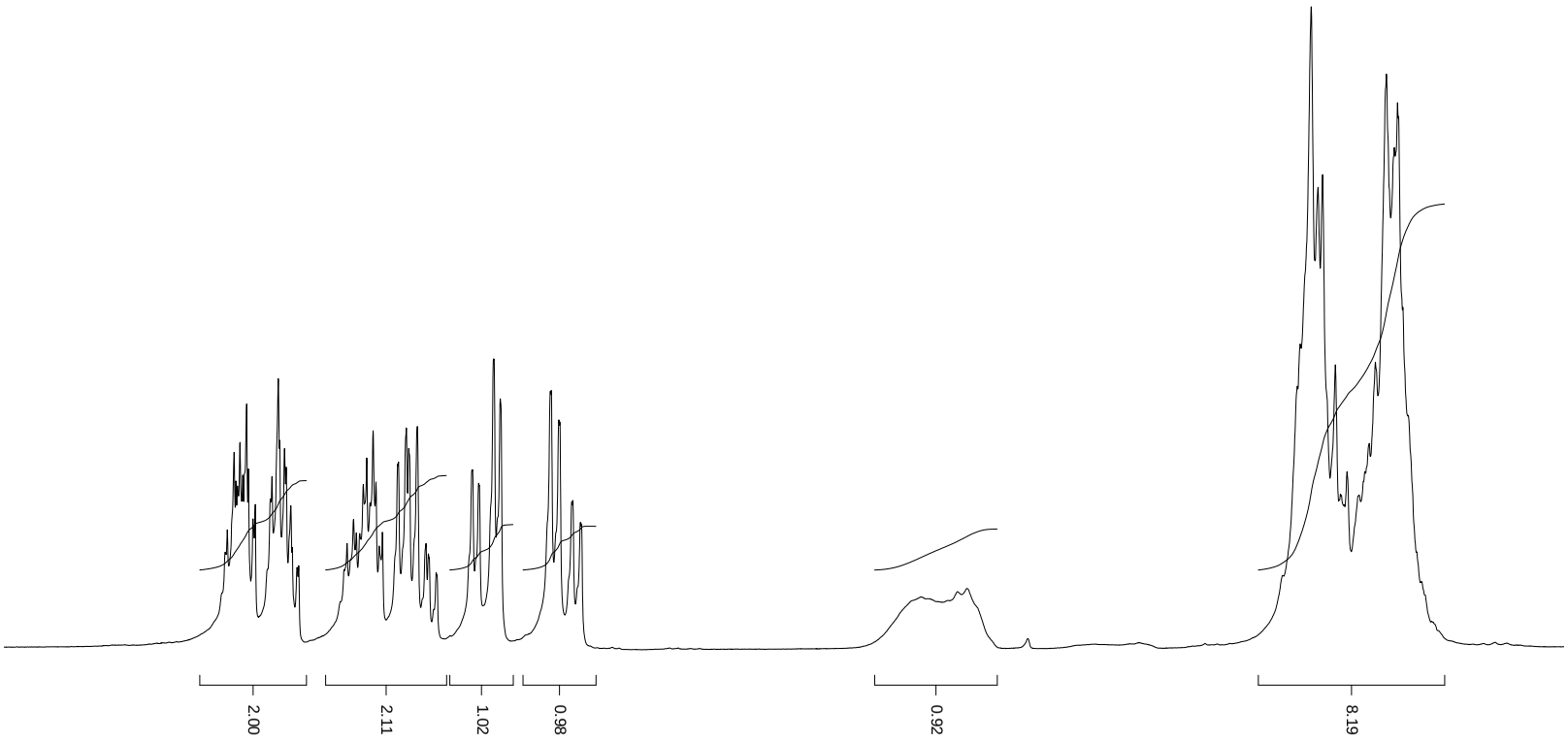

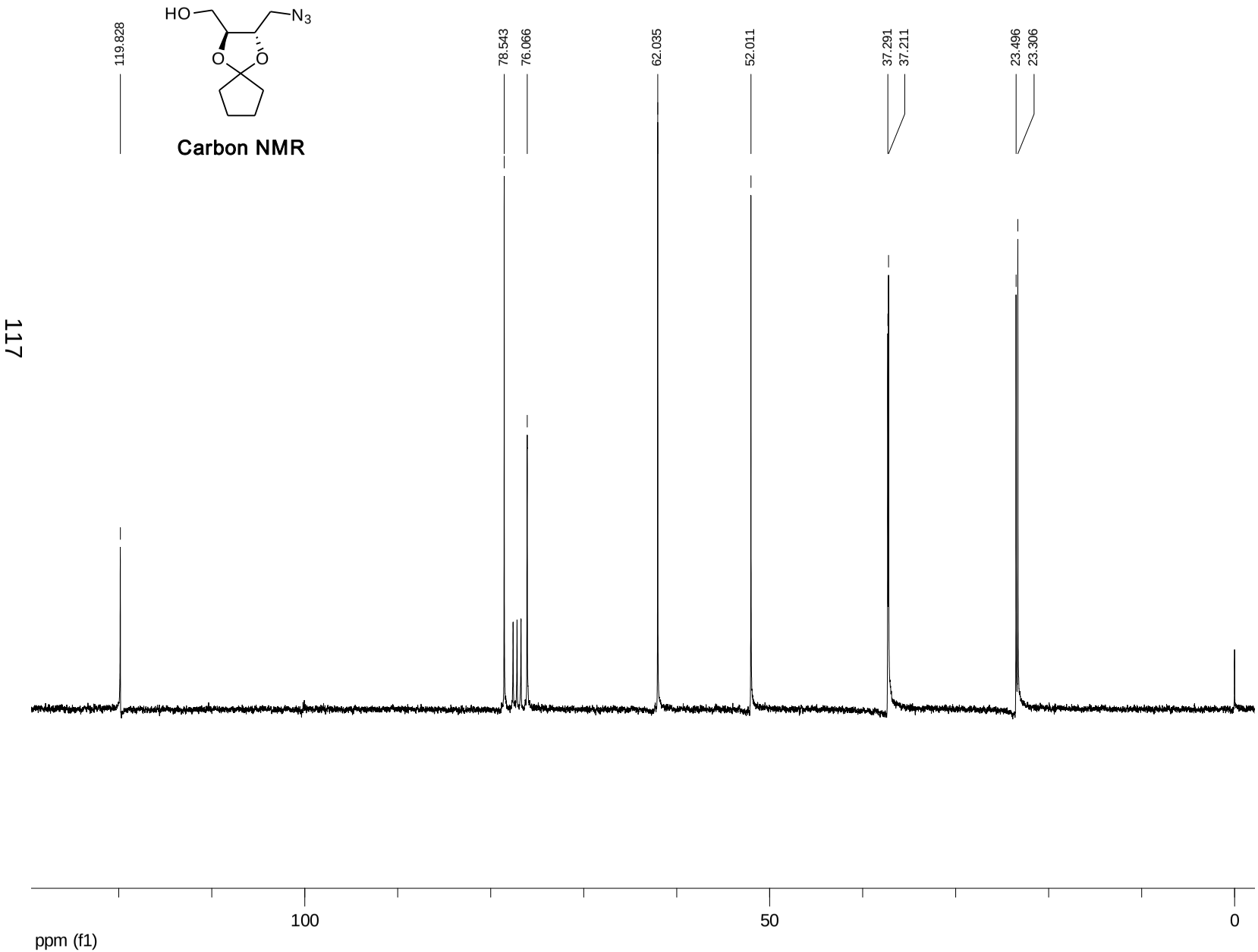
HO
N3
O
O
Carbon NMR
119.828
78.543
76.066
62.035
52.011
37.291
37.211
23.496
23.306
117
100
50
0
ppm (f1)

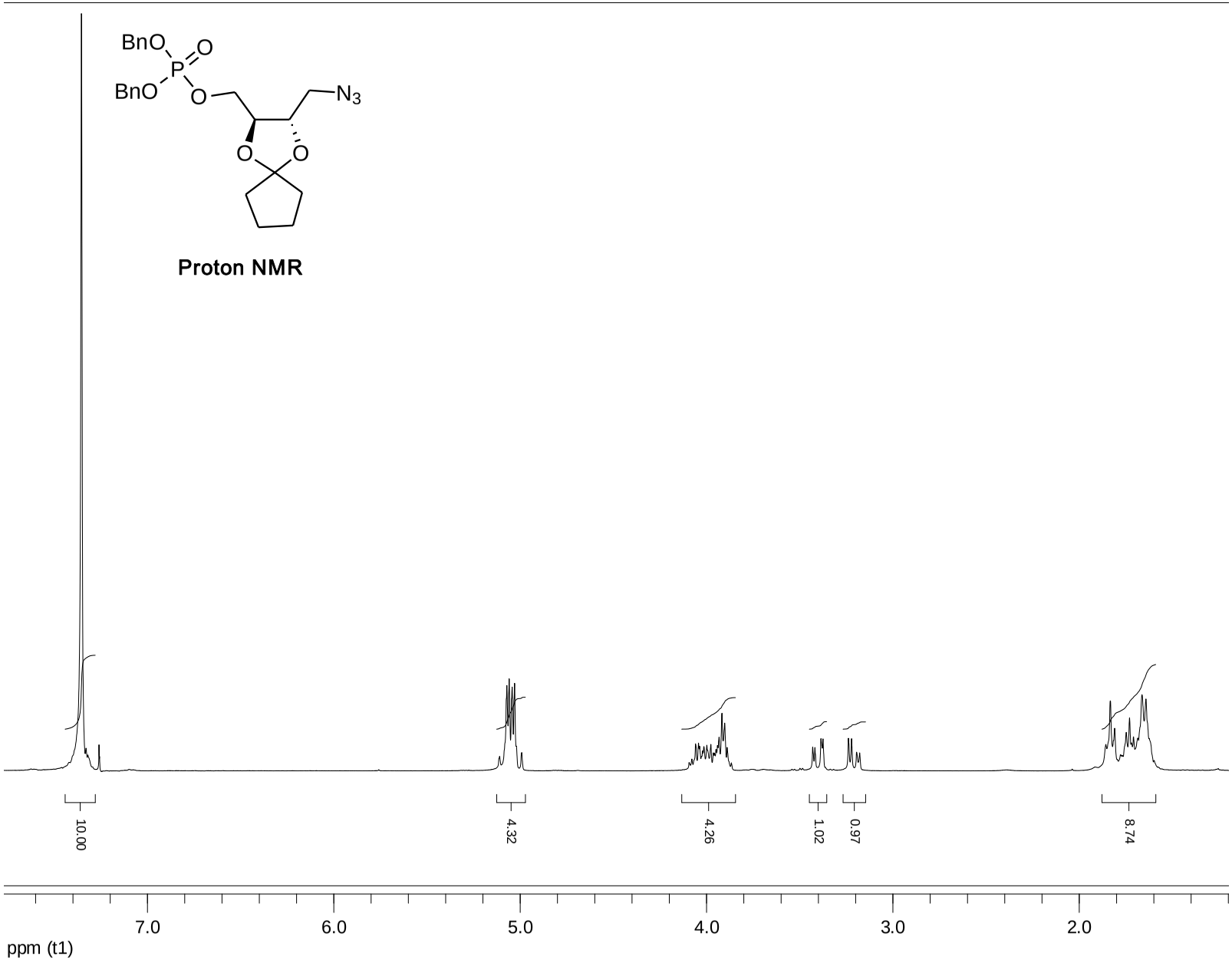
BnO
O
P
BnO
O
N3
O
O
Proton NMR
10.00
4.32
4.26
1.02
0.97
8.74
7.0
6.0
5.0
4.0
3.0
2.0
ppm (t1)

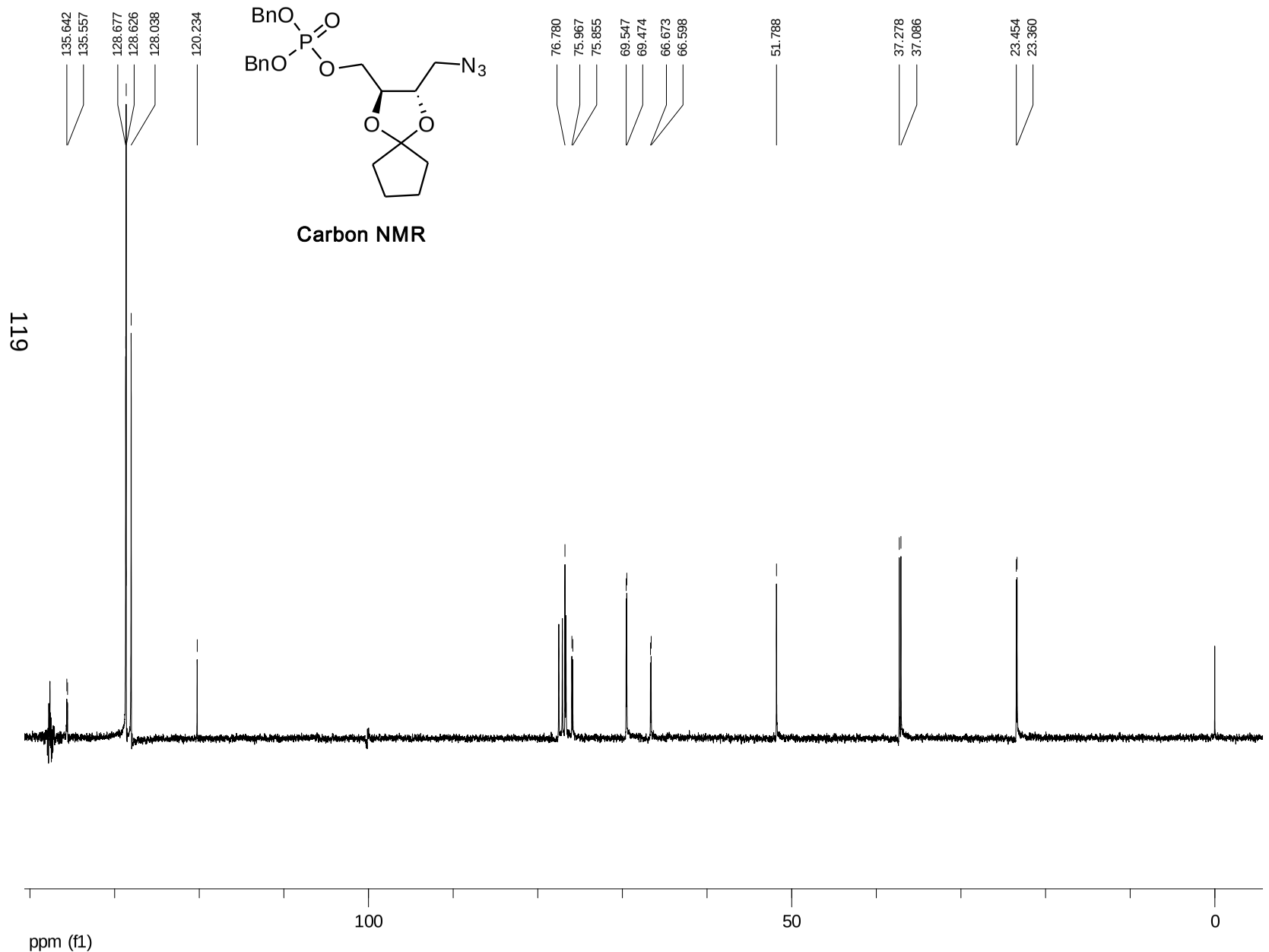
135.642
135.557
128.677
128.626
128.038
120.234
BnO
P
O
BnO
O
N3
O
O
76.780
75.967
75.855
69.547
69.474
66.673
66.598
51.788
37.278
37.086
23.454
23.360
Carbon NMR
119
100
50
0
ppm (f1)

Phosphorous NMR

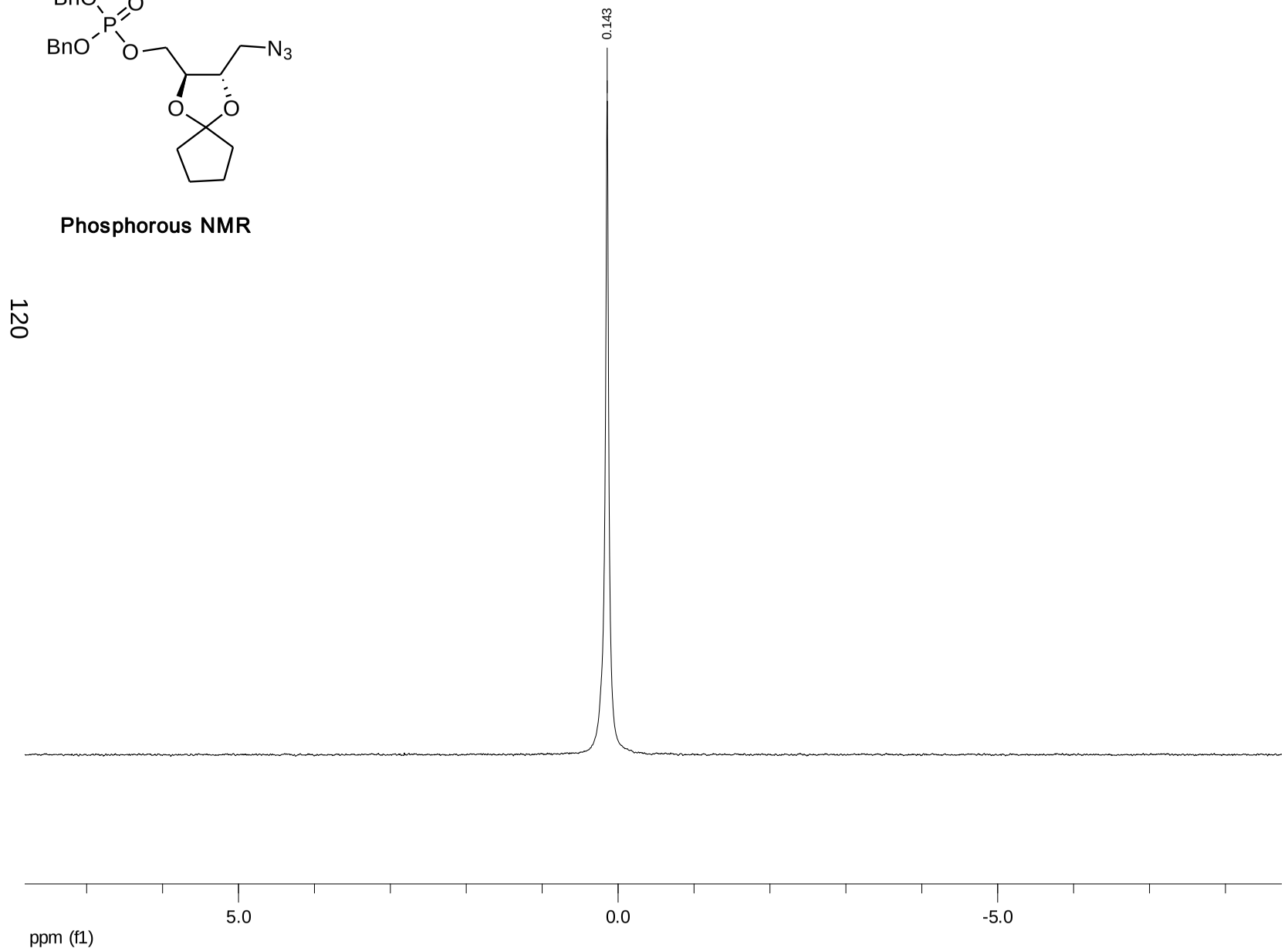

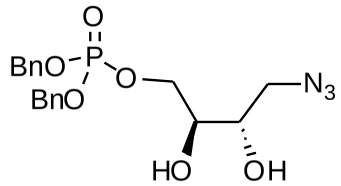
O
BnO
P
O
BnO
N3
HO
OH

Proton NMR

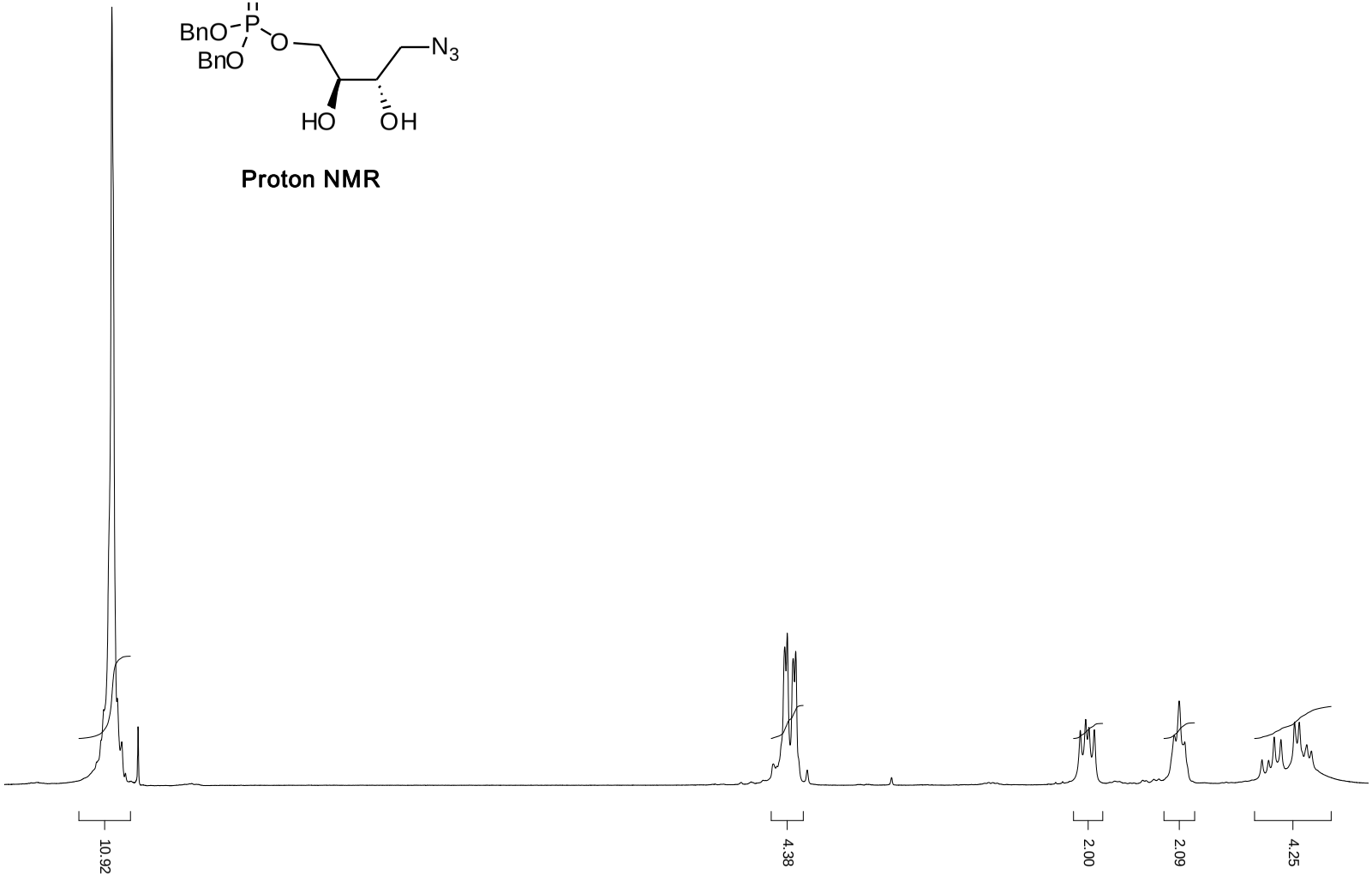
10.92
4.38
2.00
2.09
4.25
7.50
7.00
6.50
6.00
5.50
5.00
4.50
4.00
3.50
ppm (t1)

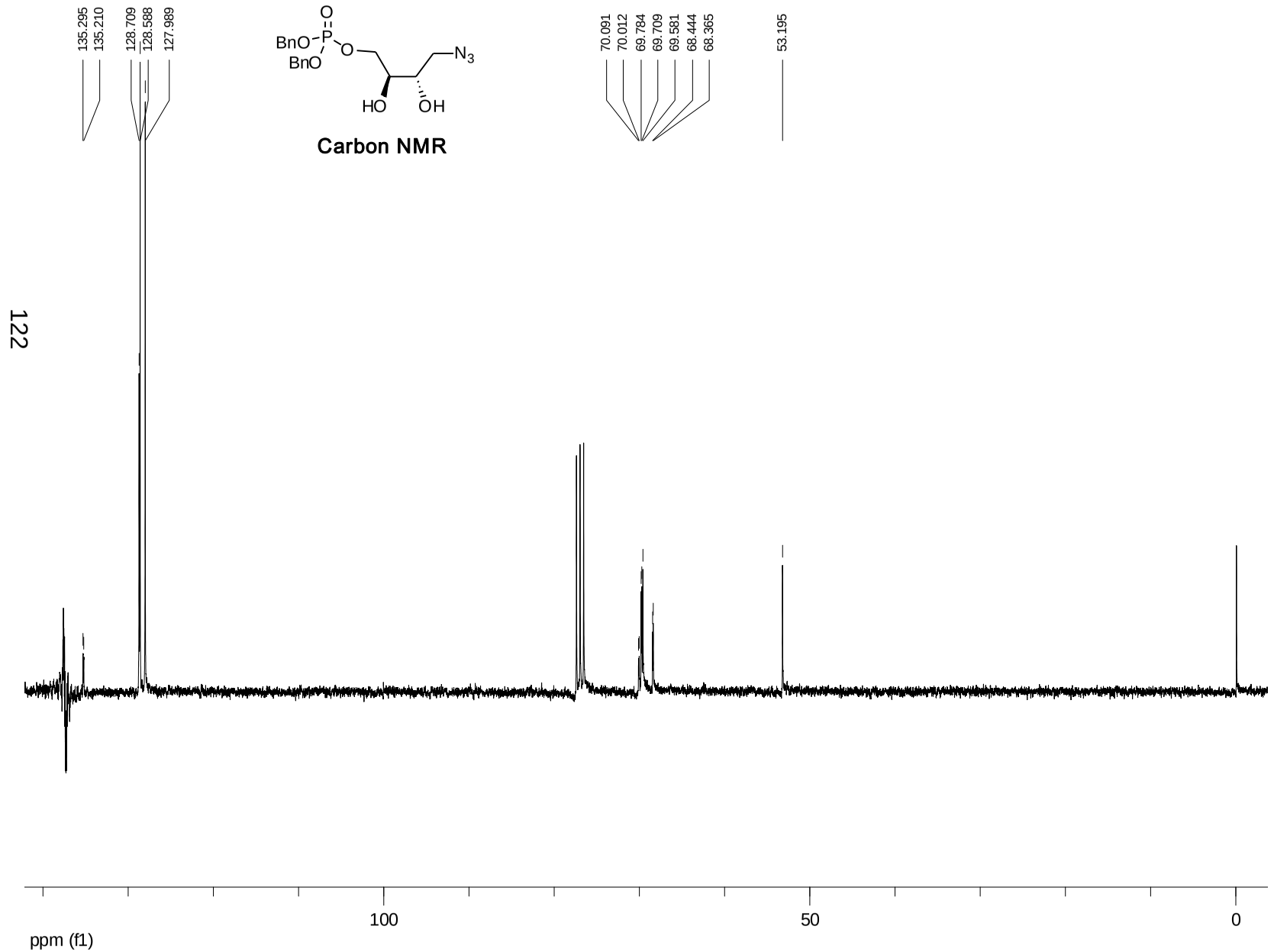
135.295
135.210
128.709
128.588
127.989
BnO
BnO
O
P
O
N3
HO
OH
70.091
70.012
69.784
69.709
69.581
68.444
68.365
53.195
Carbon NMR
122
100
50
0
ppm (f1)

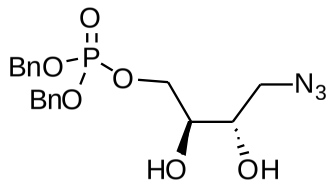

Phosphorous NMR

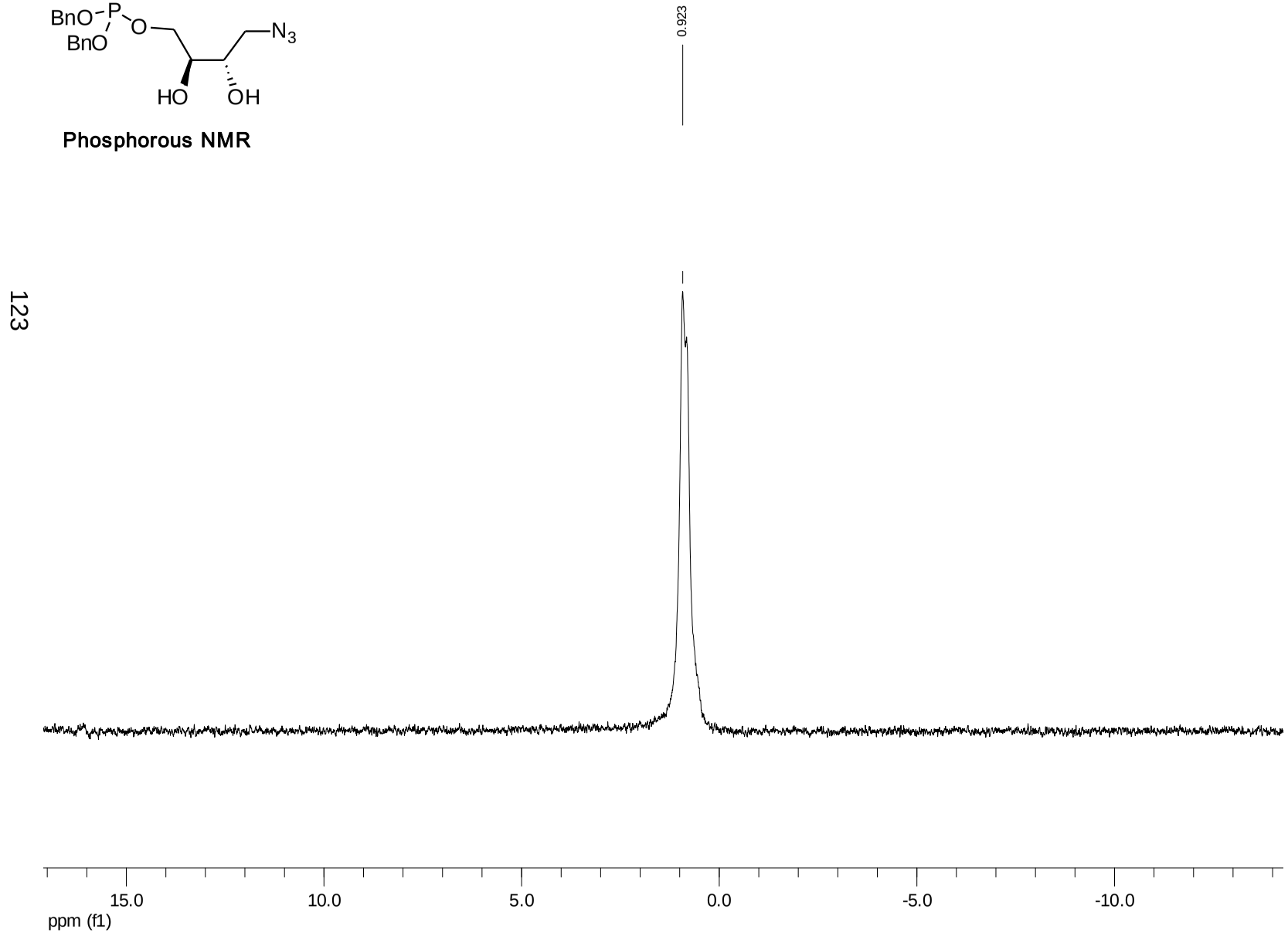

O
BnO
P
O
BnO
N3
O
O
O
O
16
16

Proton NMR

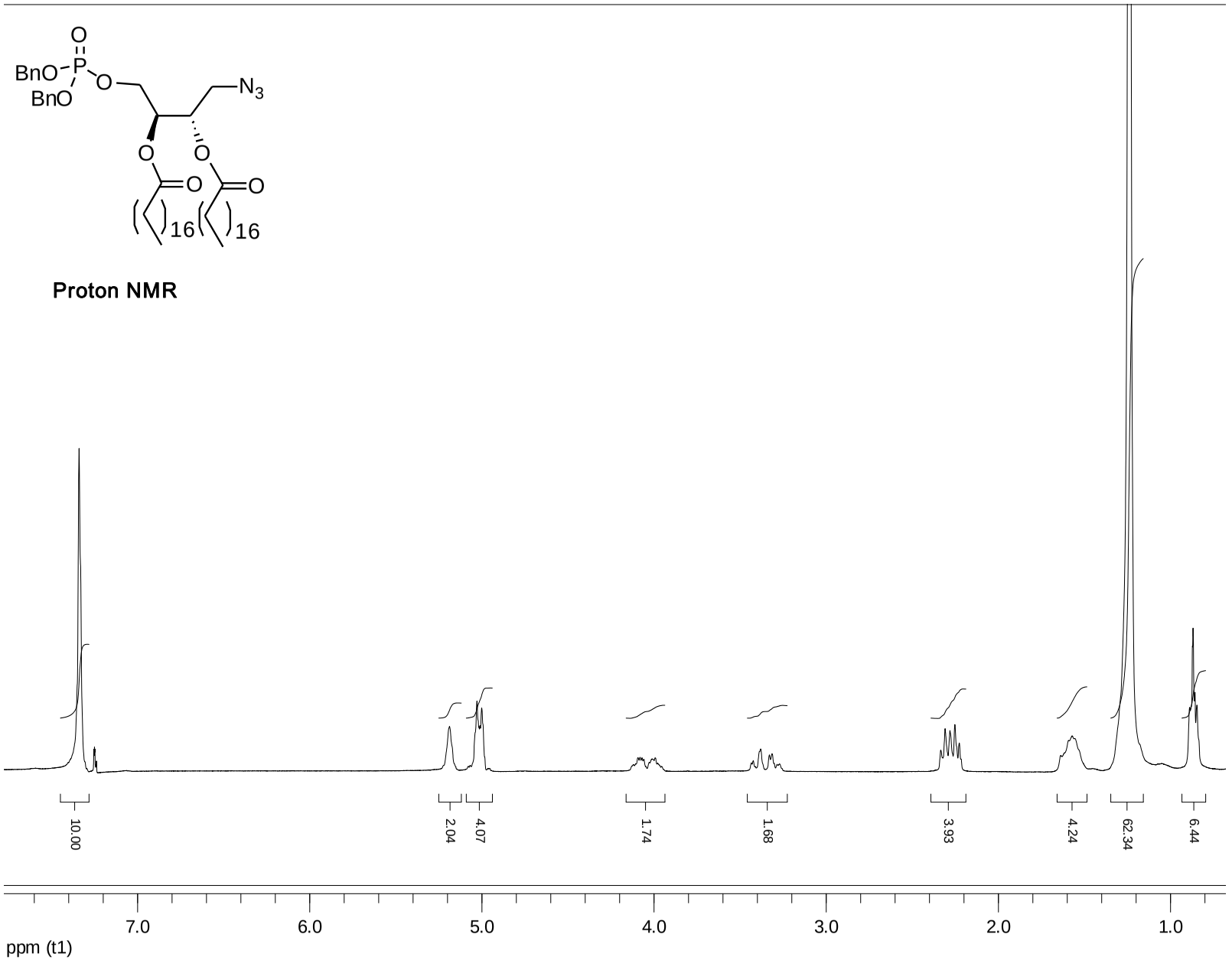
10.00
2.04
4.07
1.74
1.68
3.93
4.24
62.34
6.44
7.0
6.0
5.0
4.0
3.0
2.0
1.0
ppm (t1)

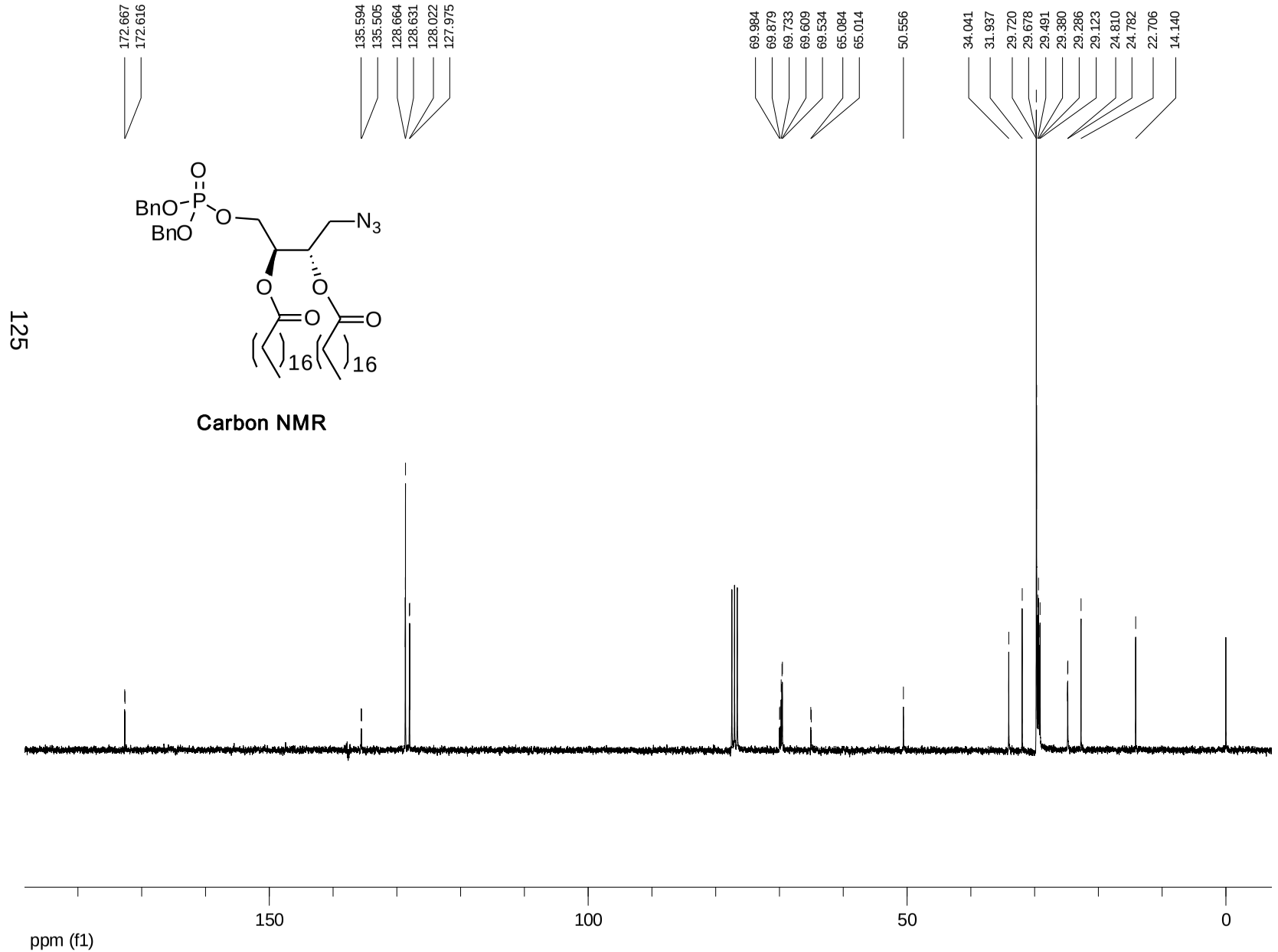
172.667
172.616
135.594
135.505
128.664
128.631
128.022
127.975
69.984
69.879
69.733
69.609
69.534
65.084
65.014
50.556
34.041
31.937
29.720
29.678
29.491
29.380
29.286
29.123
24.810
24.782
22.706
14.140
BnO
BnO
O
P
O
N3
O
O
O
O
16
16
125
Carbon NMR
150
100
50
0
ppm (f1)

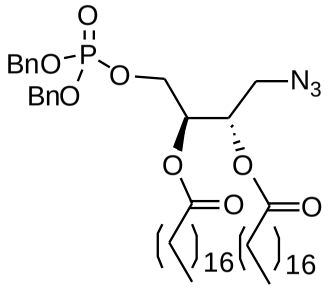

Phosphorous NMR

126

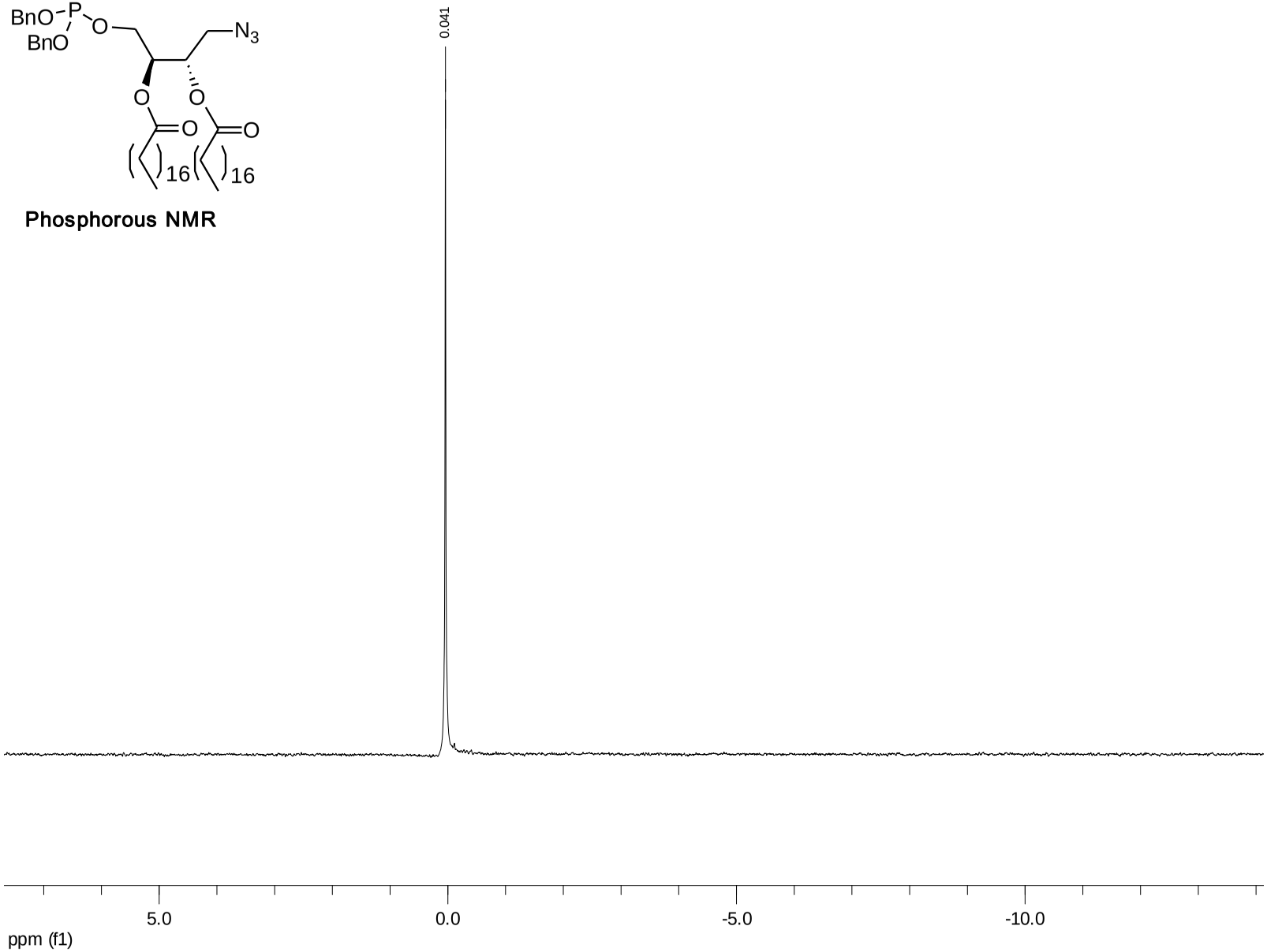

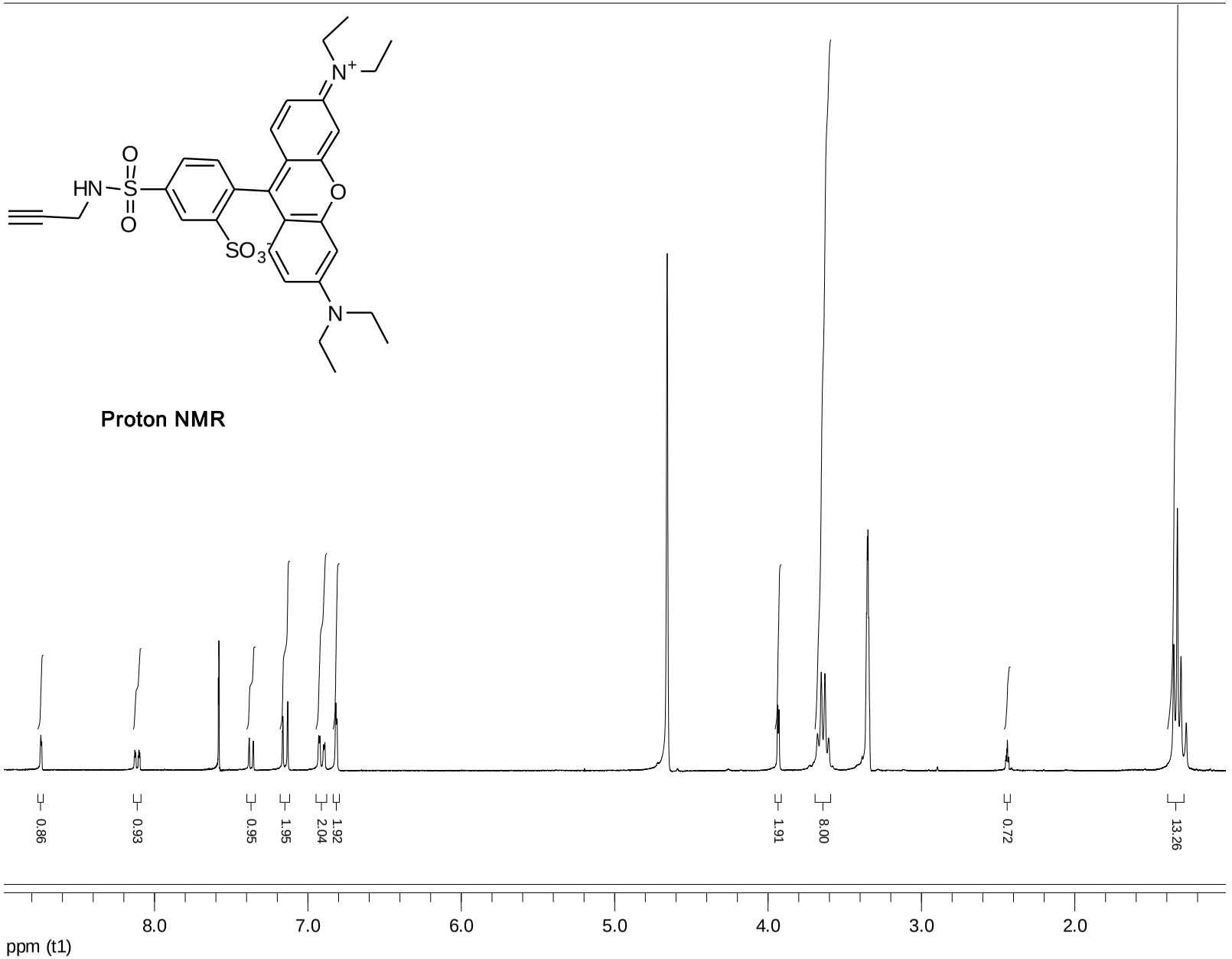
Proton NMR
0.86
0.93
0.95
1.95
2.04
1.92
1.91
8.00
0.72
13.26
8.0
7.0
6.0
5.0
4.0
3.0
2.0
ppm (t1)

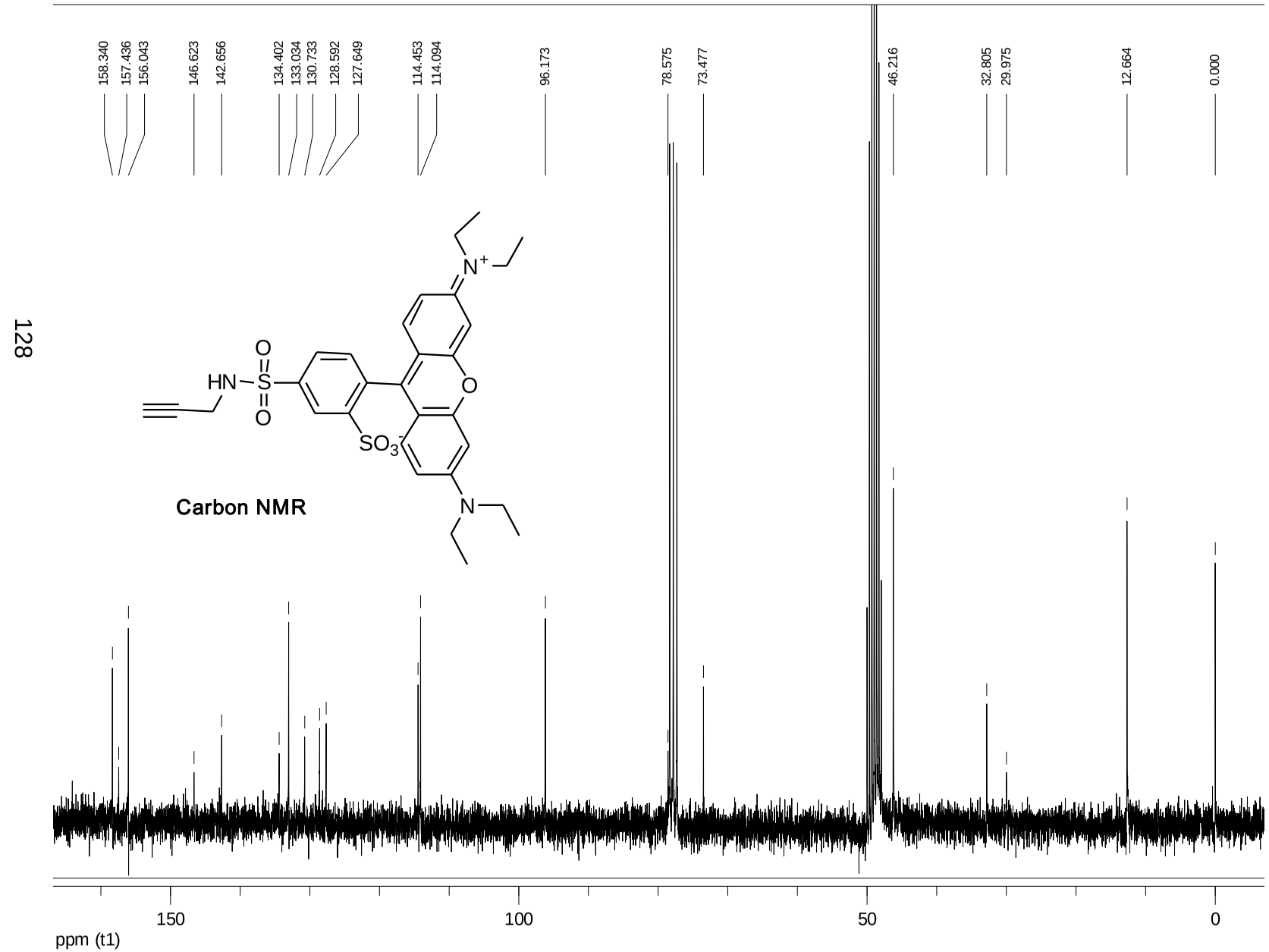
158.340
157.436
156.043
146.623
142.656
134.402
133.034
130.733
128.592
127.649
114.453
114.094
96.173
78.575
73.477
46.216
32.805
29.975
12.664
0.000
Carbon NMR
150
100
50
0
ppm (t1)

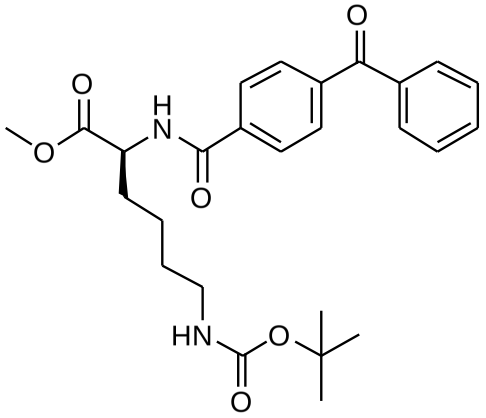
O
O
HN
O
O
HN
O
O

Proton NMR

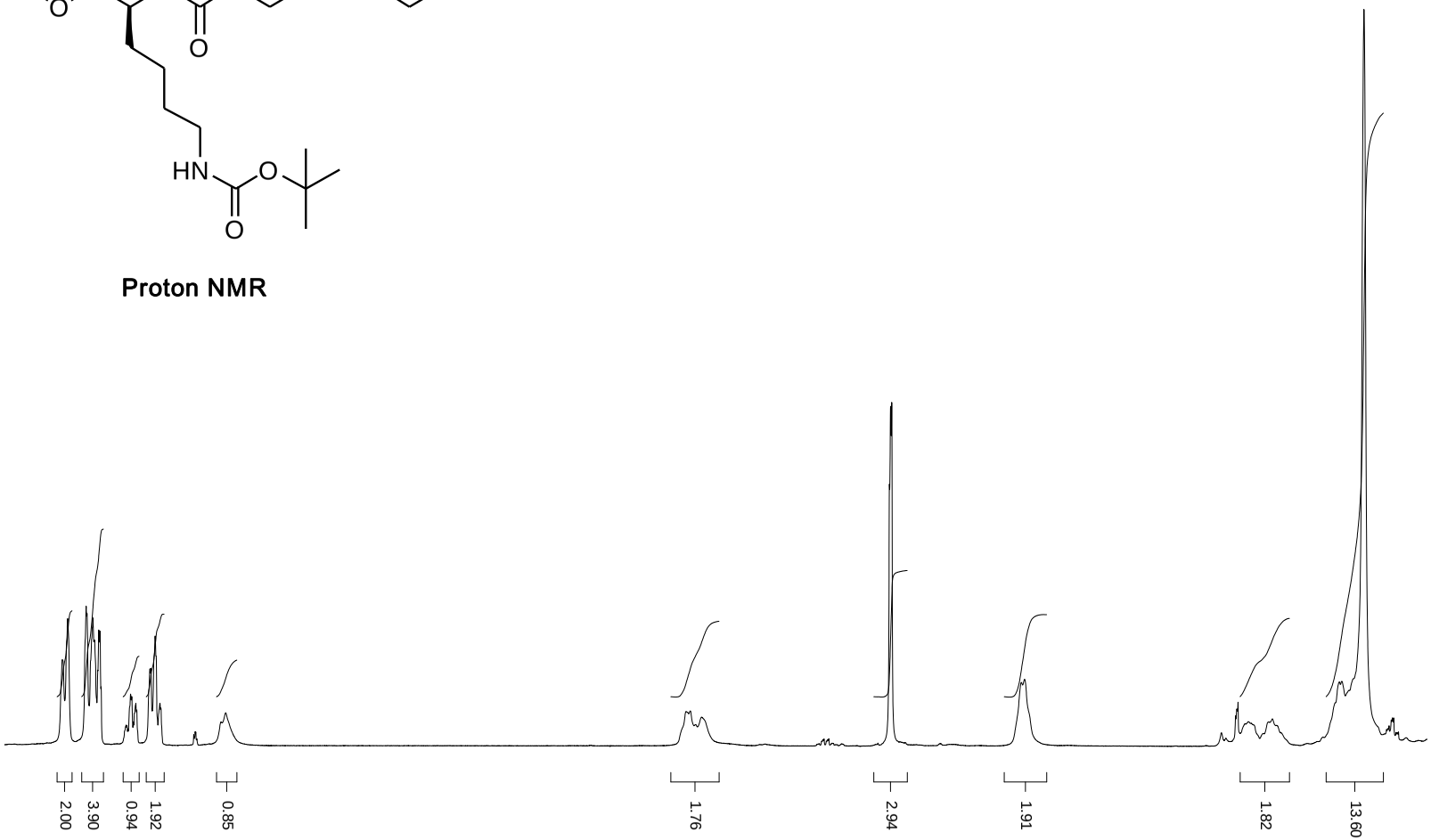
2.00
3.90
0.94
1.92
0.85
1.76
2.94
1.91
1.82
13.60
8.0
7.0
6.0
5.0
4.0
3.0
2.0
ppm (t1)

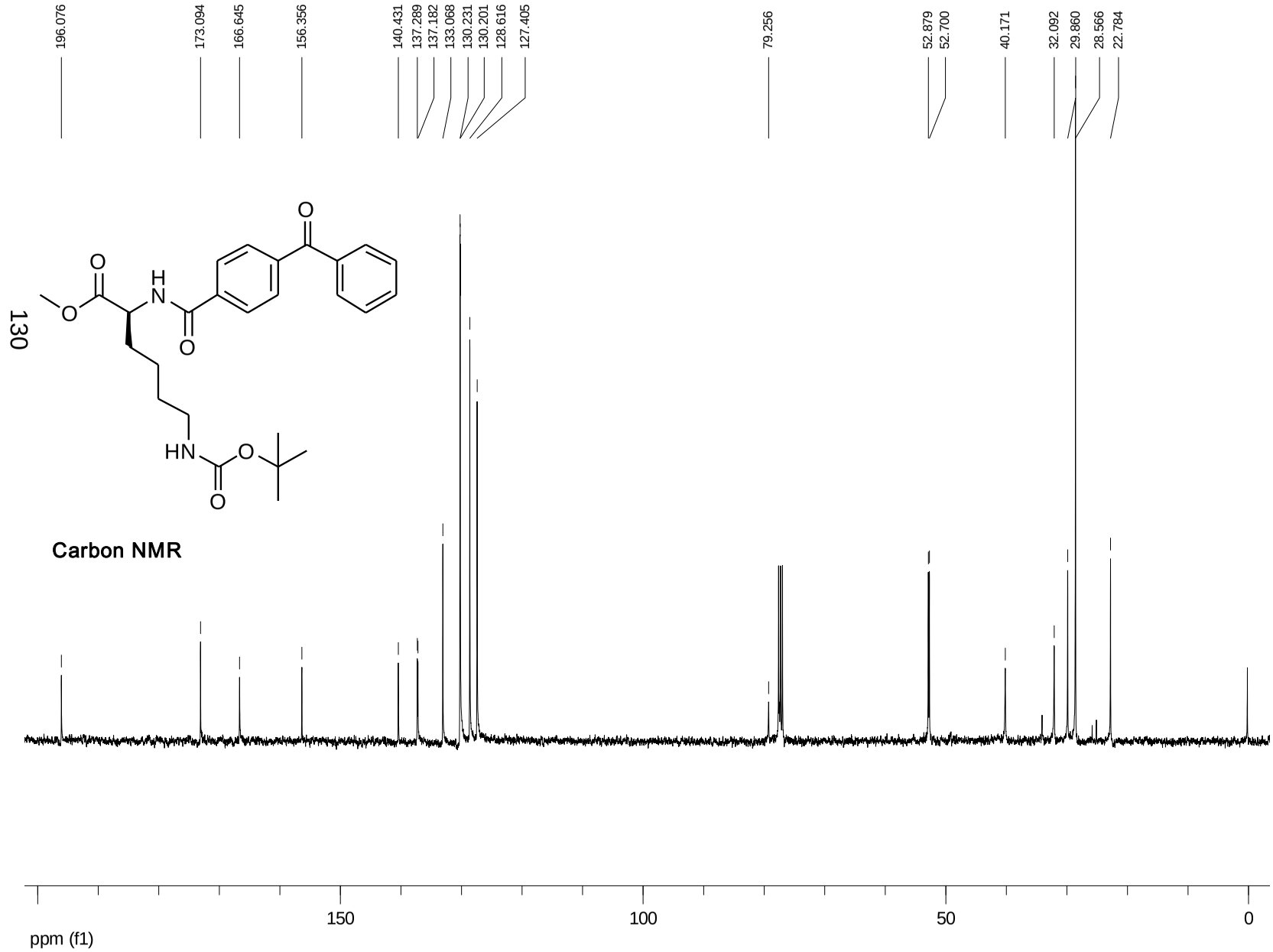
196.076
173.094
166.645
156.356
140.431
137.289
137.182
133.068
130.231
130.201
128.616
127.405
79.256
52.879
52.700
40.171
32.092
29.860
28.566
22.784
130
Carbon NMR
150
100
50
0
ppm (f1)

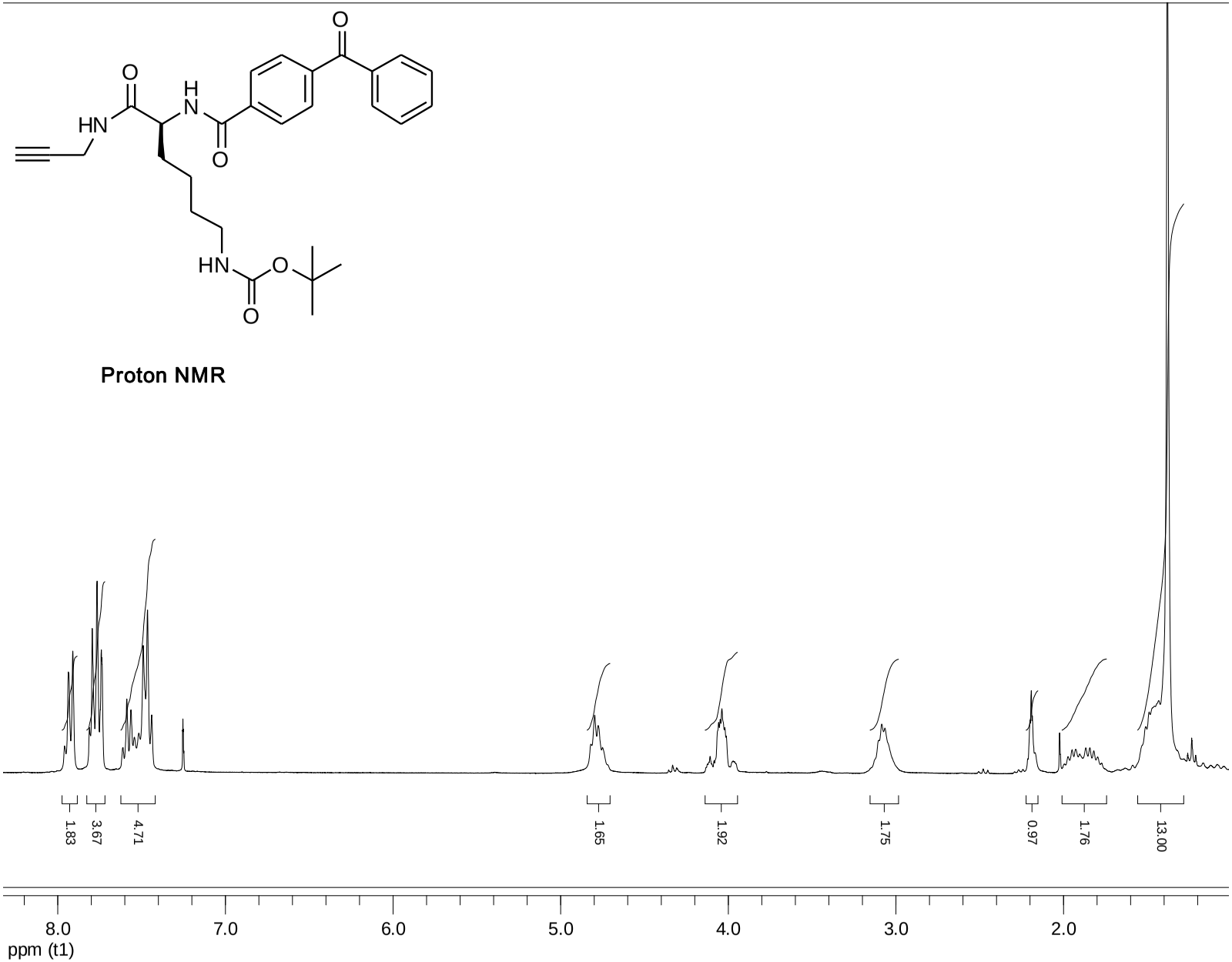
O
HN
O
H
N
O
HN
O
O
O
Proton NMR
1.83
3.67
4.71
1.65
1.92
1.75
0.97
1.76
13.00
8.0
7.0
6.0
5.0
4.0
3.0
2.0
ppm (t1)

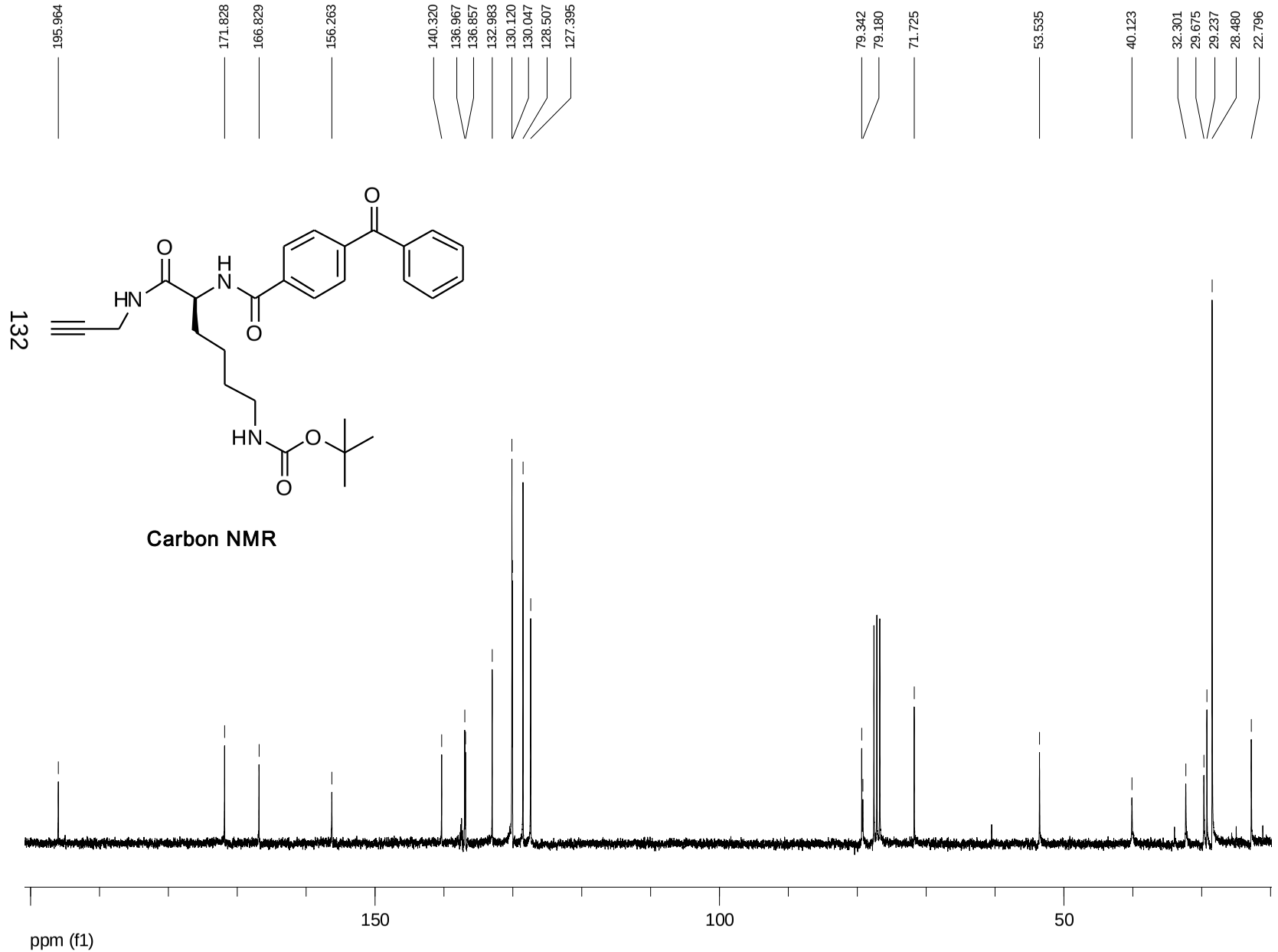
195.964
171.828
166.829
156.263
140.320
136.967
136.857
132.983
130.120
130.047
128.507
127.395
79.342
79.180
71.725
53.535
40.123
32.301
29.675
29.237
28.480
22.796
O
O
HN
H
N
O
HN
O
O
132
Carbon NMR
150
100
50
ppm (f1)

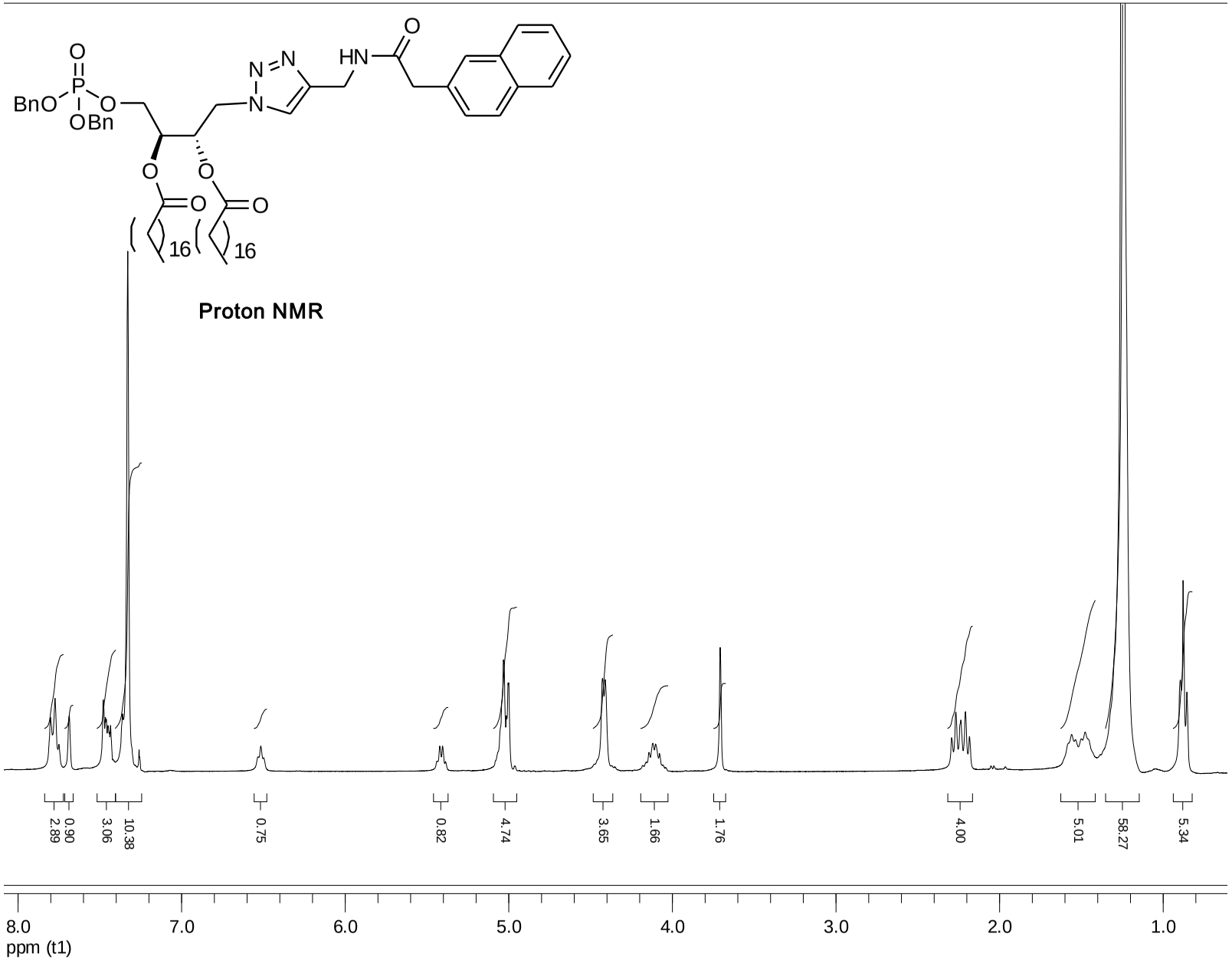
Proton NMR
8.0
7.0
6.0
5.0
4.0
3.0
2.0
1.0
ppm (t1)
2.89
0.90
3.06
10.38
0.75
0.82
4.74
3.65
1.66
1.76
4.00
5.01
58.27
5.34

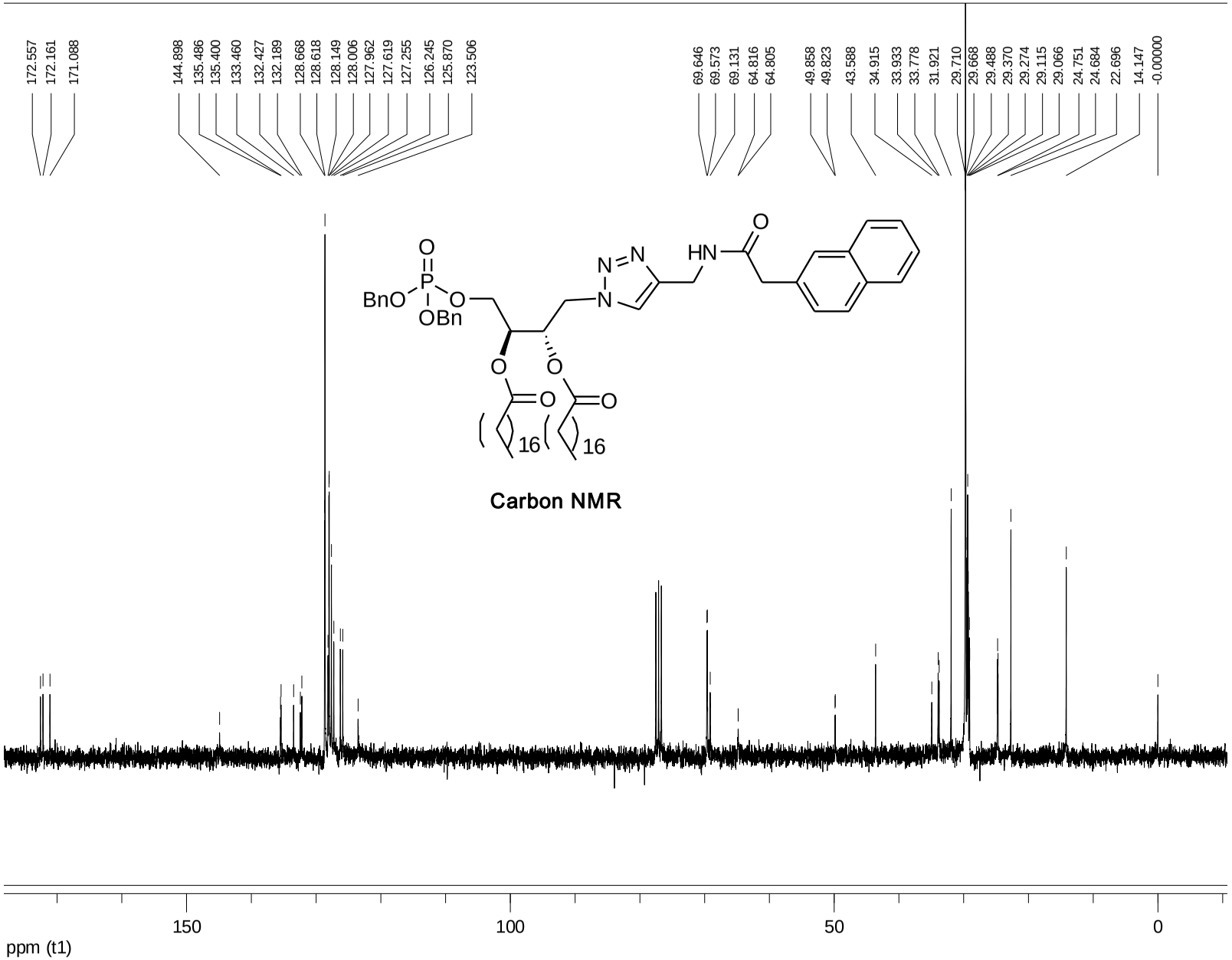
172.557
172.161
171.088
144.898
135.486
135.400
133.460
132.427
132.189
128.668
128.618
128.149
128.006
127.962
127.619
127.255
126.245
125.870
123.506
69.646
69.573
69.131
64.816
64.805
49.858
49.823
43.588
34.915
33.933
33.778
31.921
29.710
29.668
29.488
29.370
29.274
29.115
29.066
24.751
24.684
22.696
14.147
-0.00000
BnO
OBn
HN
16
16
Carbon NMR
150
100
50
0
ppm (t1)

Phosphorous NMR

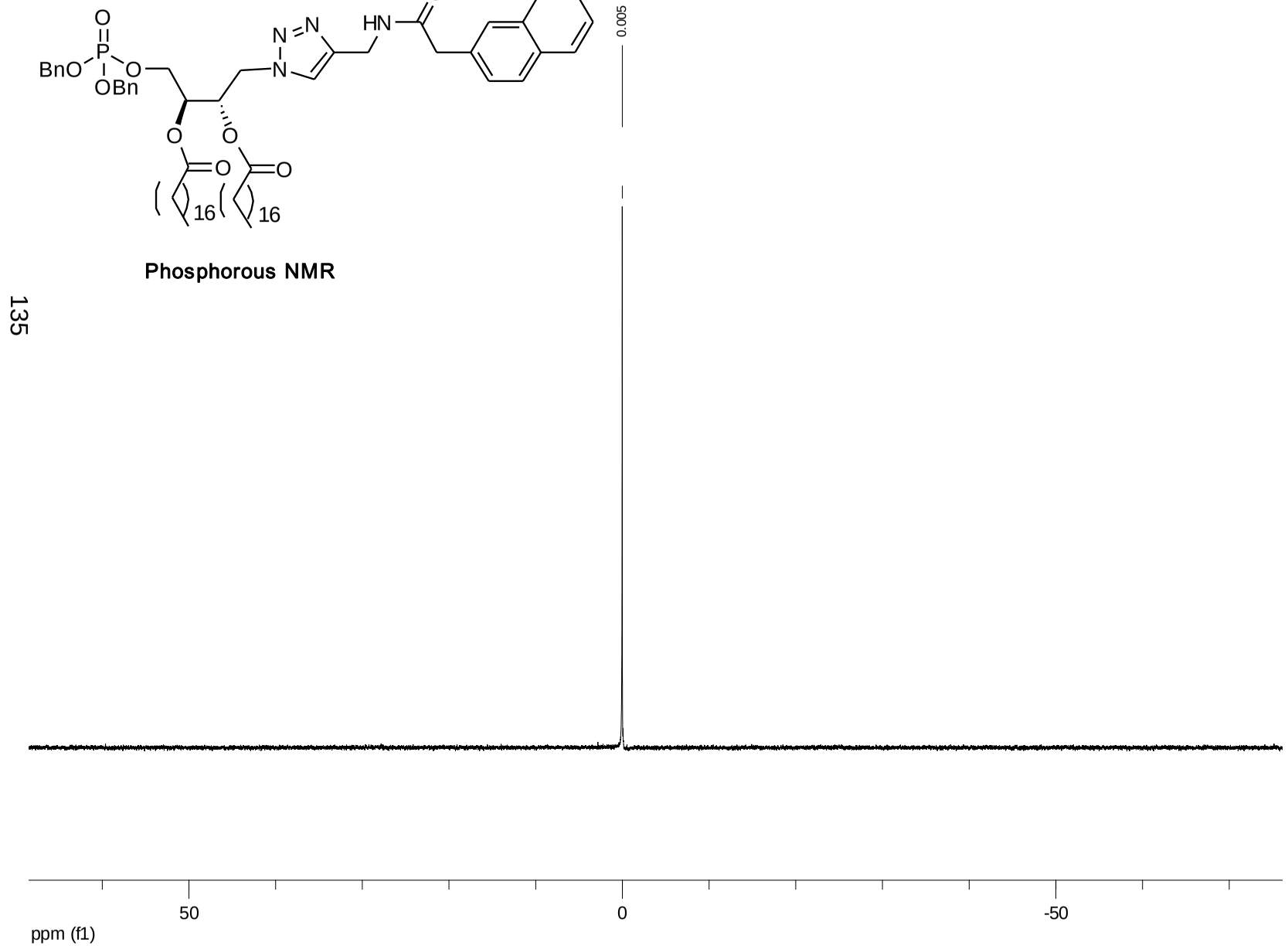

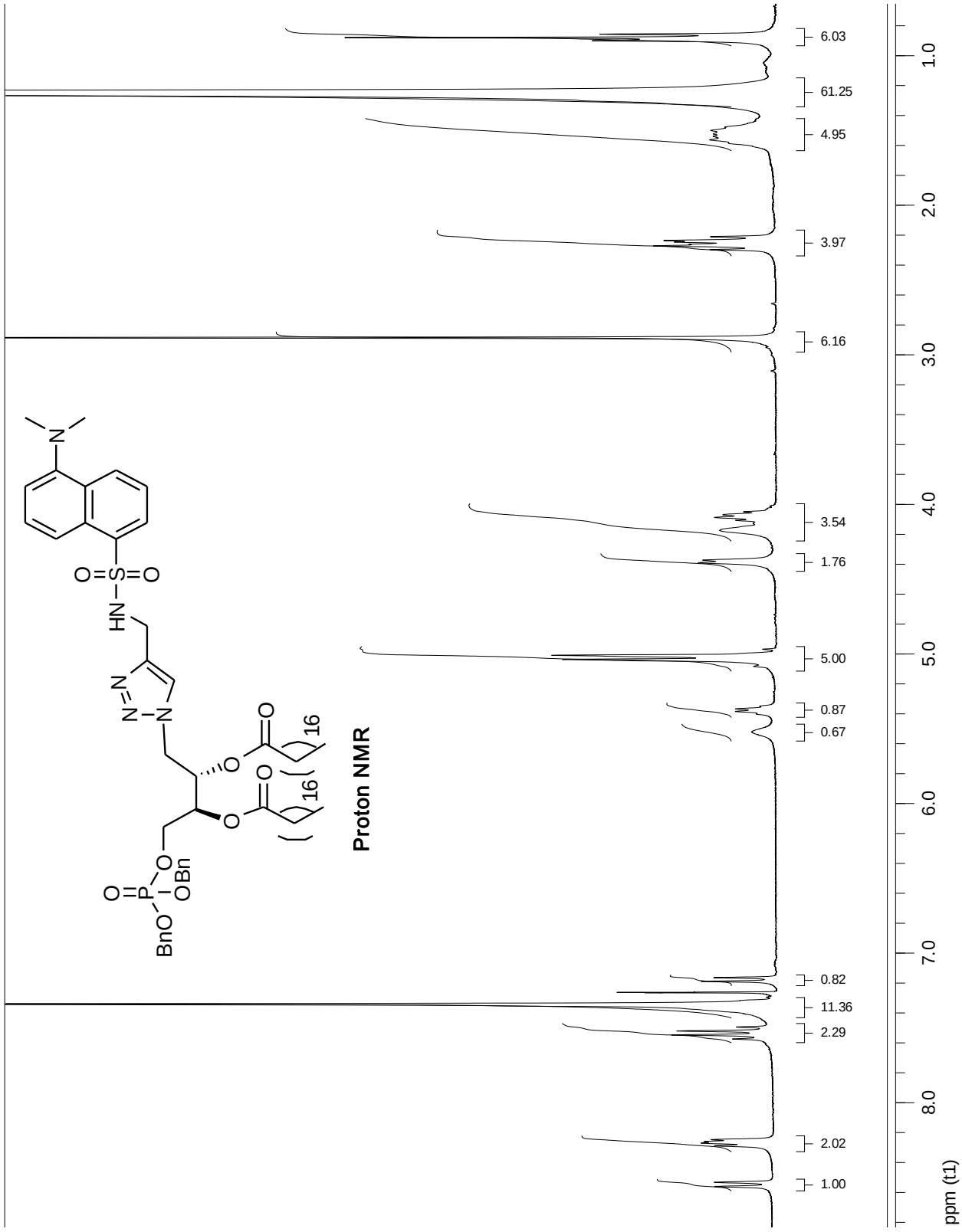
Proton NMR
6.03
61.25
4.95
3.97
6.16
3.54
1.76
5.00
0.87
0.67
0.82
11.36
2.29
2.02
1.00
ppm (t1)

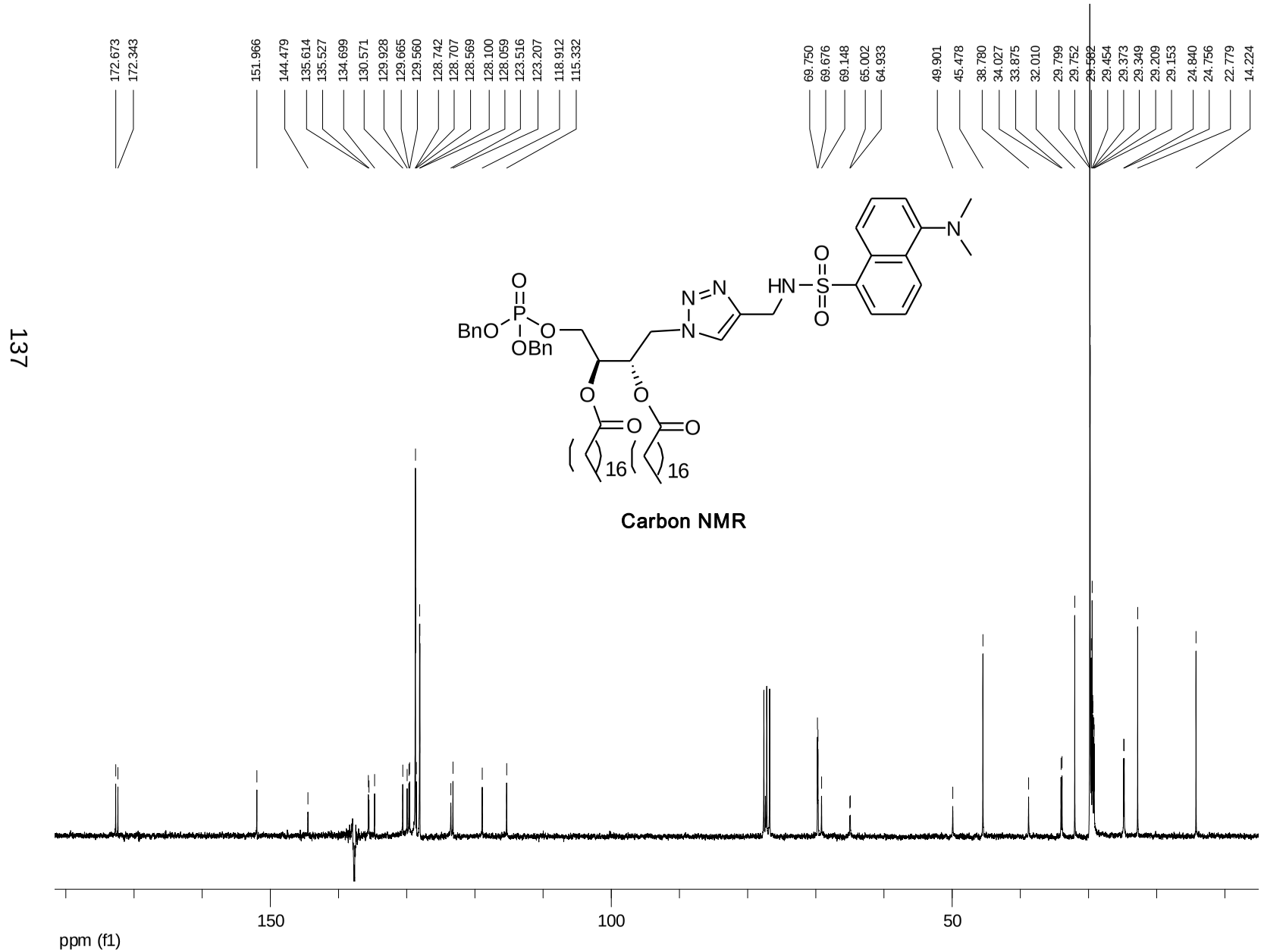
172.673
172.343
151.966
144.479
135.614
135.527
134.699
130.571
129.928
129.665
129.560
128.742
128.707
128.569
128.100
128.059
123.516
123.207
118.912
115.332
69.750
69.676
69.148
65.002
64.933
49.901
45.478
38.780
34.027
33.875
32.010
29.799
29.752
29.582
29.454
29.373
29.349
29.209
29.153
24.840
24.756
22.779
14.224
BnO
OBn
HN
16
16
150
100
50
ppm (f1)

Carbon NMR

Phosphorous NMR

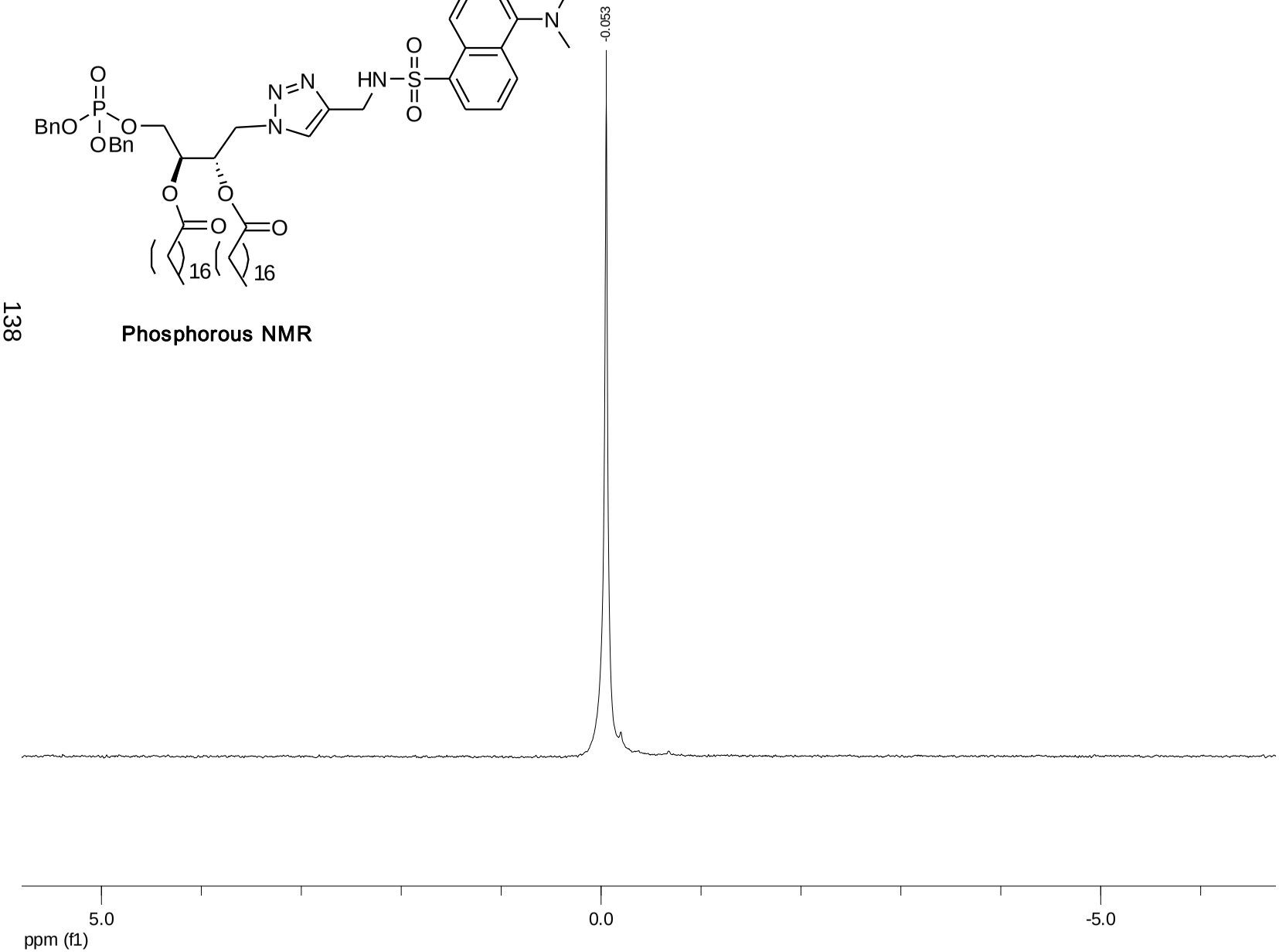

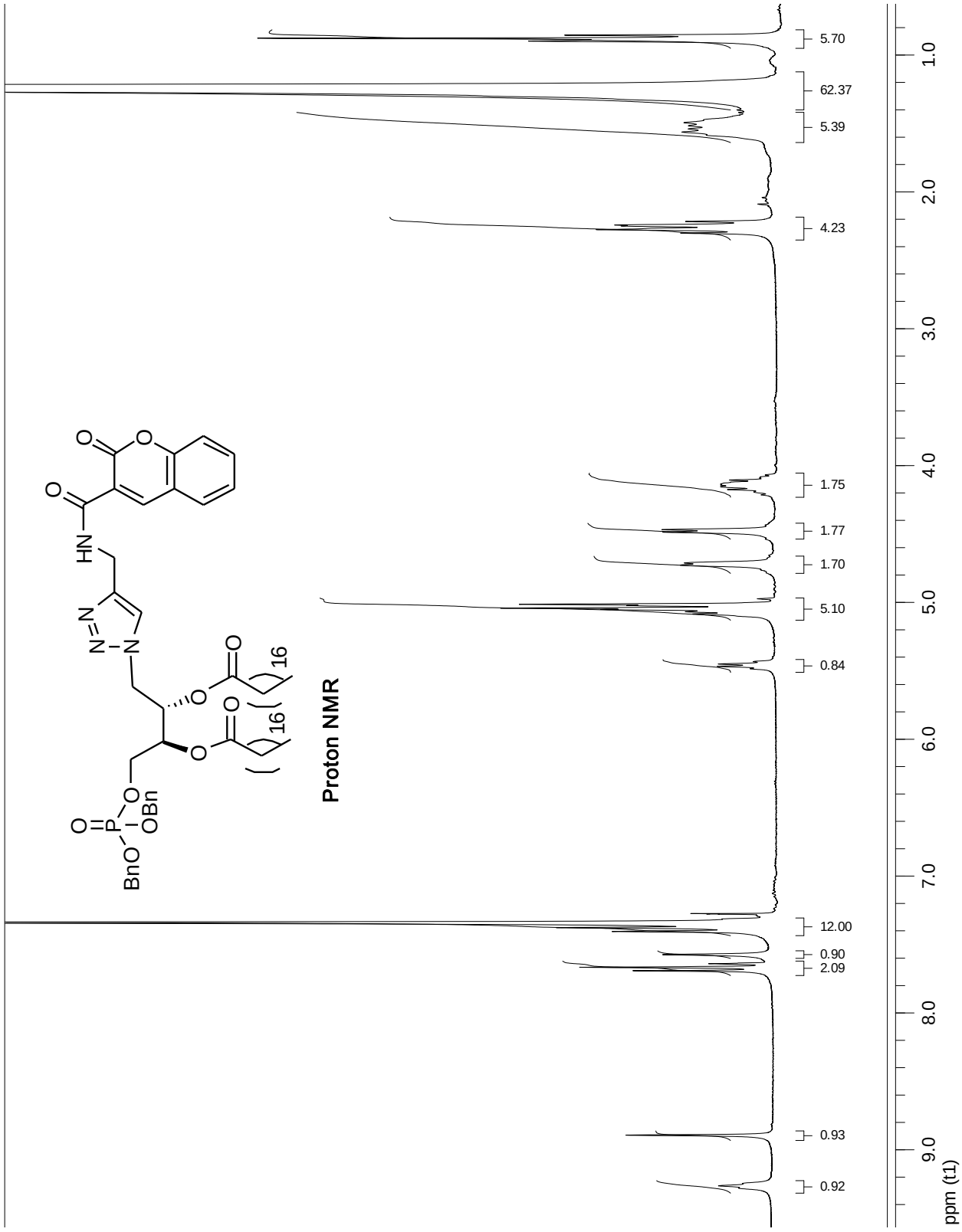
Proton NMR
5.70
62.37
5.39
4.23
1.75
1.77
1.70
5.10
0.84
12.00
0.90
2.09
0.93
0.92
1.0
2.0
3.0
4.0
5.0
6.0
7.0
8.0
9.0
ppm (t1)

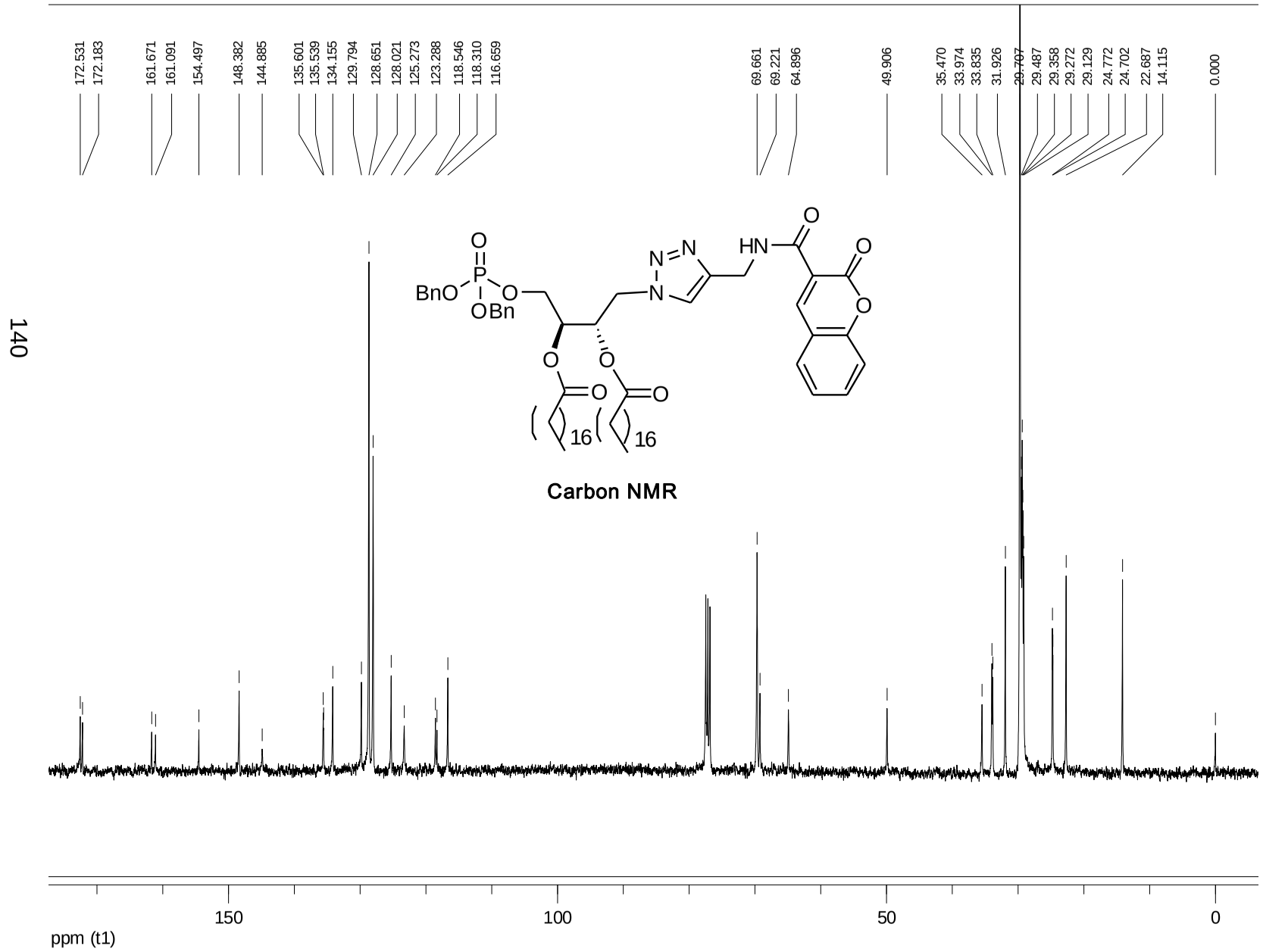
172.531
172.183
161.671
161.091
154.497
148.382
144.885
135.601
135.539
134.155
129.794
128.651
128.021
125.273
123.288
118.546
118.310
116.659
69.661
69.221
64.896
49.906
35.470
33.974
33.835
31.926
29.707
29.487
29.358
29.272
29.129
24.772
24.702
22.687
14.115
0.000
BnO
OBn
HN
16
16
Carbon NMR
140
150
100
50
0
ppm (t1)

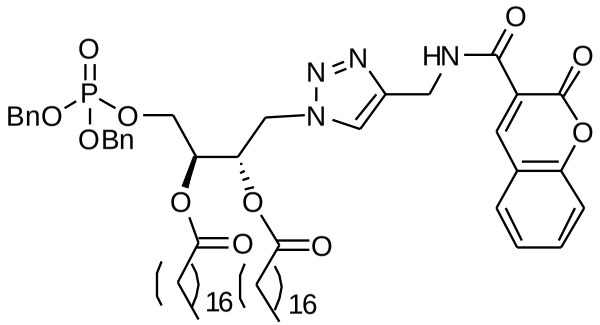

Phosphorous NMR

141

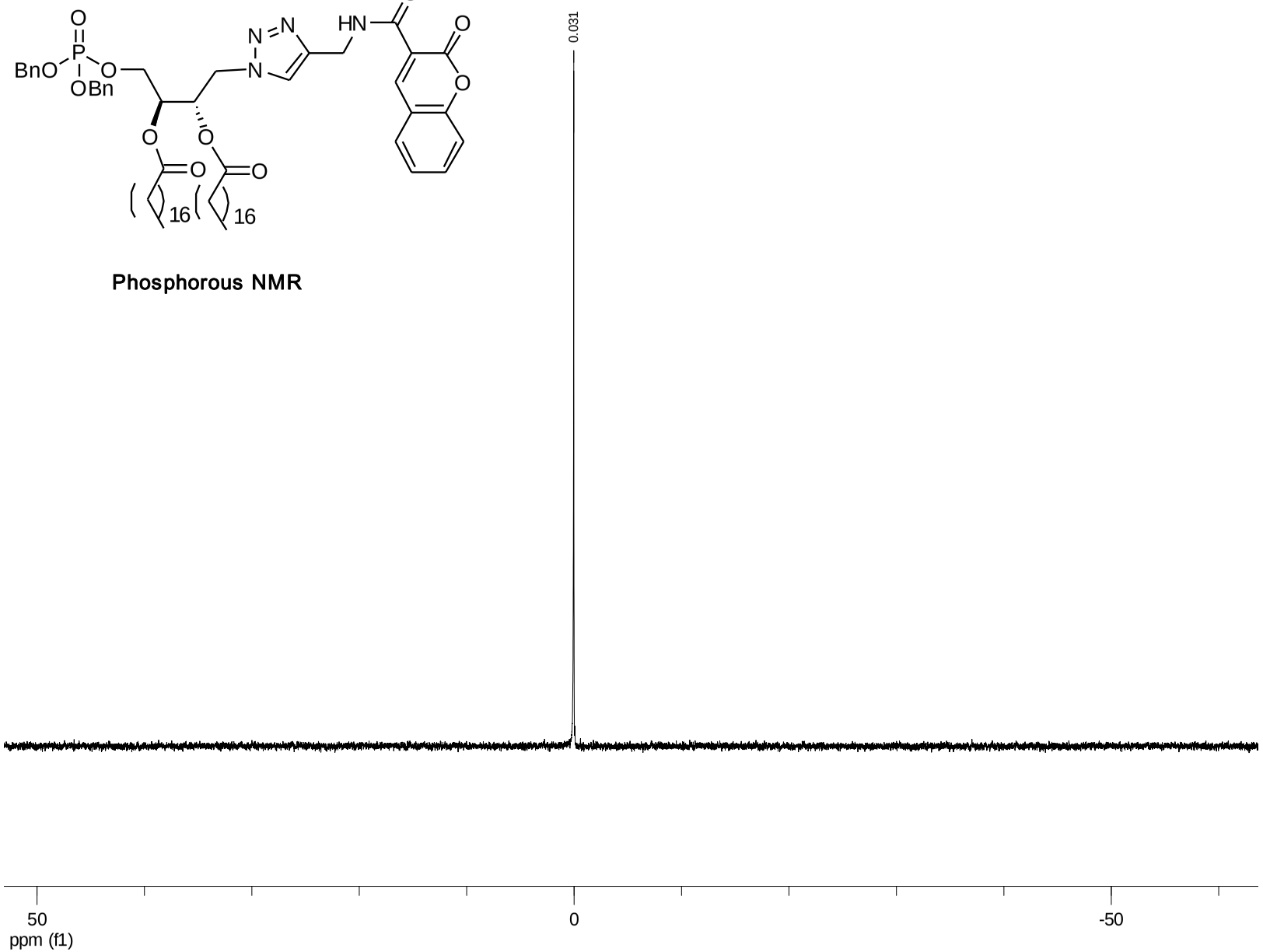

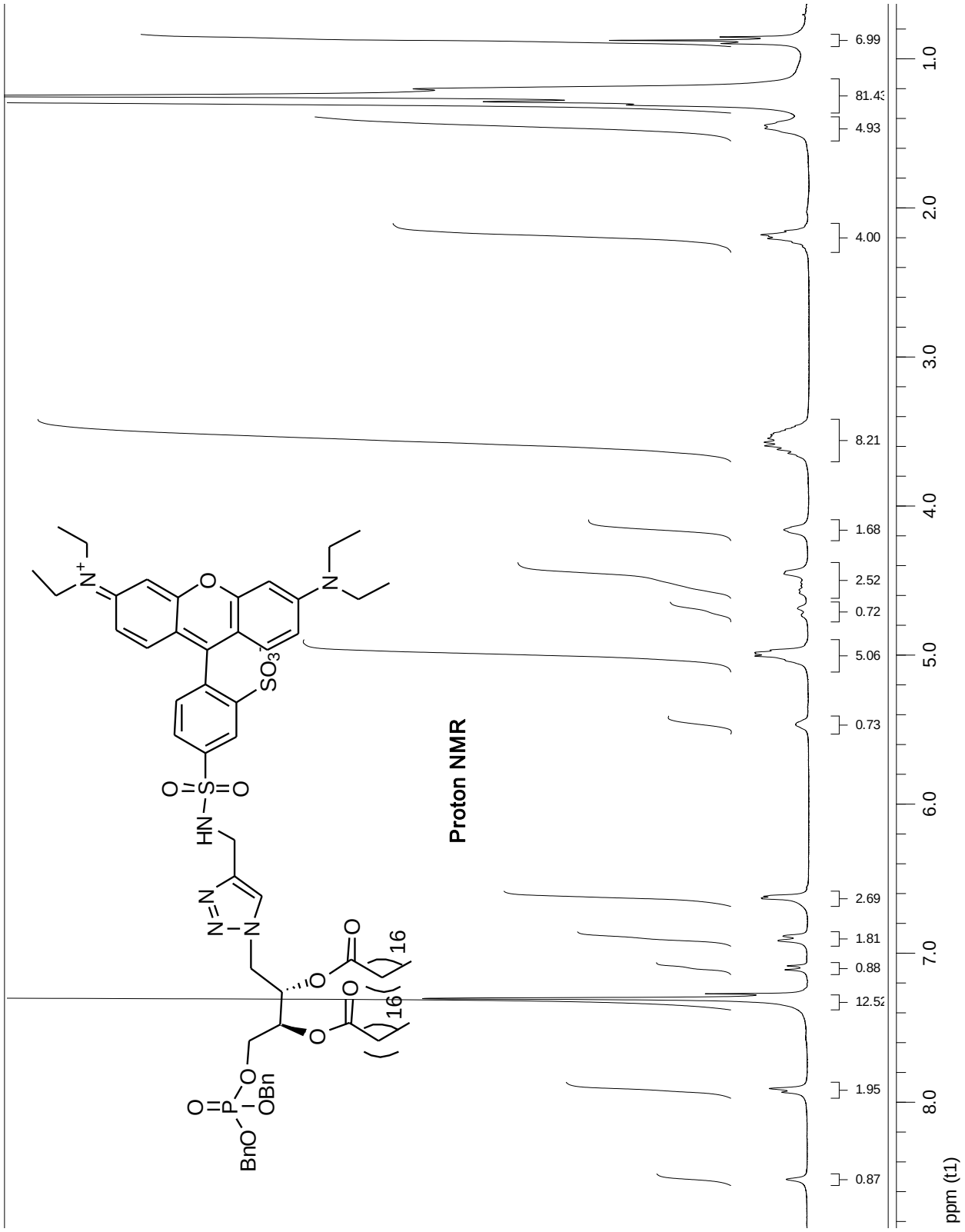
Proton NMR
6.99
81.43
4.93
4.00
8.21
1.68
2.52
0.72
5.06
0.73
2.69
1.81
0.88
12.52
1.95
0.87
1.0
2.0
3.0
4.0
5.0
6.0
7.0
8.0
ppm (t1)

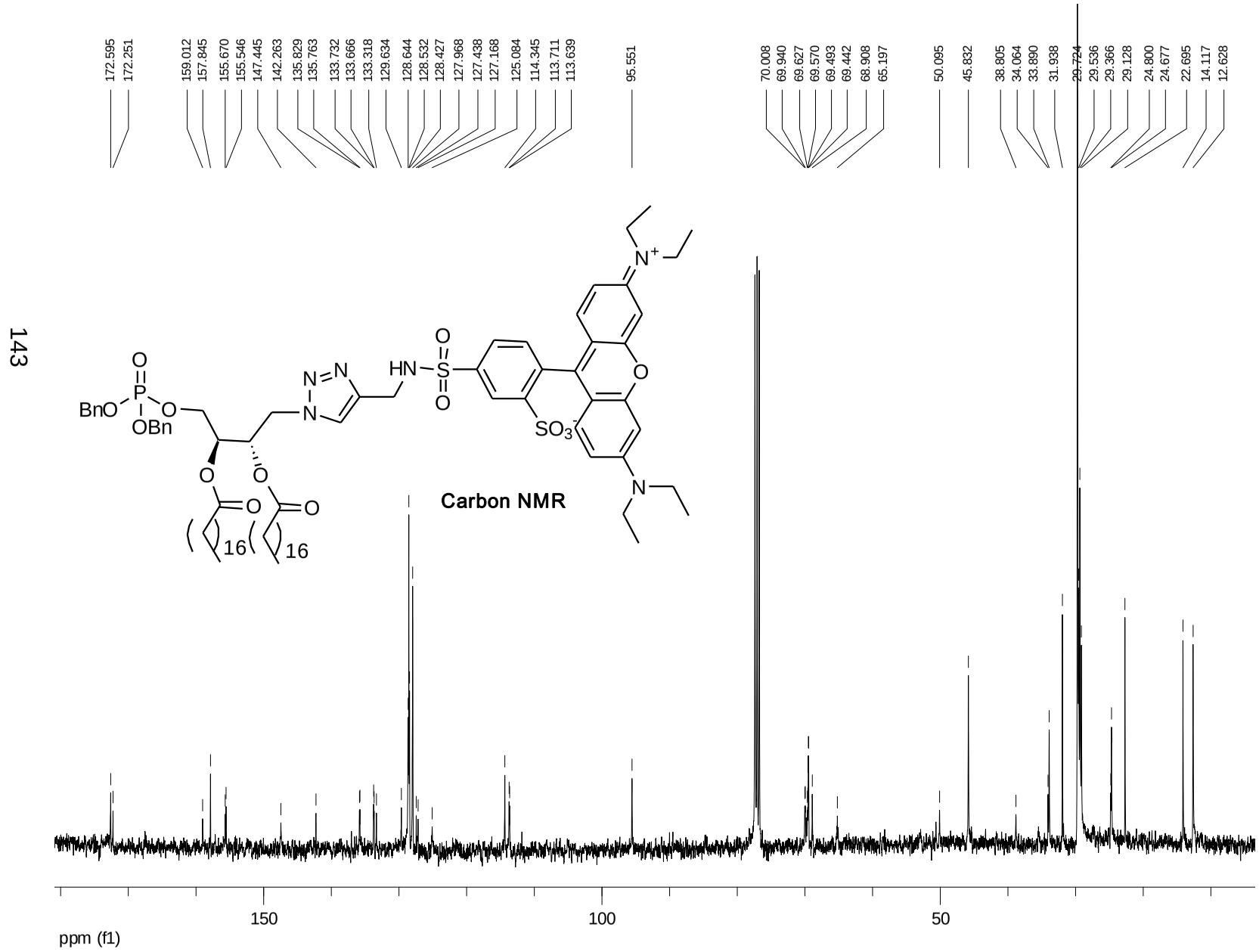
172.595
172.251
159.012
157.845
155.670
155.546
147.445
142.263
135.829
135.763
133.732
133.666
133.318
129.634
128.644
128.532
128.427
127.968
127.438
127.168
125.084
114.345
113.711
113.639
95.551
70.008
69.940
69.627
69.570
69.493
69.442
68.908
65.197
50.095
45.832
38.805
34.064
33.890
31.938
29.724
29.536
29.366
29.128
24.800
24.677
22.695
14.117
12.628
143
Carbon NMR
150
100
50
ppm (f1)

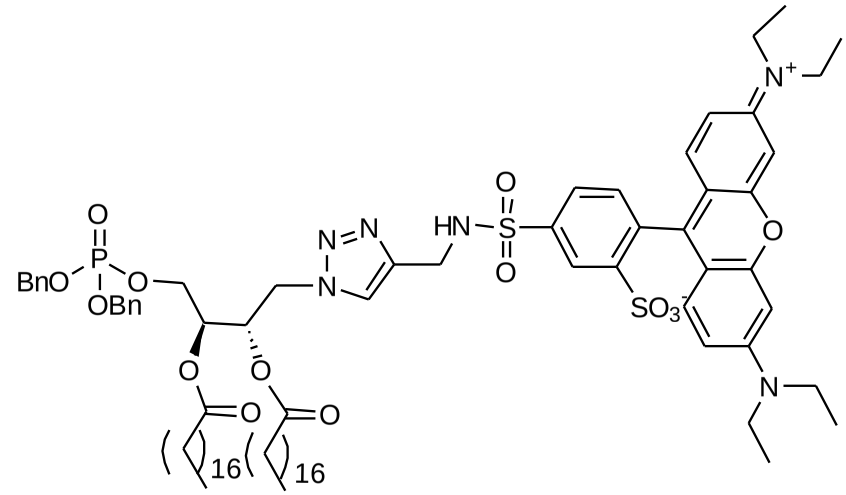

Phosphorous NMR

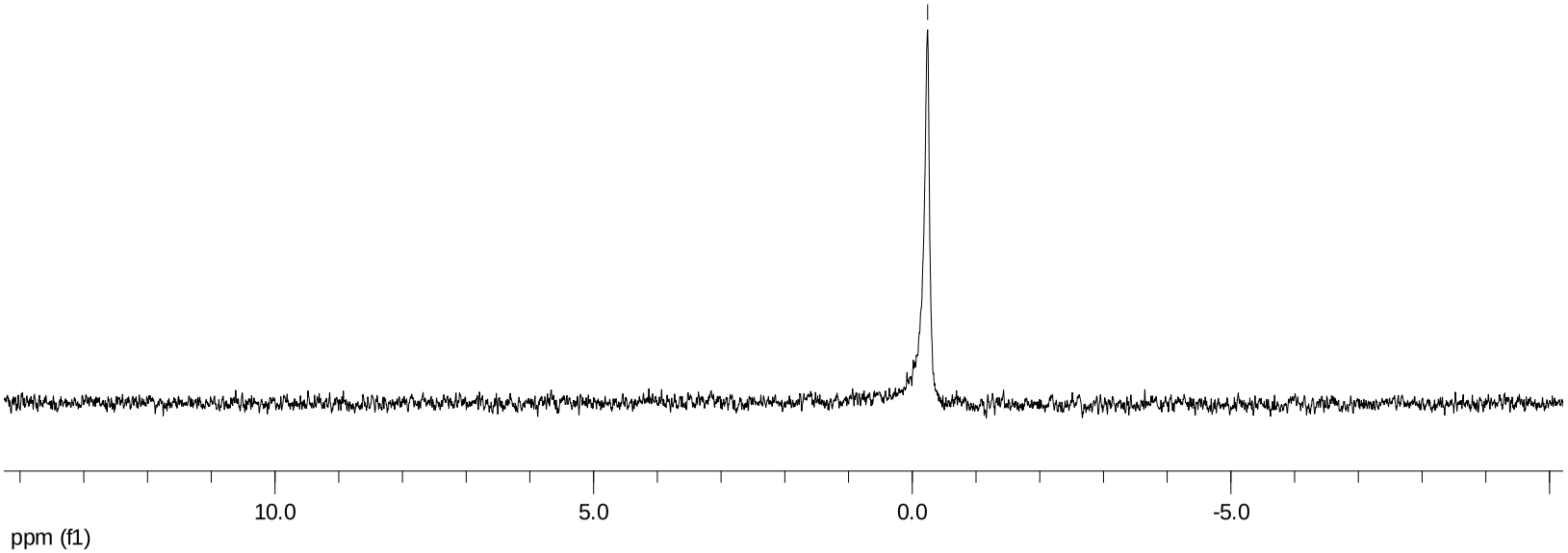

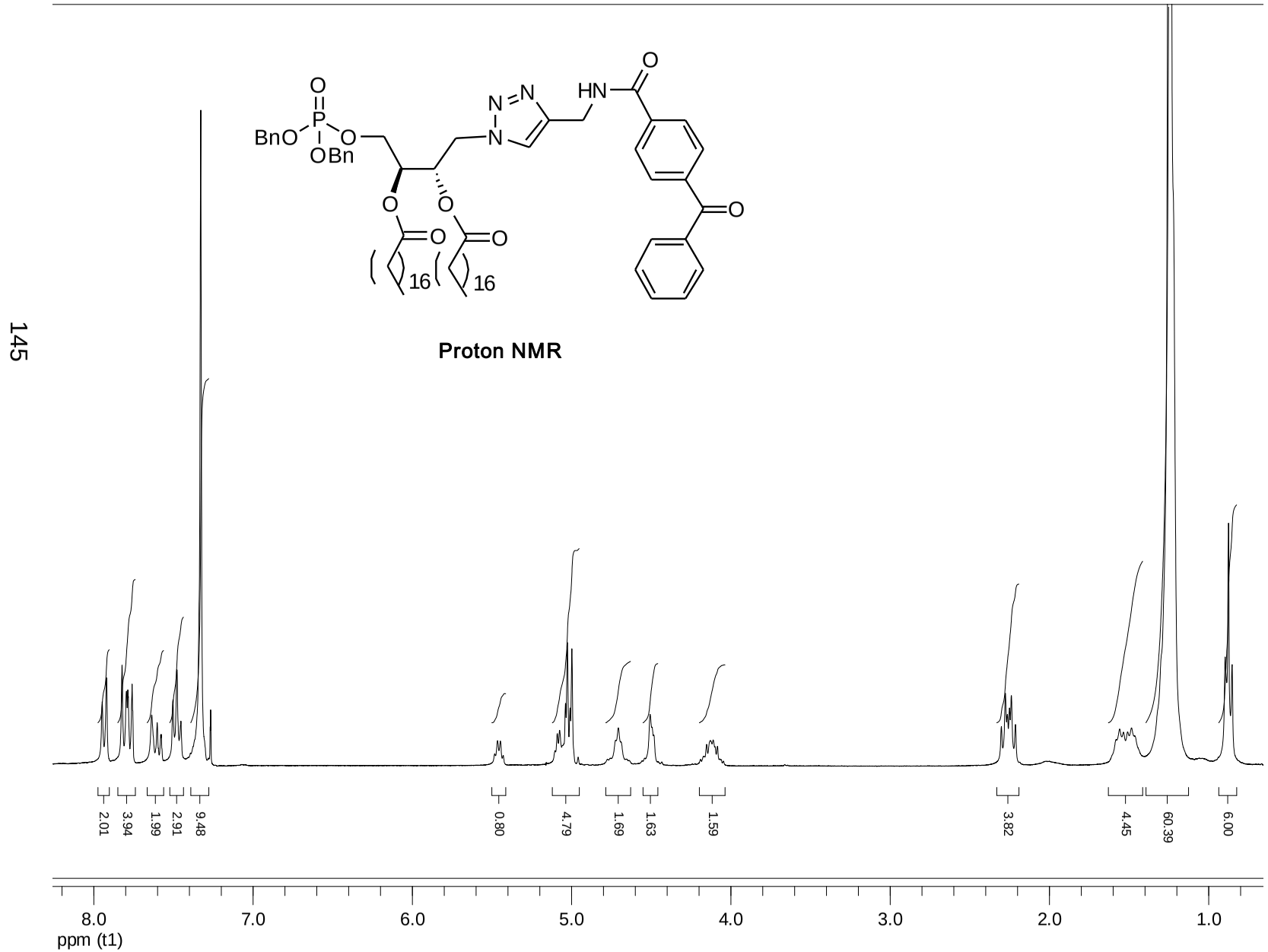
Proton NMR
2.01
3.94
1.99
2.91
9.48
0.80
4.79
1.69
1.63
1.59
3.82
4.45
60.39
6.00
8.0
7.0
6.0
5.0
4.0
3.0
2.0
1.0
ppm (t1)

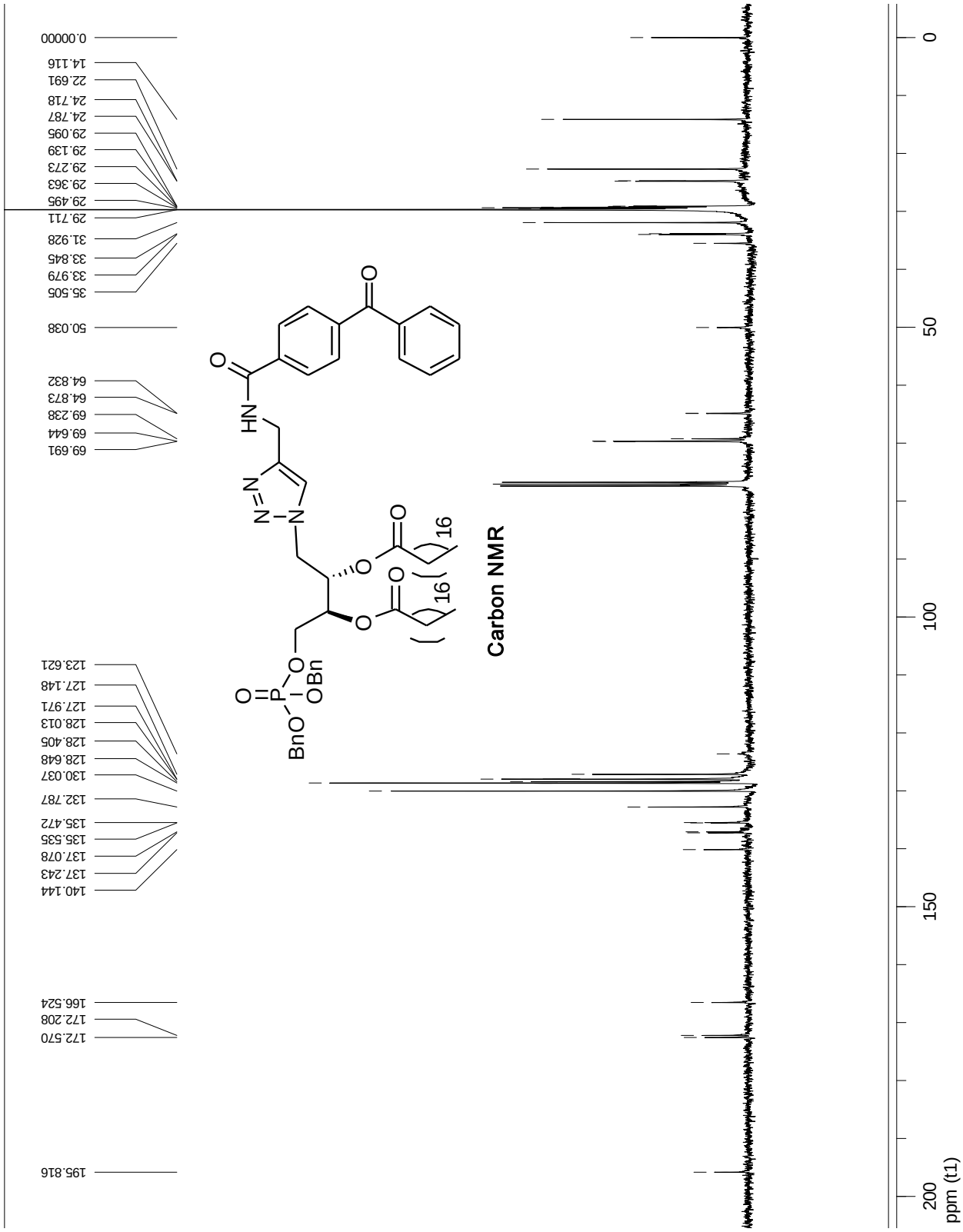
0.00000
14.116
22.691
24.718
24.787
29.095
29.139
29.273
29.363
29.495
29.711
31.928
33.845
33.979
35.505
50.038
64.832
64.873
69.238
69.644
69.691
123.621
127.148
127.971
128.013
128.405
128.648
130.037
132.787
135.472
135.535
137.078
137.243
140.144
166.524
172.208
172.570
195.816
Carbon NMR
ppm (t1)
0
50
100
150
200

Phosphorous NMR

147

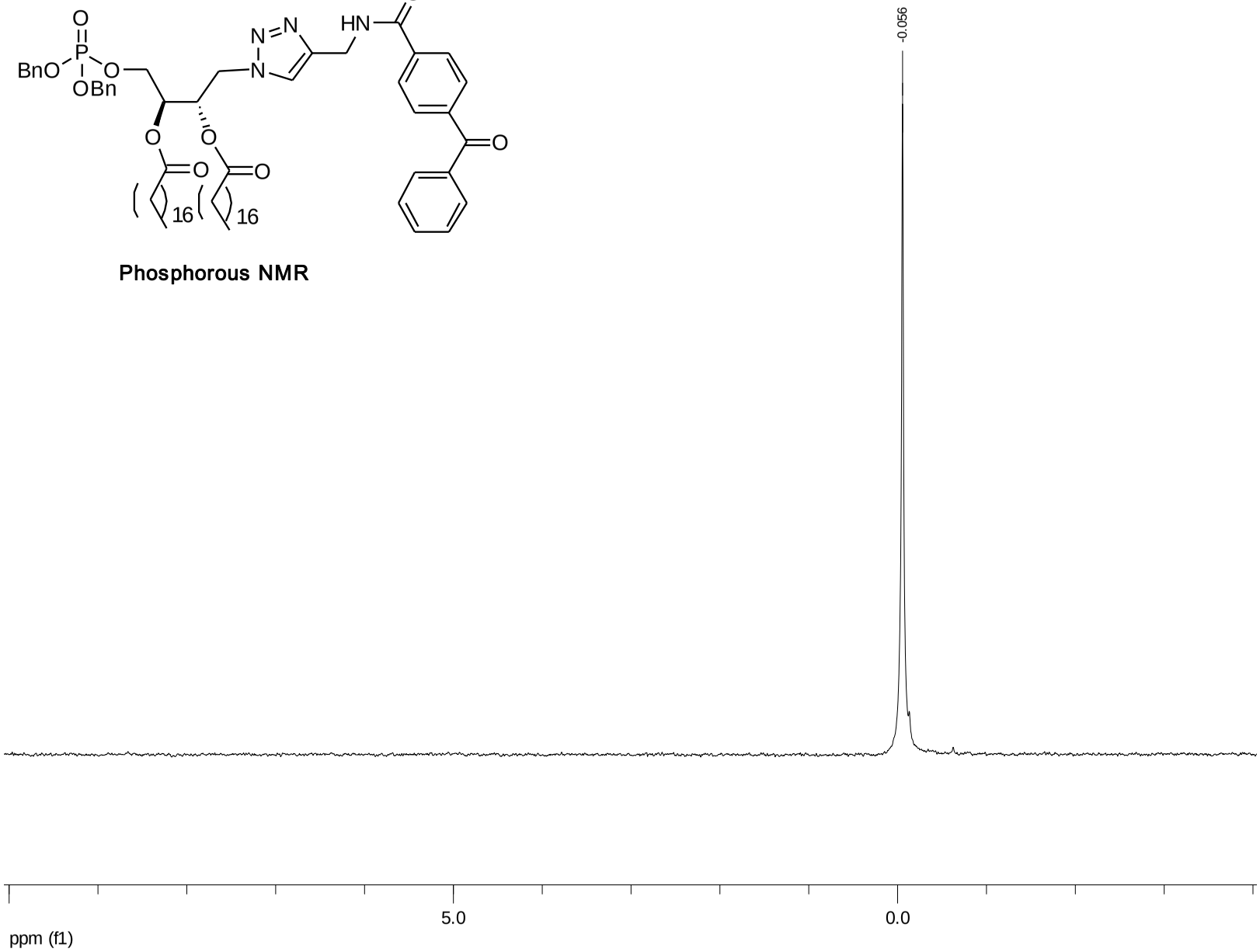

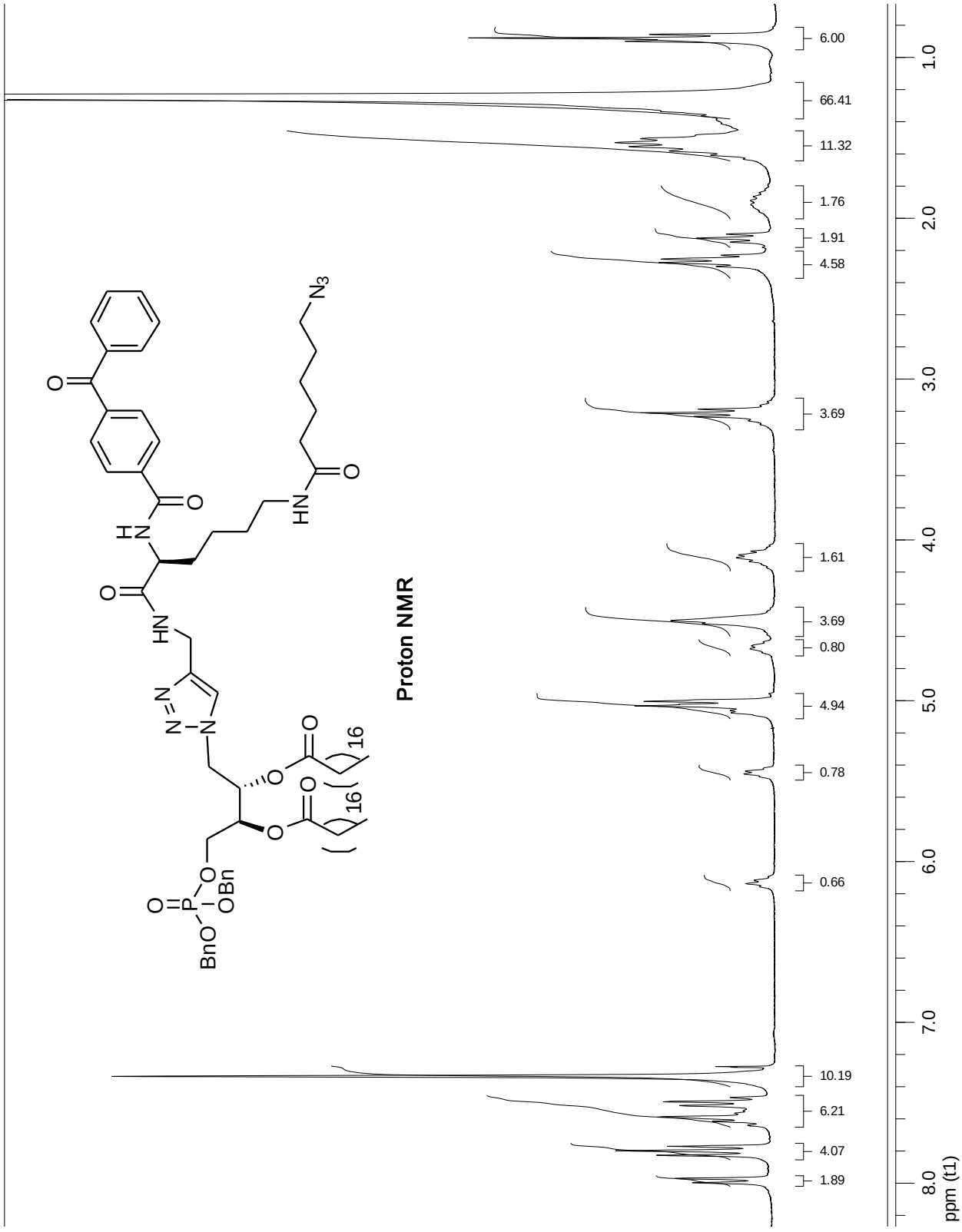
Proton NMR
6.00
66.41
11.32
1.76
1.91
4.58
3.69
1.61
3.69
0.80
4.94
0.78
0.66
10.19
6.21
4.07
1.89
1.0
2.0
3.0
4.0
5.0
6.0
7.0
8.0
ppm (t1)

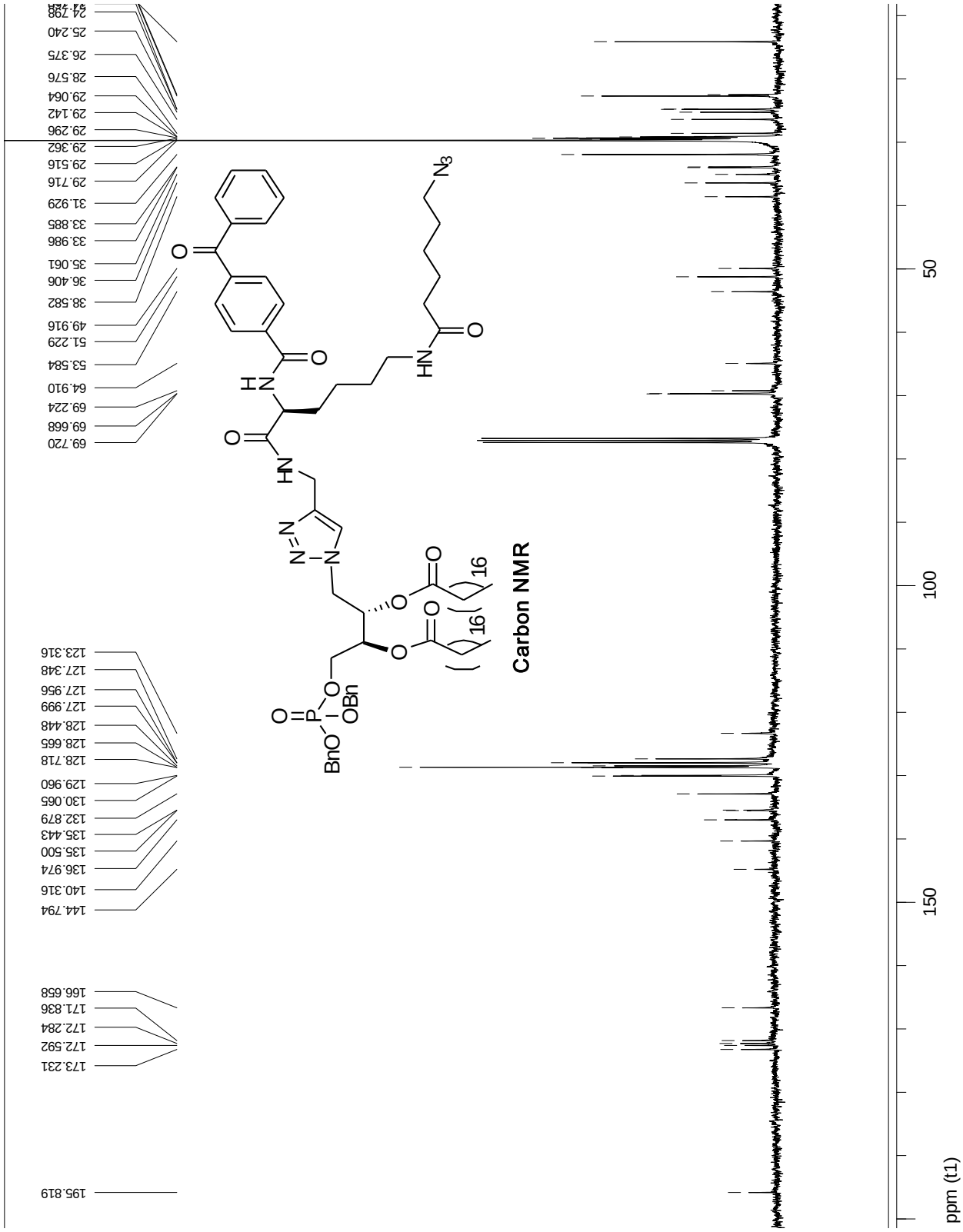
Carbon NMR
ppm (t1)
50
100
150
24.798
25.240
26.375
28.576
29.064
29.142
29.296
29.362
29.516
29.716
31.929
33.885
33.986
35.061
36.406
38.582
49.916
51.229
53.584
64.910
69.224
69.668
69.720
123.316
127.348
127.956
127.999
128.448
128.665
128.718
129.960
130.065
132.879
135.443
135.500
136.974
140.316
144.794
166.658
171.836
172.284
172.592
173.231
195.819

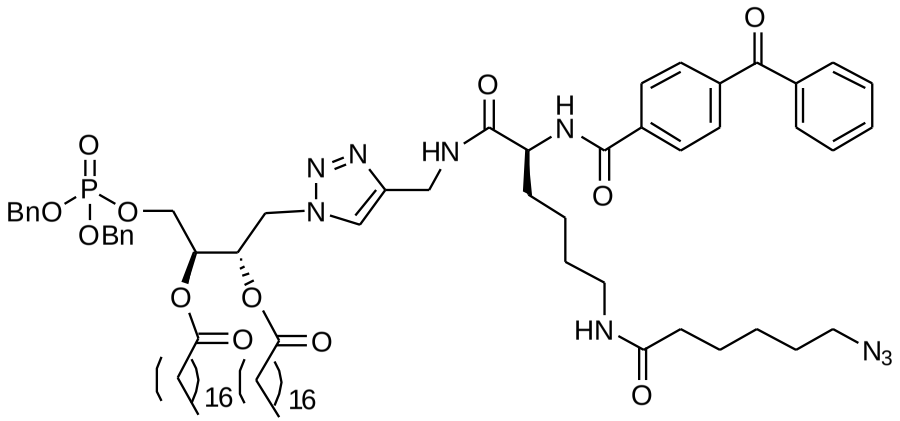

150

Phosphorous NMR

-0.251

10.0 5.0 0.0 -5.0

ppm (f1)

-2O3PO
N3
O
O
O
O
O
16
16

Proton NMR

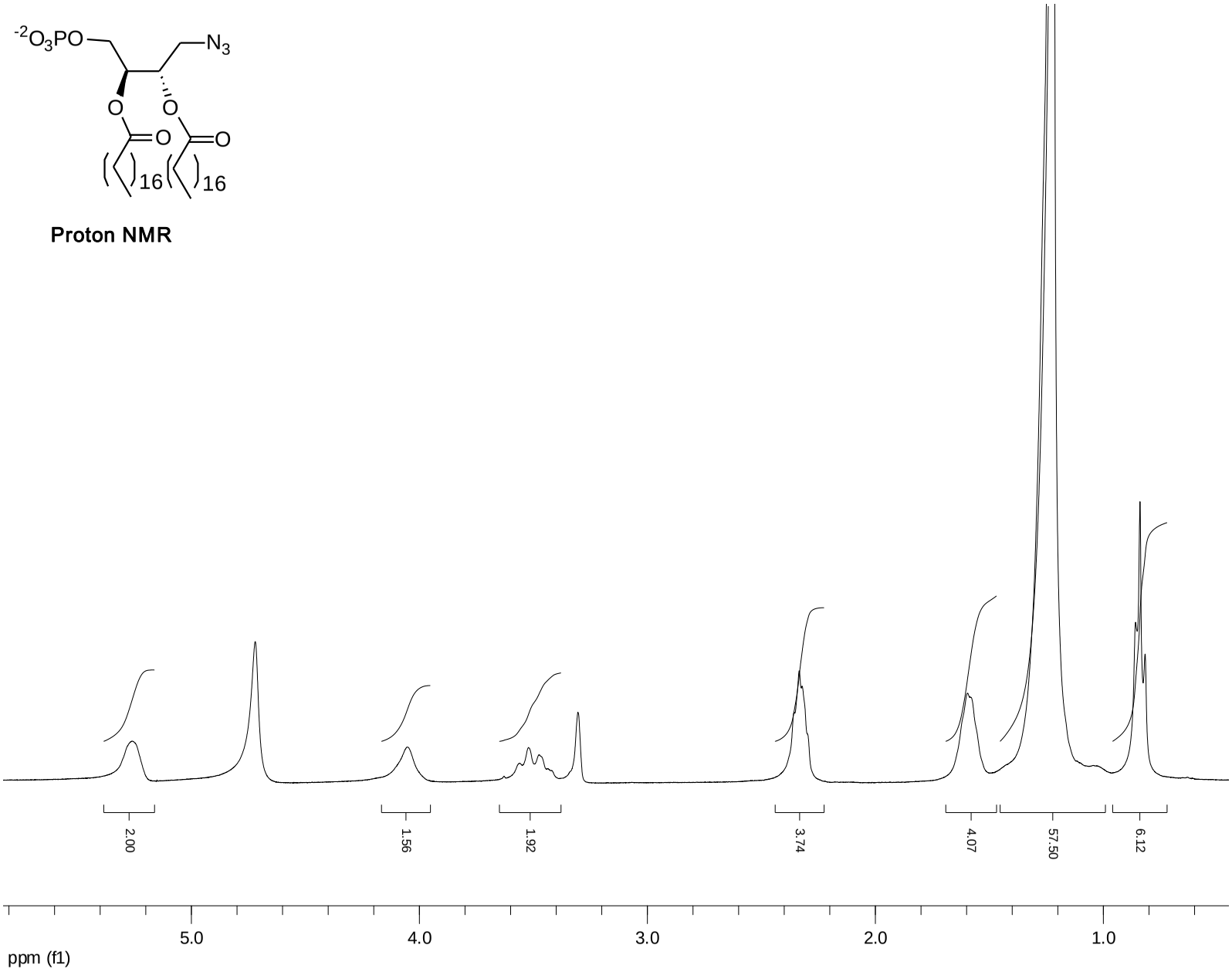
2.00
1.56
1.92
3.74
4.07
57.50
6.12
5.0
4.0
3.0
2.0
1.0
ppm (f1)

Proton NMR

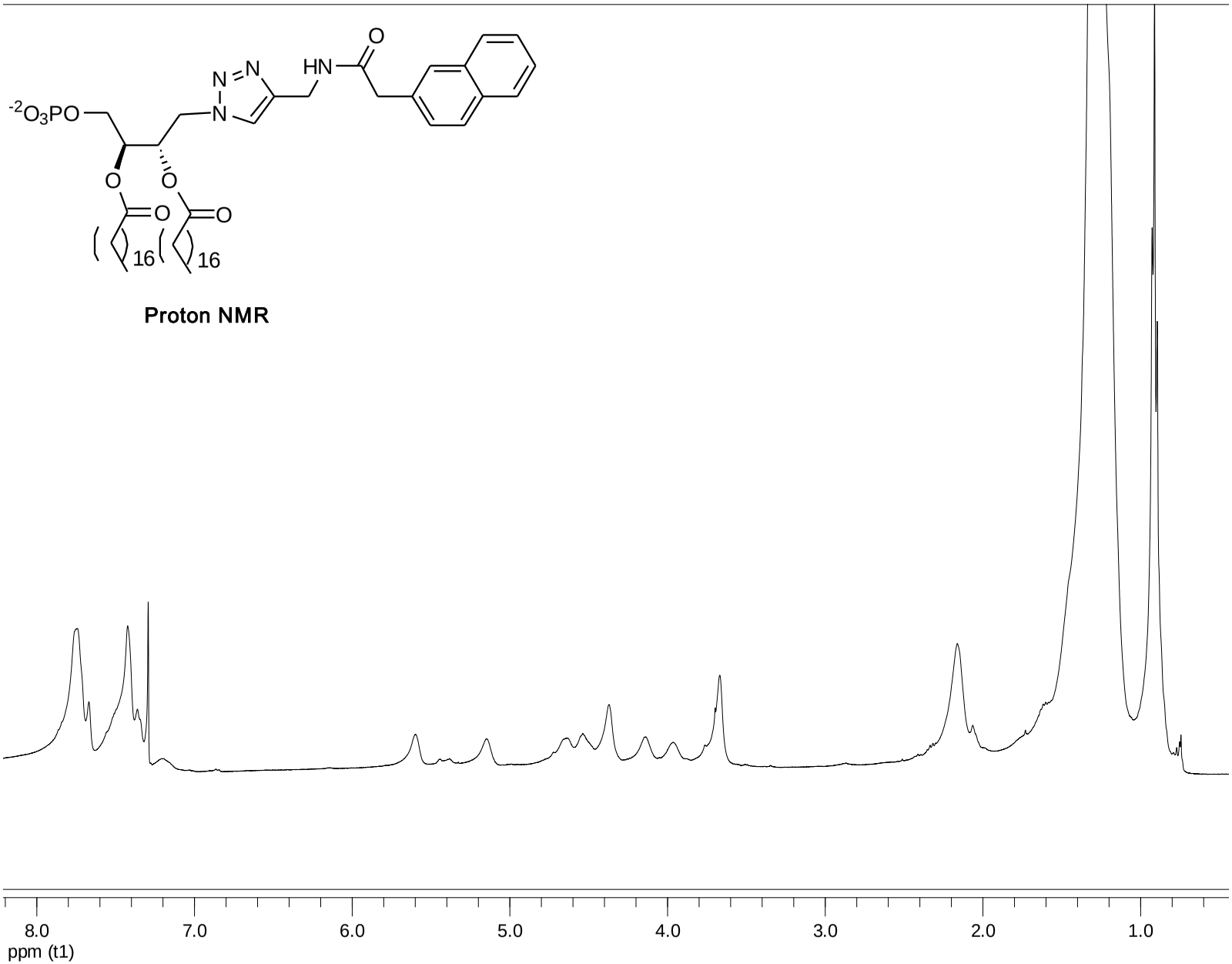

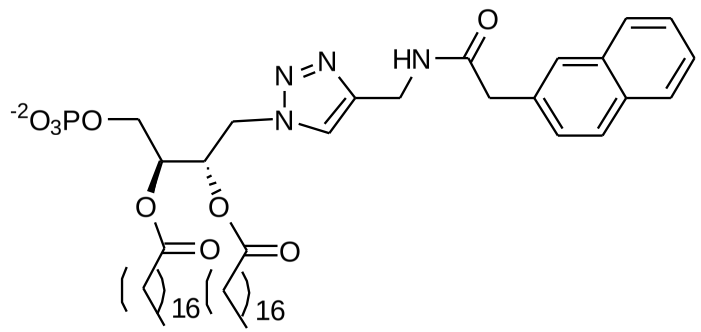

Phosphorous NMR

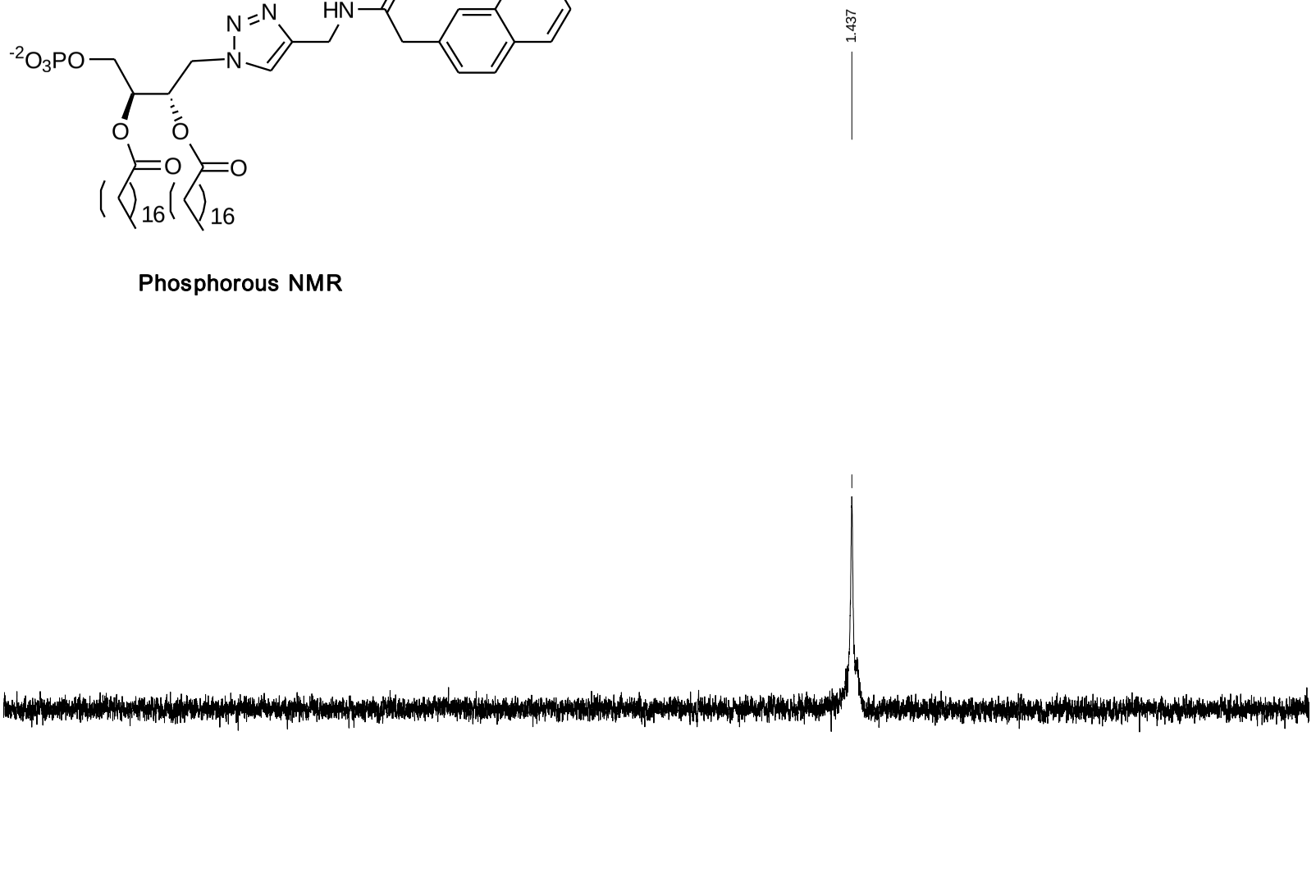

Proton NMR

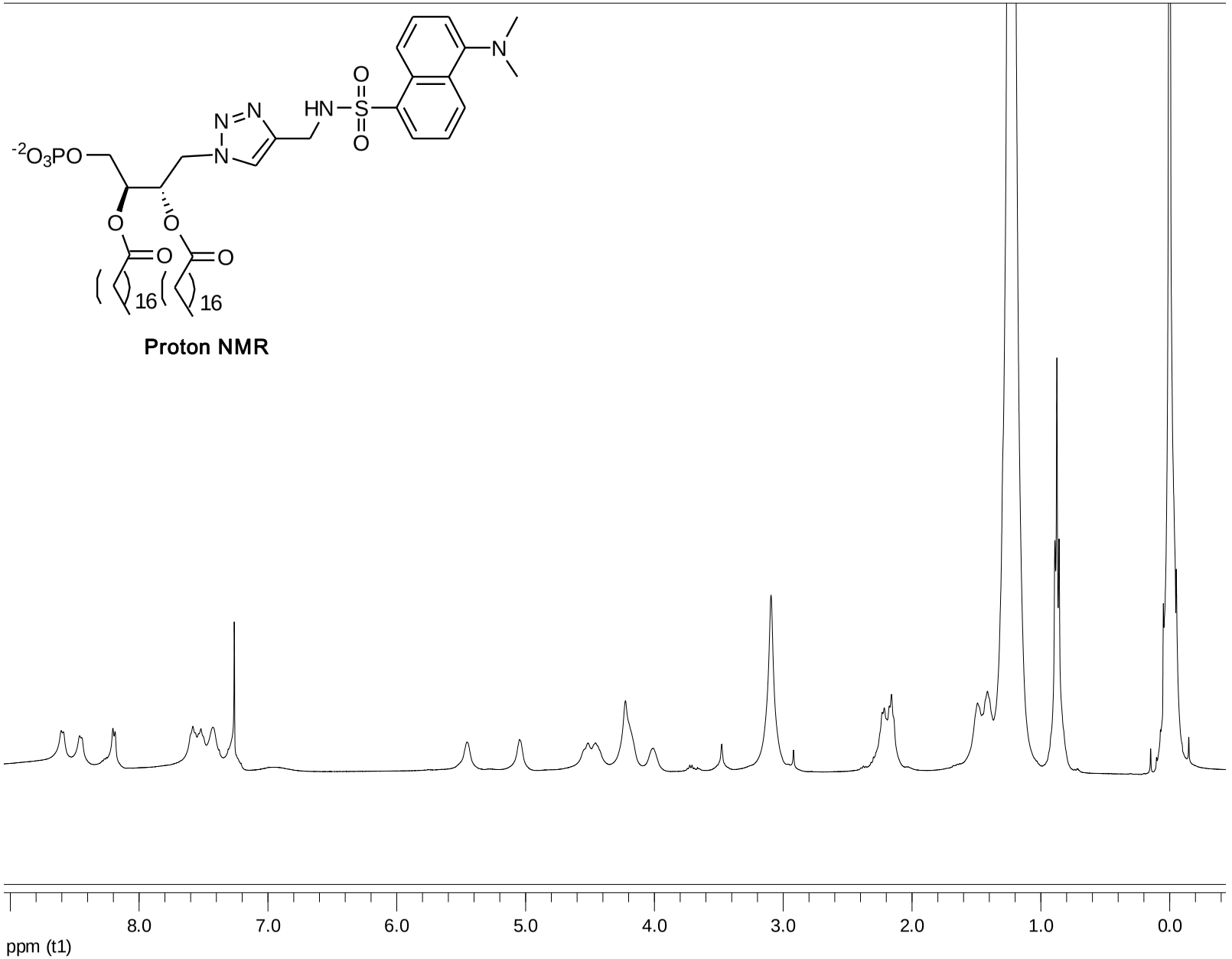

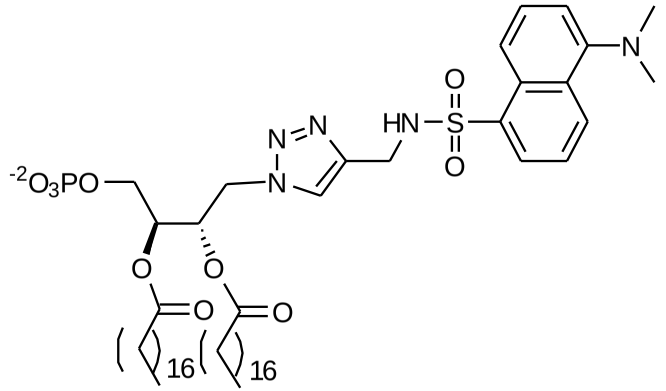

Phosphorous NMR

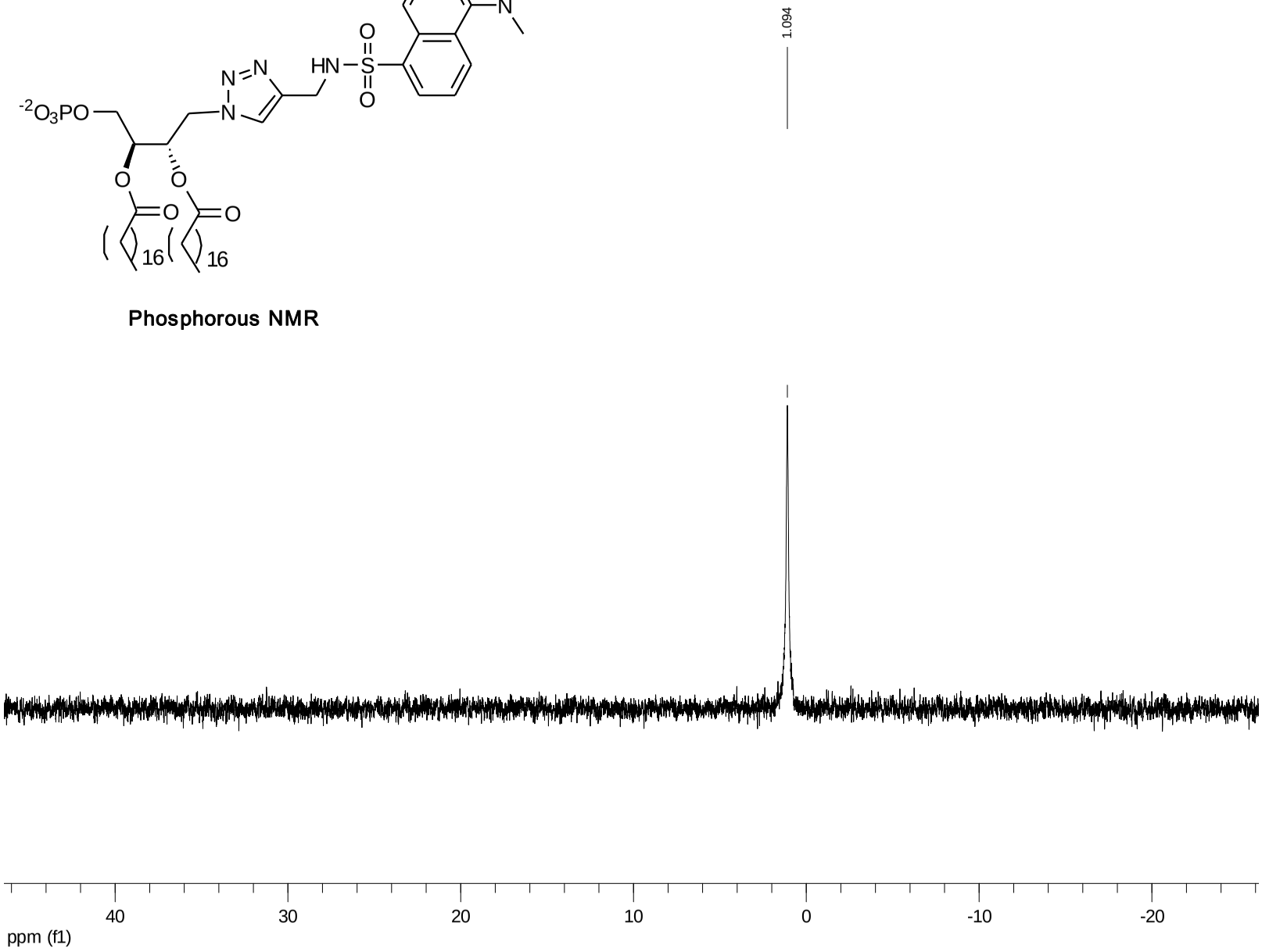

Proton NMR

156

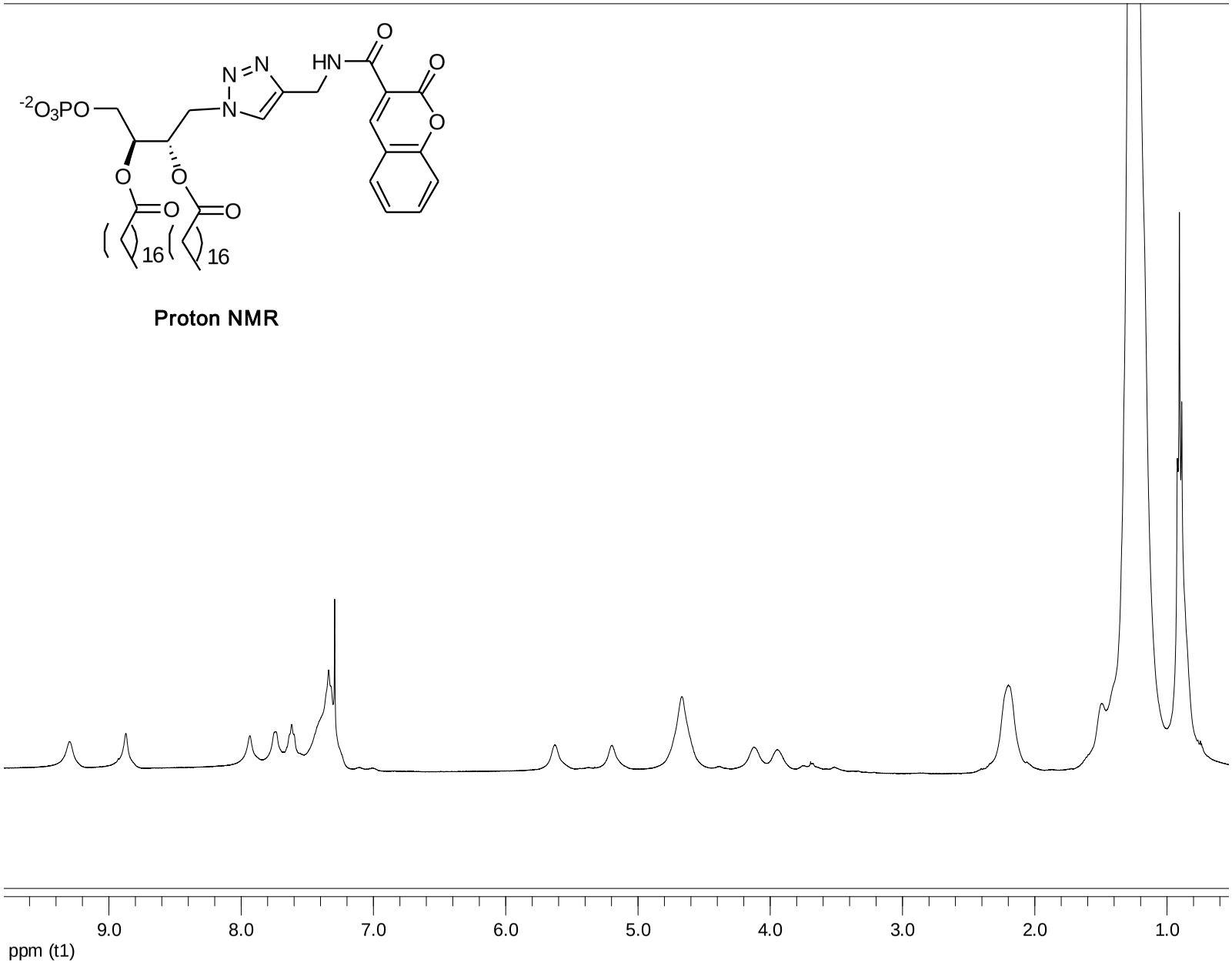

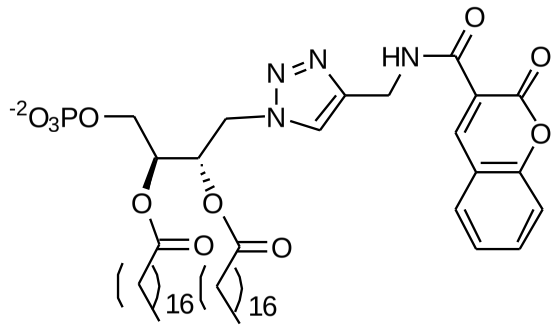

Phosphorous NMR

157

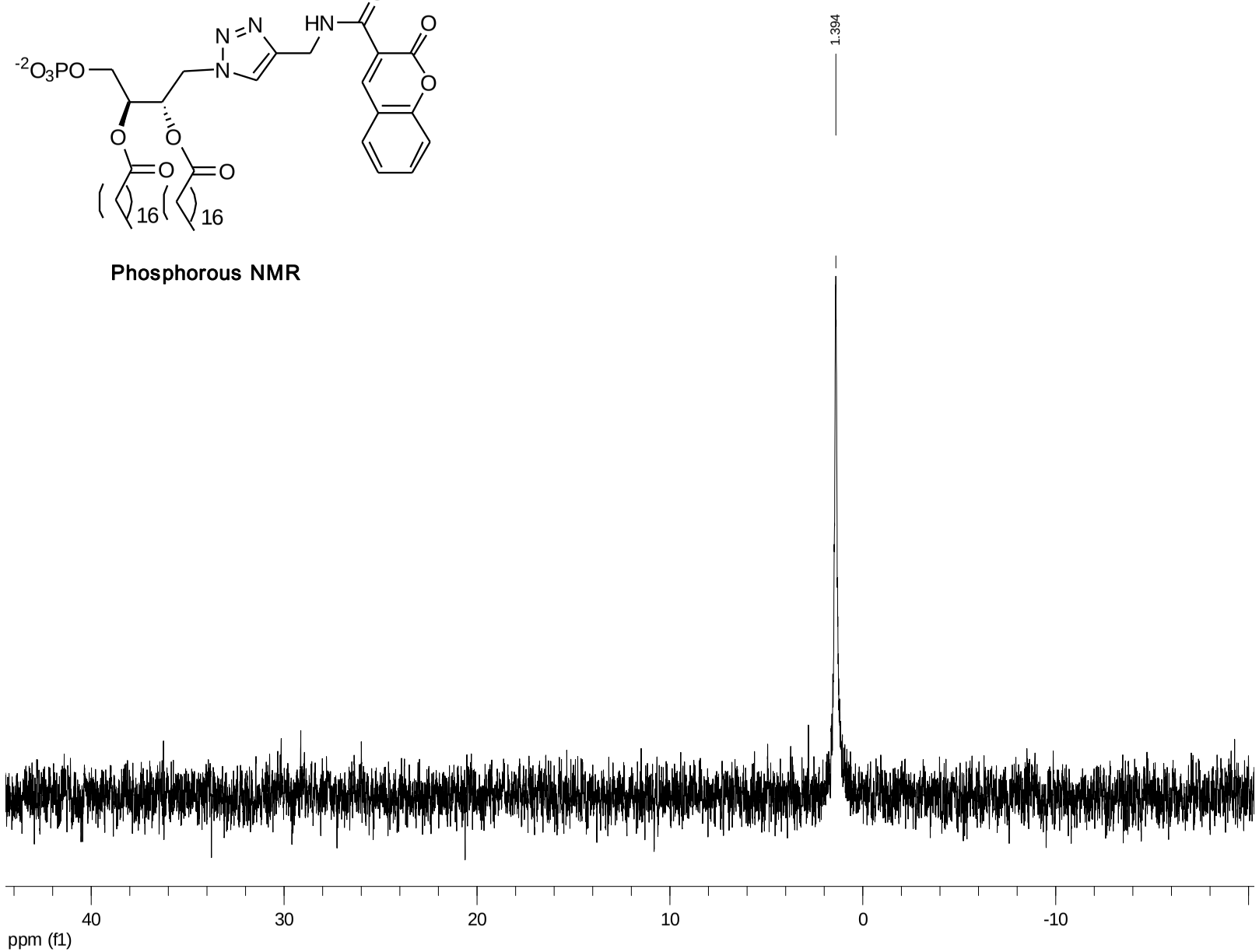

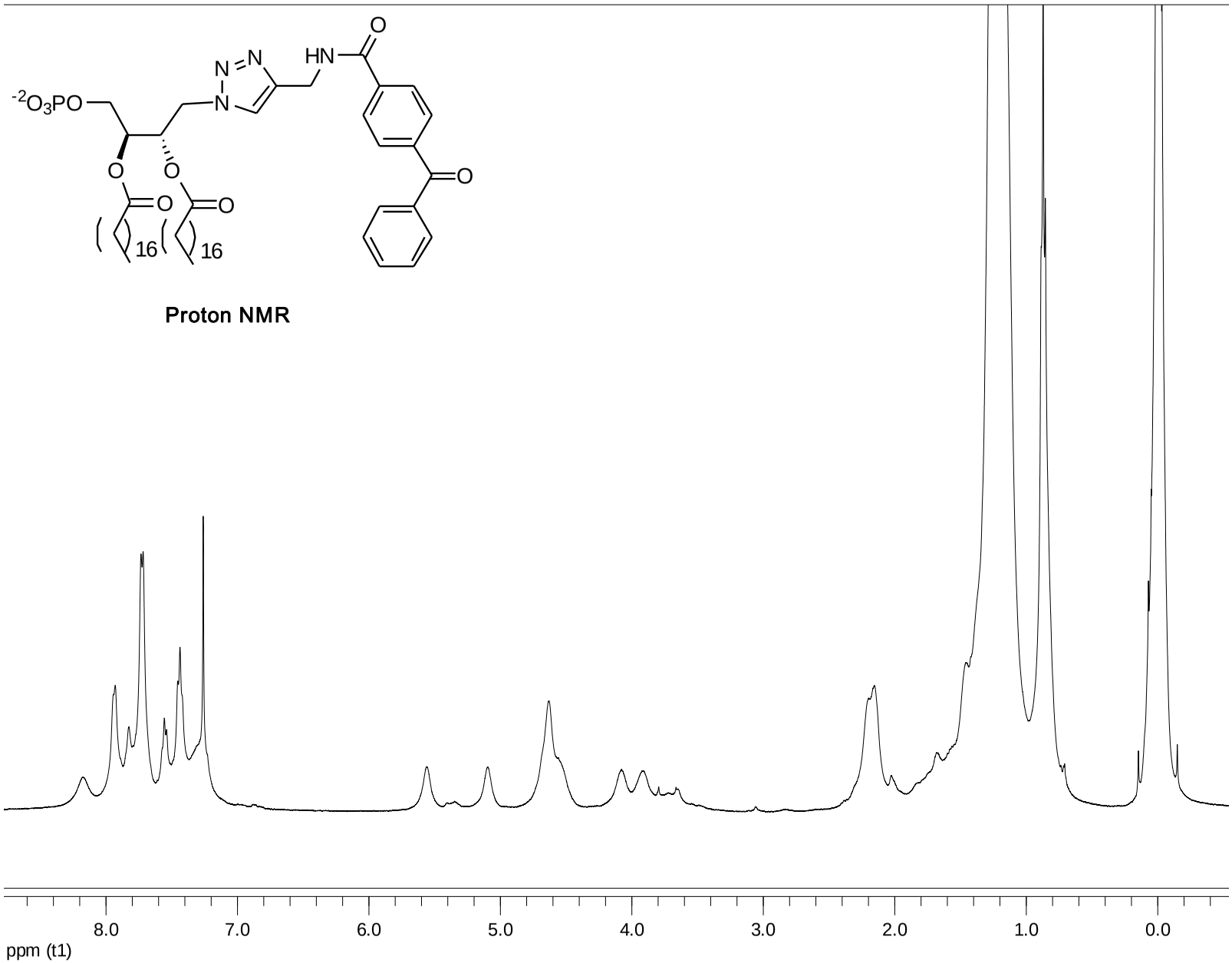

Proton NMR

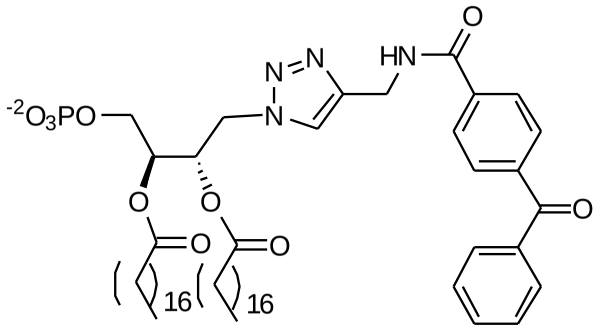

Phosphorous NMR

159

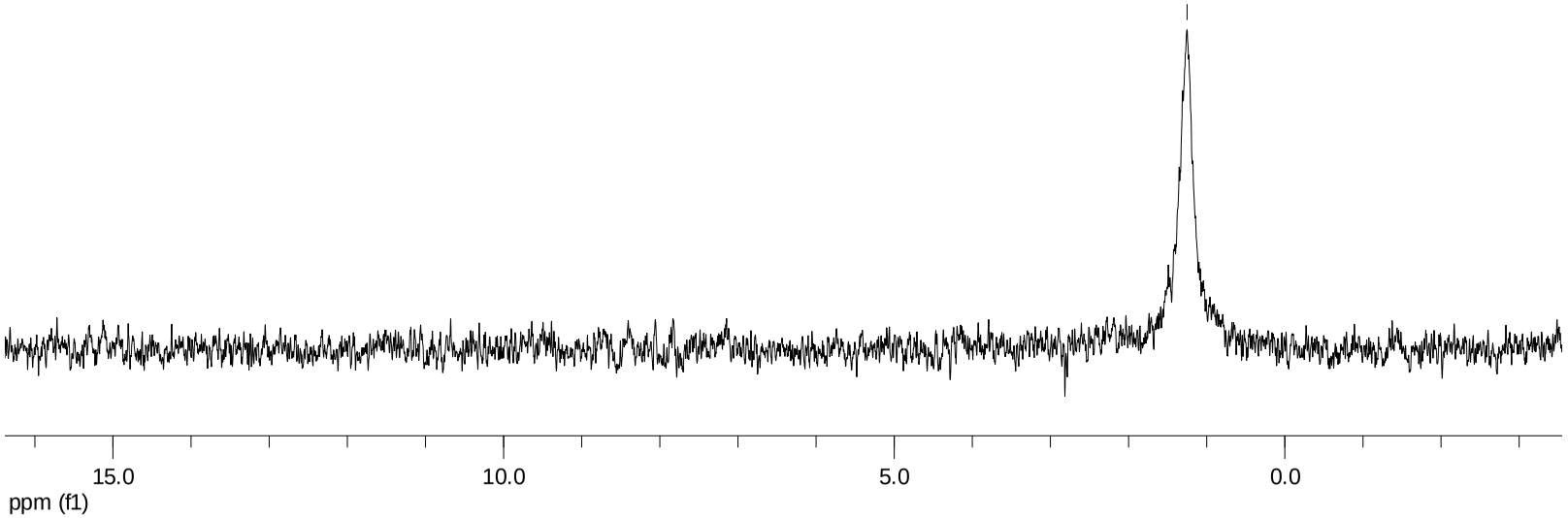

160

Proton NMR

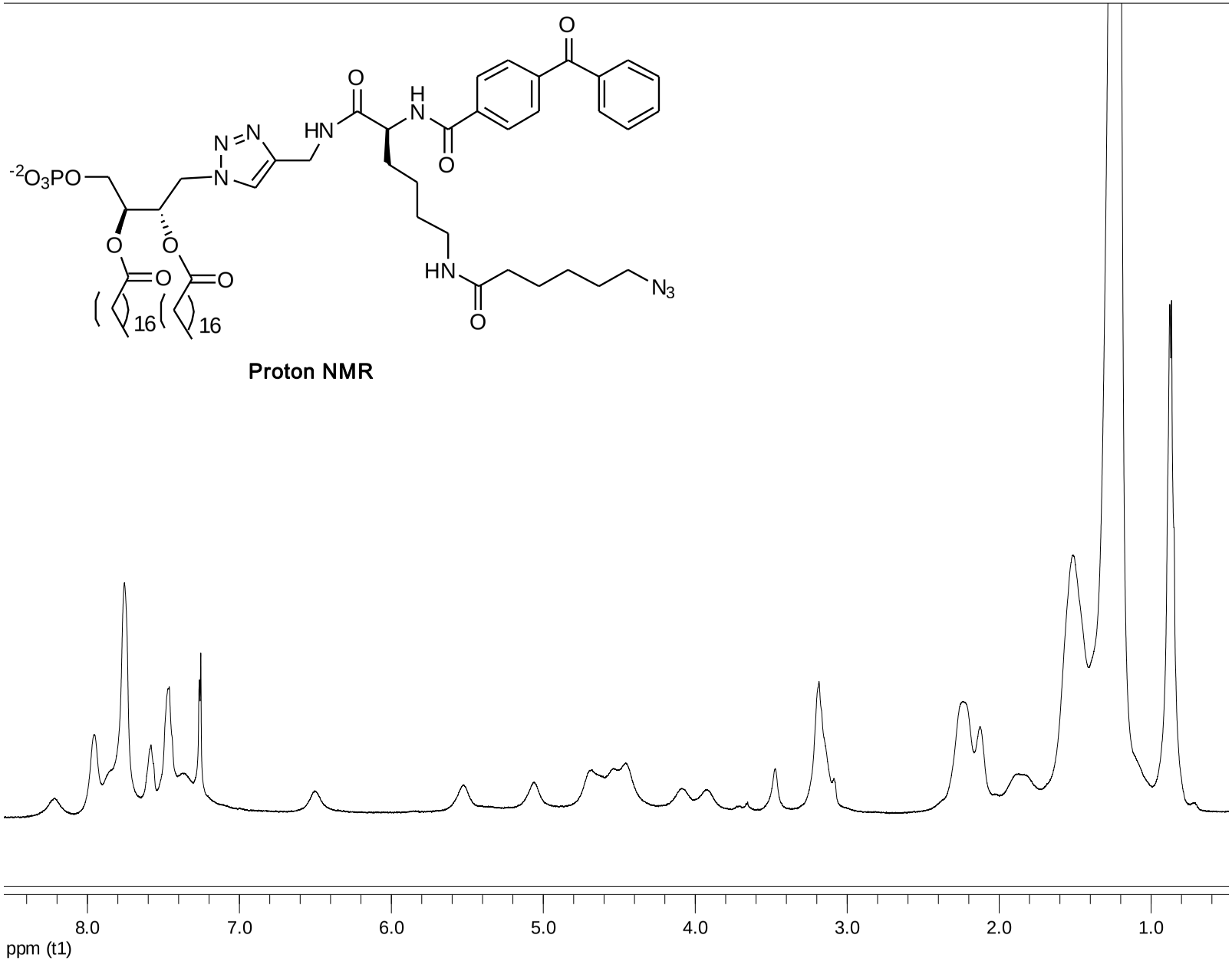

161

Phosphorous NMR

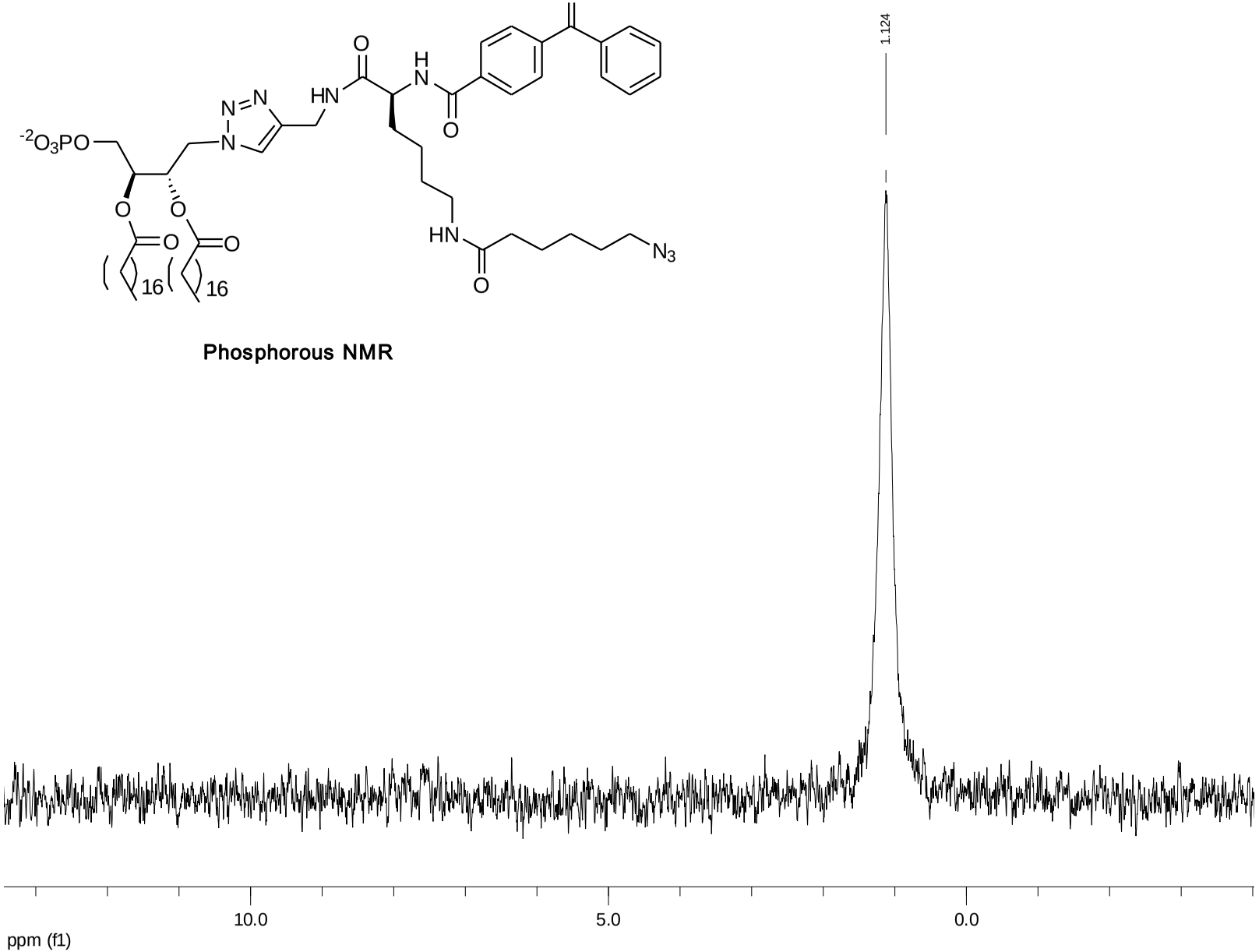

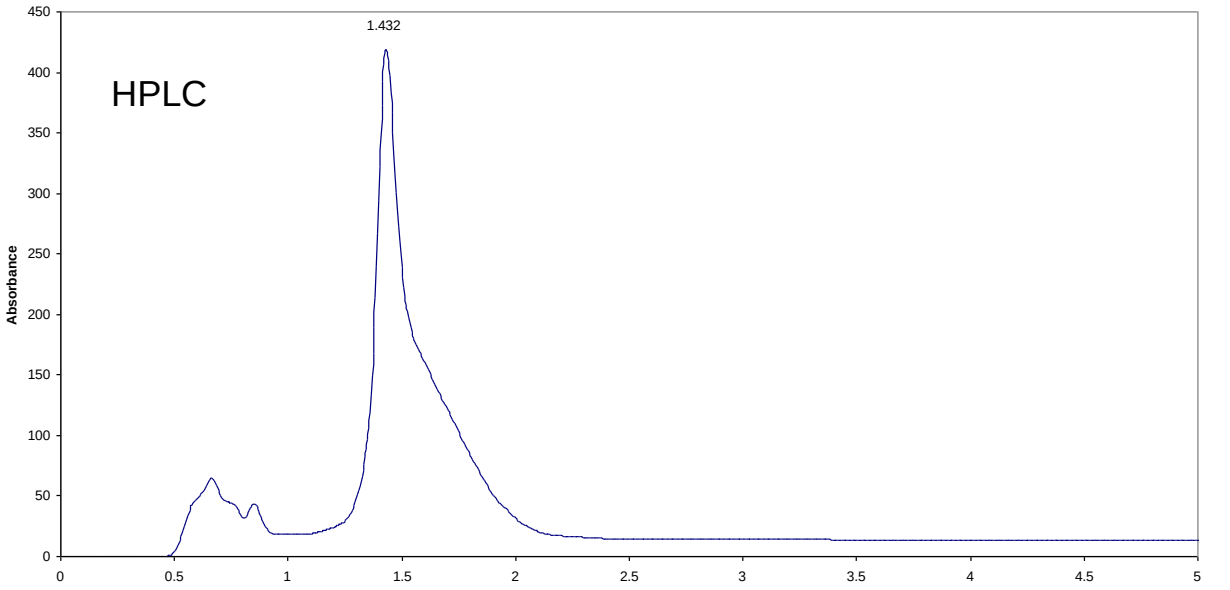
HPLC
1.432
Absorbance
450
400
350
300
250
200
150
100
50
0
0
0.5
1
1.5
2
2.5
3
3.5
4
4.5
5

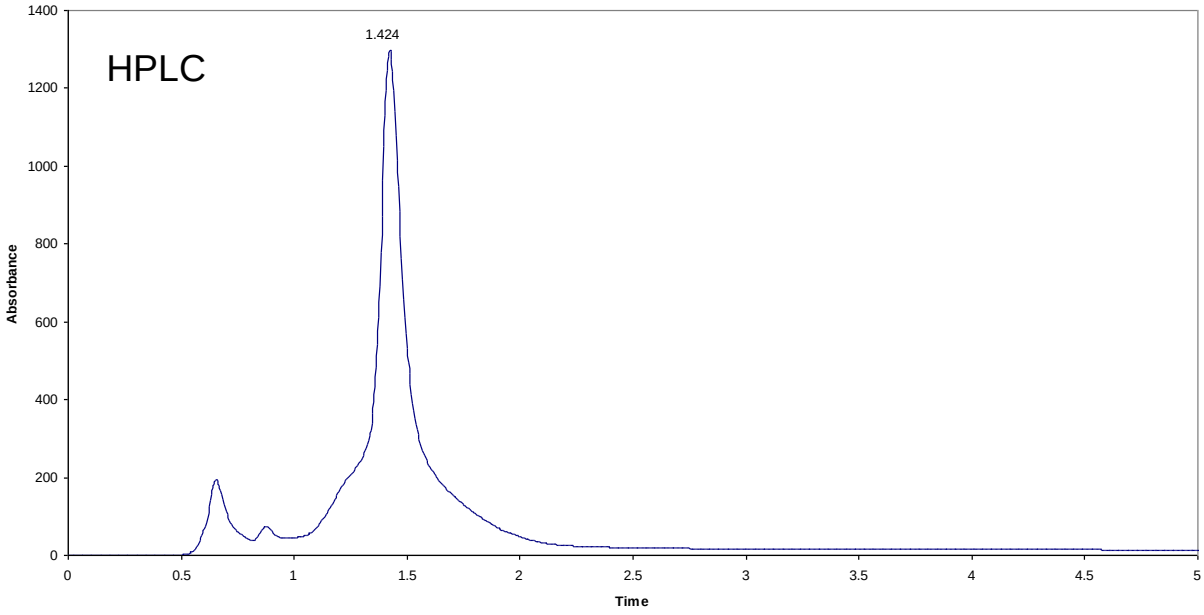
HPLC
1.424
Absorbance
1400
1200
1000
800
600
400
200
0
0
0.5
1
1.5
2
2.5
3
3.5
4
4.5
5
Time

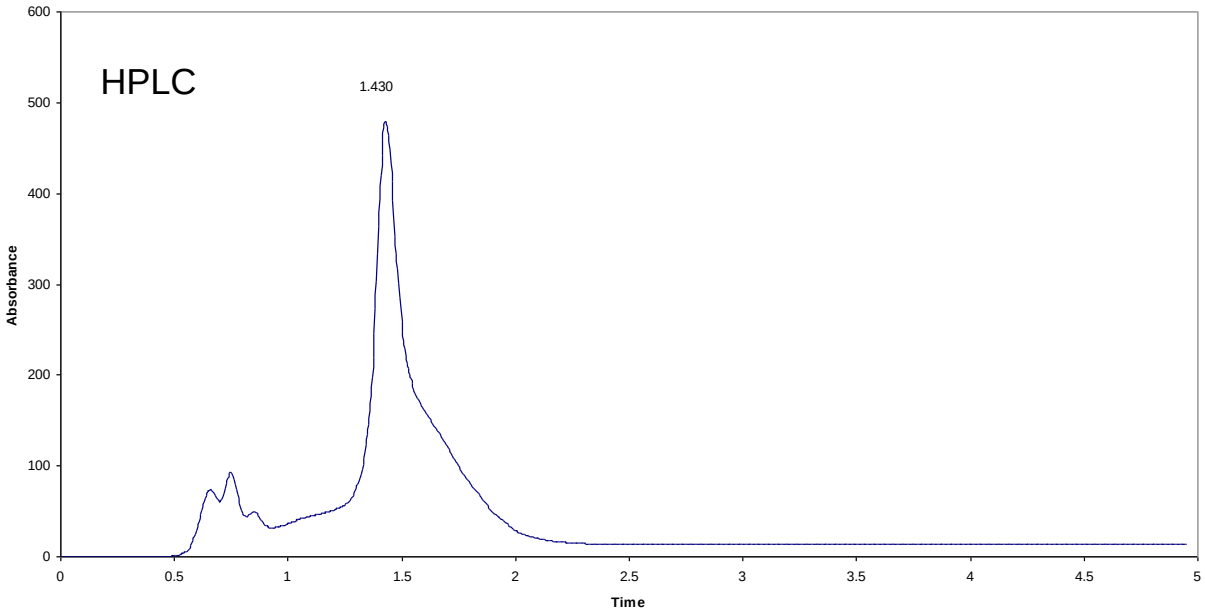
HPLC
1.430
Absorbance
Time
600
500
400
300
200
100
0
0
0.5
1
1.5
2
2.5
3
3.5
4
4.5
5

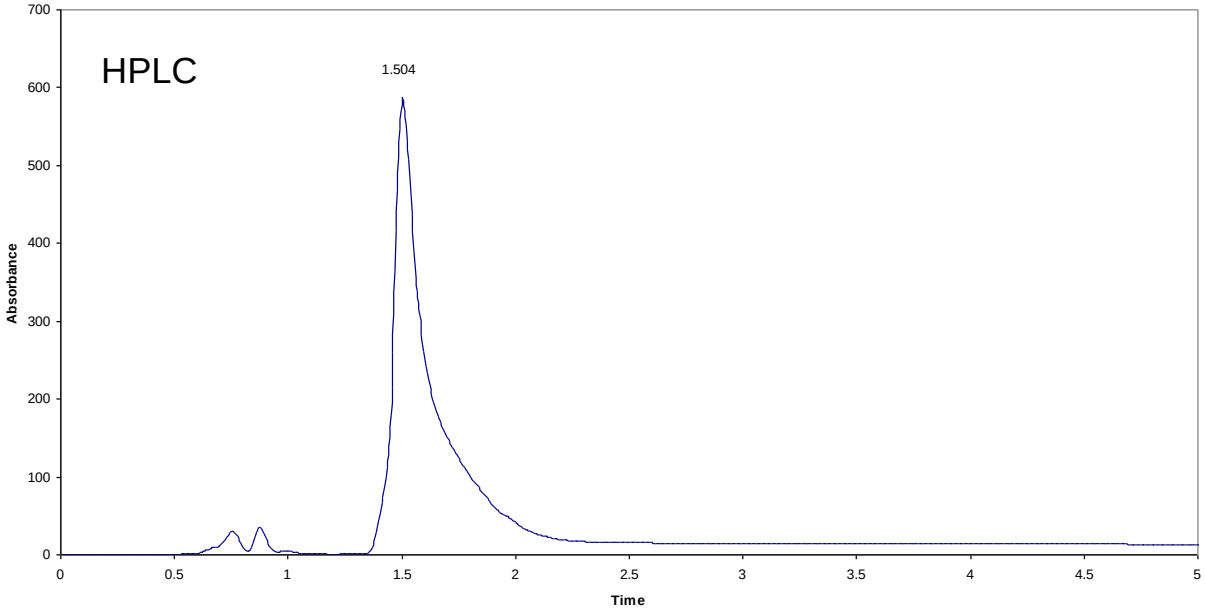
HPLC
1.504
Absorbance
Time
700
600
500
400
300
200
100
0
0
0.5
1
1.5
2
2.5
3
3.5
4
4.5
5

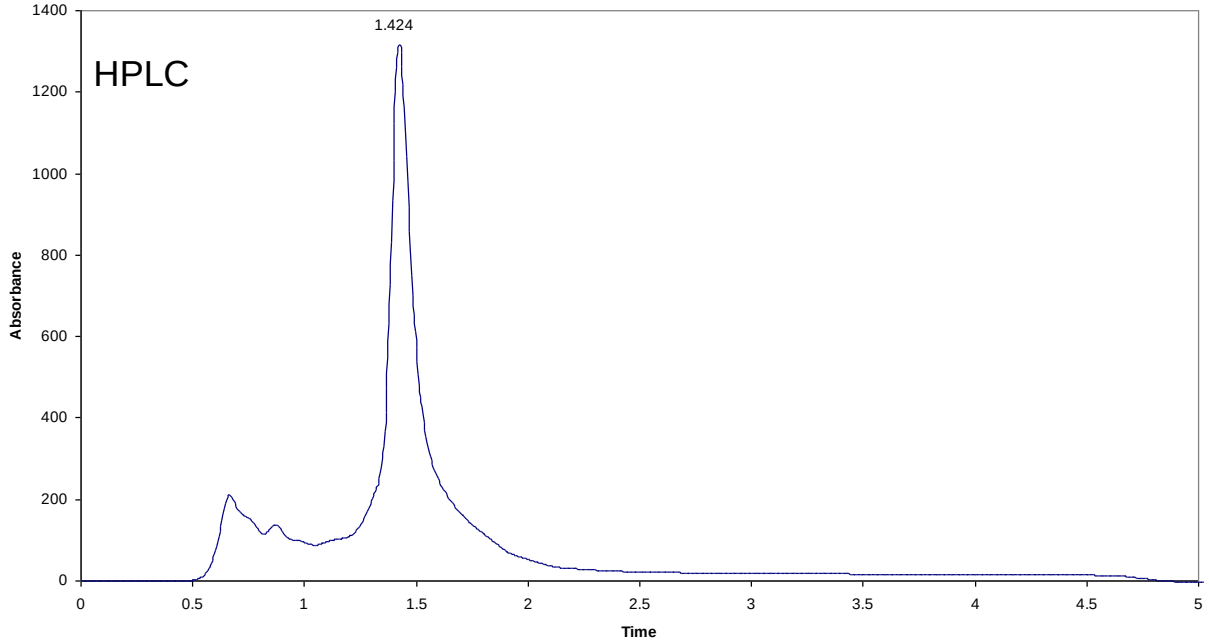
HPLC
1.424
Absorbance
Time
0
200
400
600
800
1000
1200
1400
0
0.5
1
1.5
2
2.5
3
3.5
4
4.5
5

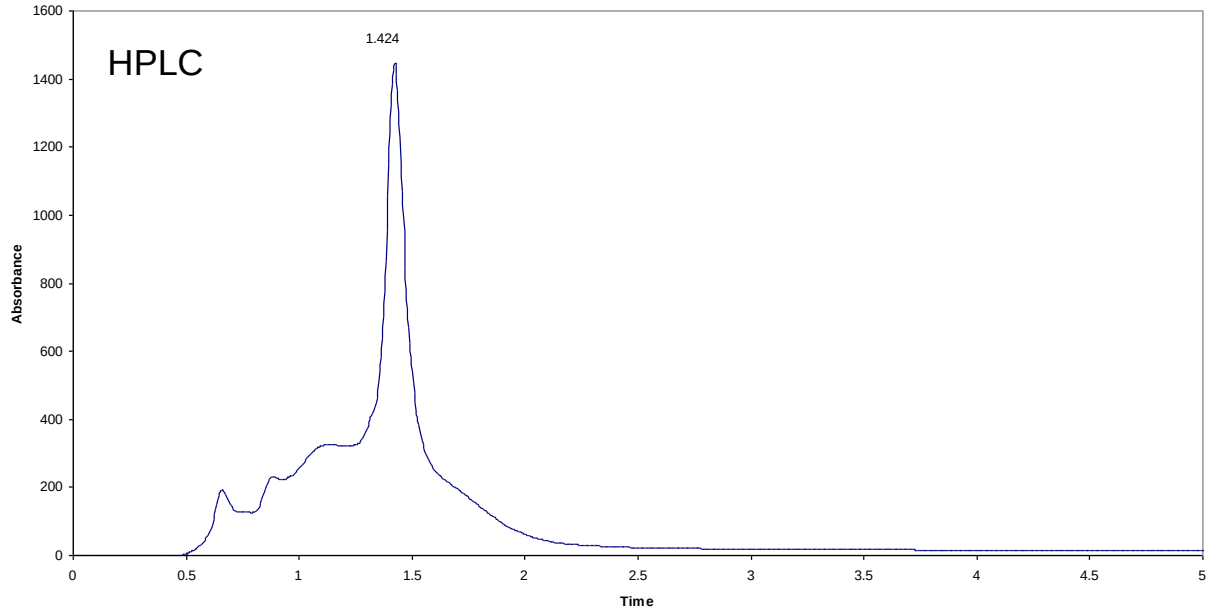
HPLC
1.424
Absorbance
Time
0
200
400
600
800
1000
1200
1400
1600
0
0.5
1
1.5
2
2.5
3
3.5
4
4.5
5

Chapter 4: Microplate-Based Analysis of Protein-Membrane Binding Interactions via Immobilization of Whole Liposomes via a Biotinylated Anchor

Background and Significance

The cellular membrane is often heavily involved in crucial intra- and extracellular recognition events that can be directly linked to a variety of important physiological and pathophysiological events. The membrane surface is decorated with a litany of biological ligands such as phospoholipids, sphingolipids, carbohydrates, peptides, and embedded proteins that can interact with solubilized proteins (figure **4.1**). These interactions directly correlate to a wide range of cellular processes including biomolecule synthesis or other cellular pathways. In addition, presentation of multiple ligands in a multivalent manner helps regulate receptor binding and function.[20, 21] Due to prominent involvement in molecular recognition during biological processes, the detection of these interactions on the molecular level is of high interest. However, as mentioned above, the membrane represents a highly complex heterogeneous environment. This leads to difficulty in investigating interactions that occur on the membrane since ligands may interact with multiple receptors, and the mechanisms of receptor-ligand interaction are often diverse and complex.

There are many mechanisms by which solubilized proteins can interact with the membrane surface. For example, carbohydrates and peptides may be presented on the

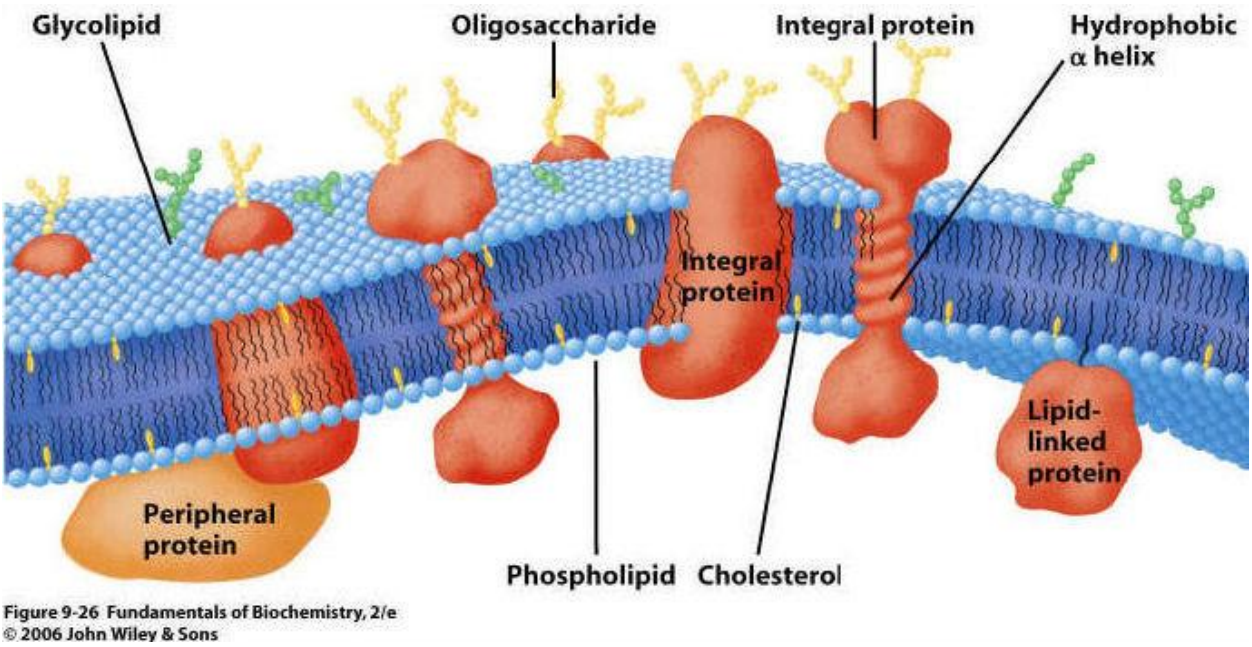

Figure 4.1. Representation of the membrane surface decorated with a variety of biological ligands.

surface leading to the interactions, as with the case of GM1 with pentavalent toxins.[124] Other proteins, such as Ras GTPases, may contain hydrophobic functionalities, such as post-translationally appended lipid tails. These will insert into the membrane bilayer and thus help regulate cellular location.[80, 125, 126] Other proteins simply insert hydrophobic residues into the non-polar regions of the membrane. Such an example is the protein hemagglutinin (HA). Following anchoring of the influenza virus to the membrane via binding to sialic acid presented on the membrane, HA inserts into the membrane promoting membrane fusion and viral entry.[127, 128] In addition, antimicrobial peptides such as gramicidin aggregrate on the membrane surface via a variety of mechanisms. This aggregration then promotes membrane insertion followed by pore formation or vesicle disruption.[129, 130]

An alternative manner in which proteins may interact with the membrane surface is through direct binding to lipids contained within the membrane, as discussed concerning DAG and PA in chapters 2 and 3, respectively. Such lipids are often present in small quantities and their expression is tightly controlled by the cell. Various proteins within the cell specifically bind to these lipids and are involved in a variety of cellular pathways. Their involvement in these processes, coupled with the finite aspects of the actual binding process, warrants the investigation of these events. As such, a high-throughput method of capable of analyzing a variety of receptors and their ability to bind membrane surfaces containing the signaling lipid would be beneficial.

To date, assays based on isothermal titration calorimetry (ITC), dye leakage,

membrane penetration, and surface palsmon resonance (SPR) have been used in the investigation of protein-membrane binding events.[131] However, such approaches do not lend themselves to high-throughput analysis due to various factors such as cost and methods of detection. Recently, a solution-phase turbidity assay was reported for the detection of protein-membrane binding.[132] While effective as a high-throughput technique, drawbacks include using absorbance, which generally limits sensitivity, as the method of detection, and the fact that the receptor is dimerized in order to promote detection. This is potentially problematic as it may not represent the true structure of the receptor in biological systems.

In order to obtain high-throughput capability and perform the analyses in an efficient manner, we sought to develop a microplate-based approach for monitoring PKC binding to DAG. Microarray techniques have proven effective for characterization of events involving DNA,[133, 134] carbohydrates,[135-143] proteins and peptides,[144-146] and more recently, lipids.[147, 148] Microarray analysis has also been extended to the deposition of membranes onto surfaces to monitor integral membrane proteins.[149, 150] The immobilization of whole liposomes has generally been carried out by the incorporation of a biotinylated anchor into the membrane.[52-56] With a few exceptions,[151, 152] membrane anchors have been accessed through the modification of phosphatidylethanolamine (PE). However, this is not an economically feasible or synthetically facile approach. Also, the biotin anchor needs to be presented at some distance from the membrane surface as liposomes are known to degrade upon contact with and to fuse to certain surfaces.[52] With these restrictions in mind, we set out to

design an efficient system that would allow immobilization of whole liposomes containing signaling lipids via a biotinylated anchor. In order to maintain cost efficient processes, all lipid analogues will be synthesized from scratch using inexpensive starting materials. In order to detect immobilization, a fluorophore-tagged lipid will be incorporated into the membrane.

Synthesis of Functionalized Lipids

Since two different lipid analogues, the biotin anchor and fluorophore-tagged lipid, needed to be synthesized, we sought to design a common scaffold so that each lipid could be accessed from a common precursor in a modular approach. This would allow quick and efficient changes in the design of the linker spacing the biotin from the surface, or in the fluorophore utilized in order to obtain the optimal system. As such, azido-lipid **4.2.2** (figure **4.2**) was synthesized as reported.[153] Modification of **4.2.2** also provides a headgroup polar enough to keep the anchor/fluorophore above the membrane surface, via formation of the triazole ring produced in the “click” reaction.

Having developed an efficient scaffold that can be efficiently derivatized by “click” chemistry,[38-40] attention was now turned towards development of a biotin-alkyne reagent that would react with **4.2.2** and serve as the biotin anchor lipid. An efficient synthesis of such a linker is outlined in figure **4.3**. Tetraethylene glycol **4.3.3** will serve as the basis for the linker that will space the biotin from the surface of the membrane. Here, **4.3.3** is converted to the mono-ethyl ester **4.3.4** in a similar approach to that previously reported.[154] The alcohol is converted into a mesylate and directly to the azide to afford

Figure 4.2. Chemical structure of azido-lipid **4.2.2**.

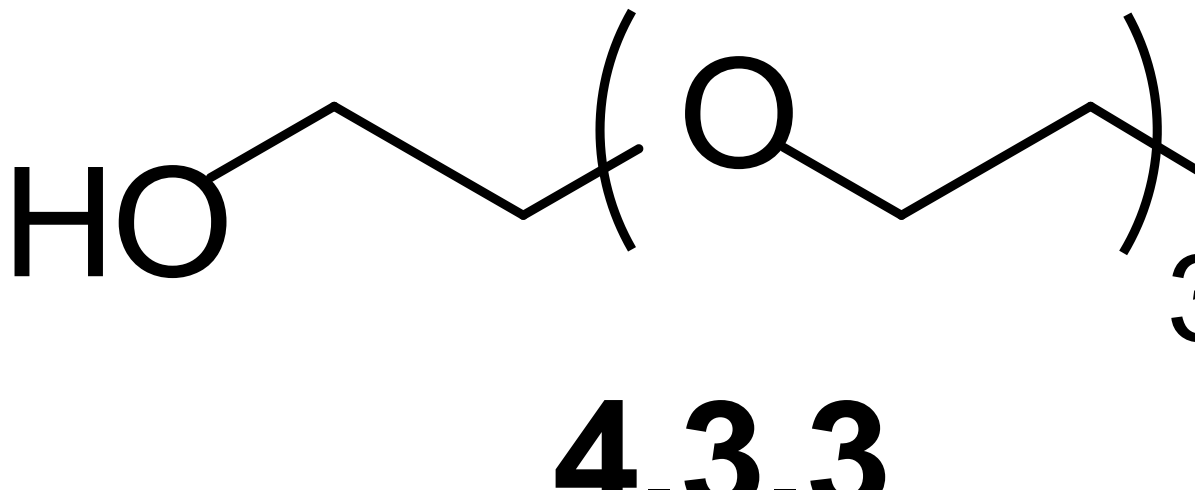

Figure 4.3. Synthesis of the biotin-TEG-alkyne linker **4.3.10**.

4.3.5. Direct reduction of the azide to an amine proved unsuccessful, but it was found that the azide of **4.3.5** could be reduced and converted to the Boc-protected amine **4.3.6** in a single step.[155] Hydrolysis of the ethyl ester under basic conditions furnished acid **4.3.7**, which was converted to alknye **4.3.8** through coupling with propargyl amine. Acidic removal of the Boc group of **4.3.8** followed by coupling with biotin-pentafluorophenyl ester **4.3.9** afforded biotin-TEG-alkyne linker **4.3.10**. Reaction of **4.3.10** with **4.2.2** via "click" chemistry afforded biotin lipid analogue **4.4.1a** (figure **4.4)**. In order to obtain the flourophore-tagged lipid that will serve as a means for detecting liposome immobilization, 5(6)-carboxyfluorescein (CBF) alkyne **2.8.17d** was attached to **4.2.2** to afford **4.4.1b.**

Immobilization of Whole Liposomes

Having developed compounds **4.4.1a** and **4.4.1b,** which can be incorporated in vesicles and should effectively facilitate the immobilization and fluorescence detection of whole liposomes, we moved on to test the efficacy of this process (figure **4.5**). Initially, unilamellar liposomes were formed using standard conditions. Vesicles composed of 98% PC, which is used as a bulk component for membranes, and 1% each of **4.4.1a** and **4.4.1b,** were prepared (Sample A), along with control vesicles that contained no biotin anchor **4.4.1a** (Sample B). The size of the vesicles was controlled via extrusion through a polycarbonate membrane with pores of 200 nm. Dynamic light scattering (DLS) was used to ensure a relative narrow polydispersity of vesicle size. Both sets of liposomes were incubated with streptavidin-coated surfaces in a 96-well microplate.

Figure 4.4. Derivatization of **4.2.2** to afford biotinylated and fluoroscein functionalized lipids.

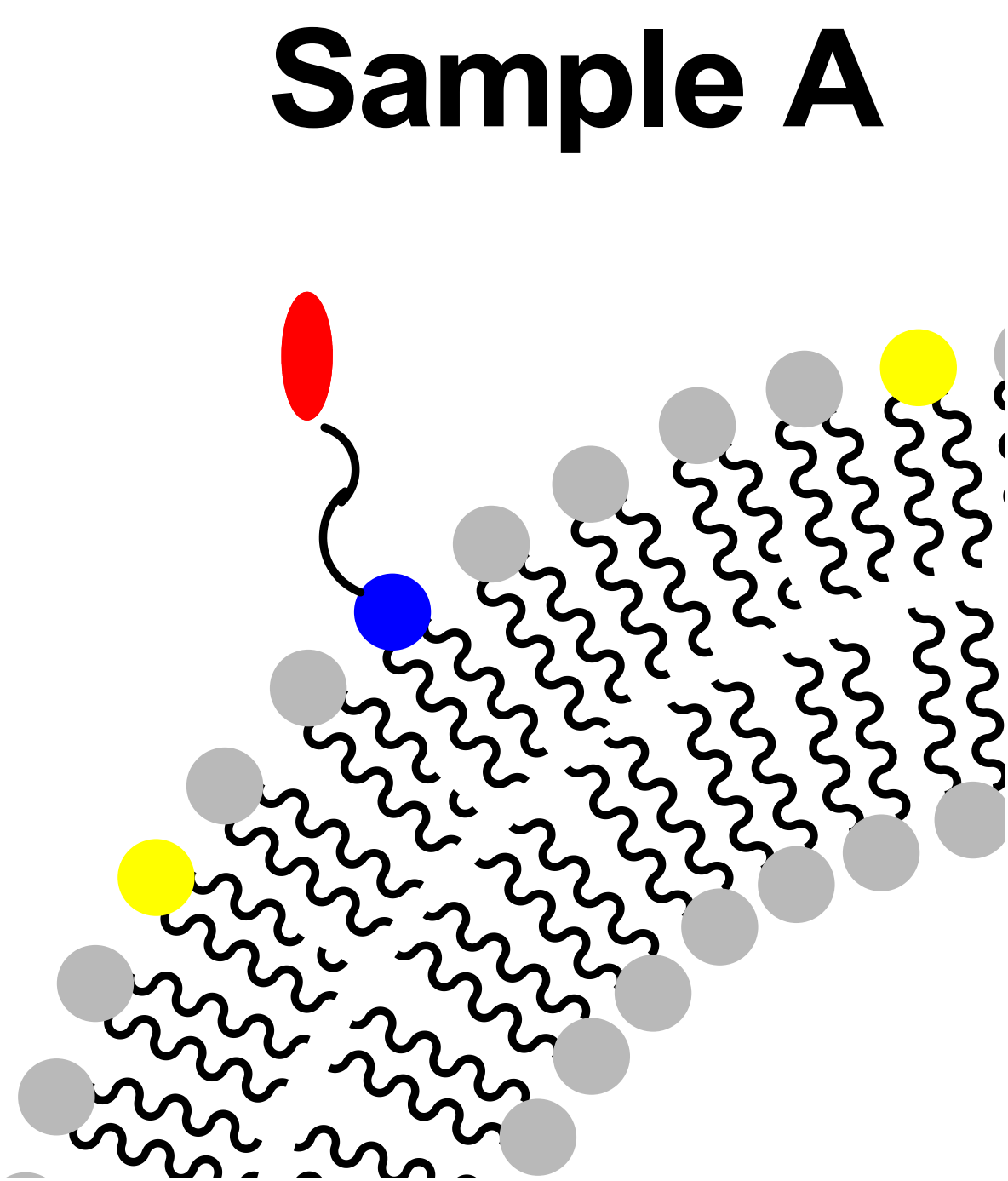

Figure 4.5. Representation of immobilization and detection of liposomes with and without **4.4.1a**.

Following incubation, the solution was removed, and the wells were thoroughly washed with buffer. Measuring the amount of fluorescence remaining after washing should give an indication as to how much immobilization occurred. This was carried out using a microplate reader. Results of multiple experiments showing standard error are given in figure **4.6**. As can be seen from the graphs, the fluorescence of sample A increased as the concentration of liposomes incubated in the well was increased, indicating that immobilization of liposomes did indeed occur. Control sample B exhibited only a small amount of background fluorescence, which further confirms the notion that liposome immobilization is driven by biotin anchor **4.4.1a**.

In a subsequent study, we sought to determine the amount of biotin required for optimal immobilization. Having obtained positive and consistent results using 1% of biotin anchor **4.4.1a** in the liposome, we were curious to see whether immobilization could be achieved using lower percentages of **4.4.1a**. Here, liposomes comprised of varying percentages of **4.4.1a** (0-2%), a constant 1% of CBF-lipid **4.4.1b** for detection purposes, and the remaining percentages comprised of PC, were incubated with streptavidin-coated wells as before. Following incubation, the wells were washed thoroughly with buffer and then measured for fluorescence on a plate reader. The results are shown in figure **4.7**. As can be seen from the graph, a plateau is reached between 0.25% and 0.5% of **4.4.1a** indicating efficient immobilization can be achieved with small percentages of **4.4.1a**.

As stated earlier, vesicles are known to fuse to certain surfaces.[52] To further prove that what we were observing is actual immobilization via a biotin-avidin interaction

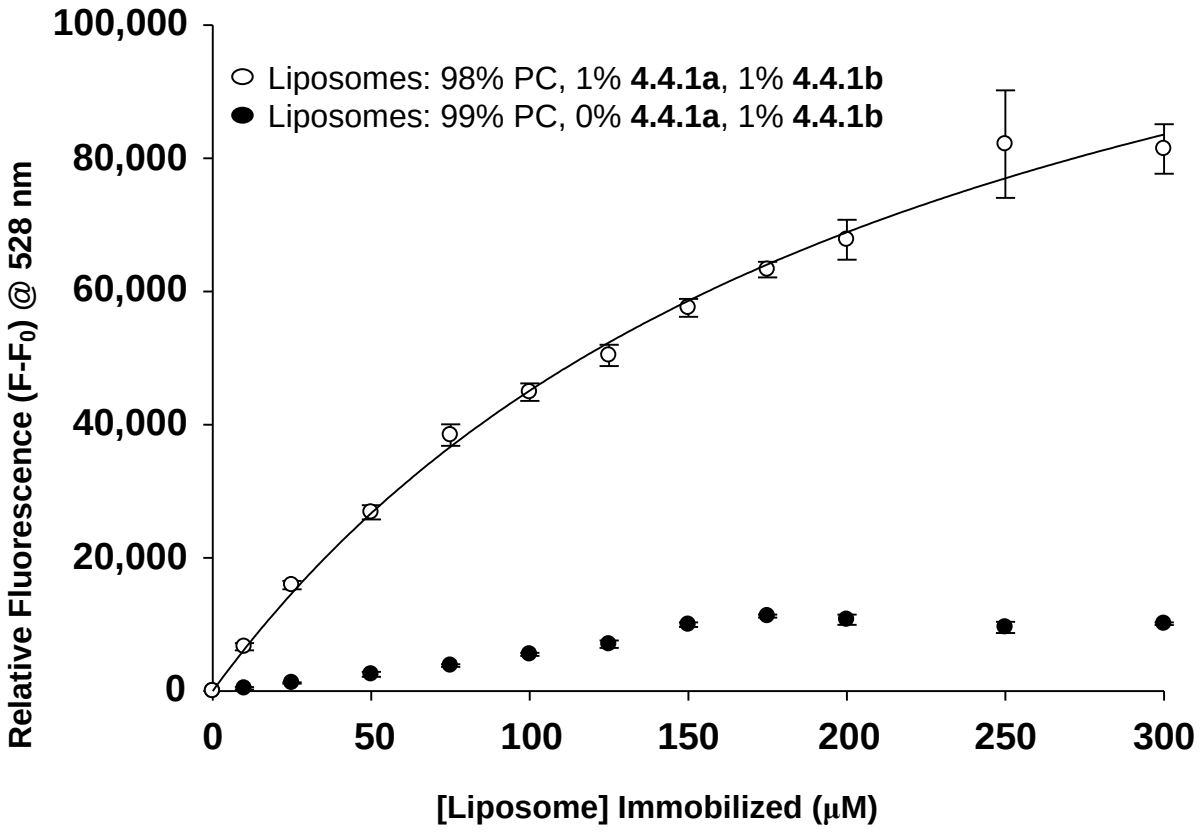

Figure 4.6. Results obtained from measuring fluorescence after liposome immobilization.

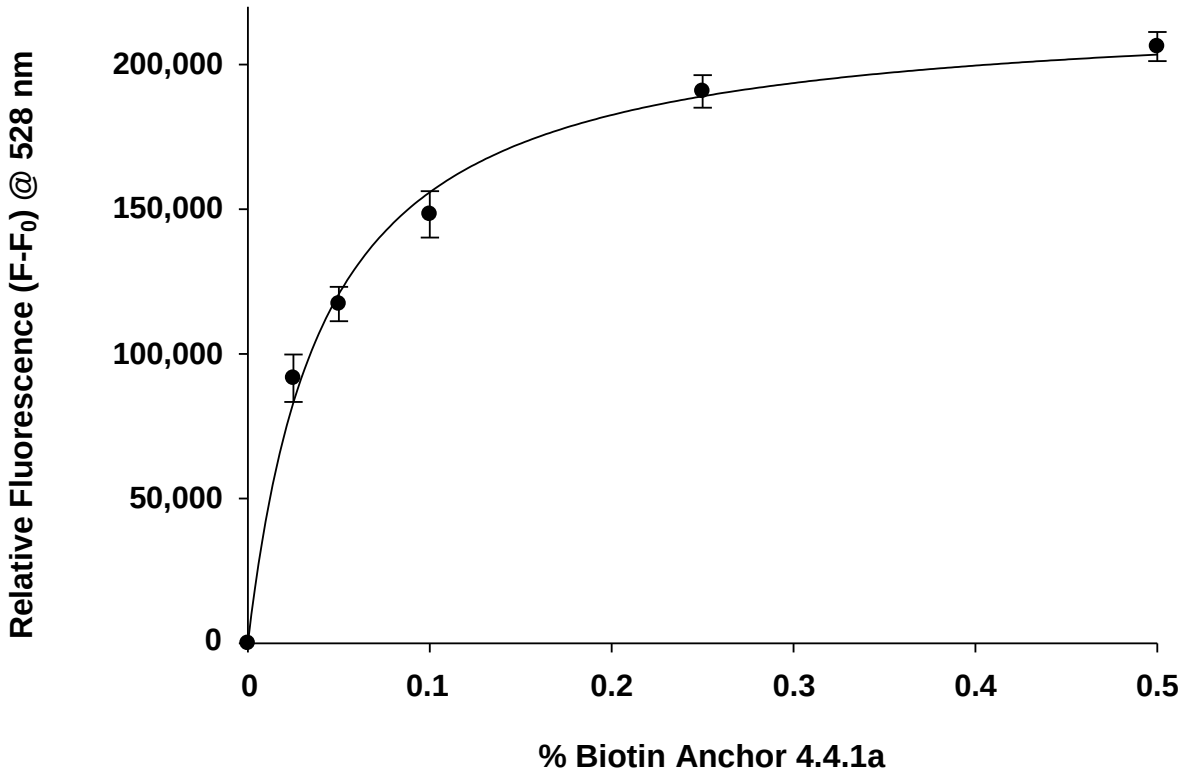

Figure 4.7. Results obtained after measuring fluorescence of immobilized liposomes containing varying percentages of **4.4.1a**.

opposed to unraveling and fusion of the vesicles to the surface, we designed a dye-leakage assay.[156] In such an experiment, vesicles are prepared with 5(6)-carboxyfluorescein encapsulated at a self-quenching concentration (50 mM). Following the removal of unencapsulated dye via size exclusion chromatography (SEC), minimal fluorescence of the liposomes will be observed. Liposomes were prepared with 1% of biotin anchor **4.4.1a**, 99% PC, and encapsulated dye. Following incubation with avidin-coated surfaces, the fluorescence of the original sample was measured on a plate reader (figure **4.8a**). Initial fluorescence was negligible and upon addition of 20% Triton X-100 detergent, the fluorescence signal drastically increased. A similar experiment was carried out, but this time, the wells were washed after incubation to remove any unbound liposomes (figure **4.8b**). Again, initial fluorescence was minimal and upon addition of the detergent, the signal increased. The combination of these results and those in figure **4.6** and **4.8** indicated that the liposomes are remaining intact during incubation and efficient immobilization of the whole vesicle is achieved.

Detection of PKCα-DAG Interactions using Whole Liposome Immobilization

Knowing that we could successfully immobilize whole liposomes, we then focused on using the technique in order to detect the binding of a protein to a ligand present in the immobilized membrane. For initial studies, we chose to incorporate DAG as the lipid and use the well known DAG receptor PKCα. PKCα is a conventional isozyme, targeting DAG with two C1 domains and the membrane with a calcium-

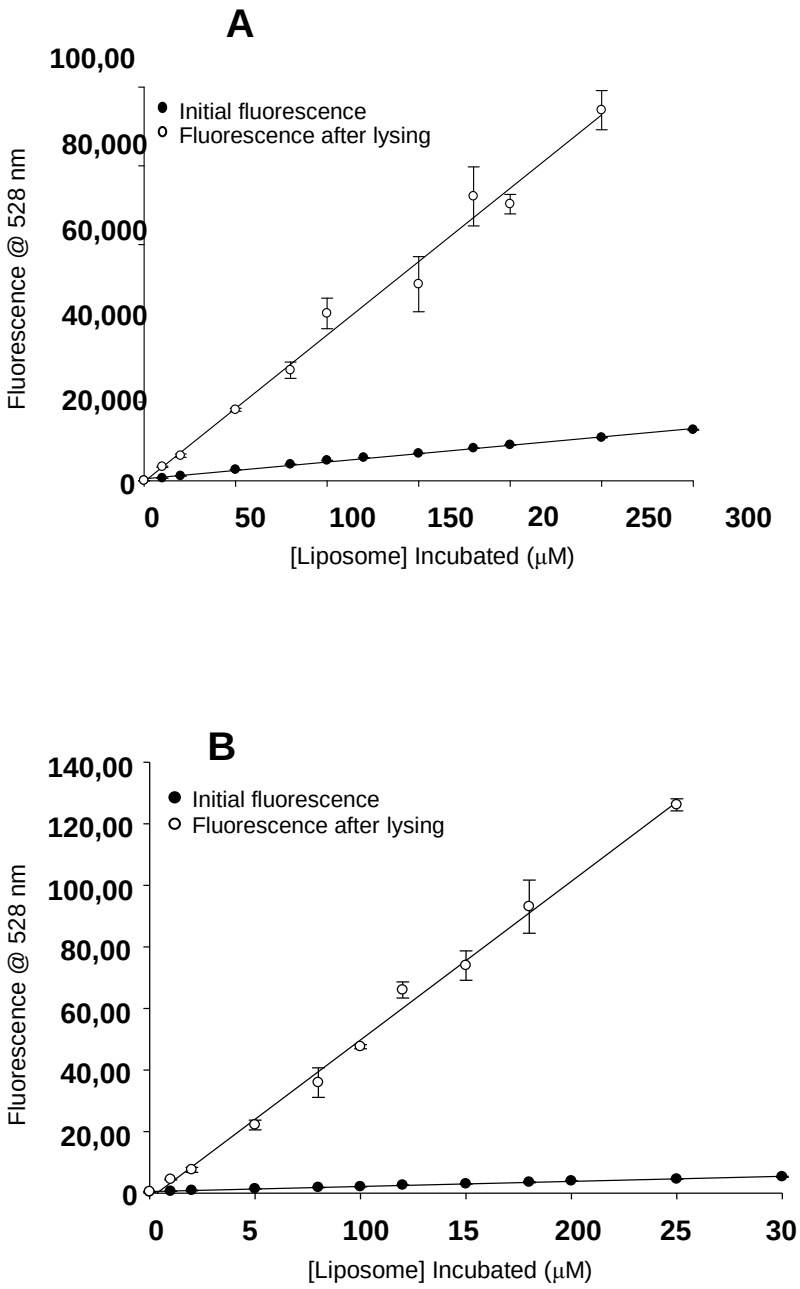

Figure 4.8. Results obtained from vesicle leakage assay of immobilized liposomes. The results in experiment **A** were obtained without a wash after immobilization. In experiment **B**, a wash after the incubation of liposomes was performed so the signal only corresponds to immobilized liposomes.

dependent interaction with PS. Liposomes similar to those reported for efficient PKCα binding[61, 122, 157] were prepared and included 1% of **4.4.1a**, 2% DAG, 20% PS, and 77% PC. The resulting liposomes were immobilized onto streptavidin-coated surfaces and binding of PKCα was detected via a dual antibody approach as shown in figure **4.9**. Following liposome incubation, PKCα was introduced to the well and allowed to incubate with the immobilized DAG-containing liposomes. Following removal of unbound protein, rabbit anti-PKCα followed by goat anti-rabbit IgG horseradish peroxidase (HRP) conjugate were introduced into the system. Following thorough washing, chemiluminescence using the HRP-tagged antibody was used to detect the amount of bound PKCα (figure **4.10**).

Results obtained were in agreement with those expected as the graph resembles a standard binding isotherm. In an effort to prove the immobilization/protein binding/detection results, we repeated the study employing liposomes that lack biotin anchor **4.4.1a**. The low background obtained confirms the validity of the results.

Development of an Immobilization Assay for the Detection of Lectin-Carbohydrate Binding

Having developed an efficient assay for the detection of DAG receptors through a liposome immobilization assay,[153] we next sought to extend the same principles to design a carbohydrate-lectin based assay. The first step was designing a lipid modified with a carbohydrate, to yield a glycolipid analogue. This was accomplished through the

one step reaction of azido-lipid **4.2.2** with mannose alkyne

Figure 4.9. Depiction of assay for the detection of PKCα binding to immobilized liposomes.

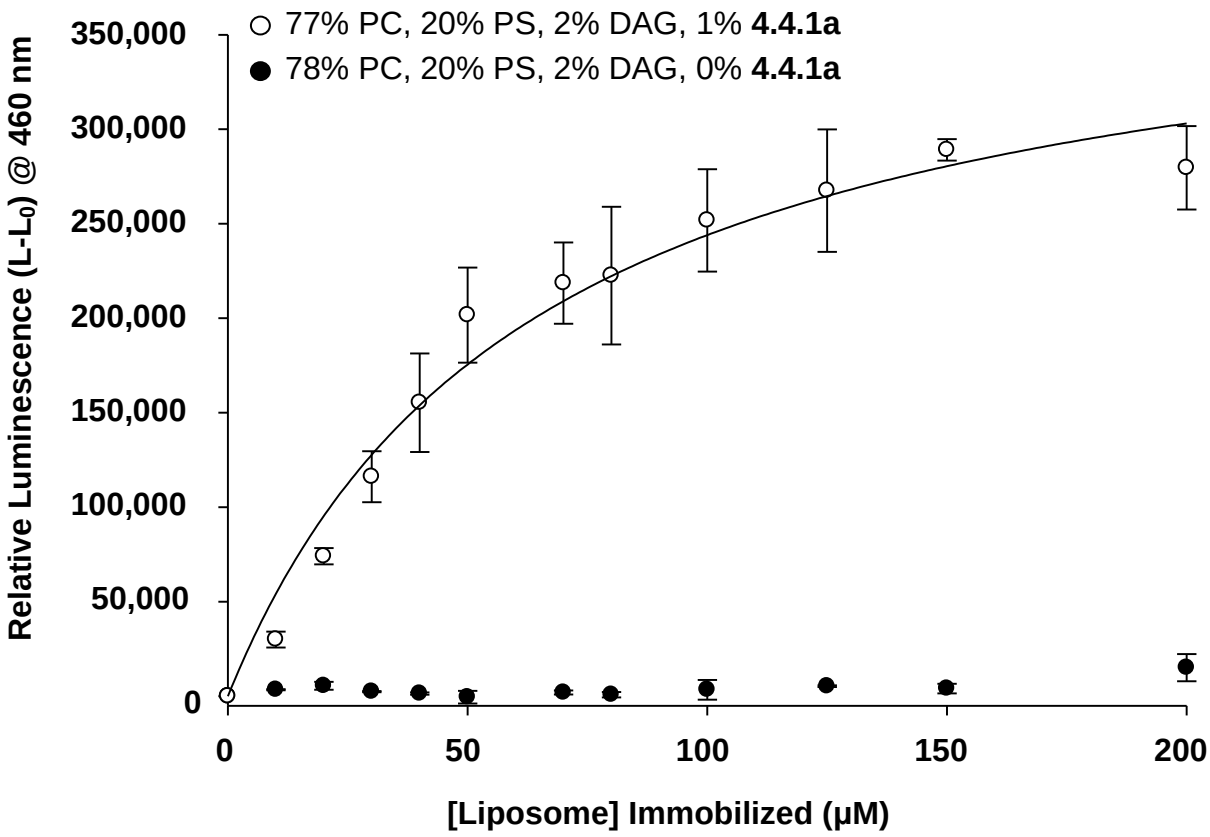

Figure 4.10. Results of whole liposome-PKCα binding.

4.11.11, which was obtained through collaboration with Dr. David Baker, University of Tennessee, to afford **4.11.1c** as shown in figure **4.11**. Arrays utilizing the immobilization of mannose and detecting the binding of ConA have previously been reported.[139] Mannose lipid **4.11.1c** was incorporated into liposomes comprised of 10% **4.11.1c**, 1% biotin anchor **4.4.1a**, and 98% PC. Liposomes were incubated with a streptavidin-coated surface and then rinsed to remove unbound liposomes. Next, fluorescein-tagged Concanavalin A (ConA) was introduced at varying concentrations along with 0.05% bovine serum albumin (BSA) as a blocking agent. As a control, ConA was also introduced to wells that had not been treated with liposomes. Initial results are shown in figure **4.12**. As seen from the graph, there is a significant amount of background signal. Various attempts at altering the percentages of BSA and mannose-lipid **4.11.1c**, along with varying the concentration of ConA, did not improve the results.

In order to determine if the background is resulting from non-specific interactions of the liposomes with the avidin surface, liposomes with 1% **4.11.1c**, 1% of CBF-lipid **4.4.1b,** and 98 % PC were introduced to wells, alongside liposomes with 0% **4.11.1c**, 1%, **4.4.1b**, and 99% PC. In order to determine if the manganese ion that is required for ConA binding played any role in the non-specific interactions, duplicate analyses were conducted in the presence of low and high concentrations of Mn^{+2}. As seen from the results in figure **4.13**, fluorescence intensity increases with the addition of Mn^{+2} and with the addition of mannose-lipid **4.11.1c.** However, a relatively small background could be obtained in the presence of the sugar with a low concentration of Mn^{+2}. As

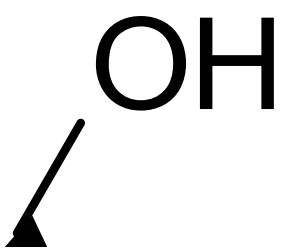

Figure 4.11. Synthesis of mannose-lipid **4.11.1c**.

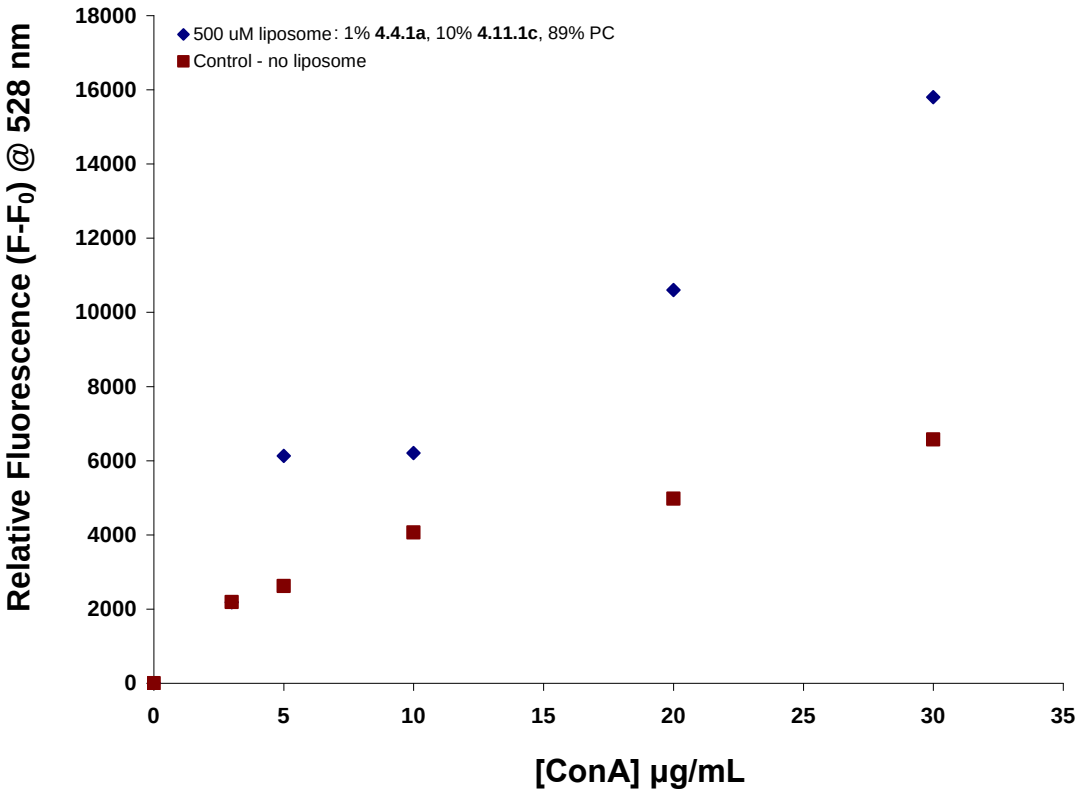

Figure 4.12. Initial attempts at detection of ConA binding to vesicles with **4.11.1c**.

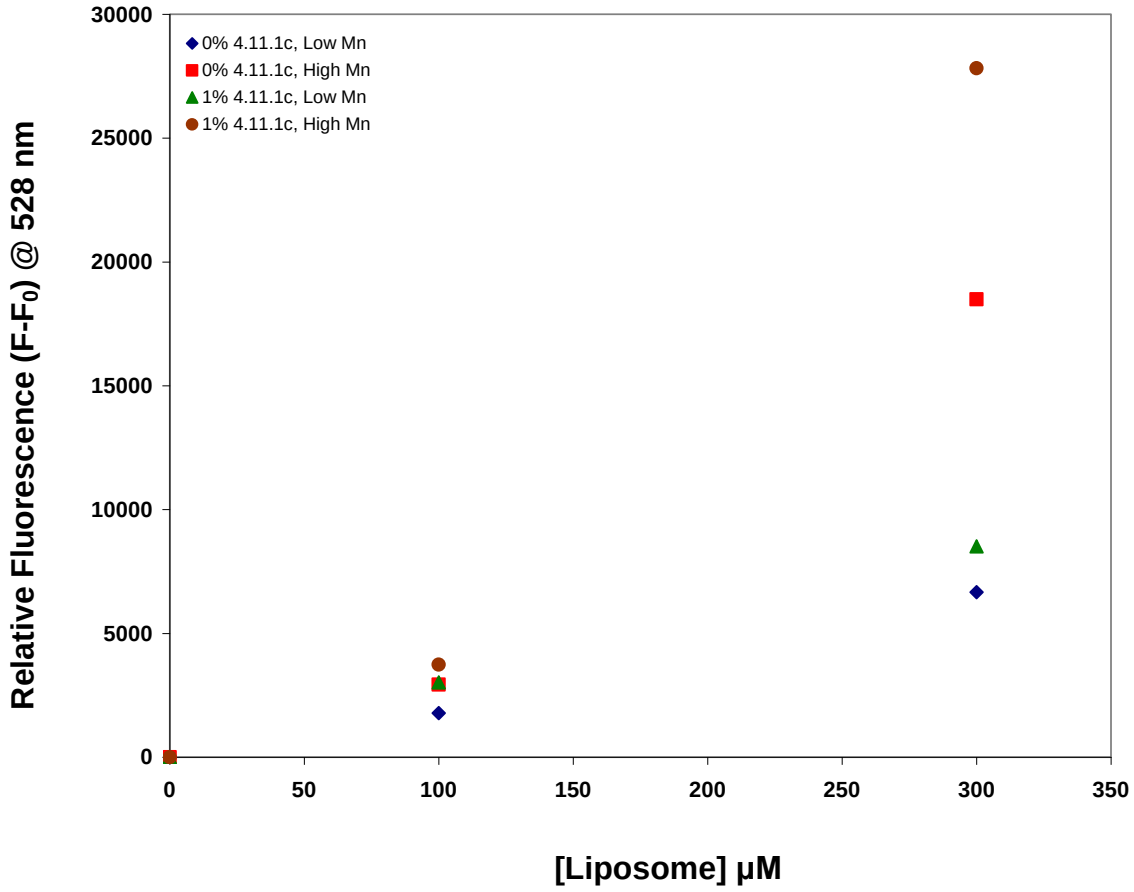

Figure 4.13. Effects of Mn^{+2} on non-specific interactions of liposomes with surface.

such, liposomes were prepared to include 5% **4.11.1c**, 1% **4.4.1a**, and 94% PC in buffer that completely excluded the Mn^{+2} and Ca^{+2} ions. These liposomes were incubated in streptavidin-coated wells and unbound liposomes were removed with washing. During the introduction of ConA, the Mn^{+2} and Ca^{+2} ions were introduced into the buffer as each is required for binding. Once again, high background signal was observed as shown in figure **4.14**.

Hoping that the non-specific binding observed could be diminished with complete exclusion of the Mn^{+2} and Ca^{+2} ions throughout the entire assay, fluorescein tagged Galanthus Nivalis lectin (GNL) was chosen as a substitute for ConA as it requires neither ion for binding. Liposomes containing 5% **4.11.1c**, 1% **4.4.1a**, and 94% PC were prepared and incubated with streptavidin-coated surfaces. Following removal of unbound liposomes, GNL was introduced at varying concentrations. Controls were simultaneously carried out by incubating GNL in wells that had not been exposed to liposomes. As before, a significant amount of nonspecific interaction was observed.

Taking into account all the experiments, several factors may be responsible as to why the assay is not working as well as the DAG-PKCα. First, using a receptor tagged with a fluorophore generally leads to increased background due to difficulty in washing away all residual fluorescence. In order to circumvent this drawback, a more sensitive technique may be employed. For example, if an HRP-tagged lectin could be obtained, chemiluminescence could be used to detect binding. However, since the concentration of the HRP tag is equal to that of the protein, a dual antibody assay may be more beneficial as this would allow the use of more protein and less of the tag for signal

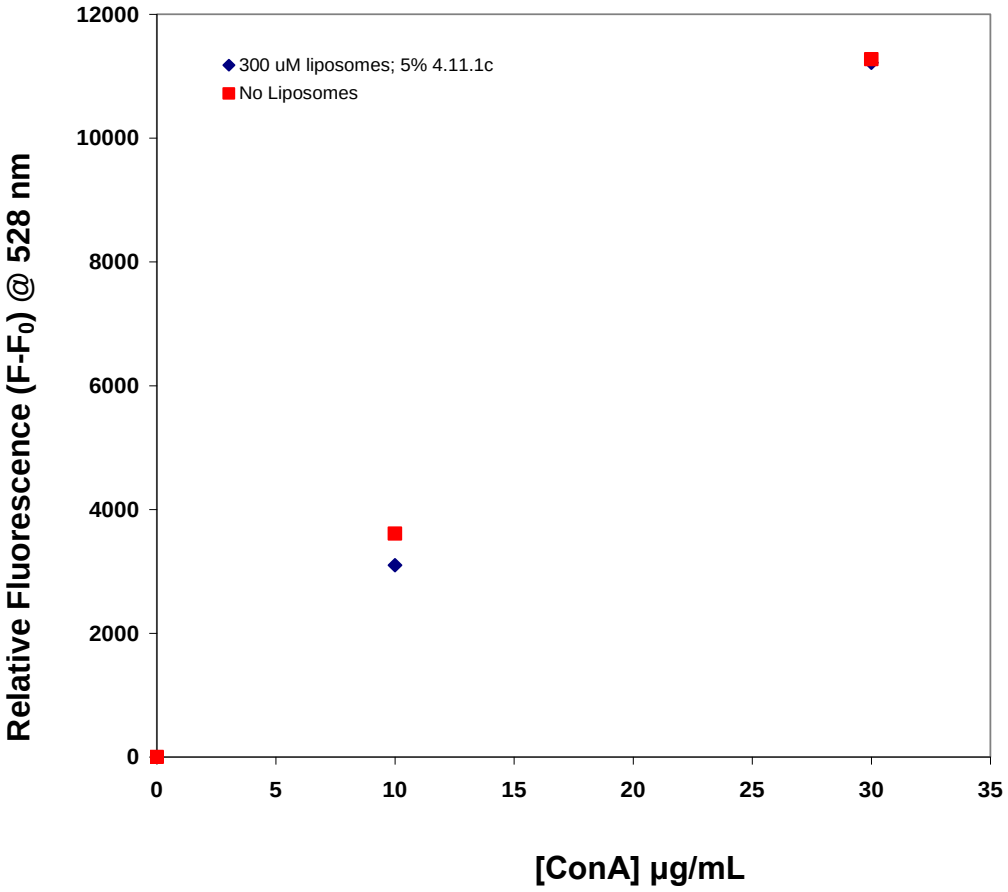

Figure 4.14. Attempts at ConA binding assay excluding Mn^{+2} and Ca ions during immobilization.

generation.

Second, since these lectins interact with mannose in a multivalent fashion, incorporating only 5-10% of the sugar may not be adequate for optimal binding. We believe that 10-15% mannose-lipid **4.11.1c** is the maximum amount that can be efficiently incorporated into vesicles. Higher concentrations of the sugar could be expressed by attaching it to a PE analogue, as it is known PE can be incorporated at much higher percentages.[158]

Third, the sugar may not be expressed far enough away from the membrane surface for optimal recognition by the receptor, as longer spacers have been reported for similar purposes.[152] This could be overcome by spacing the sugar from the surface via a TEG-based linker, similar to that used in designing **4.4.1a**.

Lastly, it is known that mannose can interfere with the binding of biotin to streptavidin,[159] and the sugar may be outcompeting the biotin leading to less sugar expressed and reduced binding. If this is the main reason for the observation of poor results, anchoring of the membrane surface would need to be achieved via alternative means. An alternative to this would be a reverse assay[160-162] in which biotin-tagged lectin is immobilized, followed by incubation with liposomes containing mannose-lipid **4.11.1c** and CBF-lipid **4.4.1b** for detection purposes.

Experimental

General Considerations

All reagents were purchased from Acros or Aldrich and used as received. Dry solvents were obtained from a Pure Solv solvent delivery system purchased from Innovative Technology, Inc. Column chromatography was performed using 230 - 400 mesh silica gel purchased from Sorbent Technologies. NMR spectra were obtained using a Bruker AC250 spectrometer updated with a TecMag data collection system, a Varian Mercury 300 spectrometer or a Bruker Avance 400 spectrometer. Mass spectra were obtained with JEOL DART-AccuTOF and ABI Voyager DE Pro MALDI spectrometers. Optical rotation values were obtained using a Perkin-Elmer 241 polarimeter. L-α-phosphatidylcholine (PC) and L-α-phosphatidylserine (PS) were purchased from Avanti Polar Lipids, Inc. (Alabaster, AL). Liposome extruder and polycarbonate membranes were obtained from Avestin (Ottawa, Canada). Microplate-based fluorescence measurements were performed using a BioTek Synergy 2 multi-detection microplate reader. Clear, white and black reacti-bind streptavidin high binding capacity (HBC) coated 96-well microplates were purchased from Pierce Biotechnology (Rockford, IL). PKCα and rabbit anti-PKCα antibody were purchased from Calbiochem (San Diego, CA). Goat anti-rabbit igG HRP-conjugate was purchased from Chemicon International (Temecula, CA). Supersignal ELISA femto maximum sensitivity substrate was purchased from Pierce Biotechnology (Rockford, IL). Characterization of 5(6)-carboxyfluorescein alkyne **2.8.17d** are given in chapter 2.

Synthetic Procedures

Ethyl 14-hydroxy-3,6,9,12-tetraoxatetradecanoate (4.3.4). In a 3-neck round bottom flask equipped with a bubbler, tetraethylene glycol **4.3.3** (43.2 mL, 250 mmol) was dissolved in anhydrous dichloromethane. Copper triflate (904.2 mg, 2.5 mmol) was added along with anhydrous tetrahydrofuran (7 mL). The solution was cooled to 0 °C and placed under a constant stream of nitrogen. Ethyl diazoacetate (5.3 mL, 50 mmol) was dissolved in anhydrous dichloromethane (34 mL) and added dropwise to the stirring solution. The solution was allowed to gradually warm to room temperature and stirring was continued overnight. The reaction was extracted with saturated NaCl and then washed with dichloromethane (100 mL). The combined organic layers were combined and dried with magnesium sulfate and filtered, and the solvent was removed under reduced pressure. Column chromatography with silica gel and a gradient solvent system of 0 - 10 % methanol/ethyl acetate afforded **4.3.4** as a yellow oil (8.9 g, 64%). ^{1}H NMR (300 MHz, $CDCl_3$) δ 4.20 (q, *J* = 7.2 Hz, 2H), 4.15 (s, 2H), 3.73-3.54 (m, 16H), 1.27 (t, *J* = 7.2 Hz, 3H); ^{13}C NMR (75 MHz, $CDCl_3$) δ 170.4, 72.6, 70.7, 70.54, 70.52, 70.44, 70.43, 70.2, 68.5, 61.4, 60.6, 14.2; HRMS $[M + H]^+$ cacld: 281.16003, found: 281.15895

Ethyl 14-azido-3,6,9,12-tetraoxatetradecanoate (4.3.5). Alcohol **4.3.4** (1.02 g, 3.64 mmol) and triethylamine (1.5 mL, 10.92 mmol) were dissolved in anhydrous diethyl ether (7 mL) at 0 °C under a nitrogen atmosphere. Methanesulfonyl chloride (285 µL, 3.68 mmol) was added dropwise with stirring. Once the addition was complete the

solution was allowed to gradually return to room temperature. Stirring was continued for a total of 1 h. At this point solvent was removed under reduced pressure. The residue was dissolved in anhydrous ethanol (10 mL) and sodium azide (239 mg, 3.68 mmol) was added. The reaction was stirred at reflux overnight. The reaction was extracted with dichloromethane (2 x 100 mL) and the organic layer was dried with magnesium sulfate, filtered and the solvent was removed under reduced pressure to yield pure **4.3.5** as a yellow oil (1.04 g, 93%).

^{1}H NMR (300 MHz, $CDCl_3$) δ 4.22 (q, *J* = 7.2 Hz, 2H), 4.15 (s, 2H), 3.73-3.67 (m, 14H), 3.40 (t, *J* = 4.8 Hz, 2H), 1.28 (t, *J* = 7.2 Hz, 3H); ^{13}C NMR (75 MHz, $CDCl_3$) δ 170.4, 70.8, 70.65, 70.62, 70.57, 70.0, 68.7, 60.8, 50.6, 14.2; HRMS $[M - N_2 + H]^+$ cacld: 278.16036, found: 278.16152

Ethyl 14-*tert*-butoxycarbonylamino-3,6,9,12-tetraoxatetradecanoate (4.3.6). Azide **4.3.5** (1.08 g, 3.55mmol) was dissolved in ethyl acetate. Di-tert-butyl dicarbonate (1.55 g, 7.1 mmol), triethyl amine (990 µL, 7.1 mmol) and Palladium on carbon (110 mg) were added with stirring. The flask was evacuated and refilled with hydrogen three times and stirred at room temperature overnight. The reaction mixture was filtered through a pad of celite and the solvent was removed under reduced pressure. Column chromatography with silica gel and and a gradient solvent of 5 : 1 - 2 : 1 chloroform/acetone with 0.1% triethylamine afforded **4.3.6** as a yellow oil (853 mg, 63%).

^{1}H NMR (300 MHz, $CDCl_3$) δ 5.10 (*b* s, 1H), 4.22 (q, *J* = 7.2 Hz, 2H), 4.16 (s, 2H), 3.73-

3.53 (m, 14H), 3.34-3.31 (m, 2H), 1.44 (s, 9H), 1.29 (t, *J* = 7.2 Hz, 3H); ^{13}C NMR (75 MHz, $CDCl_3$) δ 170.5, 156.0, 79.1, 70.8, 70.62, 70.57, 70.55, 70.51, 70.21, 68.7, 60.8, 40.3, 28.4, 14.2; HRMS $[M + H]^+$ calcd: 380.22844, found: 380.22788

.

14-*tert*-butoxycarbonylamino-3,6,9,12-tetraoxatetradecanoic acid (4.3.7). Compound **4.3.6** (379.4 mg, 1 mmol) was dissolved in methanol (2 mL) and 2M NaOH (2 mL) was added with stirring. The reaction was stirred 30 min. At this point Dowex® 50WX8-200 H^+ ion exchange resin was added until the pH was 4-5. The reaction was filtered and the solvent was removed under reduced pressure to afford **4.3.7** as a brown solid (340 mg, 97%).

^{1}H NMR (300 MHz, $CDCl_3$) δ 5.40 (*b* s, 1H), 4.08 (s, 1H), 3.66-3.54 (m, 14H), 3.34-3.24 (m, 2H) 1.44 (s, 9H); ^{13}C NMR (75 MHz, $CDCl_3$) δ 174.3, 156.3, 79.0, 70.4, 70.1, 70.0, 69.9, 69.4, 69.1, 40.1, 28.4; HRMS $[M + H]^+$ cacld: 352.19714, found: 352.19869.

***N*-(prop-2-ynyl)-14-*tert*-butoxycarbonylamino-3,6,9,12-tetraoxatetradecane carboxamide (4.3.8).** Acid **4.3.7** (340 mg, 0.968 mmol), propargylamine (73 µL, 1.06 mmol), 4-dimethylaminopyridine (DMAP, 118 mg, 0.968 mmol), and *N*-Methylmorpholine (213 µL, 1.94 mmol) were dissolved in anhydrous *N,N*-Dimethylformamide (9mL). The solution was cooled to 0 °C and stirred for 5 min. 1-Ethyl-(3-dimethylaminopropyl)carbodiimide hydrochloride (EDC-HCl, 222 mg, 1.16 mmol) was added and the reaction was stirred at room temperature overnight. Next, the solvent was removed under reduced pressure and column chromatography with a

gradient solvent system of 5 : 1 - 2 : 1 chloroform/acetone afforded **4.3.8** as a yellow oil (285 mg, 76%).

^{1}H NMR (300 MHz, $CDCl_3$) δ 7.44 (*b* s, 1H), 5.08 (*b* s, 1H), 4.11-4.09 (m, 2H), 4.03 (s, 2H), 3.70-3.53 (m, 14H), 3.33-3.31 (m, 2H), 2.24 (t, *J* = 2.3 Hz, 1H), 1.45 (s, 9H); ^{13}C NMR (75 MHz, $CDCl_3$) δ 169.9, 156.0, 79.7, 79.2, 77.3, 71.2, 71.1, 70.6, 70.5, 70.3, 70.24, 70.16, 40.3, 28.4, 28.3; HRMS $[M + H]^+$ cacld: 389.22878, found: 389.22797.

13-oxo-3,6,9,12-tetraoxa-14-azaheptadec-16-1-biotinamide (4.3.10). Synthesis of **4.3.10** was carried out by another graduate student in our lab.[153] Alkyne **4.3.8** (145 mg, 360 μmol) was dissolved in 20 mL of dry DMF. Triethylamine was added to the solution, which was then stirred for 5 minutes. Biotin-pentafluorophenyl ester **4.3.9** (148 mg, 360 μmol) was added and the solution was stirred at room temperature overnight. The solvent was then removed by rotary evaporation and the product was purified by column chromatography with a solvent system of 100% acetone - 40% methanol/dichloromethane. This yielded **4.3.10** as a colorless oil (188 mg, 100%).

$[\alpha]_D^{296K}$ + 22.19 (c = 5.25, $MeOH/CHCl_3$); ^{1}H NMR (300 MHz, $CD_3OD/CDCl_3$): δ 4.54 (m, 1H), 4.34 (m, 1H), 4.08 (s, 2H), 4.04 (d, *J* = 2.4Hz, 2H), 3.72 (m, 8H), 3.68 (m, 4H), 3.60 (t, *J* = 4.9Hz, 2H), 3.43 (m, 3H), 3.20 (m, 1H), 2.94 (dd, J_1 = 12.9Hz, J_2 = 4.8Hz, 1H), 2.76 (d, *J* = 12.9Hz, 1H), 2.24 (t, *J* = 7.2Hz, 1H), 1.65 (m, 4H), 1.46 (q, J_1 = 14.4Hz, J_2 = 7.2Hz, 2H); ^{13}C NMR (100.6 MHz, $CD_3OD/CDCl_3$): δ 174.9, 171.0, 164.5, 70.3, 70.2, 70.1, 70.0, 62.2, 60.5, 55.8, 40.3, 39.4, 39.2, 35.8, 28.6, 28.4, 25.7; MALD–HRMS $[M + H]^+$ calcd: 515.2539, found: 515.2537.

(2*S*)-3-(4-(3,18-dioxo-22-(2-oxohexahydro-1*H*-thieno[3,4-*d*]imidazol-4-yl)-5,8,11,14-tetraoxa-2,17-diazadocosyl)-1*H*-1,2,3-triazol-1-yl)propane-1,2-diyl distearate (4.4.1a) Synthesis of **4.4.1a** was carried out by another graduate student in our lab.[153] (S)-3-azidopropane-1,2-diyl distearate (**4.2.2**, 25 mg, 38.9 μmol) and biotin-TEG-alkyne **4.3.10** (20 mg, 38.9 μmol) were suspended in 1ml of THF. Copper iodide (7.4 mg, 38.9 μmol) and *N,N*-diisopropylethylamine (13μl, 77.8 μmol) were added and the resulting solution was allowed to stir at room temperature for 18 hrs. Next, the solvent was removed and the product was purified by a short column using 12 g silica gel with a solvent gradient of 2%-15% methanol/dichloromethane to obtain **4.4.1a** a white solid (20 mg, 44%).

$[\alpha]_D^{296K}$ 12.53 (c = 1.5, $CHCl_3$); ^{1}H NMR (300 MHz, $CD_3OD/CDCl_3$): δ 7.63 (s, 1H), 5.43 (m, 1H), 4.66 (m, 1H), 4.54 (m, 1H), 4.39 (m, 6H), 4.05 (m, 2H), 3.68 (m, 12H), 3.56 (m, 2H), 3.40 (m, 3H), 2.94 (d, *J* = 4.8Hz, 1H), 2.78 (m, 1H), 2.29 (m, 6H), 1.64 (m, 8H), 1.27 (m, 58H), 0.88 (m, 6H); MALDI–HRMS $[M + Na]^+$ calcd: 1186.8111, found: 1186.8082.

(*S*)-5(6)-((1-(2,3-bis(stearoyloxy)propyl)-1*H*-1,2,3-triazol-4-yl)methylcarbamoyl)-2-(6-hydroxy-3-oxo-3*H*-xanthen-9-yl)benzoic acid (4.4.1b). Synthesis of **4.4.1b** was carried out by another graduate student in our lab.[153] (S)-3-Azidopropane-1,2-diyl distearate (**4.2.2**, 58.6 mg, 0.0901 mmol) and 2-Oxo-*N*-(prop-2-ynyl)-5(6)-carboxyfluoresceinamide (**2.8.17d**, 37.2 mg, 0.0901 mmol)[103] were dissolved in 1:1 Tetrahydrofuran/water (2 mL). Copper sulfate pentahydrate (28.8 mg, 0.115 mmol) and

sodium ascorbate (35.7 mg, 0.180 mmol) were added. The reaction was stirred at room temperature in the dark overnight at which point the solvent was removed under reduced pressure. Column chromatography with a gradient solvent system of 10-20% methanol/dichloromethane afforded **4.4.1b** as a yellow solid (65.3 mg, 68%). Note: since both fluorescein isomers (5 and 6-carboxy) were present in the ^{1}H NMR spectra for compound **4.4.1b**, and the ratio of each isomer is unknown in the commercially available acid, integration values are not reported. ^{13}C NMR data for compounds **4.4.1b** is not reported due to poor solubility of the compound and the complex nature of the spectra due to the isomeric mixture.

$[\alpha]_D^{296K}$ 0.8 (C = 1.5, $CHCl_3$); δ 8.82 (*b* s), 8.41-8.29 (m), 7.99-7.87 (m), 7.42-7.26 (m), 7.12 (bs), 6.88-6.55 (m), 5.43 (*b* s), 4.74-4.58 (m), 4.38-4.30 (m), 4.11-4.08 (m), 3.72-3.67 (m), 2.40-2.27 (m), 1.64-1.59 (m), 1.26 (*b* s), 0.88 (t, *J* = 6.5 Hz); MALDI–HRMS $[M + H]^+$ calcd: 1063.6730, found: 1063.6699.

Mannose-lipid (4.11.1c). Mannose-alkyne **4.11.11** (26 mg, 0.119 mmol) and (*S*)-3-azidopropane-1,2-diyl distearate **4.2.2** (93 mg, 0.143 mmol) were dissolved in THF (2 mL). Copper sulfate pentahydrate (36 mg, 0.143 mmol) and sodium ascorbate (57 mg, 0.286 mmol) were added along with water (0.5 mL). The reaction was stirred at room temperature overnight and the solvent was removed under reduced pressure. Column chromatography with silica gel and a gradient solvent system of 100% ethyl acetate to 10% methanol-chloroform afforded **4.11.1c** as a white solid (76.5 mg, 74%).

$[\alpha]_D^{296K}$ + 25.3 (C = 3.06, $CHCl_3$); ^{1}H NMR (300 MHz, $CDCl_3/CD_3OD$) δ 7.75 (s, 1H),

5.43 (*b* s, 1H), 4.81–4.76 (m, 1H), 4.65–4.63 (m, 2H), 4.36 (dd, *J* = 3.8, 12.2 Hz, 1H), 4.09 (dd, *J* = 5.0, 11.9 Hz, 1H), 3.83–3.59 (m, 9H), 2.39–2.29 (m, 4H), 1.63–1.58 (m, 4H), 1.26 (*b* s, 56H), 0.89 (t, *J* = 5.9 Hz, 6H) ; ^{13}C NMR (100.6 MHz, $CD_3OD/CDCl_3$): δ ; MALDI–HRMS $[M + Na]^+$ calcd: 890.6440, found: 890.6402.

Liposome Immobilization Details

General procedure for liposomes preparation. Solid lipids were dissolved in chloroform to a particular concentration and a specific amount of each lipid in solution was added to a small glass container. The chloroform was removed under a constant stream of nitrogen and the resulting lipid film was dried under vacuum overnight. The appropriate volume of buffer (20 mM HEPES, pH 7.4 for studies not involving PKC or 100 mM NaCl, 20 mM HEPES, 1 mM $CaCl_2$, pH 7.4 for studies involving PKC) was added to the dried lipids in order to produce a specific concentration of liposomes after hydration and size reduction. The suspension of lipid and buffer was agitated at 40 °C for 40 min and then subjected to 10 freeze-thaw cycles. Vesicles were prepared by extrusion (19 times) through a 200 nm polycarbonate membrane to control liposome size.

Microplate liposome immobilization experiments. Analysis of liposome microplate immobilization was performed using either clear or black streptavidin-coated microplates. A solution of 20 mM HEPES buffer pH 7.4 was employed as the wash buffer. First, the wells that were to be used for analysis were incubated with 200 µL of

wash buffer for 30 minutes. This was removed, followed by introduction of 100 µL of the various liposome compositions at different concentrations. For the initial fluorescence immobilization study (Figure 1A), liposomes containing 98% PC, 1% **4.4.1a** and 1% **4.4.1b** were analyzed alongside a control with 99% PC, 0% **4.4.1a** and 1% **4.4.1b**. To determine the optimal percentage of biotin for liposome surface attachment (Figure 1B), studies utilized different liposome samples containing **4.4.1b** fixed at 1%, varying percentages of **4.4.1a** (0-2%), and the rest of the liposome was made up of PC (98-100%). After a one hour incubation, these solutions were removed and the wells were washed with 3 x 250 µL wash buffer. The microplate was then analyzed for fluorescence using a microplate reader with excitation using a 460 nm (± 40 nm) filter and emission detected with a 528 nm (± 20 nm) filter.

Procedure for immobilized vesicle leakage assay. Liposomes encapsulated with 5(6)-carboxyfluorescein (CBF) were prepared following a procedure similar to those previously reported (52). A solution of PC (99%) and biotin anchor **4.4.1a** (1%) in chloroform was dried under vacuum 4 h. The lipids were rehydrated with CBF buffer (50mM CBF, 20 mM HEPES, 150 mM NaCl, pH = 7.4) according to the general procedure cited above to give a final concentration of 5 mM liposomes. Vesicles were prepared by extrusion (19 times) through a 200 nm polycarbonate membrane. Unencapsulated dye was removed using a Sephadex G-50 column equilibrated with buffer (20 mM HEPES, 150 mM NaCl, pH = 7.4). Fractions containing liposomes were determined by measuring the fluorescence (excitation λ = 490 nm) followed by the

addition of 20 µL of 20% Triton X-100 to release the encapsulated CBF. Analysis of liposome microplate immobilization was performed using black streptavidin-coated microplates. Wells that were to be used for analysis were incubated with 200µL of was buffer (20 mM HEPES, 150 mM NaCl, pH = 7.4) for 30 min. This was removed, followed by introduction of 100 µL of liposomes at various concentrations prepared from the combined fractions after SEC chromatography. Incubation was carried out for 1 h. Following incubation, subsequent analysis was performed both with (Figure **4.8b**) and without (Figure **4.8a**) microplate washing (3 x 250 µL buffer) to remove unbound liposomes. In both cases, the microplate was initially analyzed for fluorescence using a microplate reader with excitation using a 460 nm (± 40 nm) filter and emission detected with a 528 nm (± 20 nm) filter. At this point, 30 µL of a 20% Triton X-100 solution was added to lyse the vesicles, which was followed by a repeat of the previous fluorescence measurement. Subsequent addition of the detergent did not lead to a further increase in fluorescence, indicating that all liposomes had been lysed.

Microplate analysis of whole liposome-PKCα binding: Microplate protein-binding experiments were performed using white streptavidin-coated 96-well microplates. The wash buffer that was used was 20 mM HEPES buffer pH 7.4 with 100 mM sodium chloride and 1mM calcium chloride for PKC activation. First, the wells that were to be used for analysis were washed with 200 µL of wash buffer for 30 minutes. This was removed, followed by introduction of different concentrations of liposomes (100 µL of solutions ranging from 0 to 200 µM in wash buffer) and then incubation for one hour.

Next, these solutions were removed and the wells were washed with 3 x 250 µL wash buffer. Following this, 200 µL of a 100 ng/mL solution of PKCα in wash buffer was added to each well, followed by a one-hour incubation. At this point, the protein solution was removed and the wells were washed with 3 x 250 µL wash buffer. Next, 200 µL of a 100 ng/mL solution of rabbit anti-PKCα antibody was added to each well and allowed to incubate for one hour. This solution was then removed and the wells were washed with 3 x 250 µL wash buffer. Finally, wells were incubated with goat anti-rabbit IgG HRP-conjugate for one hour and then washed with 3 x 250 µL wash buffer and 1 x 100 µL water. Chemiluminescence detection of bound antibody was next performed using supersignal ELISA femto maximum sensitivity substrate. Here, a 1:1 mixture of the substrate and peroxide solutions were mixed and 100 µL of the resulting solution was added to each well. The microplate was then immediately placed in the microplate reader and the luminescence at 425 nm was repeatedly measured for ~ 5 minutes. Assays were run numerous times, both simultaneously and on separate occasions using newly formed solutions. The chemiluminescence data was then plotted verses the original incubation concentrations using SigmaPlot to curve fit the data (non-linear regression using the Langmuir binding isotherm).

Attempts at whole liposome-lectin binding assay: Microplate protein-binding experiments were performed using black streptavidin-coated 96-well microplates. The wash buffer that was used was 20 mM HEPES buffer pH 6.5 with 100 mM sodium chloride (1 mM calcium chloride and 1 mM manganese (II) chloride were added unless

otherwise stated) for lectin activation. First, the wells that were to be used for analysis were washed with 200 µL of wash buffer for 30 minutes. This was removed, followed by introduction of different concentrations of liposomes (100 µL of appropriate solutions in wash buffer) and then incubation for one hour. Next, these solutions were removed and the wells were washed with 3 x 200 µL wash buffer. Following this, 200 µL of a appropriate µg/mL solution of lectin in wash buffer (with BSA as indicated) was added to each well, followed by a one-hour incubation. At this point, the protein solution was removed and the wells were washed with 3 x 200 µL wash buffer. The microplate was then analyzed for fluorescence using a microplate reader with excitation using a 460 nm (± 40 nm) filter and emission detected with a 528 nm (± 20 nm) filter.

- For experiments using low/hign Mn^{+2} concentrations (Figure **4.13**), liposomes were prepared in buffer with Mn^{+2}. These stock solutions were then diluted with an identical buffer solution minus the Mn^{+2} for the low samples.
- For experiments using GNL, buffer consisted of 20 mM HEPES, 150 mM NaCl, pH = 7.4.

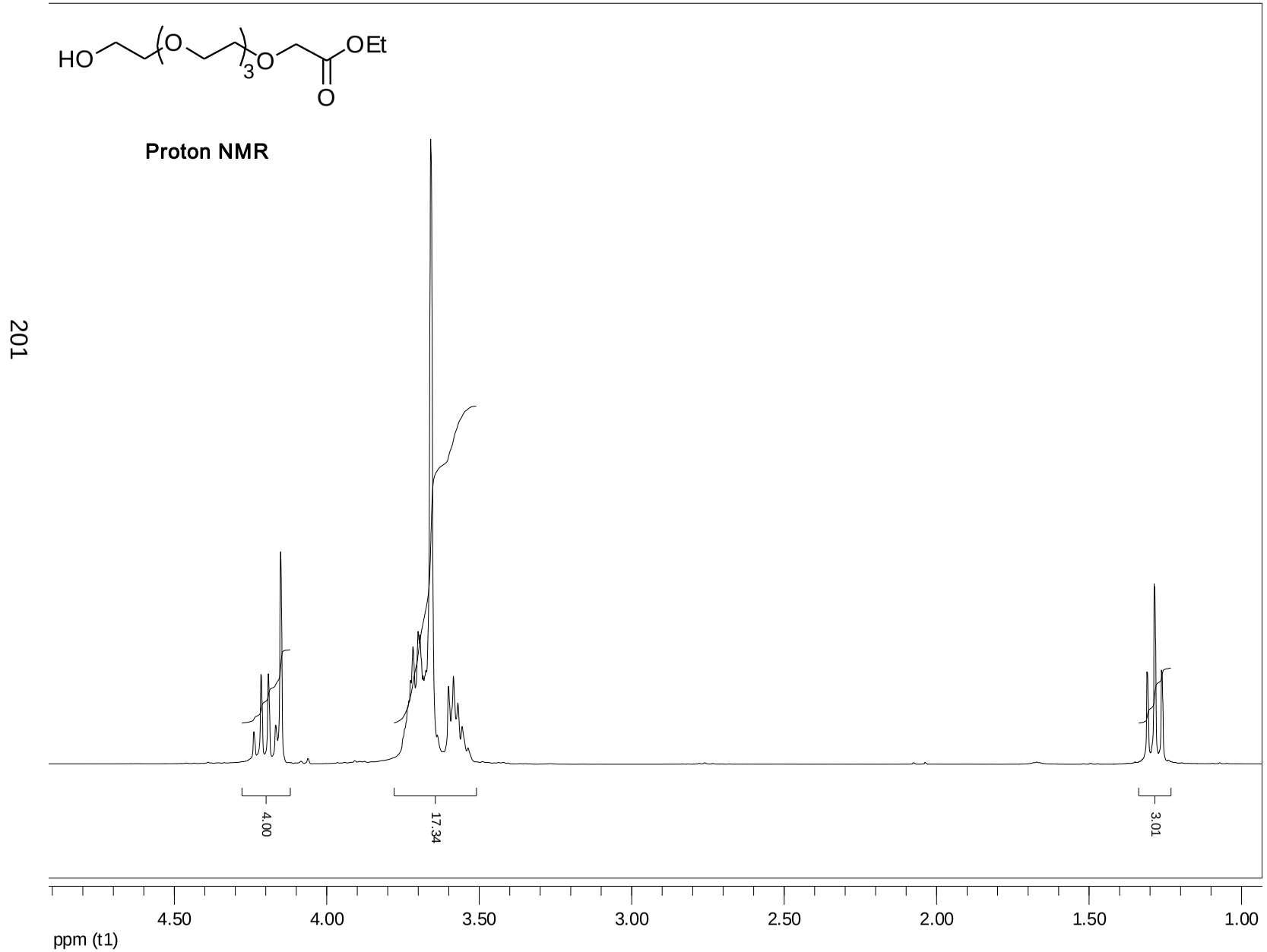
HO
O
3
O
OEt
O
Proton NMR
4.00
17.34
3.01
4.50
4.00
3.50
3.00
2.50
2.00
1.50
1.00
ppm (t1)

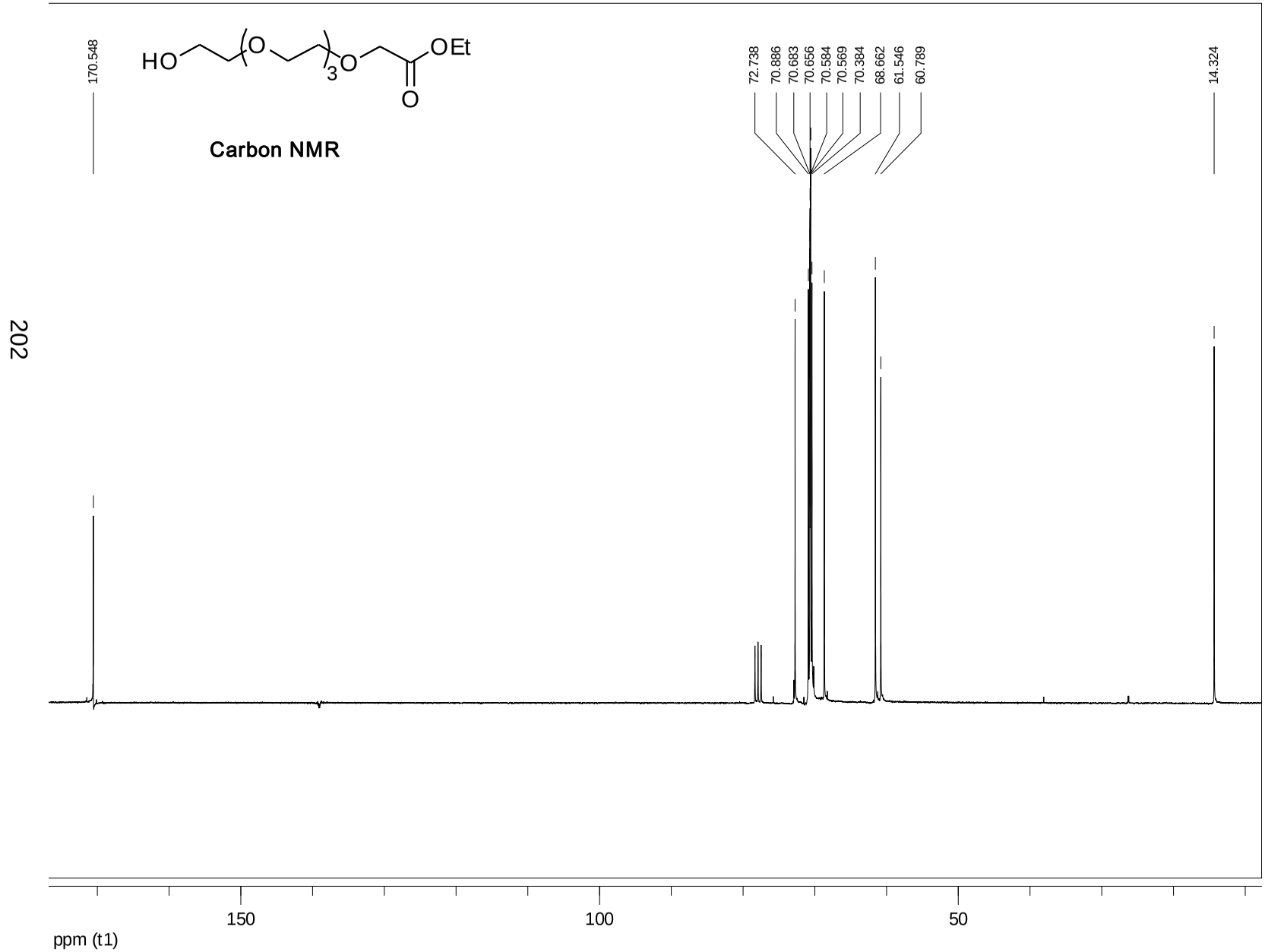
170.548
72.738
70.886
70.683
70.656
70.584
70.569
70.384
68.662
61.546
60.789
14.324
HO
O
3
O
OEt
O
Carbon NMR
202
150
100
50
ppm (t1)

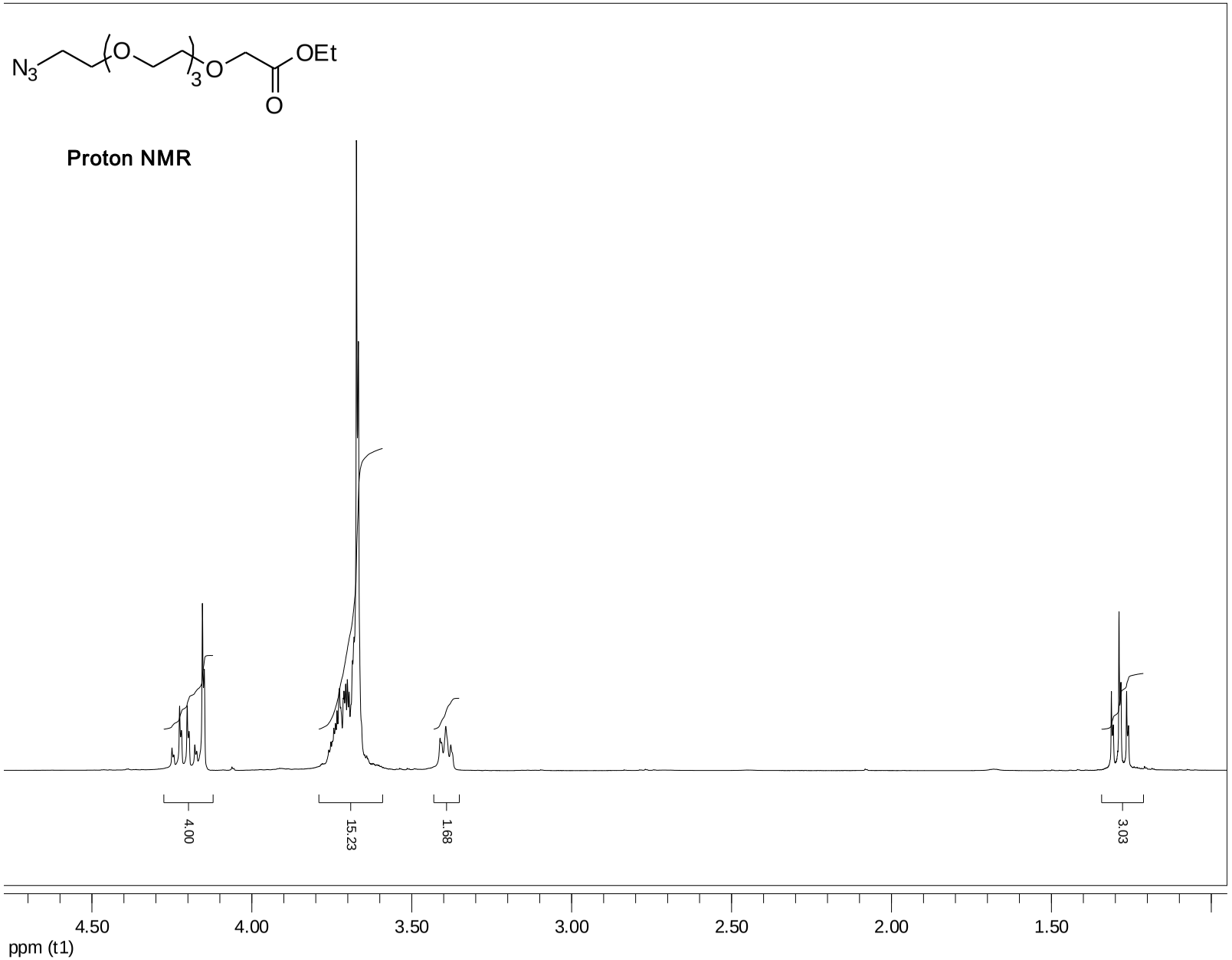
N3
O
3
O
OEt
O
Proton NMR
4.00
15.23
1.68
3.03
4.50
4.00
3.50
3.00
2.50
2.00
1.50
ppm (t1)

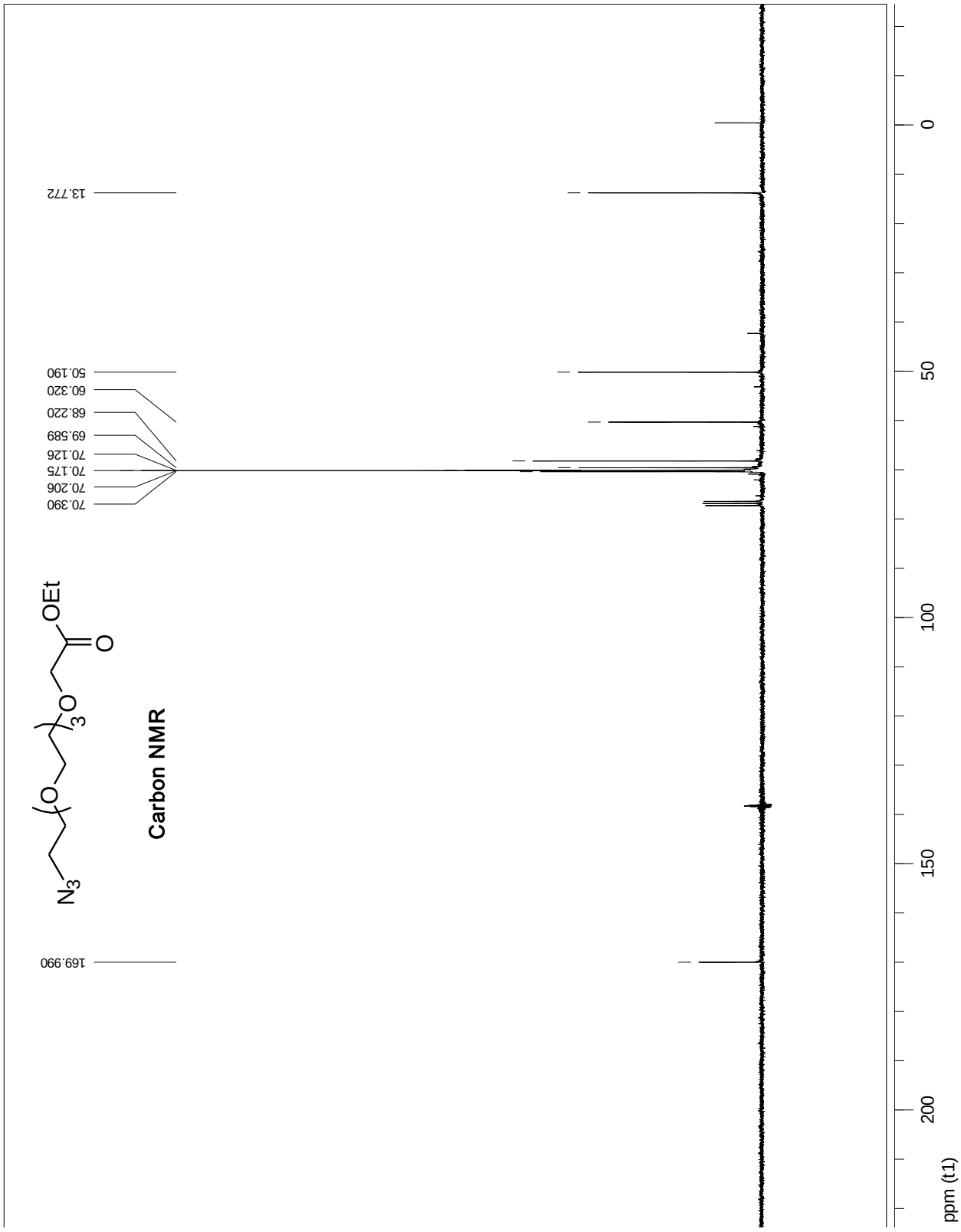
13.772
50.190
60.320
68.220
69.589
70.126
70.175
70.206
70.390
169.990
Carbon NMR
OEt
O
O
O
3
O
N3
0
50
100
150
200
ppm (t1)

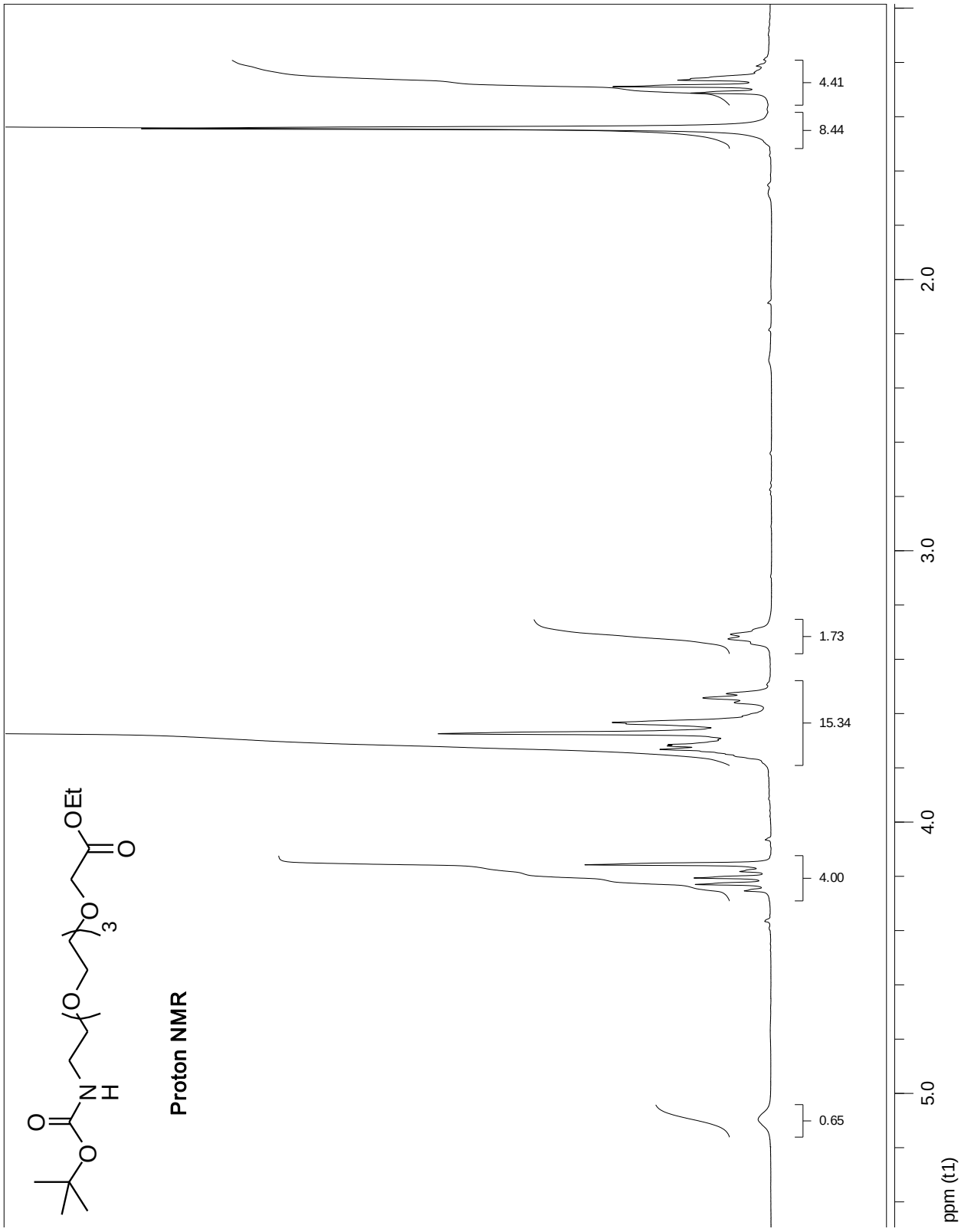
Proton NMR
4.41
8.44
1.73
15.34
4.00
0.65
2.0
3.0
4.0
5.0
ppm (t1)

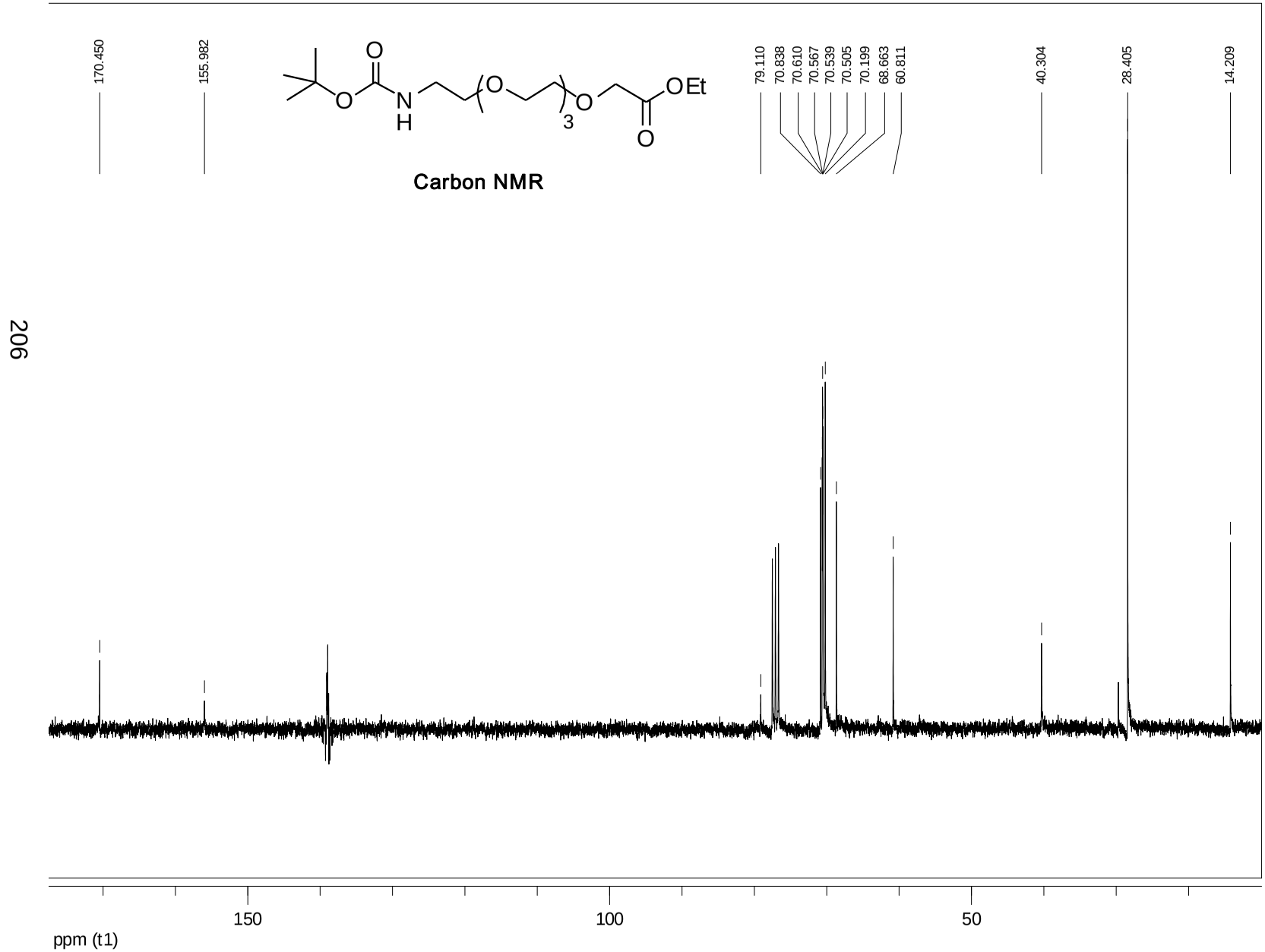
170.450
155.982
79.110
70.838
70.610
70.567
70.539
70.505
70.199
68.663
60.811
40.304
28.405
14.209
O
O
N
H
O
O
3
O
OEt
Carbon NMR
206
150
100
50
ppm (t1)

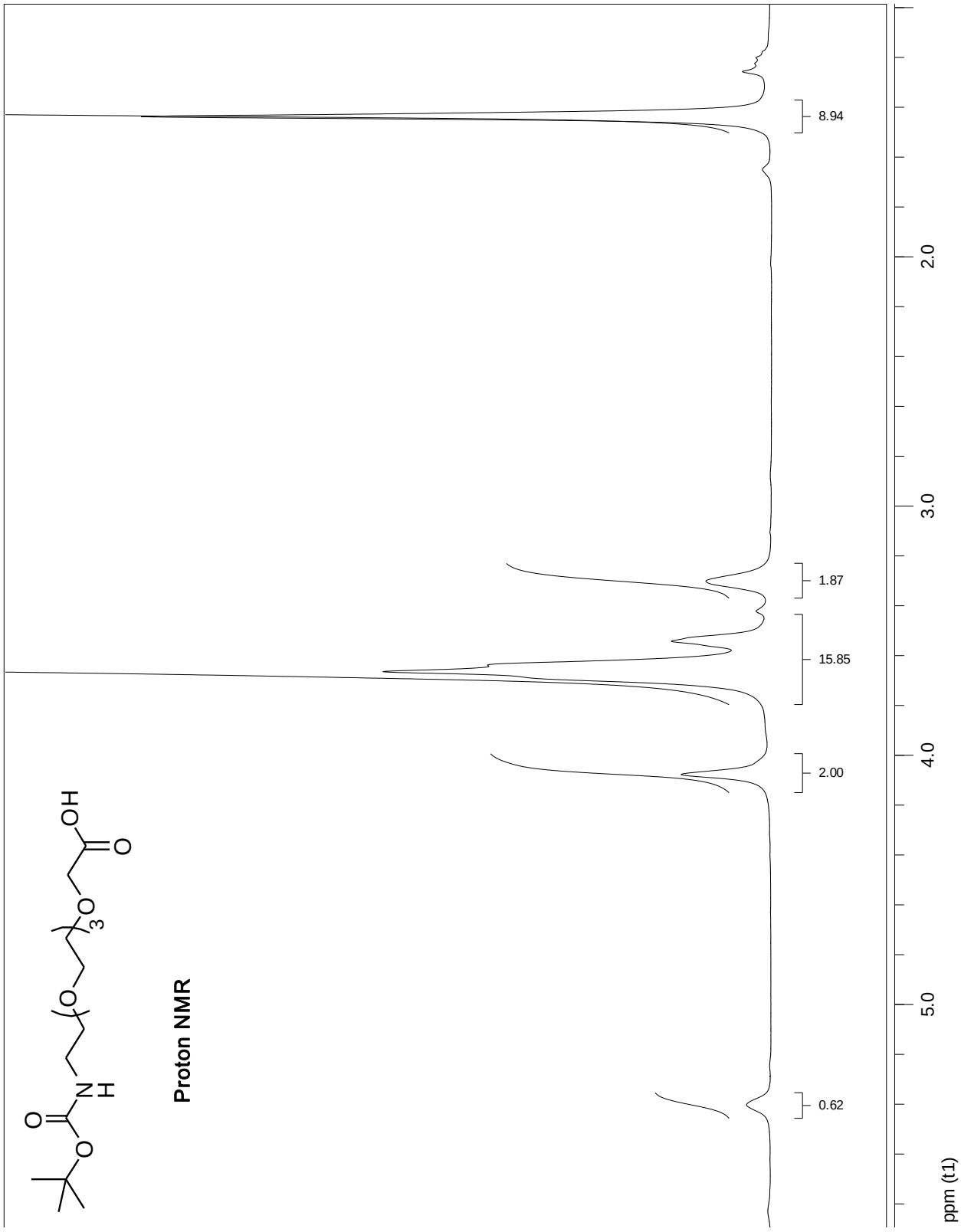
Proton NMR
8.94
1.87
15.85
2.00
0.62
2.0
3.0
4.0
5.0
ppm (t1)

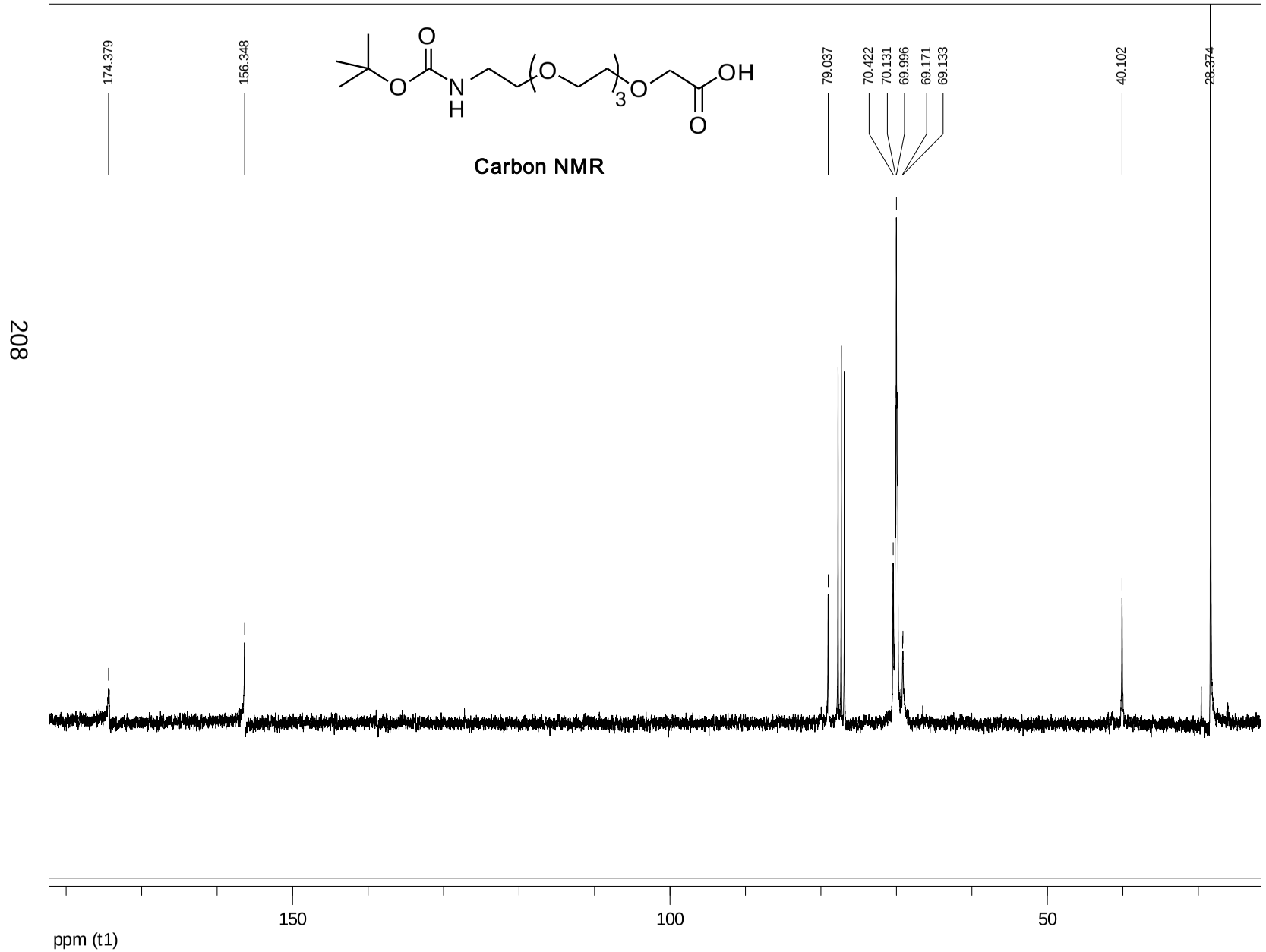
174.379
156.348
79.037
70.422
70.131
69.996
69.171
69.133
40.102
28.374
OH
Carbon NMR
208
150
100
50
ppm (t1)

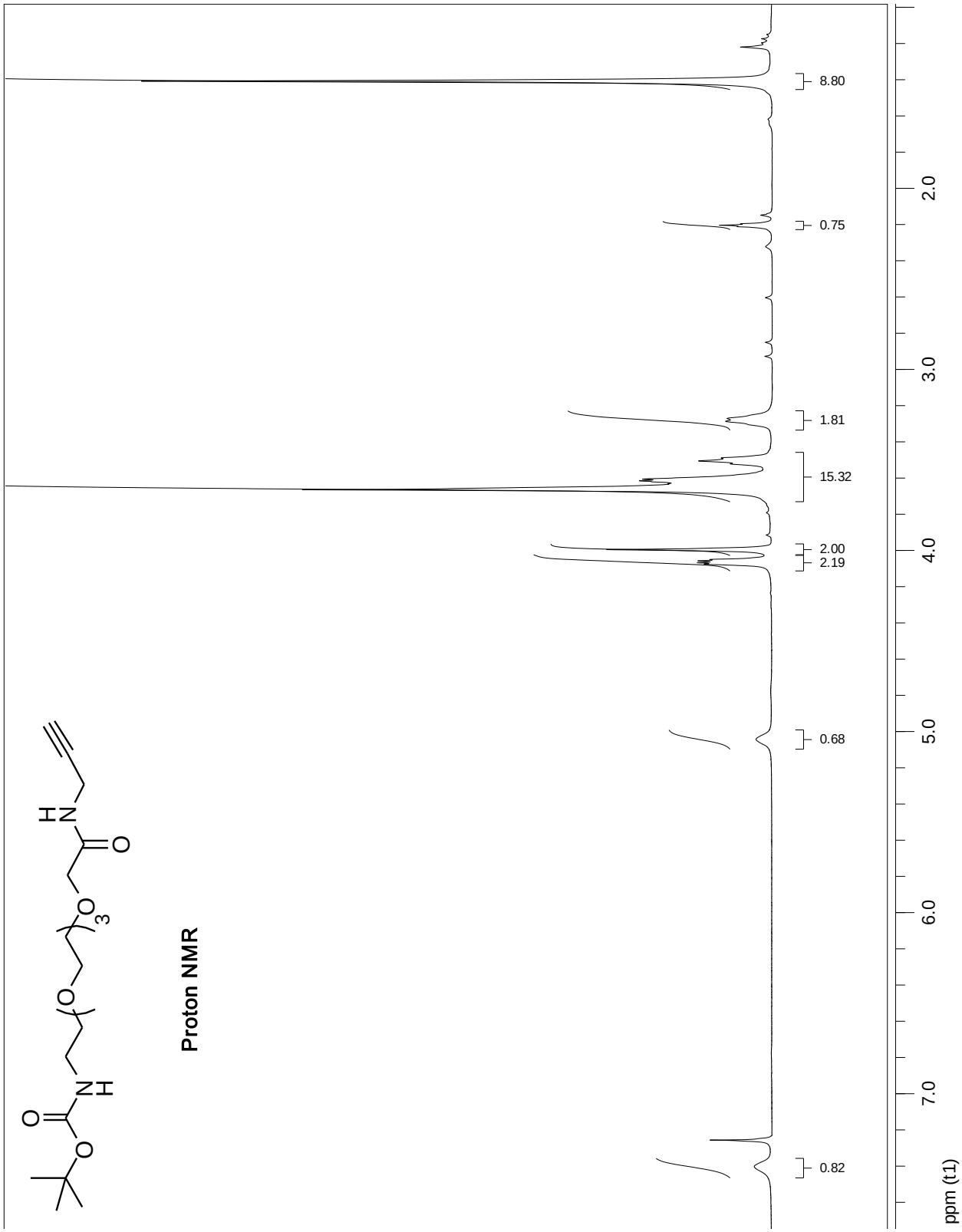
Proton NMR
8.80
0.75
1.81
15.32
2.00
2.19
0.68
0.82
2.0
3.0
4.0
5.0
6.0
7.0
ppm (t1)

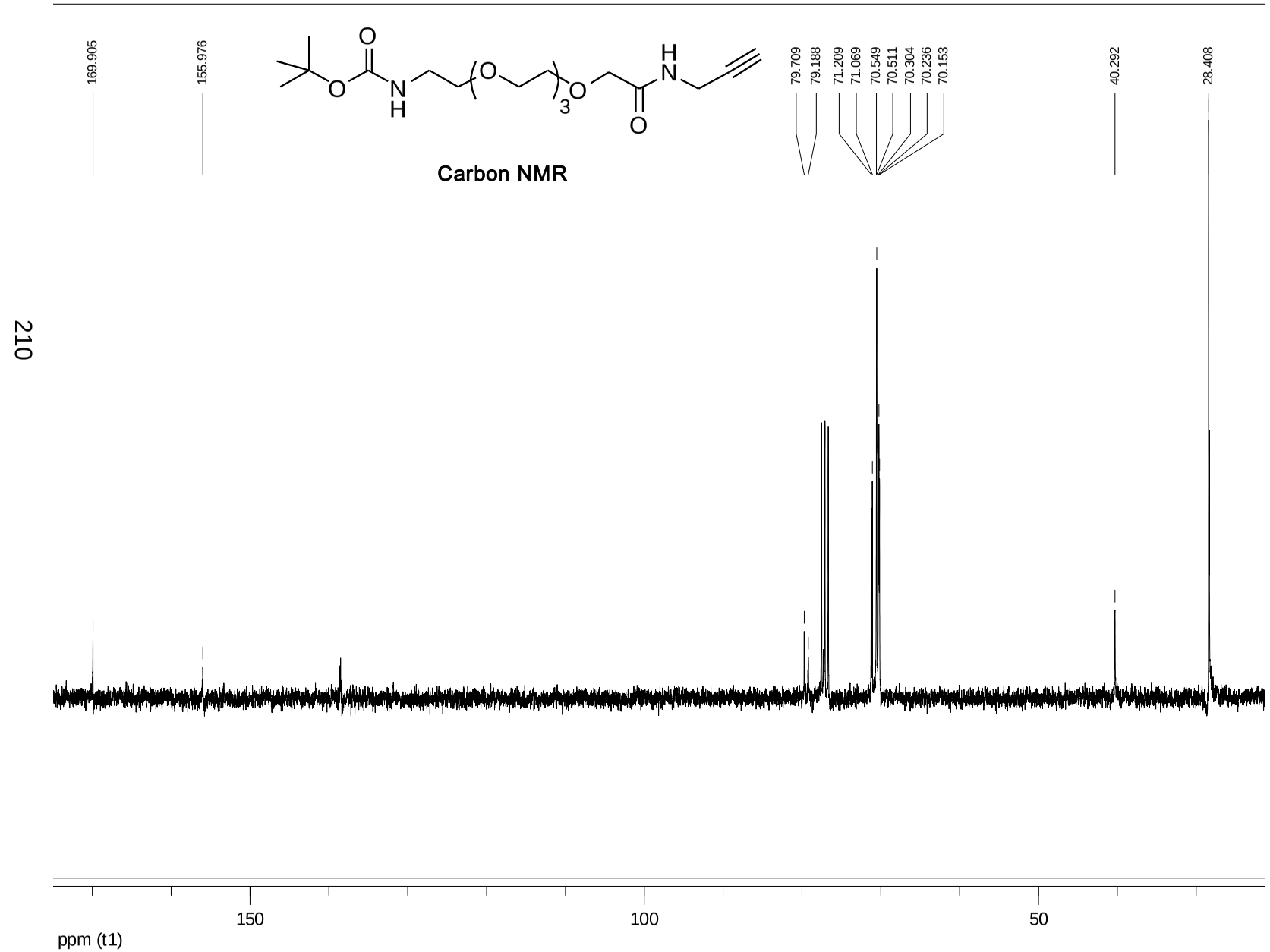
169.905
155.976
79.709
79.188
71.209
71.069
70.549
70.511
70.304
70.236
70.153
40.292
28.408
Carbon NMR
210
150
100
50
ppm (t1)

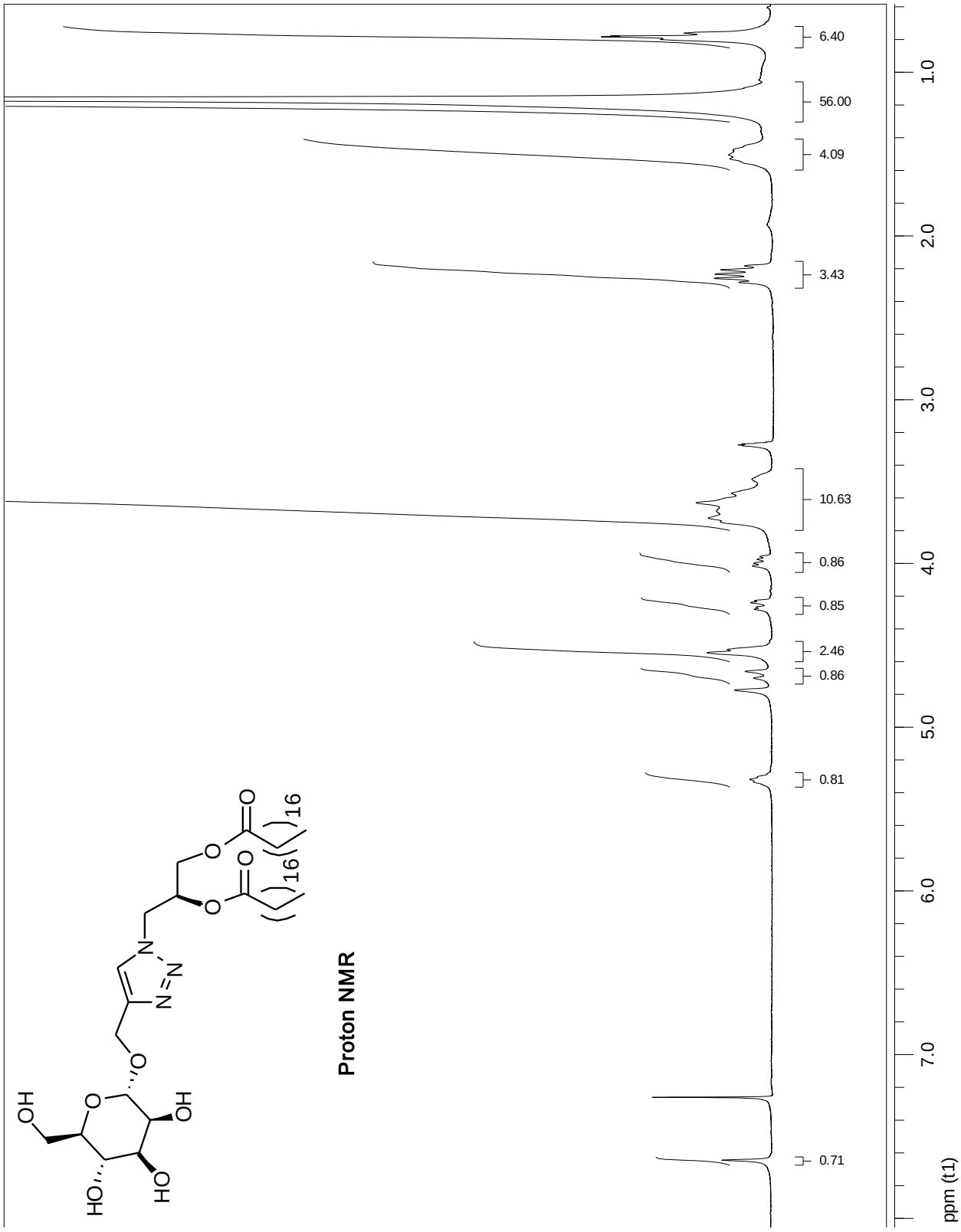
6.40
56.00
4.09
3.43
10.63
0.86
0.85
2.46
0.86
0.81
0.71
1.0
2.0
3.0
4.0
5.0
6.0
7.0
ppm (t1)
Proton NMR

Chapter 5: Click Chemistry Using Azido and Alkyne Based Lipids Presented in Liposomes: Towards a Chemical Approach for Vesicle Fusion

Background and Significance

Membrane fusion is a process that is frequently observed in cellular processes such as fertilization, endocytosis, exocytosis, and cell division. However, the fusion of membranes is not a spontaneous process and requires significant amounts of energy to occur. This energy is provided by specialized fusion proteins.[128] In order to develop a system that mimics this process without requiring fusion proteins, an environment that closely resembles that of a cell is needed.[163] Liposomes fufill this criteria as they exist in a bilayer structure and can be functionalized through the incorporation of various molecules to present specific ligands or molecules on the surface.

To date, most artificial fusion systems employ molecular recognition techniques in order to promote the process. For example, accounts of induced vesicle fusion utilizing small molecule interactions capable of producing electrostatic interactions and multiple hydrogen bonds,[163-168] such as those between vancomycin and peptides[164, 165] and between cyanuric acid and melamine,[166] have been reported. Fusion is also known to be induced through metal ion binding by amphiphilic 2,2'-bipyridine ligands.[169] A pH sensitive fusion system using coiled-coil polypeptides is also known.[170] One of the main drawbacks of such systems lies in the fact that they utilize molecules and recognition techniques that already occur within cells, which could lead to reduced specificity of

such systems *in vivo*.

Therefore, we sought to design a system that would allow specific interaction between the two liposomes that we targeted for fusion. We hypothesized that if an azide could be introduced at the surface of one liposome and an alkyne at the surface of another, then “click” chemistry could be used to covalently tether between the liposomes. This linkage would bring the liposomes into proximity in order to promote vesicle fusion. This approach is particularly appealing as both azide and alkynes are generally unreactive to cellular components, and at the same time, potentially non-toxic to the cell.

Synthesis of Lipids for Vesicle Fusion

In order to modify the surface of liposomes utilizing “click” chemistry, lipids capable of presenting azides and/or alkynes at the surface must be designed. Considerations in the design of such lipids include incorporation of a headgroup that will keep the lipid high enough in the membrane to present the azide/alkyne at the surface level of the membrane, incorporating a tether that will maintain enough distance between the azide/alkyne and the surface in order to give it ample space to react, and tethering it to the lipid in a manner that will prevent it from “dipping” back and becoming buried in the hydrophobic region of the bilayer. With these considerations in mind, we sought to utilize azido-lipid **4.2.2** (figure **5.1**) as a scaffold for incorporating azide and alkynes onto the lipid. The azide of **4.2.2** can react with a corresponding alkyne via “click” chemistry producing a triazole ring. This structure is known to be too polar to

Figure 5.1. Chemical structure of azido-lipid **4.2.2**.

exist within the bilayer, therefore maintaining presentation at the surface. The synthesis of an azide-presenting lipid **5.2.1a** using this methodology is presented in figure **5.2**. First, ester **4.3.4**[153] is converted into alkyne **5.2.2** via hydrolysis of the ethyl ester followed by coupling with propargyl amine. Next, cycloaddition with **4.2.2** furnished TEG-alcohol lipid **5.2.3**, which was converted to the azide **5.2.1a** through a mesylate intermediate. Synthesis of a TEG-alkyne lipid is presented in figure **5.3**. Initially, alkyne **4.3.8**[153] is coupled with **4.2.2** to afford Boc-protected lipid **5.3.4**. Following Boc removal and coupling to acid **5.3.5**, TEG-alkyne lipid **5.3.1b** is obtained.

In order to monitor activity and success of the "click" reactions to be carried out on the liposome surface, we chose to use a FRET based approach. It is known that carboxylates present in a fluorescent molecule can coordinate copper ions and quench fluorescence.[171] Therefore, we sought to use fluorophores that do not coordinate to copper ions and decided to develop NBD-lipid **5.4.8a** and rhodamine-lipid **5.4.8b**, as these fluorophores have proven effective in monitoring the modification of liposome surfaces via "click" chemistry.[158] The synthesis of lipids **5.4.8a** and **5.4.8b** is presented in figure **5.4**. Each was accessed from coupling of the chloro analogue of each fluorophore with propargyl amine, followed by "click" reaction with azido-lipid **4.2.2**.

Surface Modification of Liposomes via "Click" Chemistry

Having developed lipids capable of presenting "clickable" substrates on the surface of liposomes, we sought to verify that such modifications were occurring. Following similar procedures[152, 158] TEG-azido lipid **5.2.1a,** NBD-lipid **5.4.8a,** and PC

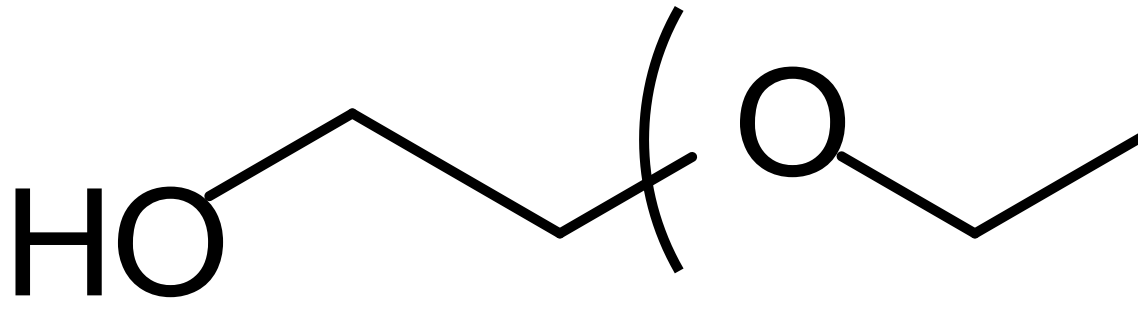

Figure 5.2. Synthesis of TEG-azido lipid **5.2.1a**.

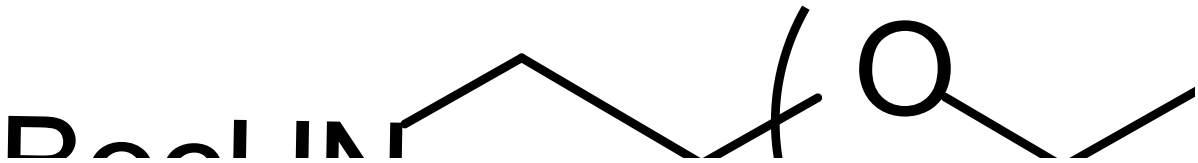

Figure 5.3. Synthesis of Teg-alkyne lipid **5.3.1b**.

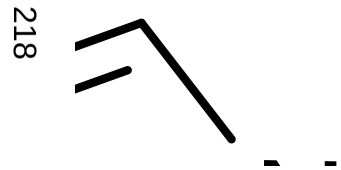

Figure 5.4. Synthesis of NBD-lipid **5.4.8a** and rhodamine-lipid **5.4.8b** via “click” chemistry with **4.2.2**.

were incorporated into liposomes at 10%, 1%, and 89% respectively. Reasoning that rhodamine-alkyne **3.7.19d** would be more water soluble than NBD-alkyne **5.4.7** due to its charge, we decided to attempt to "click" it onto TEG-azido lipid **5.2.1a**. Liposomes were added to rhodamine-alkyne and CuBr and then allowed to react 20 h with occasional monitoring of the fluorescence (figure **5.5**), the results of which are presented in figure **5.6**. Both samples exhibited a small amount of rhodamine fluorescence due to weak excitement of the rhodamine by the light used to excite the NBD. As seen from the graph, the initial fluorescence observed for the NBD-lipid (520 nm) was lower compared to that observed in the control sample without CuBr. We reasoned that the decrease of the NBD signal was not the result of FRET as the rhodamine signal was also initially lower than the control. Therefore, it seems that the NBD fluorescence is in some way being quenched by the copper ions. However, after 20 h the intensity of the rhodamine fluorescence in the "click' reaction had risen slightly above that observed for the control. This indicates that the rhodamine species is being excited more than initially observed. The possibility that energy from NBD emission is exciting the rhodamine and that FRET is being observed is indicated by two factors. First, the level of the rhodamine fluorescence does not increase in the control from the start to the end of the reaction. Also, in the "click" reaction, the rhodamine fluorescence has shifted, potentially indicating an alternative method for excitement. These results seem to indicate that indeed our system is viable for the surface modification of liposomes via click chemistry.

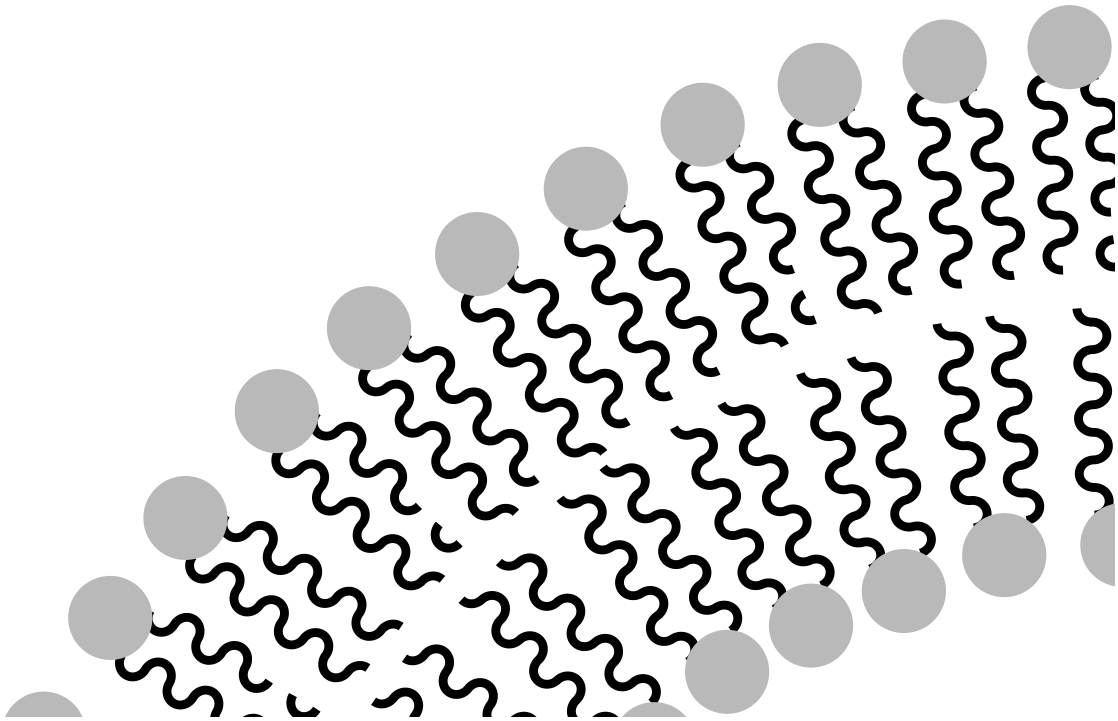

Figure 5.5. Representation of using FRET to monitor the surface modification of liposomes with “click” chemistry.

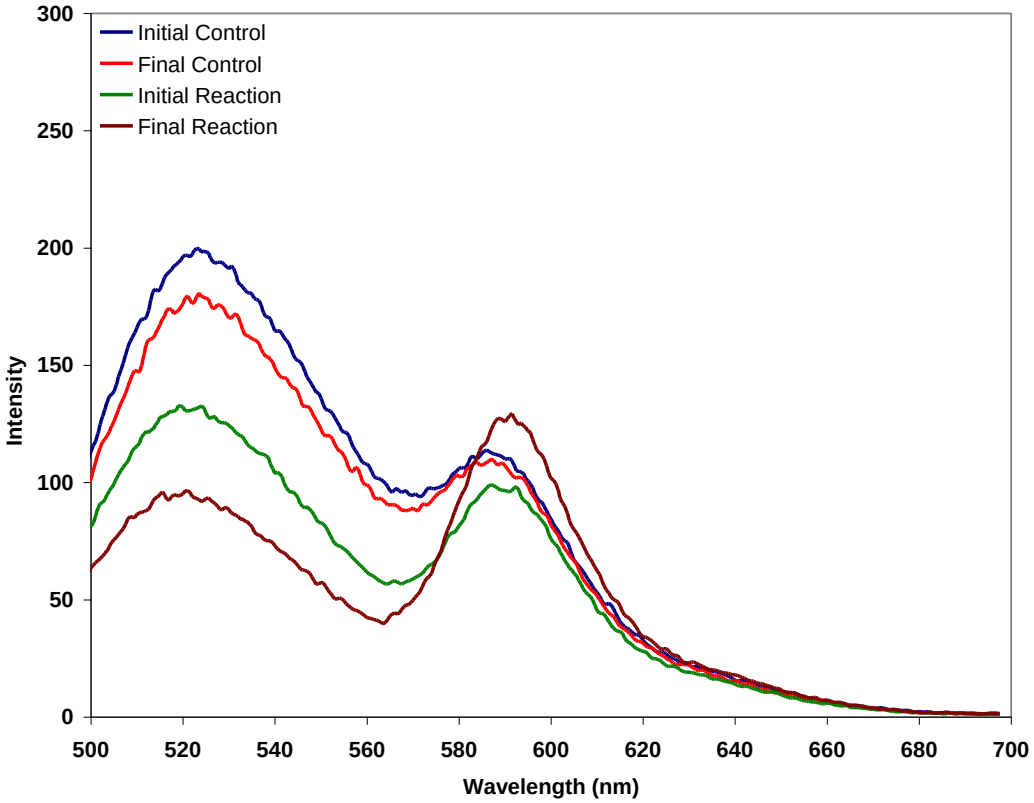

Figure 5.6. Fluorescence readings obtained during surface modification of liposomes composed of PC, **5.2.1a**, **5.4.8a** through reaction with alkyne **3.7.19d**. The blue (initial reading) and red (final reading) lines represent control experiments in which no CuBr was added. The green (initial reading) and brown (final reading) represent the actual reaction in which CuBr was added.

Attempts at Vesicle Fusion via “Click” Chemistry

In an attempt to develop a procedure for vesicle fusion promoted by an irreversible, bio-orthogonal chemical reaction, we once again turned our focus to design a system that utilizes “click” chemistry. A representation of such a system is shown in figure **5.7**.

Originally we planned on detecting the fusion with FRET. One liposome would be doped with a FRET donor lipid and the other with a FRET acceptor, which should effectively turn on FRET upon fusion. Initially, a carboxyfluorescein lipid was used as the FRET donor, but the fluorescence of the CBF was completely quenched and never regenerated during the course of the reaction. Therefore, NBD-lipid **5.4.8a** and rhodamine-lipid **5.4.8b** were used as the donor and acceptor respectively. As was observed in the surface modification experiments discussed above, the initial intensity of the NBD fluorescence was lower than that observed for the control (no CuBr). Also, the intensity for both the NBD and rhodamine fluorescence remained lower than the control during the entire course of the reaction. Due to the inability to tell how significantly the fluorescence was changing over the course of the reaction, an alternative method for the detection of fusion was sought.

A common approach used to verify the fusion of two vesicles is a dye leakage assay. Therefore, 5(6)-carboxyfluorescein was encapsulated into vesicles composed of 10% azide **5.2.1a** and 90% PC. These were then reacted with vesicles composed of 10% alkyne **5.3.1b** and 90% PC in the presence of CuBr. However, no distinct difference in the amount of CBF fluorescence after 20 h could be detected between

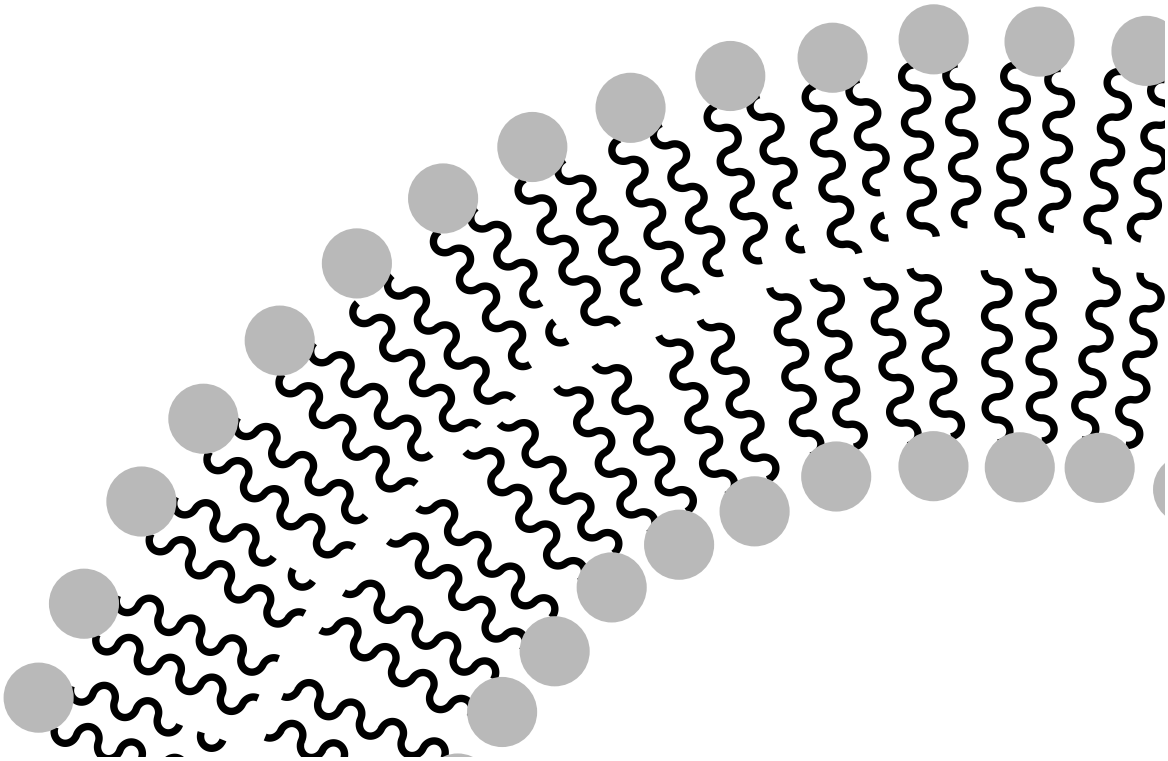

Figure 5.7. Representation of vesicle fusion promoted through covalent attachment of two vesicles via “click” chemistry.

solutions with CuBr and those without.

In a final attempt to determine if vesicle fusion promoted by “click” chemistry was occurring, the mean diameter of the vesicles was measured by dynamic light scattering over the course of the reaction. Results are shown in figure **5.8**. As can be seen from the plot, control samples containing no CuBr show a relatively constant mean diameter over a 1 h reaction time. The average diameter observed for the “click” reaction solution with azide liposomes, alkyne liposomes, and CuBr changes over time and eventually levels off at a diameter roughly twice that initially observed. Two control experiments were carried out to test the selectivity of the “click” reaction. Solutions of vesicles comprised of 10% azide **5.2.1a** and 90% PC and solutions with 10% alkyne **5.3.1b** and 90% PC were prepared and exposed to CuBr. As seen from the graph in figure **5.8**, the size of the vesicles in each of these experiments increases in a manner similar to that observed for the actual “click” reaction set. These results, along with the absence of an increase in vesicle size for those without any CuBr, seem to indicate that the copper ion is responsible in some way for the change in size.

It is known that metal ions that can complex to certain lipids exposed on the surface can induce reorganization within the bilayer.[172] If the lipids are present at relatively high concentrations (0.1 mM), then this chelation and reorganization can facilitate the formation of bilayer stacks that possess a column shape.[173] In this case, upon addition of the coordinating metal, the solution became turbid. In the three instances above that showed an increase in vesicle diameter, increased turbidity of the solution was also observed. Copper (I) ions are known to catalyze 1,3-dipolar

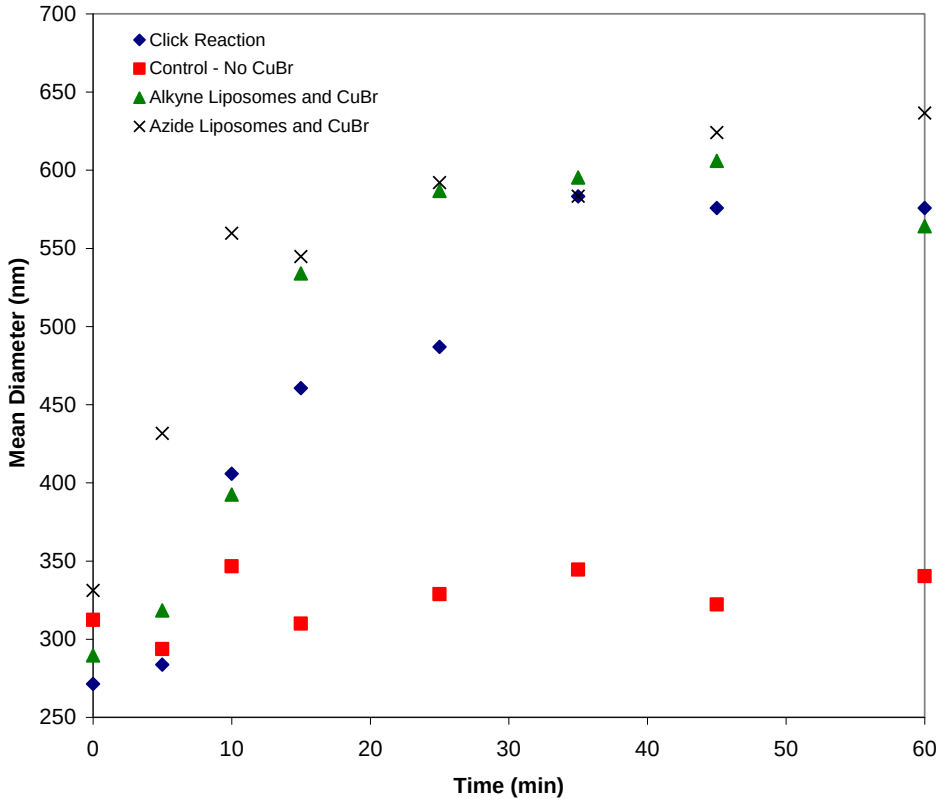

Figure 5.8. Results from DLS measurements of vesicles in fusion experiments.

cycloadditions by coordinating an azide and alkyne. This coordination brings them into proximity and forces the cycloaddition. Therefore, it seems reasonable that in the controls that contained liposomes with either the azide or alkyne, the Cu^{+} could potentially coordinate to two alkynes or two azides, thereby bringing the vesicles into proximity to each other and promoting fusion, or at least aggregation. This would explain both the increase in diameter and turbidity that was observed in all three cases. In attempts to verify whether the vesicles fuse or simply aggregrate in the presence of copper (I) ions, a copper-free version of this process is currently being developed in our lab. This approach should also lend itself compatible to monitoring the fusion event using the FRET based approach initially attempted.

Experimental

General Considerations

All reagents were purchased from Acros or Aldrich and used as received. Dry solvents were obtained from a Pure Solv solvent delivery system purchased from Innovative Technology, Inc. Column chromatography was performed using 230 - 400 mesh silica gel purchased from Sorbent Technologies. NMR spectra were obtained using a Bruker AC250 spectrometer updated with a TecMag data collection system, a Varian Mercury 300 spectrometer or a Bruker Avance 400 spectrometer. Mass spectra were obtained with JEOL DART-AccuTOF and ABI Voyager DE Pro MALDI spectrometers. Optical rotation values were obtained using a Perkin-Elmer 241 polarimeter. L-α-phosphatidylcholine (PC) was purchased from Avanti Polar Lipids, Inc. (Alabaster, AL).

Liposome extruder and polycarbonate membranes were obtained from Avestin (Ottawa, Canada). Fluorescence measurements were carried out on a PerkinElmer LS 55 Fluorescence Spectrometer. DLS measurements were carried out on a Brookhaven Instruments BI-200SM goniometer (633 nm) and a BI-9000AT digital correlator. Characterization of compounds **4.2.2**, **4.3.4**, and **4.3.8** are given in Chapter 4. Those for compound **3.7.19d** are given in Chapter 3.

Synthetic Procedures

14-Hydroxy-*N*-(prop-2-ynyl)-3,6,9,12-tetraoxatetradecan-1-amide (5.2.2). Alcohol **4.3.4** (2.32 g, 8.28 mmol) was dissolved in methanol (8 mL). With stirring 2 M NaOH was added and stirring was continued for 40 minutes. The solution was neutralized with Dowex® 50WX8-200 H^+ ion exchange resin to pH 4. The resin was removed via filtration and the filtrate was concentrated under reduced pressure. The residue was suspended in toluene and concentrated once again.

At this point, the residue was dissolved in dichloromethane (50 mL). With stirring propargyl amine (682 µL, 9.94 mmol), 1-ethyl-(3-dimethylaminopropyl)carbodiimide hydrochloride (1.9 g, 9.94 mmol), 4-dimethylaminopyridine (1.01 g, 8.28 mmol), and N-methylmorpholine (2.74 mL, 24.84 mmol) were added. The solution was stirred at room temperature overnight. The reaction mixture was extracted with 2 M HCl and dichloromethane. The organic layer was dried with magnesium sulfate, filtered, and the solvent removed under reduced pressure. Column chromatography with silica gel and a solvent system of 7% methanol-chloroform afforded **5.2.2** as a clear oil (662 mg, 28%).

^{1}H NMR (300 MHz, $CDCl_3$) δ 7.61 (s, 1H), 4.11–4.09 (m, 2H), 4.03 (s, 1H), 3.76–3.60 (m, 16H), 3.05 (s, 1H), 2.26–2.24 (t, *J* = 2.9 Hz, 1H); ^{13}C NMR (75.5 MHz, $CDCl_3$) δ170.0, 79.8, 72.5, 71.2, 71.1, 70.9, 70.5, 70.40, 70.38, 70.3, 70.2, 70.1, 61.4; HRMS $[M + H]^+$ calcd:290.16036, found: 290.16121.

(*S*)-3-(4-(16-Hydroxy-3-oxo-5,8-11,14-tetraoxa-2-azahexadecyl)-1*H*-1,2,3-triazol-1-yl)propane-1,2-diyl distearate (5.2.3). Alkyne-alcohol **5.2.2** (69 mg, 0.238 mmol) and (*S*)-3-azidopropane-1,2-diyl distearate **4.2.2** (155 mg, 0.238 mmol) were dissolved in THF (1.5 mL). Copper sulfate pentahydrate (173 mg, 3 mmol) and sodium ascorbate (275 mg, 6 mmol) were added, along with water (0.5 mL). The reaction was stirred at room temperature overnight and the solvent was then removed under reduced pressure. Column chromatography with silica gel and a solvent system of 10% methanol-chloroform afforded **5.2.3** as a white solid (131 mg, 59%).

$[\alpha]_D^{296K}$ + 1.22 (C = 5.25, $CHCl_3$); ^{1}H NMR (300 MHz, $CDCl_3$) δ 7.97 (t, *J* = 5.6 Hz, 1H), 7.65 (s, 1H), 5.39–5.36 (m, 1H), 4.64–4.54 (m, 4H), 4.32 (dd, *J* = 4.1, 12 Hz, 1H), 4.08–4.01 (m, 3H), 3.73–-3.43 (m, 17H), 2.36–2.27 (m, 4H), 1.62–1.57 (m, 4H), 1.26 (*b* s, 56H), 0.88 (t, *J* = 6.3 Hz, 6H); ^{13}C NMR (75.5 MHz, $CDCl_3$) δ 173.1, 172.6, 145.3, 123.6, 72.6, 70.9, 70.5, 70.4, 70.22, 70.18, 69.3, 62.0, 61.5, 50.0, 34.2, 34.0, 31.9, 29.72, 29.67, 29.5, 29.4, 29.3, 29.1, 29.0, 24.8, 24.7, 22.7, 14.1; MALDI–HRMS $[M + Na]^+$ calcd: 961.7175, found: 961.7190.

(*S*)-3-(4-(16-Azido-3-oxo-5,8-11,14-tetraoxa-2-azahexadecyl)-1*H*-1,2,3-triazol-1-yl)propane-1,2-diyl distearate (5.2.1a). Lipid alcohol **5.2.3** (129 mg, 0.137 mmol) was dissolved in THF (3 mL) and cooled to 0 ºC under nitrogen. With stirring triethylamine

(57 µL, 0.411 mmol) and methanesulfonyl chloride (10.8 µL, 0.138 mmol) were added. Stirring was continued at 0 ºC for 1 h. The solvent was removed under reduced pressure and the residue was dissolved in DMF. Sodium azide (17.8 mg, 0.274 mmol) was added and the reaction was heated at 85 ºC overnight. The solvent was removed under reduced pressure and column chromatography with silica gel and a solvent system of 5% methanol-chloroform afforded **5.2.1a** as a tan solid (103 mg, 78%). $[\alpha]_D^{296K}$ – 0.17 (C = 4.12, $CHCl_3$); ^{1}H NMR (300 MHz, $CDCl_3$) δ 7.72 (*b* s, 1H), 7.62 (s, 1H), 5.39–5.35 (m, 1H), 4.62–4.50 (m, 4H), 4.31 (dd, *J* = 4.2, 12 Hz, 1H), 4.08–4.00 (m, 3H), 3.77–3.61 (m, 14H), 3.39 (t, *J* = 4.8 Hz, 2H), 2.36–2.27 (m, 4H), 1.62–1.57 (m, 4H), 1.25 (*b* s, 56H), 0.88 (t, *J* = 6.3 Hz, 6H); ^{13}C NMR (75.5 MHz, $CDCl_3$) δ 173.1, 172.5, 145.2, 123.4, 71.3, 71.1, 70.7, 70.6, 70.4, 70.2, 70.0, 69.3, 62.0, 50.6, 50.0, 42.8, 34.2, 34.0, 31.9, 29.72, 29.68, 29.6, 29.5, 29.4, 29.3, 29.1, 29.0, 24.8, 24.7, 22.7, 14.1; MALDI–HRMS $[M + Na]^+$ calcd: 986.7240, found: 986.7200.

(*S*)-3-(4-(20,20-Dimethyl-3,18-dioxo-5,8,11,14,19-pentaoxa-2,17-diazahenicosyl)-1*H*-1,2,3-triazol-1-yl)propane-1,2-diyl distearate (5.3.4). Alkyne **4.3.8** (68 mg, 0.175 mmol) and (*S*)-3-azidopropane-1,2-diyl distearate **4.2.2** (155 mg, 0.238 mmol) were dissolved in THF (1.5 mL). Copper sulfate pentahydrate (131 mg, 0.525 mmol) and sodium ascorbate (208 mg, 1.05 mmol) were added along with water (0.5 mL). The reaction was stirred at room temperature overnight and the solvent was removed under reduced pressure. Column chromatography with silica gel and a solvent system of 50% acetone-chloroform afforded **5.3.4** as a white solid (107 mg, 59%).

$[\alpha]_D^{296K}$ + 0.21 (C = 4.24, $CHCl_3$); ^{1}H NMR (300 MHz, $CDCl_3$ + CD_3OD) δ 7.91 (*b* s, 1H), 7.70 (*b* s, 1H), 5.40–5.36 (m, 2H), 4.61–4.55 (m, 4H), 4.33 (dd, *J* = 4.1, 12.2 Hz, 1H), 4.09–4.01 (m, 3H), 3.66–3.52 (m, 14H), 3.31–3.29 (m, 2H), 2.37–2.28 (m, 4H), 1.64–1.55 (m, 4H), 1.44 (s, 9H), 1.26 (*b* s, 56H), 0.88 (t, *J* = 6.6 Hz, 6H); ^{13}C NMR (100.6 MHz, $CDCl_3$ + CD_3OD) δ 173.1, 172.5, 170.2, 156.0, 145.4, 123.6, 79.1, 71.1, 70.5, 70.3, 69.4, 69.3, 62.0, 50.1, 40.3, 34.0, 31.93, 31.88, 29.7, 28.4, 24.8, 22.7, 14.1; MALDI–HRMS $[M + Na]^+$ calcd: 1060.7859, found: 1060.7831.

4-Oxo-4-(prop-2-ynylamino)butanoic acid (5.3.5). Propargyl amine (200 µL, 2.92 mmol) was dissolved in acetonitrile/DMF (2/1, 20 mL) under nitrogen at 0 ºC. Succinic anhydride (292 mg, 2.92 mmol) was dissolved in acetonitrile/DMF (2/1, 10mL) and added to the stirring solution. The solution was allowed to gradually warm to room temperature and stirring was continued overnight. The solvent was removed under reduced pressure and the solid was washed with hexanes to afford **5.3.5** as a tan solid (447 mg, 99%).

^{1}H NMR (300 MHz, CD_3OD) δ 3.94 (s, 2H), 2.61–2.45 (m, 5H); ^{13}C NMR (75.5 MHz, CD_3OD) δ 176.2, 164.1, 80.6, 72.2, 31.2, 30.1, 29.5, ; HRMS $[M + H]^+$ calcd: 156.06607, found: 156.06495.

(*S*)-3-(4-(3,18,21-Trioxo-5,8,11,14-tetraoxa-2,17-22-triazapentacos-24-ynyl)-1*H*-1,2,3-triazol-1-yl)propane-1,2-diyl distearate (5.3.1b). Boc-TEG-Lipid **5.3.4** (106 mg, 0.102 mmol) was dissolved in dichloromethane (2 mL) and with stirring trifluoroacetic acid (2 mL) was added. The solution was stirred at room temperature 40 min and then

the solvent was removed under reduced pressure.

At this point, the residue was dissolved in DMF (1 mL). With stirring N-methylmorpholine (112 µL, 1.02 mmol) was added. 1-ethyl-(3-dimethylaminopropyl)carbodiimide hydrochloride (23 mg, 0.123 mmol), 4-dimethylaminopyridine (12.5 mg, 0.102 mmol), and succinic acid-alkyne **5.3.5** (19 mg, 0.123 mmol) were combined in DMF (2 mL). This solution was added with stirring to the solution prepared aboved. The combination of solutions was stirred at room temperature overnight. The solvent removed under reduced pressure. Column chromatography with silica gel and a solvent system of 10% methanol-chloroform afforded **5.3.1b** as a white solid (72 mg, 65%).

$[\alpha]_D^{296K}$ + 0.11 (C = 3.59, $CHCl_3$); ^{1}H NMR (300 MHz, $CDCl_3$) δ 7.88 (*b* s, 1H), 7.67 (*b* s, 1H), 7.06 (*b* s, 2H), 5.30–5.37 (m, 1H), 4.65–4.52 (m, 4H), 4.33 (dd, *J* = 4.2, 12 Hz), 4.09–4.00 (m, 5H), 3.66–4.43 (m, 16H), 2.55 (s, 4H), 2.36–2.27 (m, 4H), 2.23 (t, *J* = 2.4 Hz, 1H), 1.64–1.57 (m, 4H), 1.25 (*b* s, 56H), 0.88 (t, *J* = 6.6 Hz, 6H); ^{13}C NMR (75.5 MHz, $CDCl_3$) δ 173.2, 172.6, 172.1, 170.4, 169.4, 145.5, 123.7, 79.9, 71.2, 71.0, 70.54, 70.50, 70.4, 70.2, 69.8, 69.4, 62.0, 50.1, 39.3, 34.3, 34.0, 31.9, 31.6, 31.4, 29.71, 29.67, 29.5, 29.4, 29.3, 29.1, 29.0, 24.8, 24.7, 22.7, 14.1; MALDI–HRMS $[M + Na]^+$ calcd: 1097.7812, found: 1097.7857.

4-Nitro-7-*N*-(prop-2-ynyl)benzofurazan (5.4.7). 4-Chloro-7-nitrobenzofurazan **5.4.6** (100 mg, 0.501 mmol) was dissolved in THF. Diisopropylethylamine (248 µL, 1.50 mmol) and propargyl amine (41 µL, 0.601 mmol) were added and the solution was stirred at room temperature overnight. The solvent was removed under reduced pressure and column chromatography with silica gel and a gradient solvent system of

50-100% ethyl acetate-hexanes afforded **5.4.7** as an orange solid (92.4 mg, 85%).

^{1}H NMR (300 MHz, $CDCl_3$) δ 8.55 (d, *J* = 8.7 Hz, 1H), 6.41 (*b* s, 1H), 6.37 (d, *J* = 8.4 Hz, 1H), 4.34–4.31 (m, 2H), 2.45–2.43 (m, 1H); No ^{13}C NMR could be obtained; HRMS $[M + H]^+$ calcd: 219.05181, found: 219.05224.

NBD-lipid (5.4.8a). NBD-alkyne **5.4.7** (17.5 mg, 0.080 mmol) and (*S*)-3-azidopropane-1,2-diyl distearate **4.2.2** (57.4 mg, 0.088 mmol) were dissolved in THF (1.5 mL). Copper sulfate pentahydrate (60 mg, 0.240 mmol) and sodium ascorbate (95 mg, 0.480 mmol) were added along with water (0.5 mL). The reaction was stirred at room temperature overnight and the solvent was removed under reduced pressure. Column chromatography with silica gel and a gradient solvent system of 50-100% ethyl acetate-hexanes afforded **5.4.8a** as an orange solid (30.2 mg, 43%).

^{1}H NMR (300 MHz, CD_2Cl_2) δ 8.48 (d, *J* = 9 Hz, 1H), 7.72 (s, 1H), 7.26 (*b* s, 1H), 6.38 (d, *J* = 8.4 Hz, 1H), 5.40–5.37 (m, 1H), 4.81 (s, 2H), 4.62–4.61 (m, 2H), 4.28 (dd, *J* = 4.1, 12.2 Hz, 1H), 4.06 (dd, *J* = 5.4, 12 Hz, 1H), 2.33–2.21 (m, 4H), 1.60–1.47 (m, 4H), 1.25 (*b* s, 56H), 0.88 (t, *J* = 6.5 Hz, 6H); No ^{13}C NMR could be obtained; MALDI–HRMS $[M + Na]^+$ calcd: 890.6090, found: 890.6039.

Rhodamine Lipid (5.4.8b). Azido-lipid **4.2.2** (18.5 mg, 0.029 mmol) and rhodamine alkyne **3.7.19d** (17 mg, 0.029 mmol) were dissolved in THF (0.5 mL). Copper sulfate pentahydrate (21 mg, 0.086 mmol) and sodium ascorbate (34 mg, 0.171 mmol) were added along with water (0.5 mL). The reaction was stirred at room temperature

overnight and the solvent was removed under reduced pressure. Column chromatography with silica gel and a gradient solvent system of 2-5% methanol-DCM afforded **5.4.8b** as a purple solid (27.5 mg, 77%).

^{1}H NMR (300 MHz, $CDCl_3$+ CD_3OD) δ 8.36 (*b* s, 1H), 8.01 (d, *J* = 8.1 Hz, 1H), 7.83 (s, 1H), 7.23–7.13 (m, 3H), 6.96–6.88 (m, 2H), 6.75–6.74 (m, 2H), 5.41 (*b* s, 1H), 4.73–4.55 (m, 2H), 4.42 (s, 2H), 4.34 (dd, *J* = 3.9, 12 Hz, 1H), 4.00 (dd, *J* = 6.6, 12 Hz, 11.7 Hz, 1H), 3.70–3.61 (m, 8H), 2.33–2.23 (m, 4H), 1.56 (*b* s, 4H), 1.26 (*b* s, 56H), 0.88 (t, *J* = 6.3 Hz, 6H); ^{13}C NMR (100.6 MHz, $CDCl_3$ + CD_3OD) δ 173.5, 172.9, 158.04, 157.99, 142.6, 133.5, 133.4, 133.3, 130.1, 127.8, 126.9, 124.6, 114.3, 113.8, 113.7, 95.8, 69.4, 62.3, 45.9, 38.5, 34.1, 34.0, 32.0, 29.8, 29.6, 29.44, 29.38, 29.2, 29.1, 24.9, 24.8, 22.8, 14.1, 12.6; MALDI–HRMS $[M + Na]^+$ calcd: 1267.7461, found: 1267.7517.

Details for Experiments Involving Liposomes

General procedure for liposomes preparation. Solid lipids were dissolved in chloroform to a particular concentration and a specific amount of each lipid in solution was added to a small glass container. The chloroform was removed under a constant stream of nitrogen and the resulting lipid film was dried under vacuum. The appropriate volume of buffer was added to the dried lipids in order to produce a specific concentration of liposomes after hydration and size reduction. The suspension of lipid and buffer was agitated at 40 °C for 40 min and then subjected to 10 freeze-thaw cycles. Vesicles were prepared by extrusion (19 times) through a 200 nm polycarbonate

membrane to control liposome size.

General procedure for surface modification via "click' chemistry. Liposomes consisting of 10% TEG-azido lipid **5.2.1a**, 1% NBD-lipid **5.4.8a**, and 89% PC were prepared in buffer consisting of 10 mM HEPES, 145 mM NaCl, pH 6.5. Rhodamine alkyne **3.7.19d** was added to the reaction vessel in a chloroform solution to that would provide a final concentration of 200 μM (2 eq of azide concentration). Following evaporation of the chloroform and drying of the residue, liposomes (1 mM final concentration) and CuBr (2.2 mM final concentration) were added to the alkyne and diluted to a final volume of 1 mL with buffer. Fluorescence measurements (100 μL volumes) were measured at various time intervals during the 20 h reaction time.

General procedure for monitoring vesicle size with DLS. Liposomes consisting of 10% of TEG-azido lipid **5.2.1a** or 10% of TEG-alkyne lipid **5.3.1b** and 90% PC were prepared in buffer consisting of 10 mM HEPES, 145 mM NaCl, pH 6.5. Samples were prepared to provide a total liposome concentration of 1 mM. For the click reaction samples were prepared consisting of 500 μM of liposomes with **5.2.1a**, 500 μM of liposomes with **5.3.1b**, and 2.2 mM CuBr in a final volume of 1 mL. Control samples were prepared at the same concentration of liposomes with the exclusion of the CuBr. For experiments using only azide or alkyne doped liposomes, the solutions were prepared in 1 mL buffer with 1 mM appropriate liposome solution and 2.2 mM CuBr. In each case the prepared solution was filtered through a 0.45 micron Teflon filter prior to

size measurements. The change in size of the vesicles was measured over an established time scale.

Proton NMR

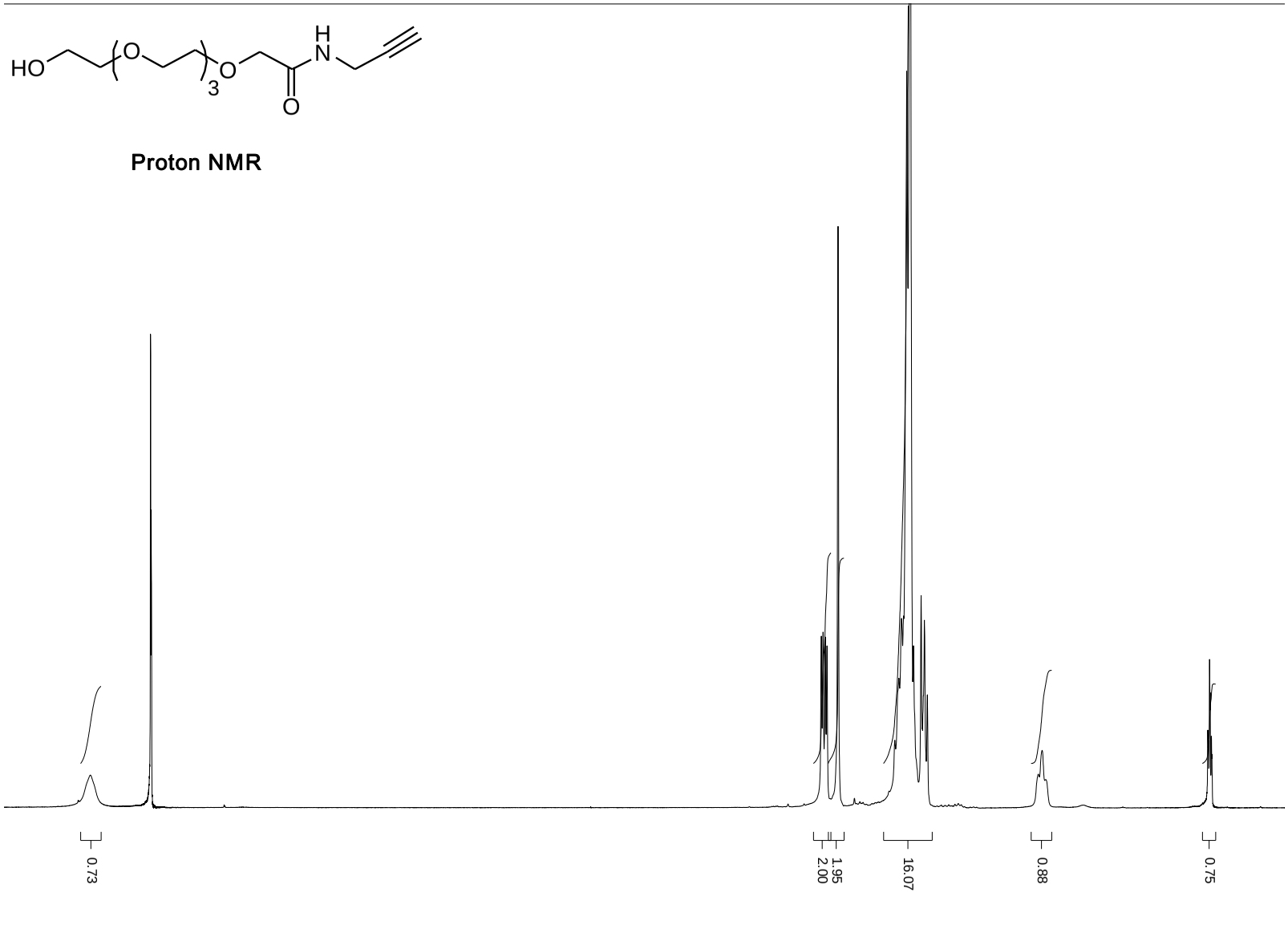

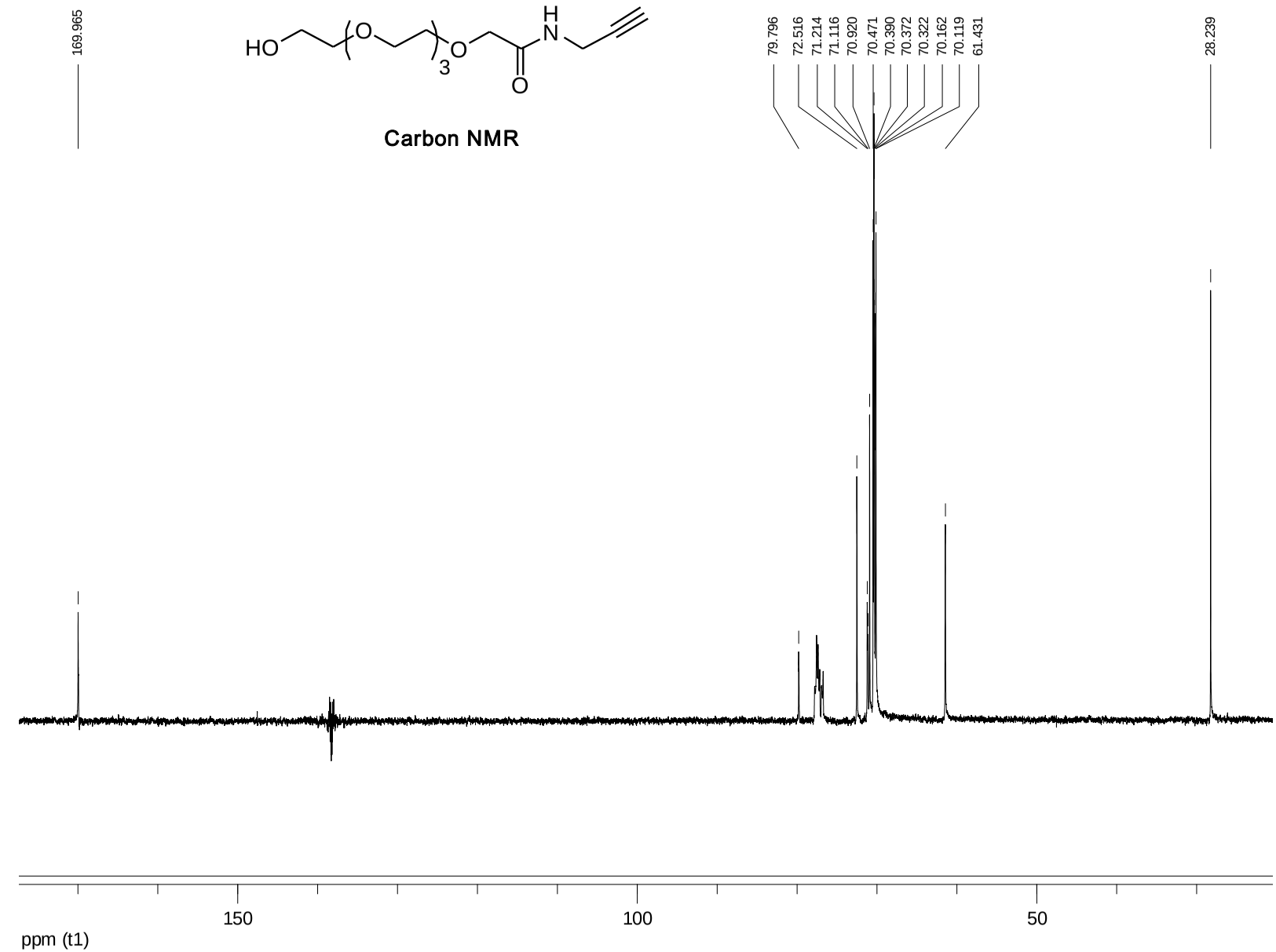
169.965
HO
O
3
O
H
N
O
Carbon NMR
79.796
72.516
71.214
71.116
70.920
70.471
70.390
70.372
70.322
70.162
70.119
61.431
28.239
150
100
50
ppm (t1)

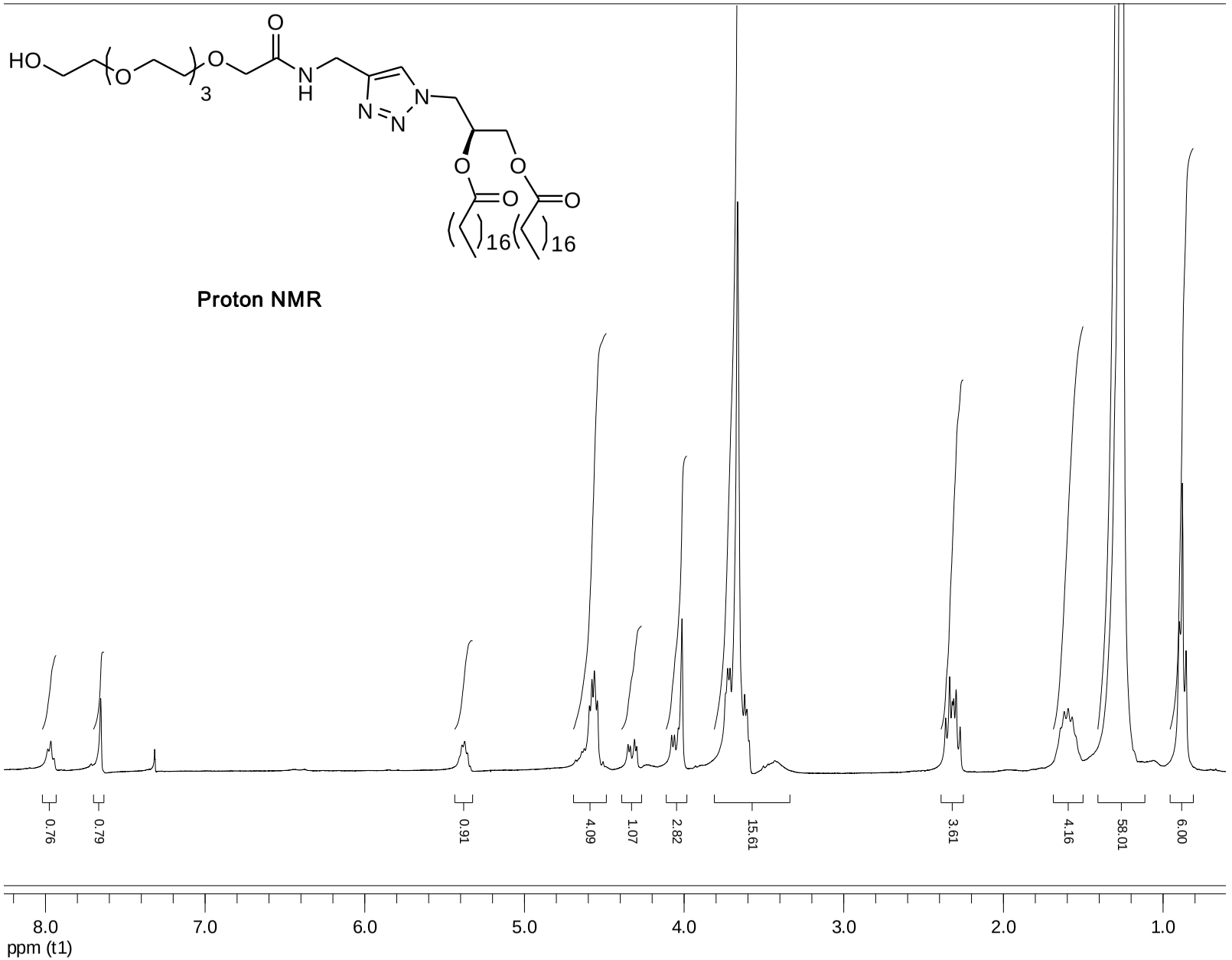
HO
O
3
O
N
H
O
N
N
N
O
O
O
O
O
16
16
Proton NMR
0.76
0.79
0.91
4.09
1.07
2.82
15.61
3.61
4.16
58.01
6.00
8.0
7.0
6.0
5.0
4.0
3.0
2.0
1.0
ppm (t1)

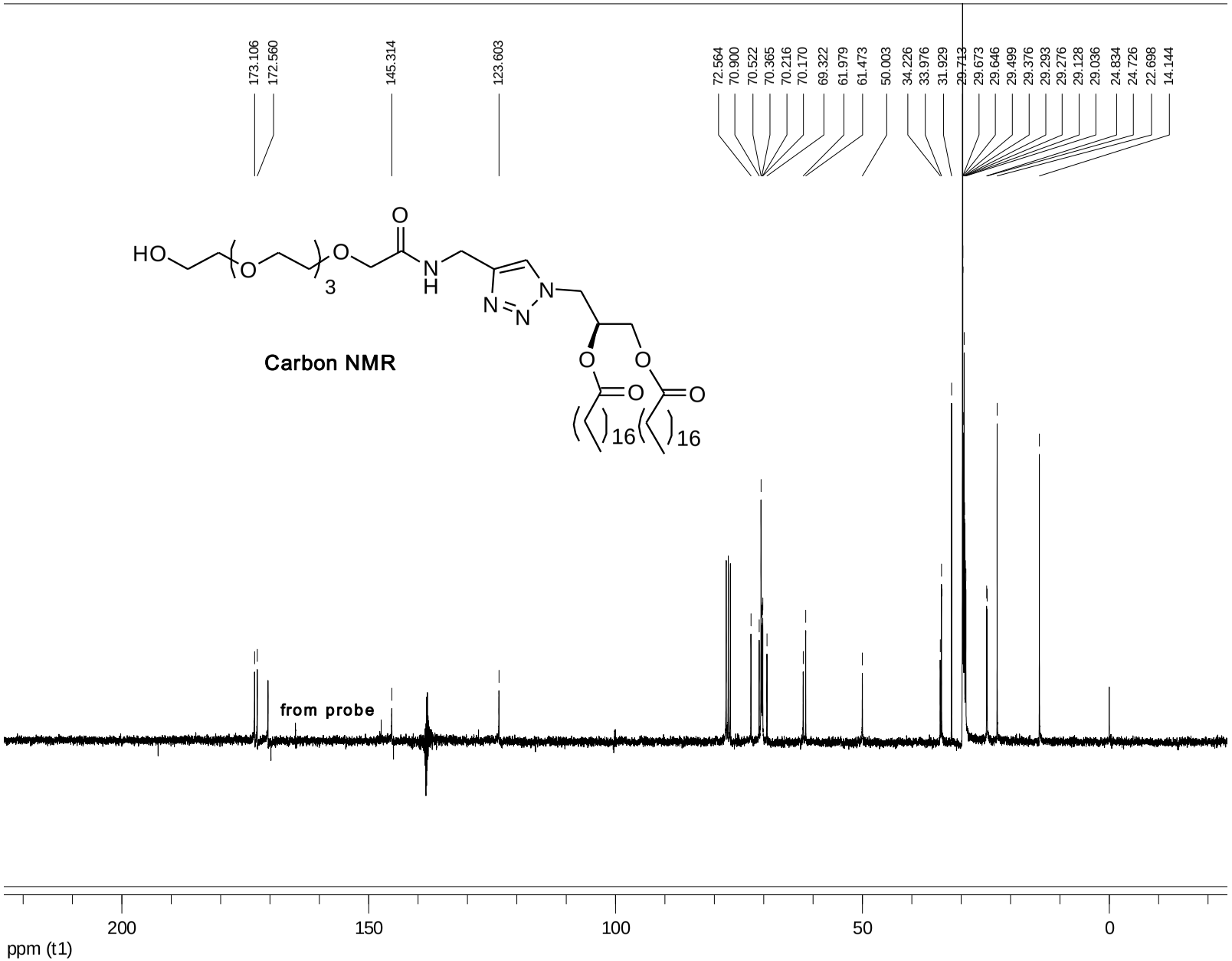
173.106
172.560
145.314
123.603
72.564
70.900
70.522
70.365
70.216
70.170
69.322
61.979
61.473
50.003
34.226
33.976
31.929
29.713
29.673
29.646
29.499
29.376
29.293
29.276
29.128
29.036
24.834
24.726
22.698
14.144
HO
O
3
N
H
N
N
N
O
O
O
O
16
16
Carbon NMR
from probe
200
150
100
50
0
ppm (t1)

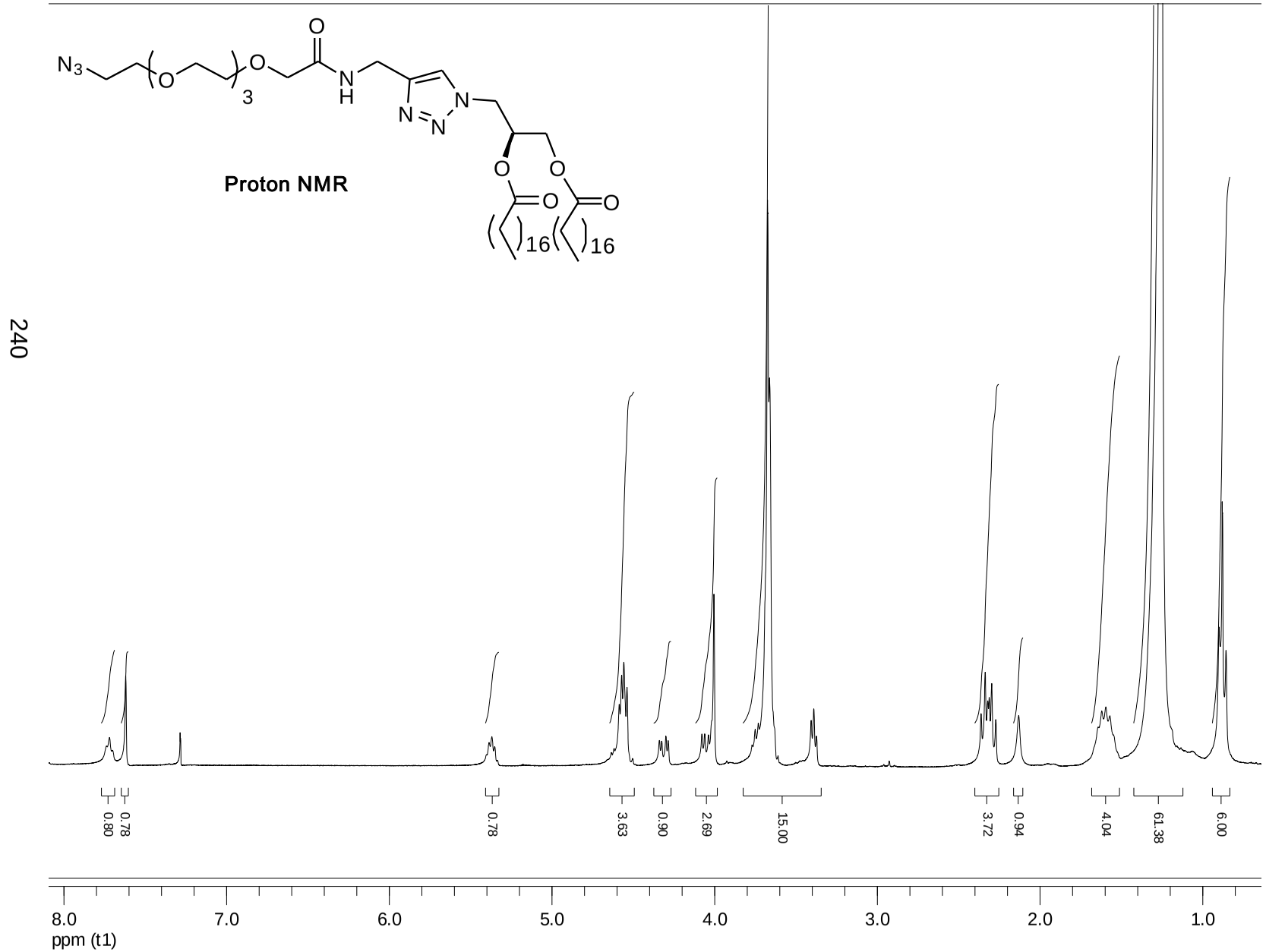
Proton NMR
240
0.80
0.78
0.78
3.63
0.90
2.69
15.00
3.72
0.94
4.04
61.38
6.00
8.0
7.0
6.0
5.0
4.0
3.0
2.0
1.0
ppm (t1)

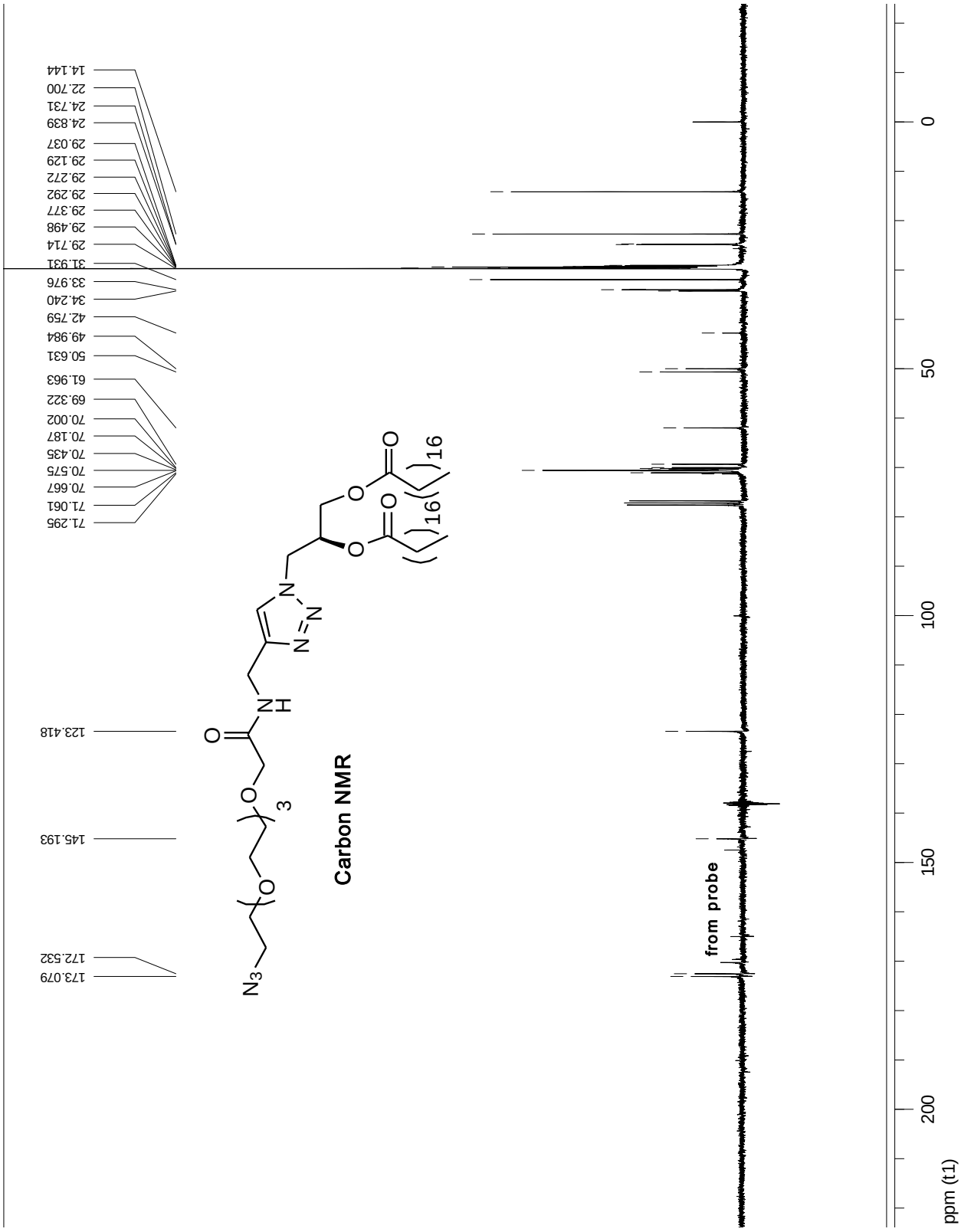
14.144
22.700
24.731
24.839
29.037
29.129
29.272
29.292
29.377
29.498
29.714
31.931
33.976
34.240
42.759
49.984
50.631
61.963
69.322
70.002
70.187
70.435
70.575
70.667
71.061
71.295
123.418
145.193
172.532
173.079
Carbon NMR
from probe
ppm (t1)
0
50
100
150
200

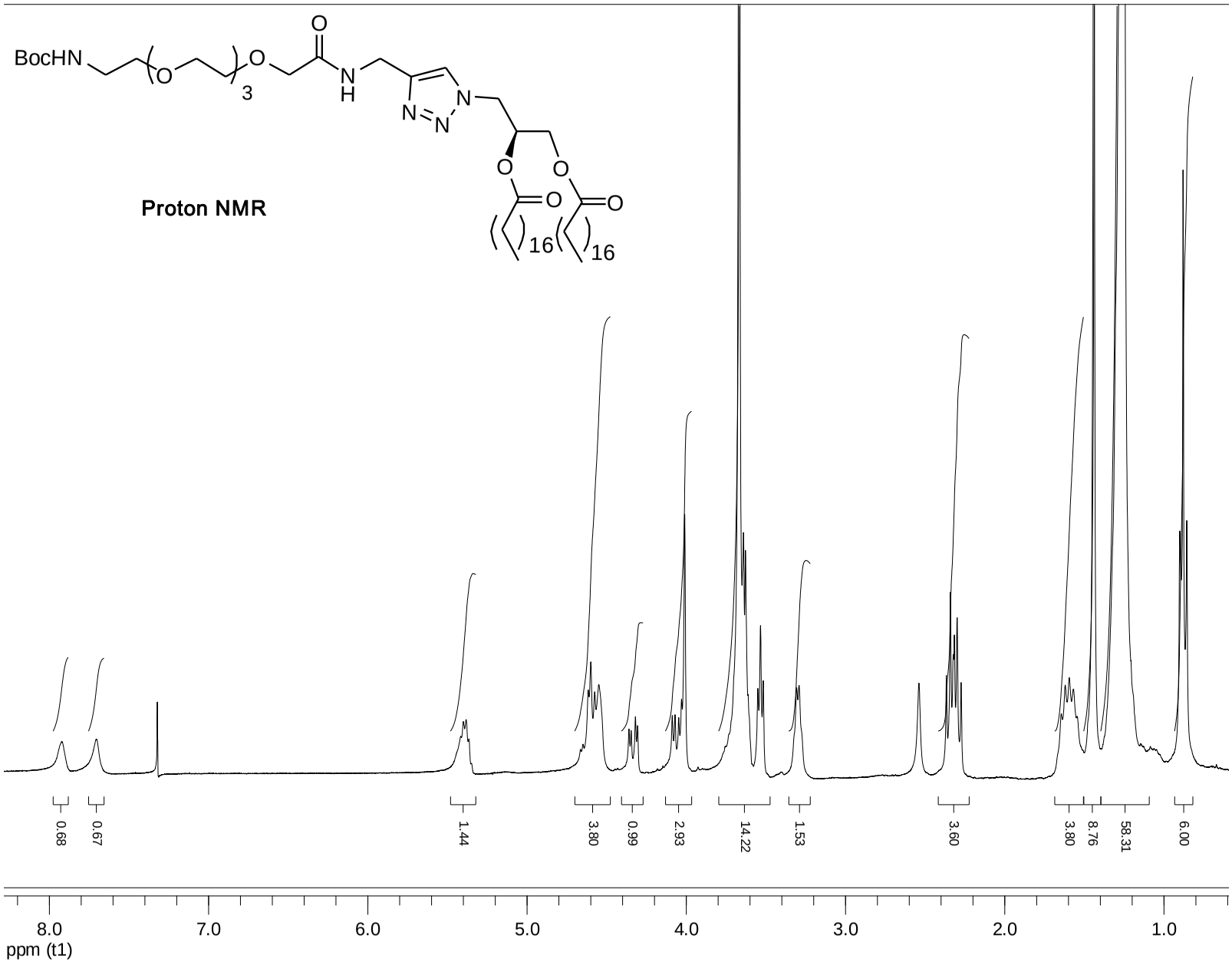
BocHN
O
3
N
H
N
N
N
O
O
O
O
16
16
Proton NMR
0.68
0.67
1.44
3.80
0.99
2.93
14.22
1.53
3.60
3.80
8.76
58.31
6.00
8.0
7.0
6.0
5.0
4.0
3.0
2.0
1.0
ppm (t1)

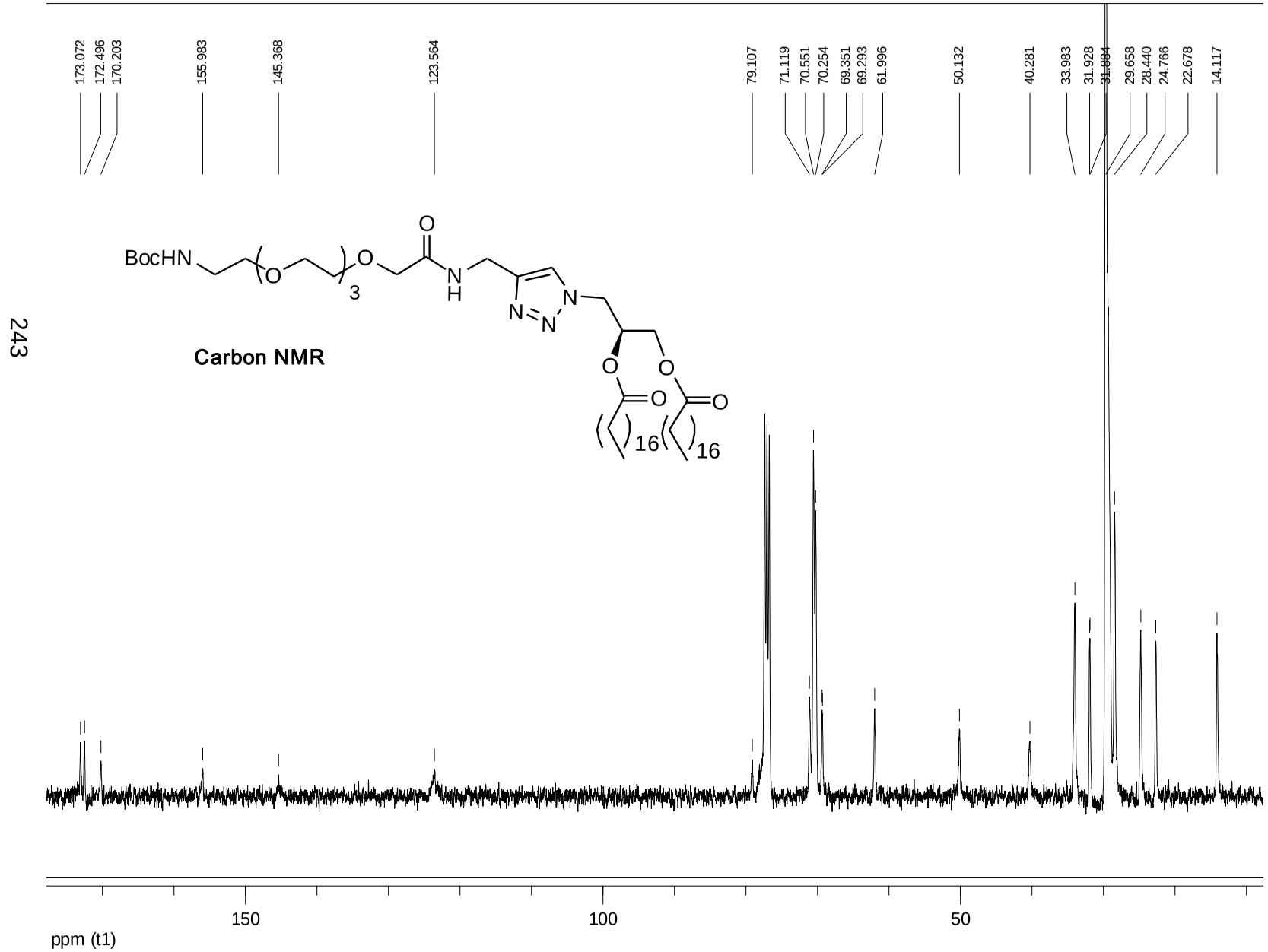
173.072
172.496
170.203
155.983
145.368
123.564
79.107
71.119
70.551
70.254
69.351
69.293
61.996
50.132
40.281
33.983
31.928
31.884
29.658
28.440
24.766
22.678
14.117
BocHN
O
O
3
O
N
H
N
N
N
O
O
O
O
16
16
Carbon NMR
150
100
50
ppm (t1)

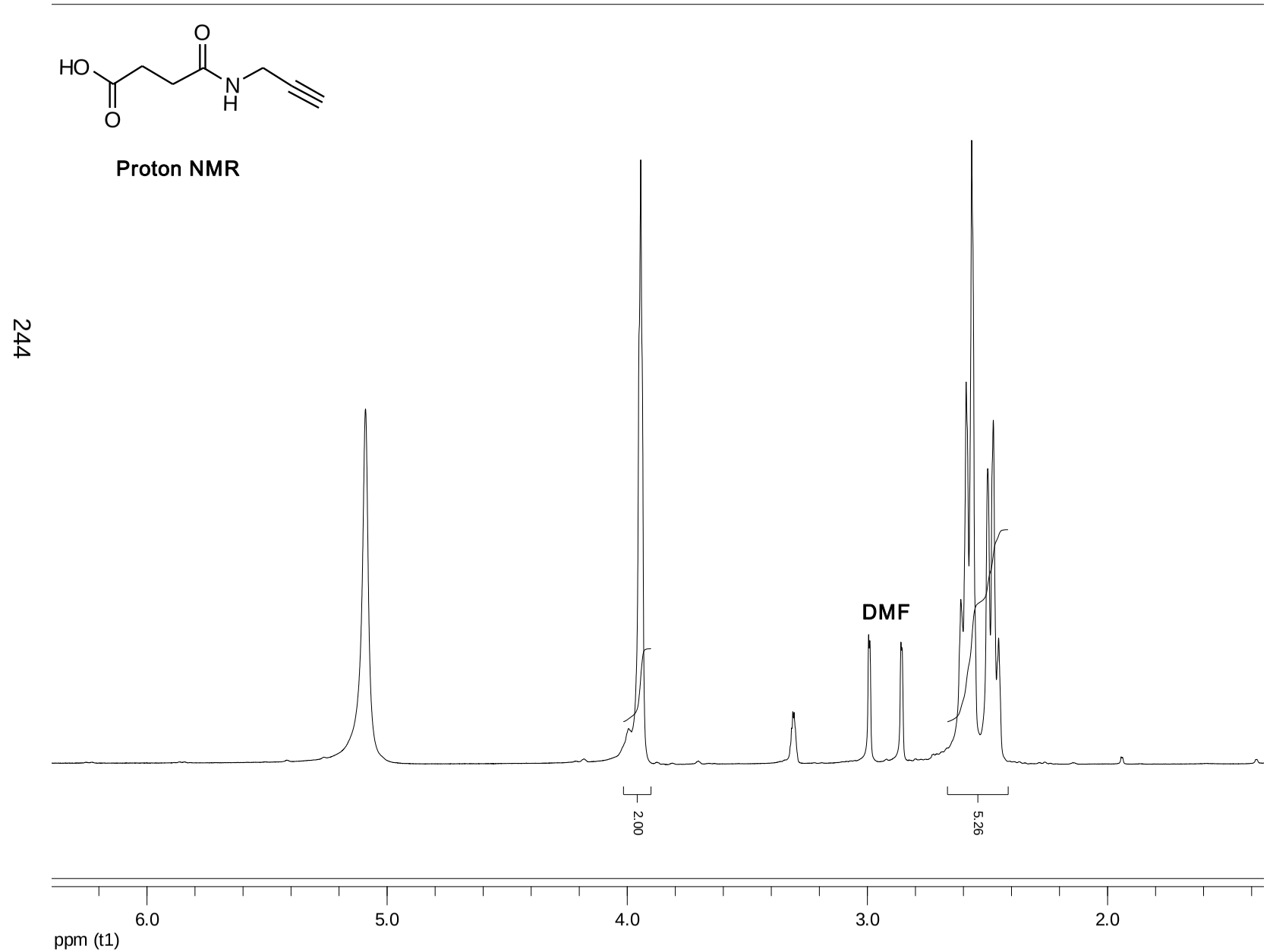
HO
O
O
N
H
Proton NMR
244
DMF
2.00
5.26
6.0
5.0
4.0
3.0
2.0
ppm (t1)

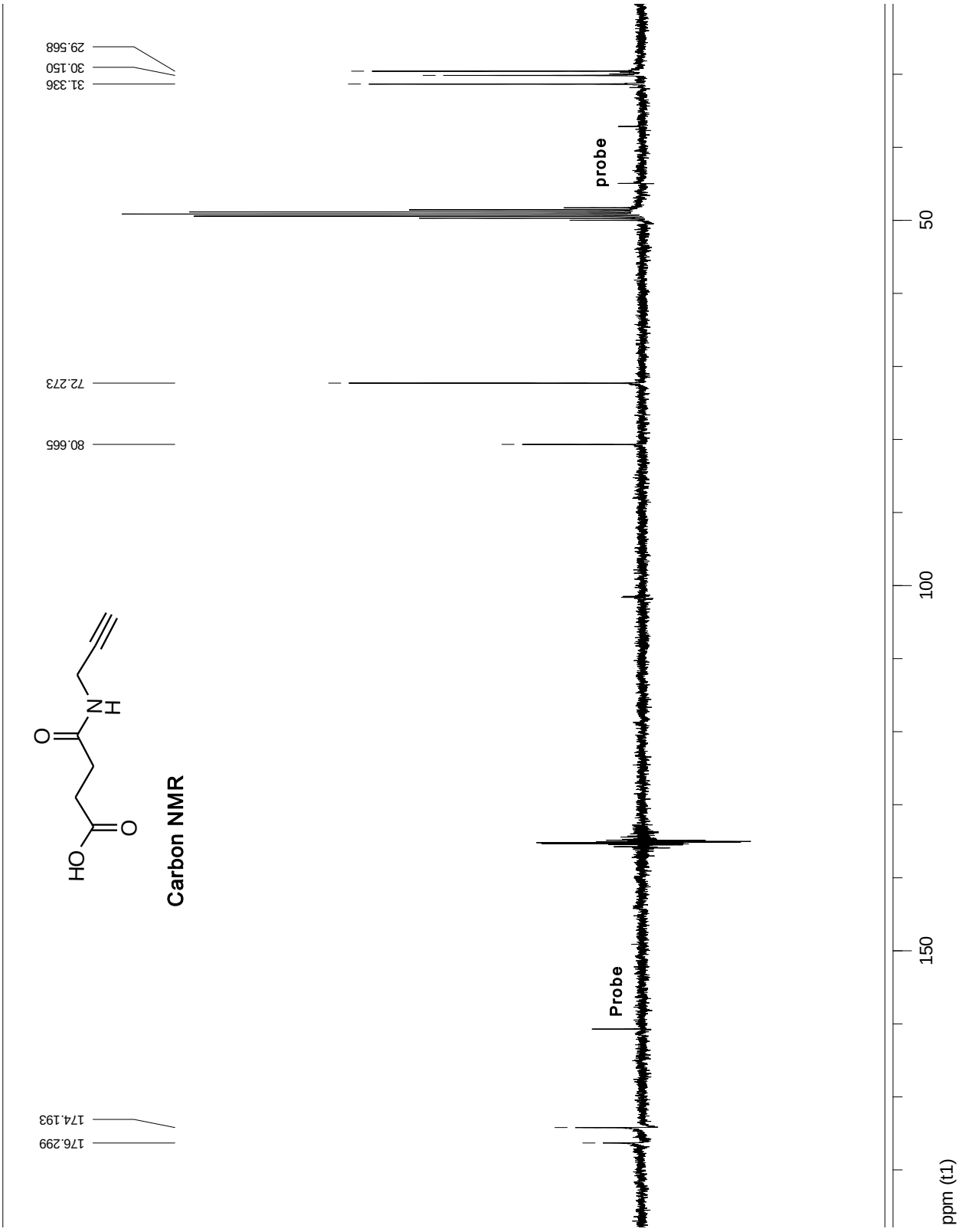
Carbon NMR
HO
O
O
H
N
O
176.299
174.193
Probe
80.665
72.273
probe
31.336
30.150
29.568
50
100
150
ppm (t1)

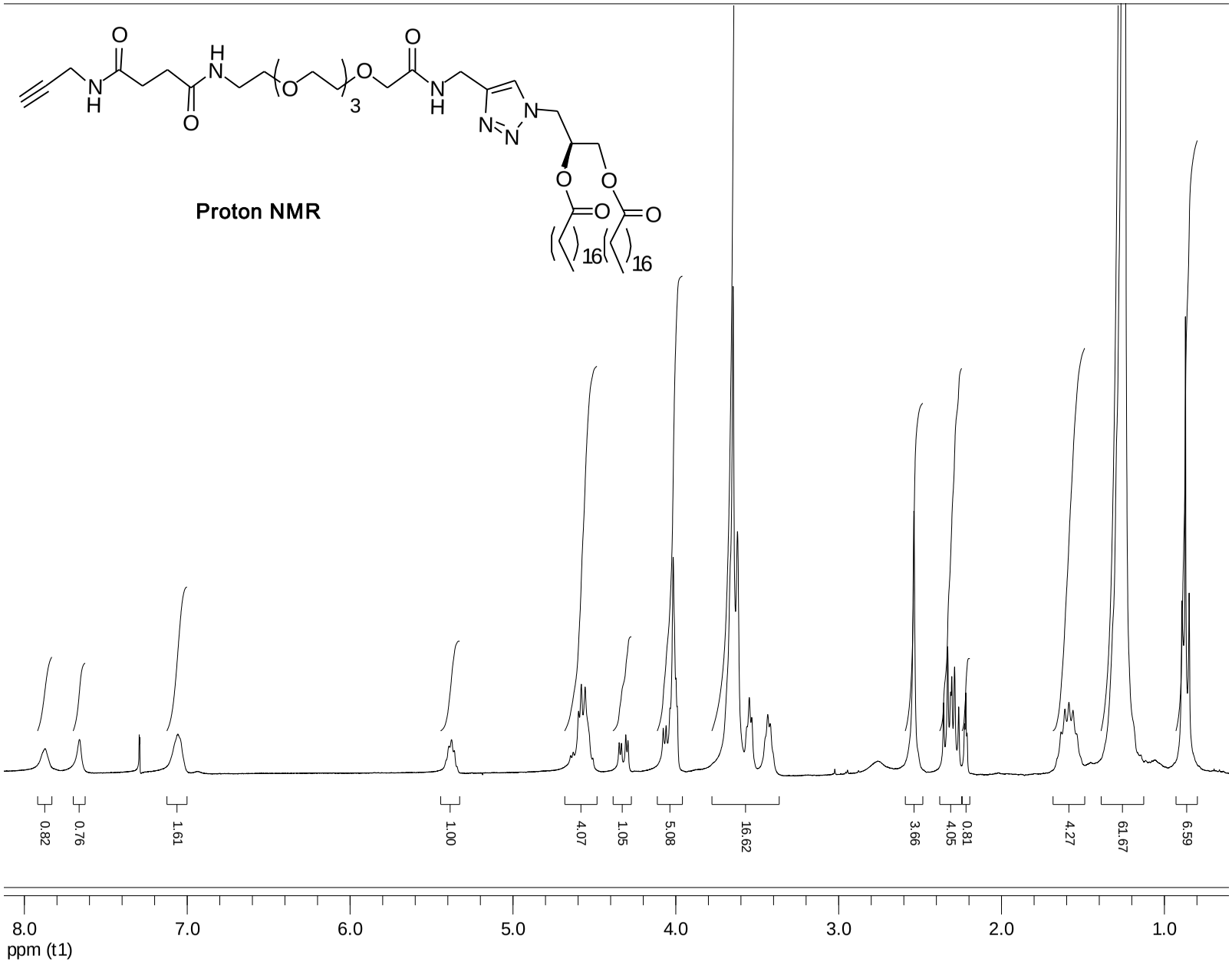
Proton NMR
0.82
0.76
1.61
1.00
4.07
1.05
5.08
16.62
3.66
4.05
0.81
4.27
61.67
6.59
8.0
7.0
6.0
5.0
4.0
3.0
2.0
1.0
ppm (t1)

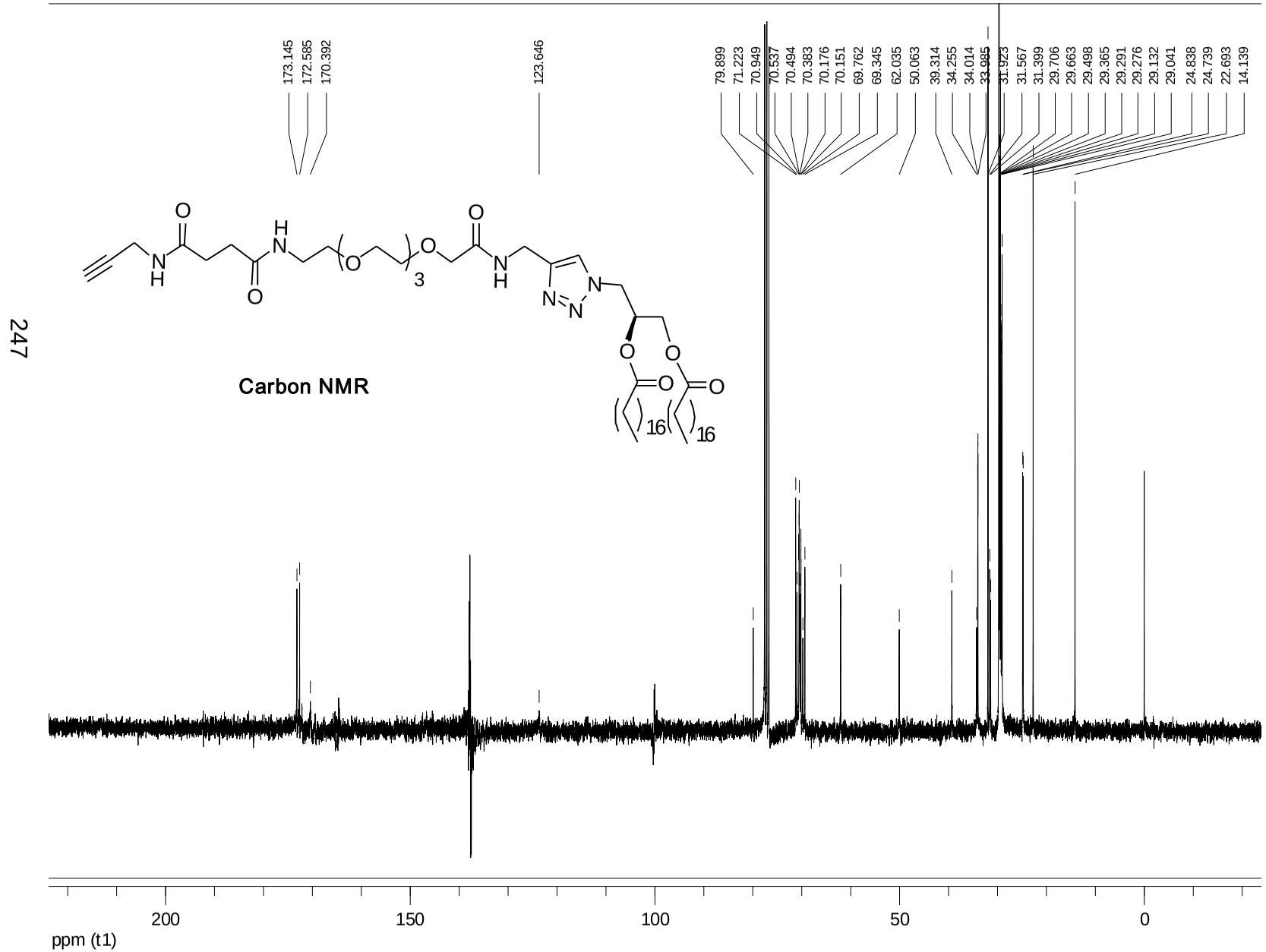
173.145
172.585
170.392
123.646
79.899
71.223
70.949
70.537
70.494
70.383
70.176
70.151
69.762
69.345
62.035
50.063
39.314
34.255
34.014
33.985
31.923
31.567
31.399
29.706
29.663
29.498
29.365
29.291
29.276
29.132
29.041
24.838
24.739
22.693
14.139
Carbon NMR
247
200
150
100
50
0
ppm (t1)

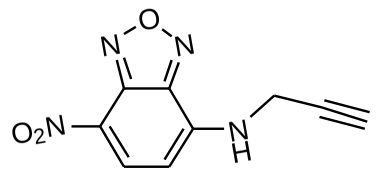

Proton NMR

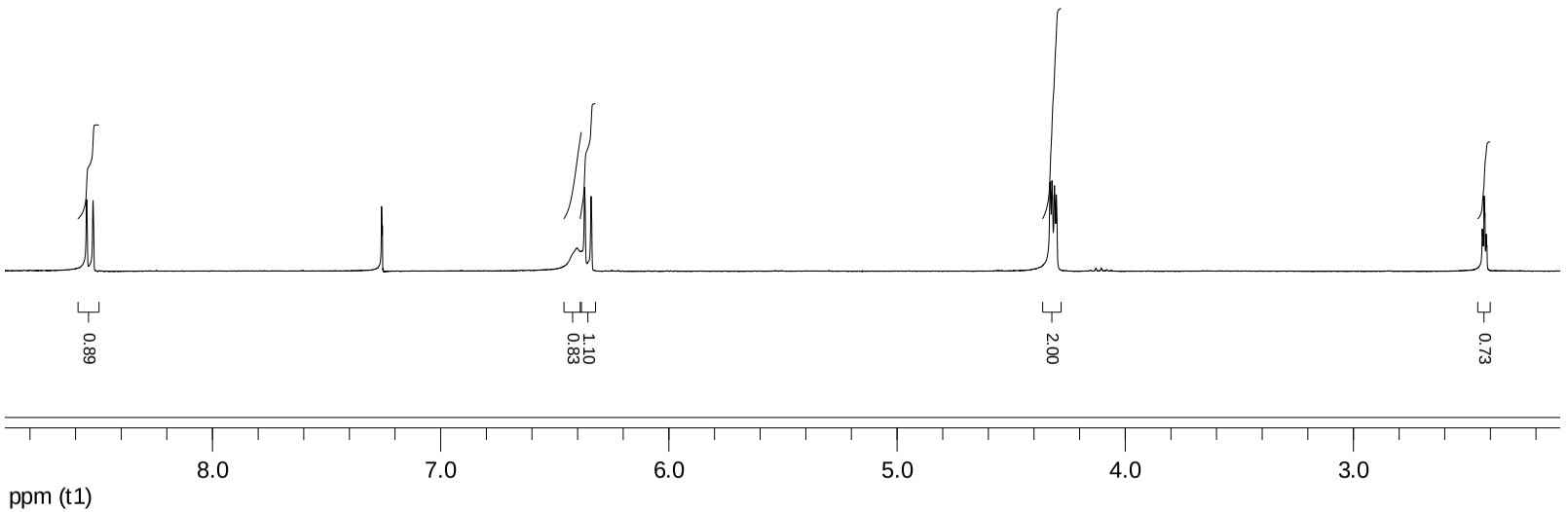

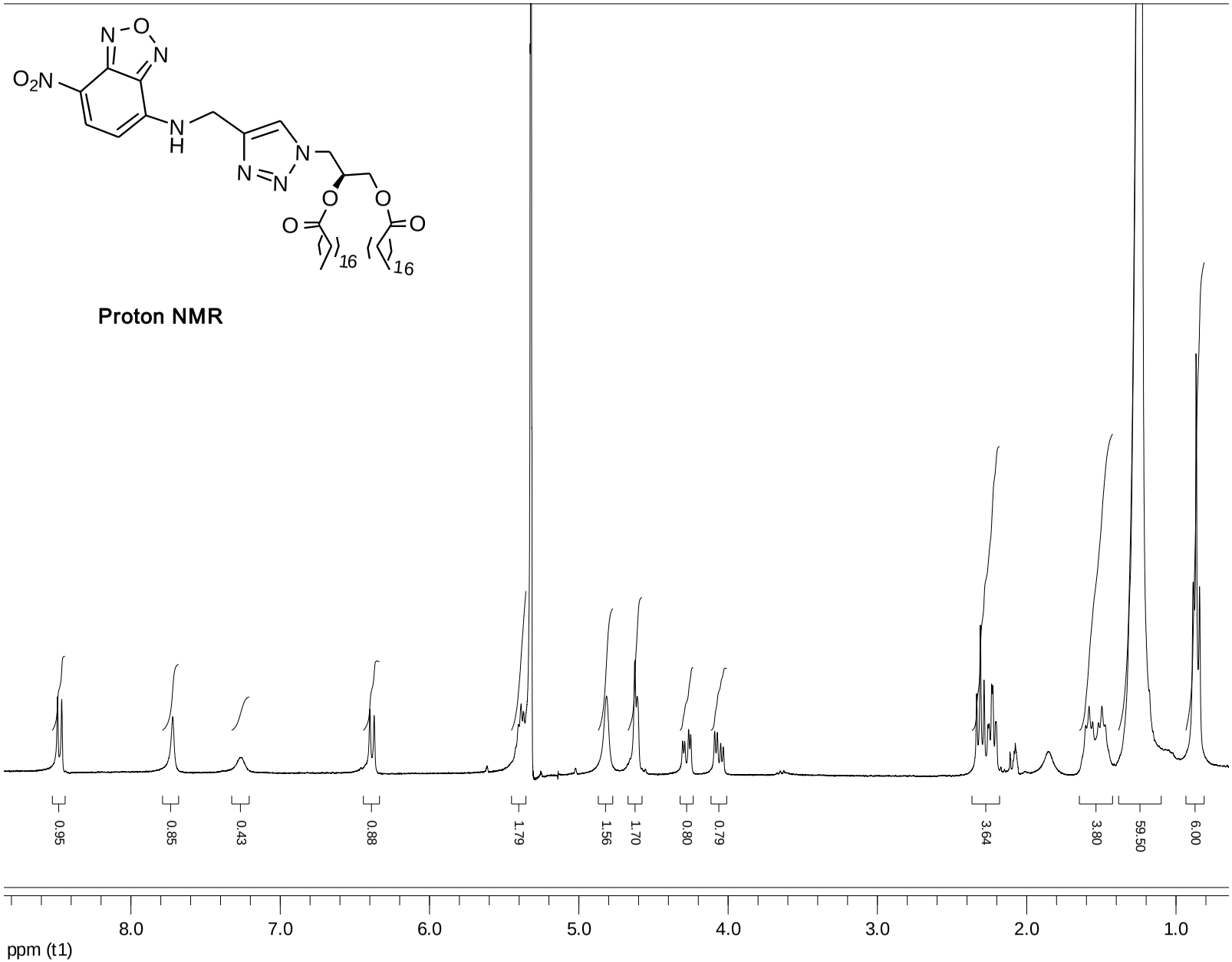
Proton NMR
0.95
0.85
0.43
0.88
1.79
1.56
1.70
0.80
0.79
3.64
3.80
59.50
6.00
8.0
7.0
6.0
5.0
4.0
3.0
2.0
1.0
ppm (t1)

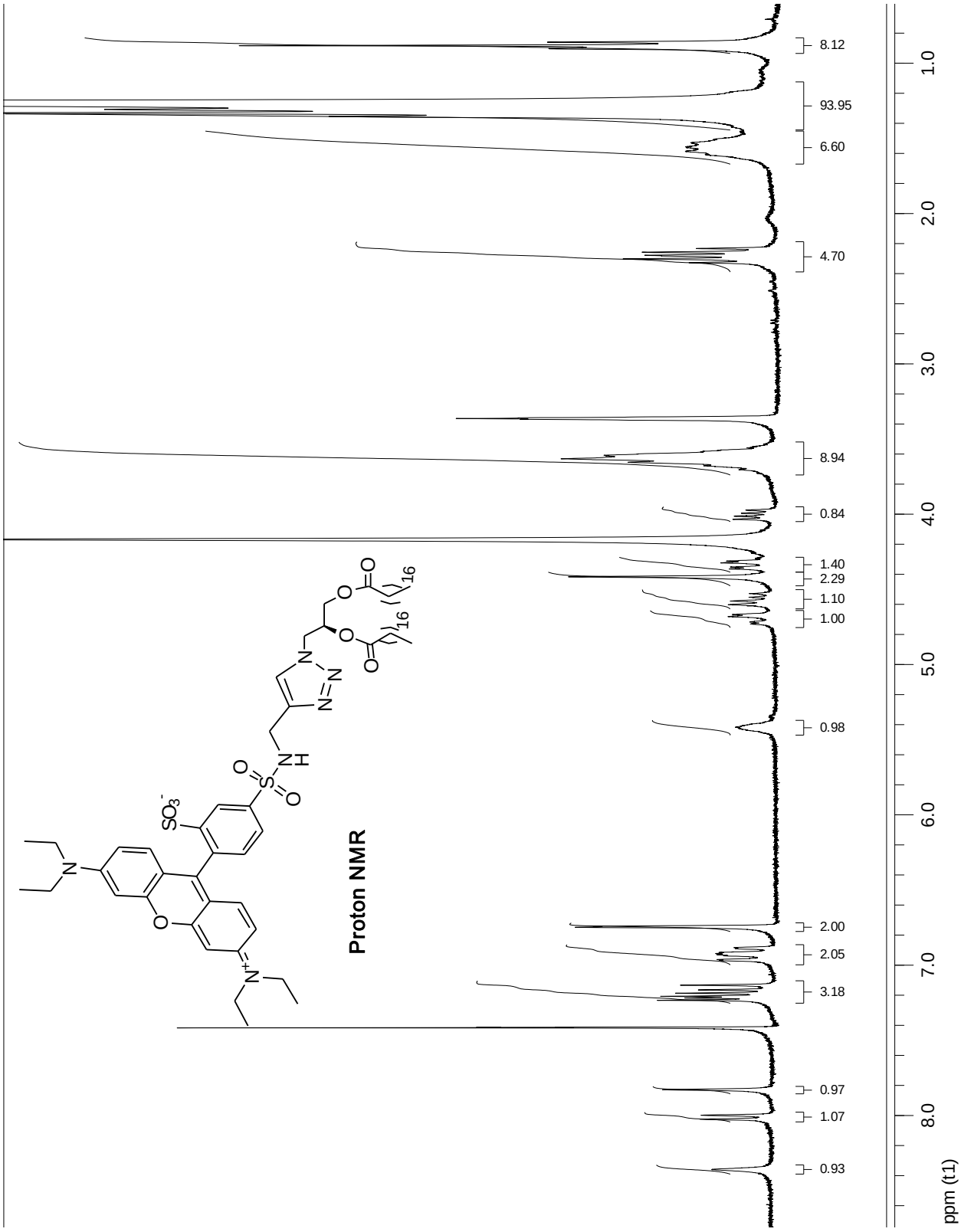
Proton NMR
8.12
93.95
6.60
4.70
8.94
0.84
1.40
2.29
1.10
1.00
0.98
2.00
2.05
3.18
0.97
1.07
0.93
1.0
2.0
3.0
4.0
5.0
6.0
7.0
8.0
ppm (t1)

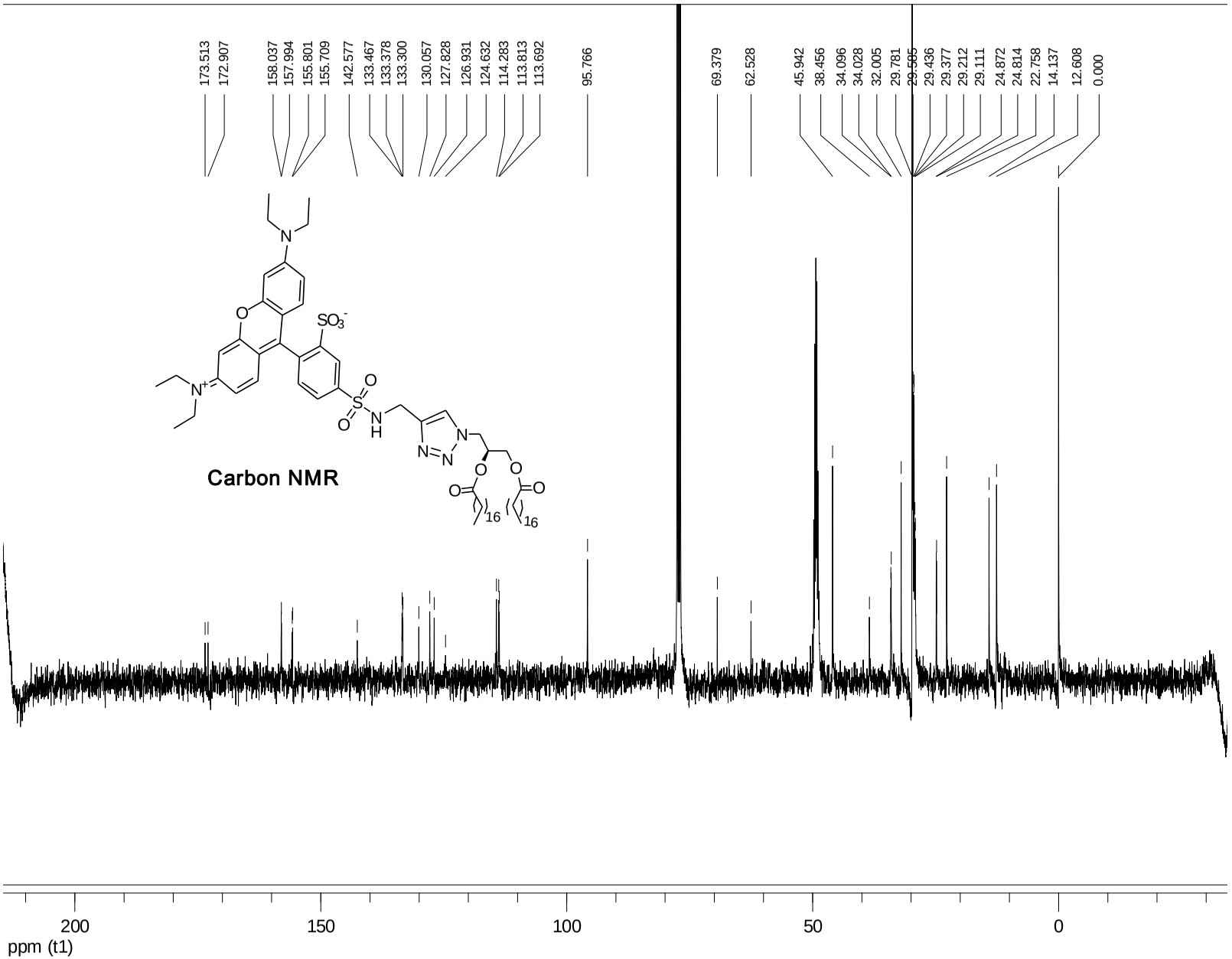
173.513
172.907
158.037
157.994
155.801
155.709
142.577
133.467
133.378
133.300
130.057
127.828
126.931
124.632
114.283
113.813
113.692
95.766
69.379
62.528
45.942
38.456
34.096
34.028
32.005
29.781
29.585
29.436
29.377
29.212
29.111
24.872
24.814
22.758
14.137
12.608
0.000
Carbon NMR
200
150
100
50
0
ppm (t1)

References

1. Carrasco, S. & Merida, I. Diacylglycerol, when simplicity becomes complex. *Trends Biochem. Sci.* **32**, 27-36 (2007).
2. Cho, W.H. & Stahelin, R.V. Membrane-protein interactions in cell signaling and membrane trafficking. *Ann. Rev. Biophys. Biomol. Struct.* **34**, 119-151 (2005).
3. Colon-Gonzalez, F. & Kazanietz, M.G. C1 domains exposed: From diacylglycerol binding to protein-protein interactions. *Biochim. Biophys. Acta* **1761**, 827-837 (2006).
4. Gomez-Fernandez, J.C. & Corbalan-Garcia, S. Diacylglycerols, multivalent membrane modulators. *Chem. Phys. Lipids* **148**, 1-25 (2007).
5. Sakane, F., Imai, S., Kai, M., Yasuda, S. & Kanoh, H. Diacylglycerol kinases: Why so many of them? *Biochim. Biophys. Acta* **1771**, 793-806 (2007).
6. Stace, C.L. & Ktistakis, N.T. Phosphatidic acid- and phosphatidylserine-binding proteins. *Biochim. Biophys. Acta* **1761**, 913-926 (2006).
7. Testerink, C. & Munnik, T. Phosphatidic acid: a multifunctional stress signaling lipid in plants. *Trends Plant Sci.* **10**, 368-375 (2005).
8. Di Paolo, G. & De Camilli, P. Phosphoinositides in cell regulation and membrane dynamics. *Nature* **443**, 651-657 (2006).
9. Lemmon, M.A. Phosphoinositide recognition domains. *Traffic* **4**, 201-213 (2003).
10. Lemmon, M.A. Membrane recognition by phospholipid-binding domains. *Nature Rev. Mol. Cell Biol.* **9**, 99-111 (2008).
11. McLaughlin, S., Wang, J.Y., Gambhir, A. & Murray, D. PIP2 and proteins: Interactions, organization, and information flow. *Annu. Rev. Biophys. Biomolec. Struct.* **31**, 151-175 (2002).
12. Misra, S., Miller, G.J. & Hurley, J.H. Recognizing phosphatidylinositol 3-phosphate. *Cell* **107**, 559-562 (2001).
13. Overduin, M. & Cheever, M.L. Signaling with phosphoinositides: better than binary. *Mol. Intervent.* **1**, 150-159 (2001).
14. Prestwich, G.D. Phosphoinositide signaling: From affinity probes to pharmaceutical targets. *Chem. Biol.* **11**, 619-637 (2004).
15. Hurley, J.H. Membrane binding domains. *Biochim. Biophys. Acta* **1761**, 805-811 (2006).
16. Schultz, A., Ling, M. & Larsson, C. Identification of an amino acid residue in the protein kinase CC1b domain crucial for its localization to the Golgi network. *J. Biol. Chem.* **279**, 31750-31760 (2004).
17. Hurley, J.H. & Misra, S. Signaling and subcellular targeting by membrane-binding domains. *Annu. Rev. Biophys. Biomolec. Struct.* **29**, 49-79 (2000).
18. Sprong, H., van der Sluijs, P. & van Meer, G. How proteins move lipids and lipids move proteins. *Nat. Rev. Mol. Cell Biol.* **2**, 504-513 (2001).
19. Griner, E.M. & Kazanietz, M.G. Protein kinase C and other diacylglycerol effectors in cancer. *Nat. Rev. Cancer* **7**, 281-294 (2007).
20. Kiessling, L.L., Gestwicki, J.E. & Strong, L.E. Synthetic multivalent ligands as probes of signal transduction. *Angew. Chem., Int. Ed.* **45**, 2348-2368 (2006).

21. Mammen, M., Choi, S.K. & Whitesides, G.M. Polyvalent interactions in biological systems: Implications for design and use of multivalent ligands and inhibitors. *Angew. Chem., Int. Ed.* **37**, 2755-2794 (1998).
22. Michell, R.H., Heath, V.L., Lemmon, M.A. & Dove, S.K. Phosphatidylinositol 3,5-bisphosphate: metabolism and cellular functions. *Trends Biochem. Sci.* **31**, 52-63 (2006).
23. Hanshaw, R.G., Stahelin, R.V. & Smith, B.D. Noncovalent keystone interactions controlling biomembrane structure. *Chem. Eur. J.* **14**, 1690-1697 (2008).
24. Murray, D., Arbuzova, A., Honig, B. & McLaughlin, S. in Peptide-Lipid Interactions 277-307 (2002).
25. Chaudhary, A. et al. Probing the phosphoinositide 4,5-bisphosphate binding site of human profilin I. *Chem. Biol.* **5**, 273-281 (1998).
26. Chen, J., Profit, A.A. & Prestwich, G.D. Synthesis of photoactivatable 1,2-*O*-diacyl-*sn*-glycerol derivatives of 1-L-phosphatidyl-D-myo-inositol 4,5-bisphosphate (PtdInsP(2)) and 3,4,5-trisphosphate (PtdInsP(3)). *J. Org. Chem.* **61**, 6305-6312 (1996).
27. Gubbens, J. et al. Photocrosslinking and Click Chemistry Enable the Specific Detection of Proteins Interacting with Phospholipids at the Membrane Interface. *Chem. Biol.* **16**, 3-14 (2009).
28. Lim, Z.Y., Thuring, J.W., Holmes, A.B., Manifava, M. & Ktistakis, N.T. Synthesis and biological evaluation of a PtdIns(4,5)P-2 and a phosphatidic acid affinity matrix. *J. Chem. Soc., Perkin Trans. 1*, 1067-1075 (2002).
29. Manifava, M. et al. Differential binding of traffic-related proteins to phosphatidic acid- or phosphatidylinositol (4,5)-bisphosphate-coupled affinity reagents. *J. Biol. Chem.* **276**, 8987-8994 (2001).
30. Picq, M., Huang, Y., Lagarde, M., Doutheau, A. & Nemoz, G. Synthesis of photoreactive phosphatidic acid analogues displaying activatory properties on cyclic AMP-phosphodiesterases. Photoaffinity labeling of an isoform of phosphodiesterase. *J. Med. Chem.* **45**, 1678-1685 (2002).
31. Prestwich, G.D. Touching all the bases: Synthesis of inositol polyphosphate and phosphoinositide affinity probes from glucose. *Acc. Chem. Res.* **29**, 503-513 (1996).
32. Rzepecki, P.W. & Prestwich, G.D. Synthesis of hybrid lipid probes: Derivatives of phosphatidylethanolamine-extended phosphatidylinositol 4,5-bisphosphate (Pea-PIP2). *J. Org. Chem.* **67**, 5454-5460 (2002).
33. Thum, O., Chen, J. & Prestwich, G.D. Synthesis of a photoaffinity analogue of phosphatidylinositol 3,4-bisphosphate, an effector in the phosphoinositide 3-kinase signaling pathway. *Tetrahedron Lett.* **37**, 9017-9020 (1996).
34. Maier, O., Oberle, V. & Hoekstra, D. Fluorescent lipid probes: some properties and applications (a review). *Chem. Phys. Lipids* **116**, 3-18 (2002).
35. Comfurius, P., Bevers, E.M. & Zwaal, R.F.A. Enzymatic-Synthesis of Phosphatidylserine on Small-Scale by Use of a One-Phase System. *J. Lipid Res.* **31**, 1719-1721 (1990).

36. Comfurius, P. & Zwaal, R.F.A. Enzymatic-Synthesis of Phosphatidylserine and Purification by Cm-Cellulose Column Chromatography. *Biochim. Biophys. Acta* **488**, 36-42 (1977).
37. Nachiappan, V. & Rajasekharan, R. Enzymatic-Synthesis of P-32 Acyl-Sn-Glycerol 3-Phosphate Using Diacylglycerol Kinase. *Anal. Biochem.* **222**, 283-285 (1994).
38. Kolb, H.C., Finn, M.G. & Sharpless, K.B. Click chemistry: Diverse chemical function from a few good reactions. *Angew. Chem., Int. Ed.* **40**, 2004-2021 (2001).
39. Lewis, W.G. et al. Click chemistry in situ: Acetylcholinesterase as a reaction vessel for the selective assembly of a femtomolar inhibitor from an array of building blocks. *Angew. Chem., Int. Ed.* **41**, 1053-1057 (2002).
40. Rostovtsev, V.V., Green, L.G., Fokin, V.V. & Sharpless, K.B. A stepwise Huisgen cycloaddition process: Copper(I)-catalyzed regioselective "ligation" of azides and terminal alkynes. *Angew. Chem., Int. Ed.* **41**, 2596-2599 (2002).
41. Kohn, M. & Breinbauer, R. The Staudinger ligation - A gift to chemical biology'. *Angew. Chem., Int. Ed.* **43**, 3106-3116 (2004).
42. Saxon, E., Armstrong, J.I. & Bertozzi, C.R. A "traceless" Staudinger ligation for the chemoselective synthesis of amide bonds. *Org. Lett.* **2**, 2141-2143 (2000).
43. Saxon, E. & Bertozzi, C.R. Cell surface engineering by a modified Staudinger reaction. *Science* **287**, 2007-2010 (2000).
44. Spencer, T.A. et al. Benzophenone-containing cholesterol surrogates: synthesis and biological evaluation. *J. Lipid Res.* **45**, 1510-1518 (2004).
45. Neef, A.B., Schultz, C. Selective Fluorescence Labeling of Lipids in Living Cells13. *Angew. Chem., Int. Ed.* **48**, 1498-1500 (2009).
46. Clegg, R.M. Fluorescence resonance energy transfer. *Curr. Opin. Biotechnol.* **6**, 103-110 (1995).
47. Sapsford, K.E., Berti, L. & Medintz, I.L. Materials for fluorescence resonance energy transfer analysis: Beyond traditional donor-acceptor combinations. *Angew. Chem., Int. Ed.* **45**, 4562-4588 (2006).
48. Wu, P.G. & Brand, L. Resonance energy-transfer: methods and applications. *Anal. Biochem.* **218**, 1-13 (1994).
49. Song, X.D., Nolan, J. & Swanson, B.I. Optical biosensor based on fluorescence resonance energy transfer: Ultrasensitive and specific detection of protein toxins. *J. Am. Chem. Soc.* **120**, 11514-11515 (1998).
50. Song, X.D., Shi, J., Nolan, J. & Swanson, B. Detection of multivalent interactions through two-tiered energy transfer. *Anal. Biochem.* **291**, 133-141 (2001).
51. Hatanaka, Y. & Sadakane, Y. Photoaffinity labeling in drug discovery and developments: Chemical gateway for entering proteomic frontier. *Curr. Top. Med. Chem.* **2**, 271-288 (2002).
52. Kalyankar, N.D. et al. Arraying of intact liposomes into chemically functionalized microwells. *Langmuir* **22**, 5403-5411 (2006).

53. Davidson, W.S. et al. The biotin-capture lipid affinity assay: a rapid method for determining binding parameters for apiloproteins. *J. Lipid Res.* **47**, 440-449 (2006).
54. Liu, X.Y., Yang, Q., Nakamura, C. & Miyake, J. Avidin-biotin-immobilized liposome column for chromatographic fluorescence on-line analysis of solute-membrane interactions. *J. Chromatogr., B* **750**, 51-60 (2001).
55. Vermette, P., Griesser, H.J., Kambouris, P. & Meagher, L. Characterization of surface-immobilized layers of intact liposomes. *Biomacromolecules* **5**, 1496-1502 (2004).
56. Vermette, P., Meagher, L., Gagnon, E., Griesser, H.J. & Doillon, C.J. Immobilized liposome layers for drug delivery applications: inhibition of angiogenesis. *J. Cont. Rel.* **80**, 179-195 (2002).
57. Sampson, S.R. & Cooper, D.R. Specific protein kinase C isoforms as transducers and modulators of insulin signaling. *Mol. Genet. Metab.* **89**, 32-47 (2006).
58. Mackay, H.J. & Twelves, C.J. Targeting the protein kinase C family: are we there yet? *Nat. Rev. Cancer* **7**, 554-562 (2007).
59. Spitaler, M. & Cantrell, D.A. Protein kinase C and beyond. *Nat. Immunol.* **5**, 785-790 (2004).
60. Gutcher, I., Webb, P.R. & Anderson, N.G. The isoform-specific regulation of apoptosis by protein kinase C. *Cell. Mol. Life Sci.* **60**, 1061-1070 (2003).
61. Stahelin, R.V. et al. Mechanism of diacylglycerol-induced membrane targeting and activation of protein kinase C delta. *J. Biol. Chem.* **279**, 29501-29512 (2004).
62. Cho, W. & Stahelin, R.V. Membrane binding and subcellular targeting of C2 domains. *Biochimica Et Biophysica Acta-Molecular and Cell Biology of Lipids* **1761**, 838-849 (2006).
63. Medkova, M. & Cho, W.H. Differential membrane-binding and activation mechanisms of protein kinase C-alpha and -epsilon. *Biochemistry* **37**, 4892-4900 (1998).
64. Kodali, D.R., Tercyak, A., Fahey, D.A. & Small, D.M. Acyl migration in 1,2-dipalmitoyl-*sn*-glycerol. *Chem. Phys. Lipids* **52**, 163-170 (1990).
65. Fernandes, R.A. An efficient synthesis of (-)-posticlure: The sex pheromone of Orgyia postica. *Eur. J. Org. Chem.*, 5064-5070 (2007).
66. Yadav, J.S., Deshpande, P.K. & Sharma, G.V.M. An Effective, Practical Method for the Synthesis of Chiral Propargyl Alcohols. *Tetrahedron* **46**, 7033-7046 (1990).
67. Jiang, G.W., Xu, Y. & Prestwich, G.D. Practical enantiospecific syntheses of lysobisphosphatidic acid and its analogues. *J. Org. Chem.* **71**, 934-939 (2006).
68. Gosse-Kobo, B., Mosset, P. & Gree, R. Total Synthesis of Unsaturated Trihydroxy C-18 Fatty-Acids. *Tetrahedron Lett.* **30**, 4235-4236 (1989).
69. Uchida, K., Kato, K. & Akita, H. A convenient synthesis of a *N*-protected L-carbamoylpolyoxamic acid derivative: Total synthesis of (+)-polyoxin J and (+)-polyoxin L. *Synthesis*, 1678-1686 (1999).

70. Baker, D.C., Haskell, T.H., Putt, S.R. & Sloan, B.J. Prodrugs of 9-(beta-D-arabinofuranosyl)adenine .2. Synthesis and evaluation of a number of 2',3'-di-*O*-acyl derivatives and 3',5'-di-*O*-acyl derivatives. *Journal of Medicinal Chemistry* **22**, 273-279 (1979).
71. Kubiak, R.J. & Bruzik, K.S. Comprehensive and uniform synthesis of all naturally occurring phosphorylated phosphatidylinositols. *J. Org. Chem.* **68**, 960-968 (2003).
72. Smith, M., Khorana, H.G., Rammler, D.H. & Goldberg, I.H. Studies on polynucleotides 14. Specific synthesis of C3'-C5' interrribonucleotide linkage - syntheses of uridylyl-(3'- 5')-uridine and uridylyl-(3'- 5')-adenosine. *J. Am. Chem. Soc.* **84**, 430-440 (1962).
73. Wroblewski, A.E. & Glowacka, I.E. Enantiomerically pure 4-amino-1,2,3-trihydroxybutylphosphonic acids. *Tetrahedron* **61**, 11930-11938 (2005).
74. Glacon, V., Benazza, M., El Anzi, A., Beaupere, D. & Demailly, G. Synthesis of alpha,omega-diazidoalditol derivatives via both bis- or tris-cyclic sulfites and peracetylated alpha,omega-dibromoalditols as bielectrophilic intermediates. *J. Carbohyd. Chem.* **23**, 95-110 (2004).
75. Reese, C.B. & Yan, H.B. Solution phase synthesis of ISIS 2922 (Vitravene) by the modified H-phosphonate approach. *J. Chem. Soc. Perkin Trans. 1*, 2619-2633 (2002).
76. Bolletta, F. et al. Synthesis and photophysical properties of fluorescent derivatives of methylmercury. *Organometallics* **15**, 2415-2417 (1996).
77. Stahelin, R.V. & Cho, W.H. Differential roles of ionic, aliphatic, and aromatic residues in membrane-protein interactions: A surface plasmon resonance study on phospholipases A(2). *Biochemistry* **40**, 4672-4678 (2001).
78. Stahelin, R.V. et al. Phosphatidylinositol 3-phosphate induces the membrane penetration of the FYVE domains of Vps27p and Hrs. *J. Biol. Chem.* **277**, 26379-26388 (2002).
79. Gupta, S. et al. Binding of Ras to phosphoinositide 3-kinase p110a Is required for Ras-driven tumorigenesis in mice. *Cell* **129**, 957-968 (2007).
80. Wittinghofer, A. & Waldmann, H. Ras - A molecular switch involved in tumor formation. *Angew. Chem., Int. Ed.* **39**, 4193-4214 (2000).
81. Fang, Y.M., Vilella-Bach, M., Bachmann, R., Flanigan, A. & Chen, J. Phosphatidic acid-mediated mitogenic activation of mTOR signaling. *Science* **294**, 1942-1945 (2001).
82. Jenkins, G.H., Fisette, P.L. & Anderson, R.A. Type-I Phosphatidylinositol 4-Phosphate 5-Kinase Isoforms are Specifically Stimulated by Phosphatidic Acid. *J. Biol. Chem.* **269**, 11547-11554 (1994).
83. Moritz, A., Degraan, P.N.E., Gispen, W.H. & Wirtz, K.W.A. Phosphatidic Acid is a Specific Activator of Phosphatidylinositol 4-Phosphate Kinase. *J. Biol. Chem.* **267**, 7207-7210 (1992).

84. Frank, C., Keilhack, H., Opitz, F., Zschornig, O. & Bohmer, F.D. Binding of phosphatidic acid to the protein-tyrosine phosphatase SHP-1 as a basis for activity modulation. *Biochemistry* **38**, 11993-12002 (1999).
85. Jones, J.A. & Hannun, Y.A. Tight binding inhibition of protein phosphatase-1 by phosphatidic acid - Specificity of inhibition by the phospholipid. *J. Biol. Chem.* **277**, 15530-15538 (2002).
86. Jones, J.A., Rawles, R. & Hannun, Y.A. Identification of a novel phosphatidic acid binding domain in protein phosphatase-1. *Biochemistry* **44**, 13235-13245 (2005).
87. Baillie, G.S. et al. TAPAS-1, a novel microdomaln within the unique N-terminal region of the PDE4A1 cAMP-specific phosphodiesterase that allows rapid, Ca2+-triggered membrane association with selectivity for interaction with phosphatidic acid. *J. Biol. Chem.* **277**, 28298-28309 (2002).
88. Grange, M. et al. The cAMP-specific phosphodiesterase PDE4D3 is regulated by phosphatidic acid binding - Consequences for cAMP signaling pathway and characterization of a phosphatidic acid binding site. *J. Biol. Chem.* **275**, 33379-33387 (2000).
89. Andresen, B.T., Rizzo, M.A., Shome, K. & Romero, G. The role of phosphatidic acid in the regulation of the Ras/MEK/Erk signaling cascade. *Febs Lett.* **531**, 65-68 (2002).
90. Ghosh, S., Moore, S., Bell, R.M. & Dush, M. Functional analysis of a phosphatidic acid binding domain in human raf-1 kinase. *J. Biol. Chem.* **278**, 45690-45696 (2003).
91. Ghosh, S., Strum, J.C., Sciorra, V.A., Daniel, L. & Bell, R.M. Raf-1 kinase possesses distinct binding domains for phosphatidylserine and phosphatidic acid - Phosphatidic acid regulates the translocation of Raf-1 in 12-*O*-tetradecanoylphorbol-13-acetate-stimulated Madin-Darby canine kidney cells. *J. Biol. Chem.* **271**, 8472-8480 (1996).
92. Hekman, M. et al. Associations of B- and C-raf with cholesterol, phosphatidylserine, and lipid second messengers - Preferential binding of Raf to artificial lipid rafts. *J. Biol. Chem.* **277**, 24090-24102 (2002).
93. Improta-Brears, T., Ghosh, S. & Bell, R.M. Mutational analysis of Raf-1 cysteine rich domain: Requirement for a cluster of basic aminoacids for interaction with phosphatidylserine. *Mol. Cell. Biochem.* **198**, 171-178 (1999).
94. Mott, H.R. et al. The solution structure of the Raf-1 cysteine-rich domain: A novel Ras and phospholipid binding site. *Proc. Natl. Acad. Sci. U.S.A.* **93**, 8312-8317 (1996).
95. Rizzo, M.A. et al. Phospholipase D and its product, phosphatidic acid, mediate agonist-dependent Raf-1 translocation to the plasma membrane and the activation of the mitogen-activated protein kinase pathway. *J. Biol. Chem.* **274**, 1131-1139 (1999).

96. Rizzo, M.A., Shome, K., Watkins, S.C. & Romero, G. The recruitment of Raf-1 to membranes is mediated by direct interaction with phosphatidic acid and is independent of association with Ras. *J. Biol. Chem.* **275**, 23911-23918 (2000).
97. Ochoa, W.F. et al. Additional binding sites for anionic phospholipids and calcium ions in the crystal structures of complexes of the C2 domain of protein kinase C alpha. *J. Mol. Biol.* **320**, 277-291 (2002).
98. Ochoa, W.F., Garcia-Garcia, J., Corbalan-Garcia, I.F.S., Verdaguer, N. & Gomez-Fernandez, J.C. Structure of the C2 domain from novel protein kinase C epsilon. A membrane binding model for Ca (2+)-independent C2 domains. *J. Mol. Biol.* **311**, 837-849 (2001).
99. Kooijman, E.E. et al. What makes the bioactive lipids phosphatidic acid and lysophosphatidic acid so special? *Biochemistry* **44**, 17007-17015 (2005).
100. Kooijman, E.E. et al. An electrostatic/hydrogen bond switch as the basis for the specific interaction of phosphatidic acid with proteins. *J. Biol. Chem.* **282**, 11356-11364 (2007).
101. Goedhart, J. & Gadella, T.W.J. Photolysis of caged phosphatidic acid induces flagellar excision in Chlamydomonas. *Biochemistry* **43**, 4263-4271 (2004).
102. Xu, Y., Fang, Y.M., Chen, J. & Prestwich, G.D. Activation of mTor signaling by novel fluoromethylene phosphonate analogs of phosphatidic acid. *Bioorg. Med. Chem. Lett.* **14**, 1461-1464 (2004).
103. Smith, M.D. et al. Synthesis and convenient functionalization of azide-labeled diacylglycerol analogues for modular access to biologically active lipid probes. *Bioconj. Chem.* **19**, 1855-1863 (2008).
104. Baldwin, J.E., Adlington, R.M., Russell, A.T. & Smith, M.L. Synthesis of a Biologically Active Analog of Antibiotic A-32390A. *J. Chem. Soc., Chem. Commun.*, 85-86 (1994).
105. Hiyama, T., Minami, T. & Takahashi, K. Synthesis of Artificial HMG-COA Reductase Inhibitors Based on the Olefination Strategy. *Bull. Chem. Soc. Jpn.* **68**, 364-372 (1995).
106. Tsuji, R., Arai, S. & Nishida, A. General method for the synthesis of chiral 2,3-bisarylmethoxy-1,4-butanediols from L-(+)-tartrate. *Synthesis*, 960-966 (2004).
107. Ahn, T., Oh, D.B., Kim, H. & Park, C. The phase property of membrane phospholipids is affected by the functionality of signal peptides from the Escherichia coli ribose-binding protein. *J. Biol. Chem.* **277**, 26157-26162 (2002).
108. Ahn, T., Oh, D.B., Lee, B.C. & Yun, C.H. Importance of phosphatidylethanolamine for the interaction of apocytochrome c with model membranes containing phosphatidylserine. *Biochemistry* **39**, 10147-10153 (2000).
109. Kim, K.H., Ahn, T. & Yun, C.H. Membrane properties induced by anionic phospholipids and phosphatidylethanolamine are critical for the membrane binding and catalytic activity of human cytochrome p450 3A4. *Biochemistry* **42**, 15377-15387 (2003).

110. Adam, G.C., Burbaum, J., Kozarich, J.W., Patricelli, M.P. & Cravatt, B.F. Mapping enzyme active sites in complex proteomes. *J. Am. Chem. Soc.* **126**, 1363-1368 (2004).
111. Ballell, L. et al. A new chemical probe for proteomics of carbohydrate-binding proteins. *ChemBioChem* **6**, 291-295 (2005).
112. Evans, M.J. & Cravatt, B.F. Mechanism-based profiling of enzyme families. *Chem. Rev.* **106**, 3279-3301 (2006).
113. Jessani, N. & Cravatt, B.F. The development and application of methods for activity-based protein profiling. *Curr. Opin. Chem. Biol.* **8**, 54-59 (2004).
114. Jessani, N. et al. Class assignment of sequence-unrelated members of enzyme superfamilies by activity-based protein profiling. *Angew. Chem., Int. Ed.* **44**, 2400-2403 (2005).
115. Kumar, S. et al. Activity-based probes for protein tyrosine phosphatases. *Proc. Natl. Acad. Sci. USA* **101**, 7943-7948 (2004).
116. Saghatelian, A., Jessani, N., Joseph, A., Humphrey, M. & Cravatt, B.F. Activity-based probes for the proteomic profiling of metalloproteases. *Proc. Natl. Acad. Sci. USA* **101**, 10000-10005 (2004).
117. Speers, A.E., Adam, G.C. & Cravatt, B.F. Activity-based protein profiling in vivo using a copper(I)-catalyzed azide-alkyne [3+2] cycloaddition. *J. Am. Chem. Soc.* **125**, 4686-4687 (2003).
118. Speers, A.E. & Cravatt, B.F. Profiling enzyme activities in vivo using click chemistry methods. *Chem. Biol.* **11**, 535-546 (2004).
119. Goddard-Borger, E.D. & Stick, R.V. An efficient, inexpensive, and shelf-stable diazotransfer reagent: Imidazole-1-sulfonyl azide hydrochloride. *Org. Lett.* **9**, 3797-3800 (2007).
120. Grandjean, C., Boutonnier, A., Guerreiro, C., Fournier, J.M. & Mulard, L.A. On the preparation of carbohydrate-protein conjugates using the traceless Staudinger ligation. *J. Org. Chem.* **70**, 7123-7132 (2005).
121. Garcia-Garcia, J., Corbalan-Garcia, S. & Gomez-Fernandez, J.C. Effect of calcium and phosphatidic acid binding on the C2 domain of PKC alpha as studied by Fourier transform infrared spectroscopy. *Biochemistry* **38**, 9667-9675 (1999).
122. Bittova, L., Stahelin, R.V. & Cho, W. Roles of ionic residues of the C1 domain in protein kinase C-alpha activation and the origin of phosphatidylserine specificity. *J. Biol. Chem.* **276**, 4218-4226 (2001).
123. Stahelin, R.V., Rafter, J.D., Das, S. & Cho, W. The molecular basis of differential subcellular localization of C2 domains of protein kinase C-alpha and group IVa cytosolic phospholipase A(2). *J. Biol. Chem.* **278**, 12452-12460 (2003).
124. Kitov, P.I. et al. Shiga-like toxins are neutralized by tailored multivalent carbohydrate ligands. *Nature* **403**, 669-672 (2000).
125. Silvius, J.R. Mechanisms of Ras protein targeting in mammalian cells. *J. Membr. Biol.* **190**, 83-92 (2002).

126. Volkert, M., Wagner, M., Peters, C. & Waldmann, H. The chemical biology of Ras lipidation. *Biol. Chem.* **382**, 1133-1145 (2001).
127. Tamm, L.K. Hypothesis: spring-loaded boomerang mechanism of influenza hemagglutinin-mediated membrane fusion. *Biochim. Biophys. Acta* **1614**, 14-23 (2008).
128. Tamm, L.K., Crane, J. & Kiessling, V. Membrane fusion: a structural perspective on the interplay of lipids and proteins. *Curr. Opin. Struct. Biol.* **13**, 453-466 (2003).
129. Brogden, K.A. Antimicrobial peptides: Pore formers or metabolic inhibitors in bacteria? *Nat. Rev. Microbiol.* **3**, 238-250 (2005).
130. Zasloff, M. Antimicrobial peptides of multicellular organisms. *Nature* **415**, 389-395 (2002).
131. Cho, W.W., Bittova, L. & Stahelin, R.V. Membrane binding assays for peripheral proteins. *Anal. Biochem.* **296**, 153-161 (2001).
132. Connell, E., Scott, P. & Davletov, B. Real-time assay for monitoring membrane association of lipid-binding domains. *Anal. Biochem.* **377**, 83-88 (2008).
133. Bulyk, M.L. DNA microarray technologies for measuring protein-DNA interactions. *Curr. Opin. Biotechnol.* **17**, 422-430 (2006).
134. Stoughton, R.B. Applications of DNA microarrays in biology. *Annu. Rev. Biochem* **74**, 53-82 (2005).
135. Bryan, M.C. et al. Covalent display of oligosaccharide arrays in microtiter plates. *J. Am. Chem. Soc.* **126**, 8640-8641 (2004).
136. Calarese, D.A. et al. Dissection of the carbohydrate specificity of the broadly neutralizing-anti-HIV-1 antibody 2G12. *Proc. Natl. Acad. Sci. USA* **102**, 13372-13377 (2005).
137. Feizi, T., Fazio, F., Chai, W.C. & Wong, C.H. Carbohydrate microarrays - a new set of technologies at the frontiers of glycomics. *Curr. Opin. Struct. Biol.* **13**, 637-645 (2003).
138. Huang, C.Y. et al. Carbohydrate microarray for profiling the antibodies interacting with Globo H tumor antigen. *Proc. Natl. Acad. Sci. USA* **103**, 15-20 (2006).
139. Liang, P.H., Wang, S.K. & Wong, C.H. Quantitative analysis of carbohydrate-protein interactions using glycan microarrays: Determination of surface and solution dissociation constants. *J. Am. Chem. Soc.* **129**, 11177-11184 (2007).
140. Pilobello, K.T. & Mahal, L.K. Deciphering the glycocode: the complexity and analytical challenge of glycomics. *Curr. Opin. Chem. Biol.* **11**, 300-305 (2007).
141. Pohl, N.L. Fluorous tags catching on microarrays. *Angew. Chem., Int. Ed.* **47**, 3868-3870 (2008).
142. Ratner, D.M., Adams, E.W., Disney, M.D. & Seeberger, P.H. Tools for glycomics: Mapping interactions of carbohydrates in biological systems. *ChemBioChem* **5**, 1375-1383 (2004).
143. Werz, D.B. & Seeberger, P.H. Carbohydrates as the next frontier in pharmaceutical research. *Chem. Eur. J.* **11**, 3194-3206 (2005).

144. Kung, L.A. & Snyder, M. Proteome chips for whole-organism assays. *Nat. Rev. Mol. Cell Biol.* **7**, 617-622 (2006).
145. Min, D.H. & Mrksich, M. Peptide arrays: towards routine implementation. *Curr. Opin. Chem. Biol.* **8**, 554-558 (2004).
146. Wilson, D.S. & Nock, S. Recent developments in protein microarray technology. *Angew. Chem., Int. Ed.* **42**, 494-500 (2003).
147. Kanter, J.L. et al. Lipid microarrays identify key mediators of autoimmune brain inflammation. *Nature Med.* **12**, 138-143 (2006).
148. Liang, P.H. et al. Quantitative microarray analysis of intact glycolipid-CD1d interaction and correlation with cell-based cytokine production. *J. Am. Chem. Soc.* **130**, 12348-12354 (2008).
149. Deng, Y. et al. Fluidic air-stable supported lipid bilayer and cell-mimicking microarrays. *J. Am. Chem. Soc.* **130** (2008).
150. Fang, Y., Frutos, A.G. & Lahiri, J. Membrane protein microarrays. *J. Am. Chem. Soc.* **124**, 2394-2395 (2002).
151. Elliott, J.T. & Prestwich, G.D. Maleimide-functionalized lipids that anchor polypeptides to lipid bilayers and membranes. *Bioconj. Chem.* **11**, 832-841 (2000).
152. Hassane, F.S., Frisch, B. & Schuber, F. Targeted liposomes: Convenient coupling of ligands to preformed vesicles using "click chemistry". *Bioconjugate Chem.* **17**, 849-854 (2006).
153. Losey, E.A., Smith, M.D., Meng, M. & Best, M.D. Microplate-Based Analysis of Protein-Membrane Binding Interactions via Immobilization of Whole Liposomes Containing a Biotinylated Anchor. *Bioconjugate Chem.* **20**, 376-383 (2009).
154. Jullien, L. & Lehn, J.M. The Chundle Approach to Molecular Channels Synthesis of a Macrocycle Based Molecular Bundle. *Tetrahedron Lett.* **29**, 3803-3806 (1988).
155. Shirude, P.S., Kumar, V.A. & Ganesh, K.N. BisPNA targeting to DNA: Effect of neutral loop on DNA duplex strand invasion by aepPNA-N7G/aepPNA-C substituted peptide nucleic acids. *Eur. J. Org. Chem.*, 5207-5215 (2005).
156. Forbes, C.C., DiVittorio, K.M. & Smith, B.D. Bolaamphiphiles promote phospholipid translocation across vesicle membranes. *J. Am. Chem. Soc.* **128**, 9211-9218 (2006).
157. Bolen, E.J. & Sando, J.J. Effect of Phospholipid Unsaturation on Protein-Kinase-C Activation. *Biochemistry* **31**, 5945-5951 (1992).
158. Cavalli, S., Tipton, A.R., Overhand, M. & Kros, A. The chemical modification of liposome surfaces via a copper-mediated 3+2 azide-alkyne cycloaddition monitored by a colorimetric assay. *Chem. Commun. (Cambridge)*, 3193-3195 (2006).
159. Houen, G. & Hansen, K. Interference of sugars with the binding of biotin to streptavidin and avidin. *J. Immunol. Methods* **210**, 115-123 (1997).
160. Hsu, K.L. & Mahal, L.K. A lectin microarray approach for the rapid analysis of bacterial glycans. *Nat. Protoc.* **1**, 543-549 (2006).

161. Hsu, K.L., Pilobello, K.T. & Mahal, L.K. Analyzing the dynamic bacterial glycome with a lectin microarray approach. *Nat. Chem. Biol.* **2**, 153-157 (2006).
162. Pilobello, K.T., Krishnamoorthy, L., Slawek, D. & Mahal, L.K. Development of a lectin microarray for the rapid analysis of protein glycopatterns. *ChemBioChem* **6**, 985-989 (2005).
163. Paleos, C.M. & Tsiourvas, D. Interaction between complementary liposomes: a process leading to multicompartment systems formation. *J. Mol. Recognit.* **19**, 60-67 (2006).
164. Gong, Y., Luo, Y.M. & Bong, D. Membrane activation: Selective vesicle fusion via small molecule recognition. *J. Am. Chem. Soc.* **128**, 14430-14431 (2006).
165. Gong, Y., Ma, M., Luo, Y. & Bong, D. Functional determinants of a synthetic vesicle fusion system. *J. Am. Chem. Soc.* **130**, 6196-6205 (2008).
166. Ma, M.M., Paredes, A. & Bong, D. Intra- and Intermembrane Pairwise Molecular Recognition between Synthetic Hydrogen-Bonding Phospholipids. *J. Am. Chem. Soc.* **130**, 14456-14458 (2008).
167. Marchi-Artzner, V. et al. Selective adhesion, lipid exchange and membrane-fusion processes between vesicles of various sizes bearing complementary molecular recognition groups. *Chemphyschem* **2**, 367-376 (2001).
168. Marchi-Artzner, V., Jullien, L., Gulik-Krzywicki, T. & Lehn, J.M. Molecular recognition induced aggregation and fusion between vesicles containing lipids bearing complementary hydrogen bonding head-groups. *Chem. Commun.*, 117-118 (1997).
169. Richard, A. et al. Fusogenic supramolecular vesicle systems induced by metal ion binding to amphiphilic ligands. *Proc. Natl. Acad. Sci. USA* **101**, 15279-15284 (2004).
170. Kashiwada, A., Matsuda, K., Mizuno, T. & Tanaka, T. Construction of a pH-responsive artificial membrane fusion system by using designed coiled-coil polypeptides. *Chem. Eur. J.* **14**, 7343-7350 (2008).
171. Mancin, F., Rampazzo, E., Tecilla, P. & Tonellato, U. Self-assembled fluorescent chemosensors. *Chem. Eur. J.* **12**, 1844-1854 (2006).
172. Sasaki, D.Y., Shnek, D.R., Pack, D.W. & Arnold, F.H. Metal-induced dispersion of lipid aggregates - A simple, selective, and sensitive fluorescent metal-ion sensor *Angew. Chem., Int. Ed.* **34**, 905-907 (1995).
173. Waggoner, T.A., Last, J.A., Kotula, P.G. & Sasaki, D.Y. Self-assembled columns of stacked lipid bilayers mediated by metal ion recognition. *J. Am. Chem. Soc.* **123**, 496-497 (2001).

Vita

Matthew D. Smith was born in Hattiesburg, Mississippi in 1982. He is the son of Robert and Naomi Smith. After growing too old to play “army fort” in the woods, he attended Oak Grove High School in Hattiesburg. Upon graduation, he attended college at William Carey University, also in Hattiesburg. He married Beth Ann McGraw and upon completion of a B.S. in chemistry, they moved to Tennessee where Matt attended the University of Tennessee. He completed a doctorate of philosophy in chemistry in May 2009. He currently has one daughter, Norah Anne-Claire.